

STUDIES ON THE MOBILITY OF
SITES IN POLYSTYRENE POLYMERS OF DIFFERENT
DEGREES OF CROSSLINKING

By

KENNETH M. JONES

A DISSERTATION PRESENTED TO THE GRADUATE SCHOOL
OF THE UNIVERSITY OF FLORIDA IN PARTIAL FULFILLMENT
OF THE REQUIREMENTS FOR THE DEGREE OF
DOCTOR OF PHILOSOPHY

UNIVERSITY OF FLORIDA

1991

To My Parents and My Wife for Their Loving Support

ACKNOWLEDGEMENTS

I appreciate Dr. James A. Deyrup for the suggestion of this research project and his guidance during its progression.

I am grateful for the efforts of Dr. Richard Yost with whom I worked in the preparation of the theoretical model (Appendix A) and the final draft of this dissertation.

I thank Dr. Nigel Richards for agreeing to serve on the committee at the last minute when Dr. Katritzky was unavailable.

I appreciate that Dr. Enholm generously allowed the use of his Chem Draw program and printer by which many of the figures in this document were prepared.

I acknowledge Dr. John Zoltewicz for his explanations of some of the problems which had to be addressed in this dissertation.

I thank Drs. Alan R. Katritzky and Kenneth Sloan for taking the time to serve on my supervisory committee.

For the time that I spent teaching organic laboratory, I am grateful to have worked with Steve Webb for his good company.

Because this work has involved the use of infrared spectroscopy, I feel that I am fortunate to have had Dr. Willis B. Person for consultation about this field. His

advice has allowed me not to worry excessively about the validity of some of the methods used for quantification of species and the possible identification of interactions.

Finally I am indebted to Dr. William M. Jones and especially to Dr. James D. Winefordner for the use of their word processing and computing equipment, without which the process of writing would have been much more difficult and the theoretical section (Appendix A) would have been nearly impossible.

TABLE OF CONTENTS

ACKNOWLEDGEMENTS	iii
ABSTRACT	xx
LIST OF TABLES	ix
LIST OF FIGURES	xiii
KEY TO SYMBOLS	xviii
CHAPTERS	
1 REVIEW OF POLYMER-SUPPORTED REAGENTS	1
1.1 Introduction	1
1.2 Introduction to Site Isolation	4
1.2.1 Claims of Site Isolation	4
1.2.2 Claims of No Site Isolation	10
1.2.3 Efforts to Clarify the Claims about Site Isolation	18
1.3 Characteristics of Crosslinked Polymers	25
1.3.1 Difficulties in Studying Crosslinked Polymers	25
1.3.2 Residual Vinyl Groups	27
1.3.3 Polymeric Heterogeneity	28
1.3.4 Microporous and Macroporous Polymers	29
1.4 Proposal of Research	30
2 SYNTHESIS OF MONOMERS AND POLYMERS	32
2.1 Introduction	32
2.2 Preparation of Ordered Amine Polymers	33
2.2.1 Silanediamines of Pyrrolidine	33
2.2.2 Preparation of 4-Vinylbenzylamine	36
2.2.3 Model Silanediamines of Benzylamine	38
2.2.4 Silanediamine Monomers	38
2.2.5 Preparation of Silanediamine- loaded Polymers and the Removal of the Di- <i>tert</i> -butylsilyl Protecting Group	39
2.3 Preparation of Random Amine Polymers	41

2.3.1	Selection and Preparation of a Monomer for the Preparation of the Random Amine Prepolymer	41
2.3.2	Removal of the <i>tert</i> -Butoxycarbonyl (BOC) Protecting Group	42
2.4	Preparation of N-(4-Vinylbenzyl)acetamide Calibration Curves for the Spectroscopic Quantification of Amine Groups in Polymers	44
2.4.1	Justification for the Use of Infrared Spectroscopy	44
2.4.2	Preparation of 4-Vinylbenzylacetamide and its Polymers for Calibration Curves	44
2.4.3	Analysis of the Calibration Data	45
3	MEASURE OF PROXIMITY AND MOVEMENT OF AMINE GROUPS IN POLYMERS	52
3.1	Introduction	52
3.1.1	Quantitative Infrared (IR) Spectroscopy	54
3.1.2	Extraction of Data from IR Spectra	64
3.2	Measure of Proximity by Formation of Urea and Urethane Moieties	66
3.2.1	Coupling of Amines to Form Urea and Urethane Moieties	66
3.2.2	Coupling Reaction	67
3.2.3	Analysis of Polymer Samples Containing Urea and Urethane Moieties	68
3.2.4	Conditions and Results of the Coupling Reaction	71
3.2.5	Discussion of the Results of the Coupling Reaction	80
3.2.6	Conclusions	85
3.3	Measure of Proximity by Hydrogen Bonding	85
3.3.1	Advantages for the Use of Hydrogen Bonding to Measure Proximity	85
3.3.2	Acetylation Reaction	86
3.3.3	Analysis of Hydrogen Bonding in Polymer Samples	90
3.3.4	Conditions and Results of the Acetylation Reaction	90
3.3.5	Discussion of the Acetylation Results	91
3.3.6	Conclusions	100
3.4	Measure of Proximity by the Amine-catalyzed Aldol Condensation of Phenylacetaldehyde	101
3.4.1	The Rationale for the Use of the Amine-catalyzed Aldol Condensation of Phenylacetaldehyde for the Measure of Proximity	101

3.4.2	The Amine-catalyzed Aldol Condensation of Phenyl-acetaldehyde	102
3.4.3	Conditions, Analysis and Results of the Condensation Reaction . . .	103
3.4.4	Discussion of the Condensation Results	104
CHAPTER 4 CONCLUSIONS	109
CHAPTER 5 EXPERIMENTAL SECTION	113
5.1	Introduction	113
5.2	Syntheses	114
5.2.1	Silanediamine Compounds	114
5.2.2	1,1'-(Diphenylsilylene)bis-(pyrrolidine), <u>10</u>	114
5.2.3	1,1'-(Bis(1-methylethyl)silylene)-bis(pyrrolidine), <u>11</u>	115
5.2.4	1,1'-(<i>(1,1-Dimethylethyl)</i> Phenylsilylene)bis(pyrrolidine), <u>12</u> . . .	115
5.2.5	Bis(<i>1,1-Dimethylethyl</i> chlorosilylpyrrolidine, <u>13</u>	116
5.2.6	4-Vinylbenzoic acid, <u>14</u>	117
5.2.7	4-Vinylbenzamide, <u>15</u>	118
5.2.8	4-Vinylphenylmethanamine, <u>16</u>	119
5.2.9	1,1-Diphenyl- <i>N,N'</i> -dibenzyl-silanediamine, <u>17</u>	120
5.2.10	1,1-Bis(<i>1-methylethyl</i>)- <i>N,N'</i> -dibenzylsilanediamine, <u>18</u>	121
5.2.11	1-(<i>tert-Butyl</i>)-1-phenyl- <i>N,N'</i> -dibenzylsilanediamine, <u>19</u>	121
5.2.12	1,1-Di- <i>tert-butyl</i> - <i>N,N'</i> -dibenzylsilanediamine, <u>20</u>	122
	5.2.12.1 First method	122
	5.2.12.2 Second method	123
5.2.13	1,1-Di- <i>tert-butyl</i> - <i>N,N'</i> -bis(4-vinylbenzyl)silanediamine, <u>21</u>	123
5.2.14	<i>O</i> -(<i>tert-butyl</i>)- <i>N</i> -(4-vinylbenzyl)carbamate, <u>22</u>	125
5.2.15	<i>N</i> -(4-Vinylbenzylacetamide, <u>23</u>	126
5.2.16	<i>O</i> -(<i>tert-butyl</i>)- <i>N</i> -benzylcarbamate, <u>24</u>	127
5.2.17	<i>O</i> -(<i>tert-butyl</i>)- <i>N</i> -(4-Methylbenzyl)carbamate, <u>25</u>	128
5.2.18	<i>N</i> -Benzylacetamide, <u>26</u>	129
5.2.19	<i>N</i> -(4-Methylbenzyl)acetamide, <u>27</u>	129
5.2.20	<i>N,N'</i> -Dibenzylurea, <u>28</u>	130
5.3	Polymer Preparation	133
5.3.1	General Synthetic Method for the Preparation of Polymers (Known to be Macroporous)	133

5.3.2	Preparation of N-(4-Vinylbenzyl)-acetamide Copolymers	133
5.3.2.1	Preparation of 20 mol% Crosslinked Polymers	133
5.3.2.2	Preparation of 80 mol% Crosslinked Polymers	136
5.3.3	Preparation and Silanediamine-loaded Polymers	137
5.3.4	Preparation and Carbamate-loaded Copolymers	140
5.4	Infrared Analysis Methods	144
5.4.1	Determination of Relative Molar Absorptivities	144
5.4.2	Extraction of Data from IR Spectra	145
5.5	Reactions on Polymers	145
5.5.1	Conditions Used for the Coupling of Amine Groups with Carbonyldiimidazole	145
5.5.2	Conditions Used for the Acetylation of Random and Ordered Polymers	147
5.5.3	Amine-catalyzed Reactions of Phenylacetaldehyde	147
APPENDICES		
A	THEORETICAL MODEL FOR RANDOMLY DISTRIBUTED AMINES	154
B	CHN CALCULATIONS	178
C	TREATMENT OF SPECTRA FOR THE DETERMINATION OF URETHANE AND UREA CONCENTRATIONS	186
BIBLIOGRAPHY		196
REFERENCES		197
BIOGRAPHICAL SKETCH		201

LIST OF TABLES

Table 1-1	Results of the Acylation of Polymer-bound Esters	7
Table 1-2	Composition of 4-Vinylbenzoic Acid-Styrene(ST)-Divinylbenzene(DVB) Copolymer	11
Table 1-3	Relative Intensities of Infrared Absorption Bands (KBr) for Various Carboxylated Polystyrenes, before and after Treatment with Dicyclohexyl-carbodiimide (DCC)	17
Table 1-4	Characteristics of Random (R) and Ordered (NR) Polymers Containing Bound Benzylthiol Moieties	24
Table 1-5	Reduction and Reoxidation Yields of Polymer-bound Benzylthiol Polymers	24
Table 2-1	Silanediamines of Pyrrolidine	35
Table 2-2	Silanediamines of Benzylamine	37
Table 2-3	Calibration Curve Data of N-(4-Vinylbenzyl)acetamide <u>23</u> Versus its Concentration in 20X Comonomer Solution	47
Table 2-4	Least Squares Analysis of the Calibration Data of 20X N-(4-Vinylbenzyl)-acetamide <u>23</u> (from the Lotus program) . .	49
Table 2-5	Calibration Data of N-(4-Vinylbenzyl)-acetamide <u>23</u> Versus its Concentration in 80X Comonomer Solution	49
Table 2-6	Least Square Analysis of the 80X Calibration Curve Data of N-(4-Vinylbenzyl)acetamide <u>23</u> (from Lotus program)	51
Table 3-1	Probability of Proximity of Spherical Groups	53

Table 3-2	Calibration Curve Data of the N-Benzylacetamide <u>26</u> /Toluene Solutions . . .	56
Table 3-3	Least Squares Analysis of the N-Benzylacetamide <u>26</u> /Toluene Calibration Curve Data	58
Table 3-4	Relative Molar Absorptivities of Model Carbonyl Compounds (Versus Toluene) . . .	59
Table 3-5	Molar Absorptivities of Model Carbonyl Compounds Relative to Polymer-bound Benzylacetamide	60
Table 3-6	Results of IR Measurements on the Carbamate-loaded Polymers	62
Table 3-7	Results of the Coupling of Polymer-bound Amines to form Urea and Urethane	72
Table 3-8	Results of Analysis of Figures 3-6 through 3-9	80
Table 3-9	Hypothetical Urethane/Urea Ratios Based on the Best Lines (and Curves) for the Data in Table 3-8	82
Table 3-10	Average Site Accessibility Data Obtained from the Coupling of Amine Polymers with 1,1'-Carbonyl-diimidazole	83
Table 3-11	Results of the Acetylation of Amine Polymers	88
Table 3-12	Summary of Accessibility Data Obtained from the Acetylation Reaction	90
Table 3-13	Results of Amine-catalyzed Aldol Condensation of Phenylacetaldehyde . . .	107
Table 3-14	Results of Amine-catalyzed Aldol Condensation of Phenylacetaldehyde (On an equivalent basis)	108
Table 5-1	Composition of Reagents Used for the Preparation of 20X N-(4-Vinylbenzyl)-acetamide <u>23</u> Copolymer Calibration Samples	134

Table 5-2	Data from IR Measurements of 20X N-(4-Vinylbenzyl)acetamide <u>23</u> Calibration Samples	135
Table 5-3	Composition of Reagents used for the Preparation of 80X N-(4-Vinylbenzyl)-acetamide <u>23</u> Calibration Curve Samples .	136
Table 5-4	Data from IR Measurements on 80X N-(4-Vinylbenzyl)acetamide <u>23</u> Calibration Curve Samples	137
Table 5-5	Composition of Reagents Used for the Preparation of Silanediamine-loaded Polymers	139
Table 5-6	Amounts of Reagents used for the Preparation of Silanediamine-loaded Polymers	139
Table 5-7	Calculated Composition of the Silanediamine-loaded Polymers	140
Table 5-8	Amounts of Reagents Used for the Preparation of Carbamate-loaded Polymers	141
Table 5-9	Calculated Composition of the Carbamate-loaded Polymers	142
Table 5-10	Results of IR Measurements of the Carbamate-loaded Polymers	143
Table 5-11	Schedule for the Addition of Carbonyldiimidazole to Amine Copolymers	146
Table 5-12	Results of the IR Measurements on the Amine-Polymer Samples Coupled with 1,1'-Carbonyldiimidazole	148
Table 5-13	Results of the IR Measurements on the Acetylated Amine-polymer Samples	149
Table 5-14	Characteristics of Reactions of Amine-polymer-catalyzed Aldol Condensation of Phenylacetalddehyde	151
Table 5-15	Results of Analyses on the Amine-polymer-catalyzed Reaction Mixtures	152
Table A-1	Values for Various Quantities Related to the Random Distribution of Spheres .	159

Table A-2	Values of the Coefficients in Equation A-13	161
Table A-3	Estimations of the Values of Z at Various Distances (L) from a Central Sphere for Various Degrees of Functionalization	163
Table A-4	Theoretical Values Expected for the Urethane Concn/Urea Concn Ratios (assuming different mobilities, i.e. distances moved)	166
Table A-5	Values of the Constants k and c for Integral Values of the Mobility Parameter m	168
Table A-6	Values of m Obtained by Best Fits of the Theoretical R_m Curve to the Experimental Data for the Random Polymers	169
Table A-7	Conversion of Urea Fractions into Distance Moved	176
Table B-1	Calculation of the Atomic Mass Balance of a Silanediamine-loaded Polymer (J4-A) (20X)	179
Table B-2	Calculation of the Atomic Mass Balance of a Silanediamine-loaded Polymer (J4-D) (80X)	180
Table B-3	Calculation of the Atomic Mass Balance of a Carbamate-loaded Polymer (20X)-Sample (J8-A)	181
Table B-4	Calculation of the Atomic Mass Balance of a Carbamate-loaded Polymer (80X)-Sample (J8-D)	183
Table B-5	Calculation of the Atomic Mass Balance of a Acetamide-loaded Polymer (20X)-Sample (I38-A)	185

LIST OF FIGURES

Figure 1-1	Reaction Scheme for the Monoacylation of Polymer-bound Esters	6
Figure 1-2	Polymer-supported Cross Aldol Reactions .	9
Figure 1-3	Formation of Polymer-bound Sebacyl Ester .	13
Figure 1-4	Products of the Attempted Cyclization of Polymer-bound Sebacyl Ester	13
Figure 1-5	Formation of Polymer Bound ω -Cyano-pelargonyl Thiol Ester	15
Figure 1-6	Product of Attempted Cyclization of Thiol Ester Using Lithium Bistriethyl-disilazide	15
Figure 1-7	Reactions of Polymer-bound Carboxylic Acid with Dicyclohexylcarbodiimide (DCC) .	16
Figure 1-8	Spectra of the Carbonyl Region of a Carboxylated Polystyrene, before and after Reaction with DCC. The Spectra Pictured are for SX-2 (see Table 1-3) [77JA625]	16
Figure 1-9	Reactions Forming and Consuming Monomeric Benzyne	20
Figure 1-10	Reactions Forming and Consuming Polymer-bound Benzyne	21
Figure 2-1	5-Vinylisoindoline <u>8</u> and 6-Vinyl-1,2,3,4-tetrahydroisoquinoline <u>9</u>	35
Figure 2-2	Preparation of 4-vinylbenzylamine <u>16</u> . . .	36
Figure 2-3	Preparation of Bifunctional Amine Sites in Crosslinked Polystyrene	40
Figure 2-4	Preparation of O-(<i>tert</i> -butyl)-N-(4-vinylbenzyl)carbamate <u>22</u>	42

Figure 2-5	Preparation of Randomly Distributed Amine Copolymers	43
Figure 2-6	Preparation of N-(4-Vinylbenzyl)acetamide <u>23</u>	46
Figure 2-7	Calibration Curve of N-(4-Vinylbenzyl)-acetamide <u>23</u> Versus its Concentration in 20X Comonomer Solution	48
Figure 2-8	Calibration Curve of N-(4-Vinylbenzyl)-acetamide <u>23</u> Versus its Concentration in 80X Comonomer Solution	50
Figure 3-1	N-benzylacetamide/Toluene Calibration Curve	57
Figure 3-2	IR Spectra of "Blank" 20X, 40X, 60X and 80X Polystyrene	63
Figure 3-3	Typical Results Obtained from the Subtraction of Spectra	65
Figure 3-4	Reaction for the Coupling of Monomeric Amines with 1,1'-Carbonyldiimidazole	67
Figure 3-5	Coupling of Polymer-bound Amines with 1,1'-Carbonyldiimidazole	70
Figure 3-6	Graphical Presentation of Coupling Reaction Data (20X)	73
Figure 3-7	Graphical Presentation of Coupling Reaction Data (40X)	74
Figure 3-8	Graphical Presentation of Coupling Reaction Data (60X)	75
Figure 3-9	Graphical Presentation of Coupling Reaction Data (80X)	76
Figure 3-10	Graphical Presentation of the Coupling Data as a Function of Crosslinking (nominally 1.5 mol% Random and Ordered Polymers)	77
Figure 3-11	Graphical Presentation of the Coupling Data as a Function of Crosslinking (nominally 3.0 mol% Random and Ordered Polymers)	78

Figure 3-12	Reaction of Polymer-bound Amines with Acetylimidazole	88
Figure 3-13	Spectra of the Carbonyl Region of Acetylated Random Polymer Samples (3%; 20X, 40X, 60X and 80X) (Polystyrene Subtracted) (Nujol Mulls)	93
Figure 3-14	Spectra of the Carbonyl Region of Acetylated Ordered Polymer Samples (3%; 20X, 40X, 60X and 80X) (Polystyrene Subtracted) (Nujol Mulls)	94
Figure 3-15	Spectra of the Carbonyl Region of Acetylated Ordered Polymer Samples (1.5%; 20X, 40X, 60X and 80X) (Polystyrene Subtracted) (Nujol Mulls)	95
Figure 3-16	Spectrum of 7.3 mol% Polymer-bound Benzylacetamide	96
Figure 3-17	Spectrum of 7.3 mol% Polymer-bound Benzylacetamide Superimposed with the 3 mol% NR (80X) Carbonyl Spectrum	97
Figure 3-18	IR Spectra of the Carbonyl Region of Various Concentrations of N-Benzylacetamide in Toluene (Toluene Subtracted)	98
Figure 3-19	IR Spectra of the NH Region of Various Concentrations of N-Benzylacetamide in Toluene (Toluene Subtracted)	99
Figure 3-20	Stoichiometry of the Amine-catalyzed Aldol Condensation of the Phenylacetaldehyde	102
Figure 3-21	Possible Mechanism of the Amine-catalyzed Aldol Condensation of the Phenylacetaldehyde	105
Figure 3-22	GC Trace of an Extract of the Aldol Reaction	106
Figure 5-1	Gas chromatograms of compounds <u>24</u> and <u>25</u>	131
Figure 5-2	Gas chromatograms of compounds <u>26</u> , <u>27</u> and <u>28</u>	132

Figure 5-3	Stoichiometry of Reaction for the Formation of Urea from Amine-loaded Copolymers with Carbonyldiimidazole . . .	146
Figure A-1	Graphical Presentation of the Values of the Function Y	158
Figure A-2	Plot of the Values of Z for Various Degrees of Functionalization versus L . .	162
Figure A-3	Graphical Presentation of the Theoretical R_m Values	167
Figure A-4	Theoretical R_m Values along with the Fitted Curves of the Form: $Y = k/DF + C$	170
Figure A-5	Graphical Presentation of the Fitting of the Theoretical R_m Curve to the Experimental Data for the 20X Random Polymer	171
Figure A-6	Graphical Presentation of the Fitting of the Theoretical R_m Curve to the Experimental Data for the 40X Random Polymer	172
Figure A-7	Graphical Presentation of the Fitting of the Theoretical R Curve to the Experimental Data for the 60X Random Polymer	173
Figure A-8	Graphical Presentation of the Fitting of the Theoretical R Curve to the Experimental Data for the 80X Random Polymer	174
Figure C-1	IR Spectrum of a Random Polymer Sample after Coupling with Carbonyldiimidazole ($CHBr_3$ Mull)	187
Figure C-2	Magnified View of the IR Spectrum shown in Figure C-1 ($CHBr_3$ Mull)	188
Figure C-3	IR Spectrum of the Carbonyl Region of a Coupled Ordered Polymer after the Aromatic Overtones have been Subtracted	189
Figure C-4	An Expanded View of the IR Spectrum in Figure C-3 with the Baseline and Integration Bounds	190

Figure C-5	IR Spectrum of an Ordered Polymer Sample after Coupling with Carbonyldiimidazole (CHBr ₃ Mull)	192
Figure C-6	Magnified View of the IR Spectrum shown in Figure C-5 (CHBr ₃ Mull)	193
Figure C-7	IR Spectrum of the Carbonyl Region of a Coupled Ordered Polymer after the Aromatic Overtones have been Subtracted	194
Figure C-8	An Expanded View of the IR Spectrum in Figure C-7 with the Baseline and Integration Bounds	195

KEY TO SYMBOLS AND ABBREVIATIONS

AIBN	Azo-isobutyronitrile
AMIDE	N-(4-Vinylbenzyl)acetamide <u>23</u>
br	Broad
BOC	<i>tert</i> -Butoxycarbonyl group
BuLi	Butyllithium
CALIB	Calibration (or calibrated)
CARB	<i>O-tert-Butyl-N-(4-Vinylbenzyl)carbamate</i>
CDCl ₃	Chloroform (deuterated)
CH ₂ Cl ₂	Methylene chloride
CHBr ₃	Bromoform
CHN	Carbon, hydrogen and nitrogen combustion analysis
c(m)	Constant determined by least square best fit in equations
CONCN	Concentration
d	Doublet
DCC	Dicyclohexylcarbodiimide
dd	Doublet of doublets
df	Degrees of freedom
DF	Degree of functionalization
D(L)	Cubic polynomial (aL ³ + bL ² + cL)
DMSO	Dimethylsulfoxide
DMSO-d ₆	Dimethylsulfoxide (deuterated)
DVB	Divinylbenzene
eq.	Equivalent
EtOH	Ethanol
FTIR	Fourier transform infrared (spectroscopy)
g	Gram
GC/MS	Gas chromatography/mass spectroscopy
h	Hour
HB	Hydrogen bonded
IBD	Iodobenzene diacetate
IR	Infrared
K _L	The probable occupancy of a layer when that layer is the nearest <u>occupied</u> layer
k(m)	Constant determined by least square best fit in equations
L	Layer number (see Appendix A) or the thickness of one layer
LiAlH ₄	Lithium aluminum hydride
LTA	Lead tetraacetate
m	Mobility (i.e. distance moved)
M	Molar (moles/liter)

m^2	Meter squared (for the measure of area)
m	Multiplet (when applied to NMR spectra)
mg	Milligram
mL	Milliliter
$mmol$	Millimole
mol	Mole
m/p	Ratio of meta/para isomers
MS	Mass spectrometry (spectrum)
MS(CI)	Mass spectrometry (spectrum) by chemical ionization
MS(EI)	Mass spectrometry (spectrum) by electron ionization
MS(HR)	Mass spectrum (high resolution)
m/z	Mass-to-charge ratio
NHB	Non-hydrogen bonded
n_L	Number of spheres in a given layer = $12 \cdot L^2$
NR	Ordered
NMR	Nuclear Magnetic Resonance
OTf	Triflate group ($CF_3-SO_3^-$)
$P(0, i)$	The probability of finding no (zero) amine "spheres" in the i^{th} layer
$P(\geq 1, i)$	The probability of finding one or more amine "spheres" in the i^{th} layer
$P_{N,L}$	The probability of finding N amine "spheres" in the L^{th} layer
R	Random
R_m	Theoretical urethane/urea ratio (a function of mobility)
s	Second (time)
s	Singlet (when applied to NMR spectra)
S.D.	Standard deviation
SiN_2	Silanediamine monomer--N,N-bis(4-vinylbenzyl)-1,1-di- <i>tert</i> -butylsilane 21
S_L	The product, S_L , of eqns (A-7) and (A-9)
ST	Styrene
t	"Student's" distribution value for the given degrees of freedom
t	Triplet (when applied to NMR spectra)
TC	Tetraphenylcyclopentadienone
THF	Tetrahydrofuran
UV	Ultraviolet
VIS	Visible
X	Qualitative measure of crosslinking as determined by the mol% of divinylbenzene (DVB) used in the initial monomer mixtures
Y	The fraction of nearest amines found in each layer
Z	The cumulative distribution, obtained by forming the cumulative sum of the terms of Y
δ	Measure of deviation of the NMR signal from

that of tetramethylsilane in parts per
million

π Numerical constant, approxiamately 3.14
 μ Micro (10^{-6})

Σd_i^2 Summation of the squares of the deviations

Σd_i Summation of the deviations

Abstract of Dissertation Presented to the Graduate School
of the University of Florida in Partial Fulfillment of the
Requirements for the Degree of Doctor of Philosophy

STUDIES ON THE MOBILITY OF
SITES IN POLYSTYRENE POLYMERS OF DIFFERENT
DEGREES OF CROSSLINKING

By

KENNETH M. JONES

December, 1991

Chairperson: Dr. James A. Deyrup
Major Department: Chemistry

The purpose of the research was to assess the mobility of functional groups that are bound on a polystyrene matrix. The synthetic methodology of binding two amines under mild conditions using dialkylsilyl ditriflates was developed. The research involved the preparation and the testing of the stability of various silanediamines for the purposes of purification and incorporation into polystyrene of different degrees of crosslinking. Once incorporated the silanediamine sites were cleaved to create sites containing two primary amines. For comparison, polymers were prepared in which the amine groups were randomly distributed.

Polystyrene samples, nominally crosslinked at 20 mol%, 40 mol%, 60 mol% and 80 mol%, were loaded at 1.5 mol% and 0.75 mol% with di-*tert*-butyl-N,N'-di(4-vinylbenzyl)silanediamine,

which upon cleavage yielded ordered polymers loaded at 3.0 mol% and 1.5 mol% in amine groups. Polystyrene was loaded with randomly placed carbamate groups by copolymerization of O-(*tert*-butyl)-N-(4-vinylbenzyl)carbamate with styrene and divinylbenzene which were also loaded at 3.0 mol% and 1.5 mol%. These polymers were treated to generate randomly placed amine groups in the polystyrene matrix.

The proximity of the amines was tested in three ways. In one method the random and ordered amine polymers were treated with 1,1'-carbonyldiimidazole followed by ethanol. This sequence of reagents resulted in the formation of urea and urethane groups in the polymer samples. The ratio of the two functional groups was determined from calibration curves of IR absorption intensities and was used to judge the mobility of the amino groups. The second method by which evidence of proximity of amino groups was obtained involved the examination of hydrogen bonding in the polymer samples. The random and ordered amine polymers were treated with acetic anhydride and pyridine in order to form acetamide groups from the amine groups. The degrees of hydrogen bonding in the random and ordered polymers were then compared. The last method involves the testing of random and ordered polymers loaded at 3.0 mol%, 1.5 mol%, 0.5 mol% and 0.1 mol% as amine catalysts of the aldol condensation of phenylacetaldehyde.

CHAPTER 1
REVIEW OF POLYMER-SUPPORTED REAGENTS

1.1 Introduction

In 1963 Merrifield [63JA2149] reported the synthesis of a tetrapeptide by the novel technique of immobilization of an amino acid in a polymeric gel. Since then the study of polymer-supported reagents and catalysts has developed into a discipline of chemistry in its own right. Polymer-supported species offer some interesting distinctions to molecular species capable of existing in solution. Polymer-bound species include enzymes, Wittig reagents, photosensitizers, reductants, oxidants and others [80MI1]. Reagents which are bound in polymers offer the following potential advantages:

- (i) The work-up is simplified since the excess and spent reagent can be easily removed from the final reaction mixture by simple filtration.
- (ii) Excess reagent can be used to achieve higher yields without causing separation problems.
- (iii) It is possible to regenerate and re-use the reagent since it is easily recovered. Since polymer-supported reagents will generally be more expensive than the analogous nonsupported reagents, it might

then become worthwhile to prepare complex reagents which would otherwise be prohibitively expensive.

Other advantages result from the insolubility and nonvolatility of the polymer. For example, polymer-supported reagents will be non-toxic and odorless. These are characteristics especially appreciated by those who must work with the reagents. Finally it should be noted that a number of microenvironmental effects are possible with polymer-supported reagents.

One possibility is that the environment of the polymeric material may favor a given reaction. The difference in polarity between the polymer and the reaction solvent might cause the substrate to concentrate within the polymer. This could cause an increase in the reaction rate, although it is also possible that the change in polarity may diminish the reaction rate more so than the higher concentration will increase it.

Sites may be created in a polymer in which two or more functional groups act in a cooperative manner, as they are considered to do in enzymes. The functional groups may be the same or different, depending on the reaction to be catalyzed.

In contrast to the preparation of cooperative sites, it is possible, depending on the mobility of the polymer chains, to isolate one species from another. This can have dramatic chemical reactivity effects, for example with organotransition metal species such as titanocene (see section 1.2.1). The

activity of the species may be the same as if the species were approaching infinite dilution.

Another possibility which depends on the mobility of the polymer chains is that of template formation in crosslinked polymers. The method depends on the incorporation of the template during the polymerization followed by the removal of the template after the polymerization is complete. The template may be used to position functional groups which remain in the polymer after the template is removed. The cavity that is left in the polymer may be useful, for example, in the resolution of enantiomers by chromatography. [77MI1].

Obviously, with polymeric reagents having all of these advantages, they are worthy of and will receive further investigation. Mobility in and stability of bifunctional sites in crosslinked polystyrene are the subjects of this investigation and merit further discussion.

The integrity of bifunctional sites or the isolation of separated species depends in part on the mobility of the polymer chains to which the functional groups are attached. This parameter, i.e., mobility of the polymer chains, was at least one design factor in the experiments described below.

Numerous review articles are available concerning polymeric reagents and a few are listed here. These references contain references to many more papers on the subjects of site-site isolation/interaction, polymer-supported

reagents and catalysts, and their uses in organic synthesis [75PAC503, 76ACR135, 86MI1, 80MI2].

1.2 Introduction to Site Isolation

A motivation for the development of polymer-bound reagents has been the potential immobilization of a chemical species in a reaction. This phenomenon has suggested the name "hyperentropic efficacy" or the high dilution principle. The bound species remains isolated during subsequent reactions, as though the species were approaching infinite dilution. In some cases the reactivity of the species changes upon isolation.

1.2.1 Claims of Site Isolation

As stated above, in 1963 Merrifield [63JA2149] reported the synthesis of a tetrapeptide using immobilization of an amino acid in a polymeric gel to develop a practical peptide synthetic technique. He claimed that the binding of the growing peptide chains to the polymer backbone provided isolation of one chain from another which prevented inter-peptide reactions such as unwanted couplings. This along with the ability to remove excess reagents (which helped to achieve high yields) by simple washing made the synthetic technique practical since purification of the intermediate peptide chains was eliminated. He investigated polymers that were 1%, 2%, 8% and 16% crosslinked and chose 2% crosslinked polymers

since lesser crosslinked polymers were too fragile and higher crosslinked polymers did not allow sufficiently rapid penetration of reagents.

Following Merrifield's results others applied the use of polymer supports to nonpeptide organic syntheses. Patchornik and Kraus [70JA7587] reported on the generation and directed monoacylation of polymer-bound ester enolates. Two side reactions, which affect esters in solution, were avoided by binding the esters to a polymer: 1) self-condensation of the ester to be acylated, and 2) diacylation which results from proton exchange between an enolate and an already acylated ester followed by a second acylation of the newly formed acylated enolate.

Phenylacetic and acetic acids were reacted with chloromethylated polystyrene-2% divinylbenzene (DVB) to prepare the corresponding polymer esters (0.1-0.3 mmol of ester/g of polymer (Degree of Functionalization, DF = 1-3%)). The polymer ester was swelled and one equivalent of trityllithium in tetrahydrofuran at 0°C under dry argon was added to form the enolate. The reactions involved are shown in Figure 1-1.

After the red color of the base had disappeared (1-5 min), 1.5 equiv of an acid chloride or anhydride were added. The mixture was then stirred for 1 hour at room temperature. The polymer was then filtered, thoroughly washed and dried. Upon cleavage with dry HBr in trifluoroacetic acid, a single

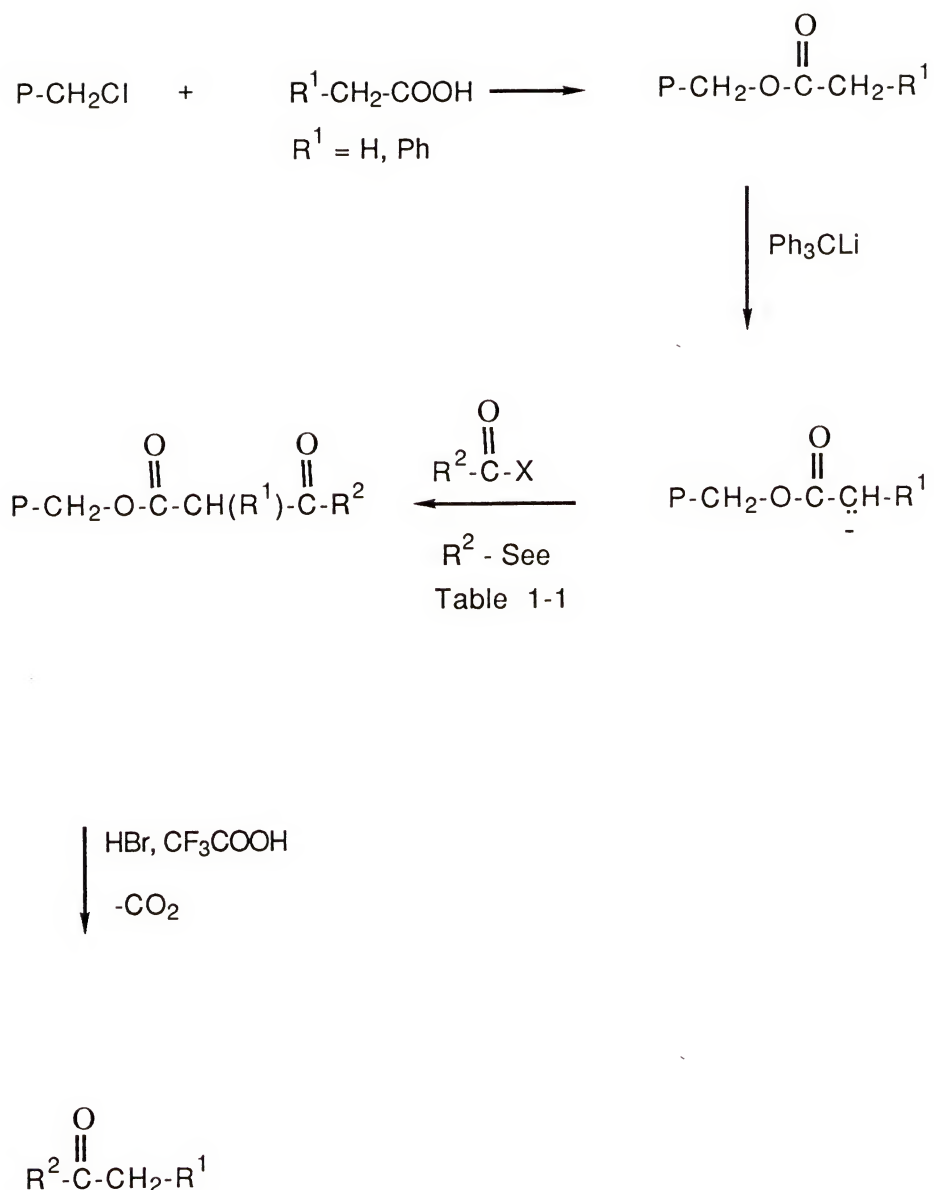


Figure 1-1 Reaction Scheme for the Monoacetylation of Polymer-bound Esters

Table 1-1 Results of Acylation of Polymer-bound Esters

Ester	Acylating Agent	Product	Yield %	Yield Unreacted Acid %
<i>p</i> -CH ₃ OOCCH ₂ C ₆ H ₅	<i>p</i> -O ₂ NC ₆ H ₄ COCl	<i>p</i> -O ₂ NC ₆ H ₄ COCH ₂ C ₆ H ₅	43	40
<i>p</i> -CH ₃ O-COCH ₂ C ₆ H ₅	<i>p</i> -BrC ₆ H ₄ -CO-Cl	<i>p</i> -BrC ₆ H ₄ COCH ₂ C ₆ H ₅	40	45
<i>p</i> -CH ₃ OOCCH ₂ C ₆ H ₅	(α -C ₁₀ H ₇ CH ₂ CO) ₂ O	α -C ₁₀ H ₇ CH ₂ COCH ₂ C ₆ H ₅	40	55
<i>p</i> -CH ₃ O-CO-CH ₃	<i>p</i> -O ₂ N-C ₆ H ₄ -CO-Cl	<i>p</i> -O ₂ N-C ₆ H ₄ CO-CH ₃	20	45

ketone and unreacted acid were obtained in every case. The results of their investigation are summarized in Table 1-1. Analogous reactions in solution with ethyl phenylacetate, performed under identical conditions, resulted in the formation of several ketone products.

Leznoff and Wong reported the selective blocking of one hydroxy group in symmetrical diols [72CJC2892]. A single hydroxy group of symmetrical diols was derivatized by reacting 2% crosslinked polystyrene supported carboxylic acid chlorides with an excess of the diol. A major advantage of the polymer-supported derivatization was that the excess diol could be removed by simple washing and filtration. The yields of recovered monotritylated diols ranged from 37% to 51% based on the amount of diol bound to the polymer. Some have claimed [76ACR135] that this experiment is not a true demonstration of site isolation, since monofunctionalization of diols has been achieved by using excess diol plus trityl chloride [23CB769];

however, the authors of the solution-chemistry paper did not report yields for much of their work.

Leznoff and Wong also reported the protection of a single aldehyde group of symmetrical dialdehydes via acetal formation on a 2% crosslinked polystyrene resin, again using excess dialdehyde to ensure monofunctionalization [73CJC3756]. Wittig reactions, crossed aldol condensations, benzoin condensations, Grignard reactions and metal hydride reductions were carried out on the unprotected aldehyde groups. Interestingly, attempts to conduct mixed benzoin condensations with excess benzaldehyde and sodium cyanide invariably led to intractable mixtures of symmetrical benzoins and mixed or crossed benzoins, perhaps demonstrating that the free aldehydes groups were in fact not isolated. The crossed aldol condensations of 1 and 2 with acetophenone yielded the chalcones 3 and 4 in 100% and 96% yields, respectively, as shown in Figure 1-2. The chalcone 3 had previously been obtained in only 30% yield [06M969].

W.D. Bonds, Jr. et al. reported the site isolation of titanocene species on 20% crosslinked polystyrene resin [75JA2128]. Site isolation of an organometallic species is important since monomeric organometallic species, which are active for a given reaction because they have open coordination sites, tend to polymerize by forming ligand bridges or metal-metal bonds when they are free to associate, as they are in solution. The titanocene species which was

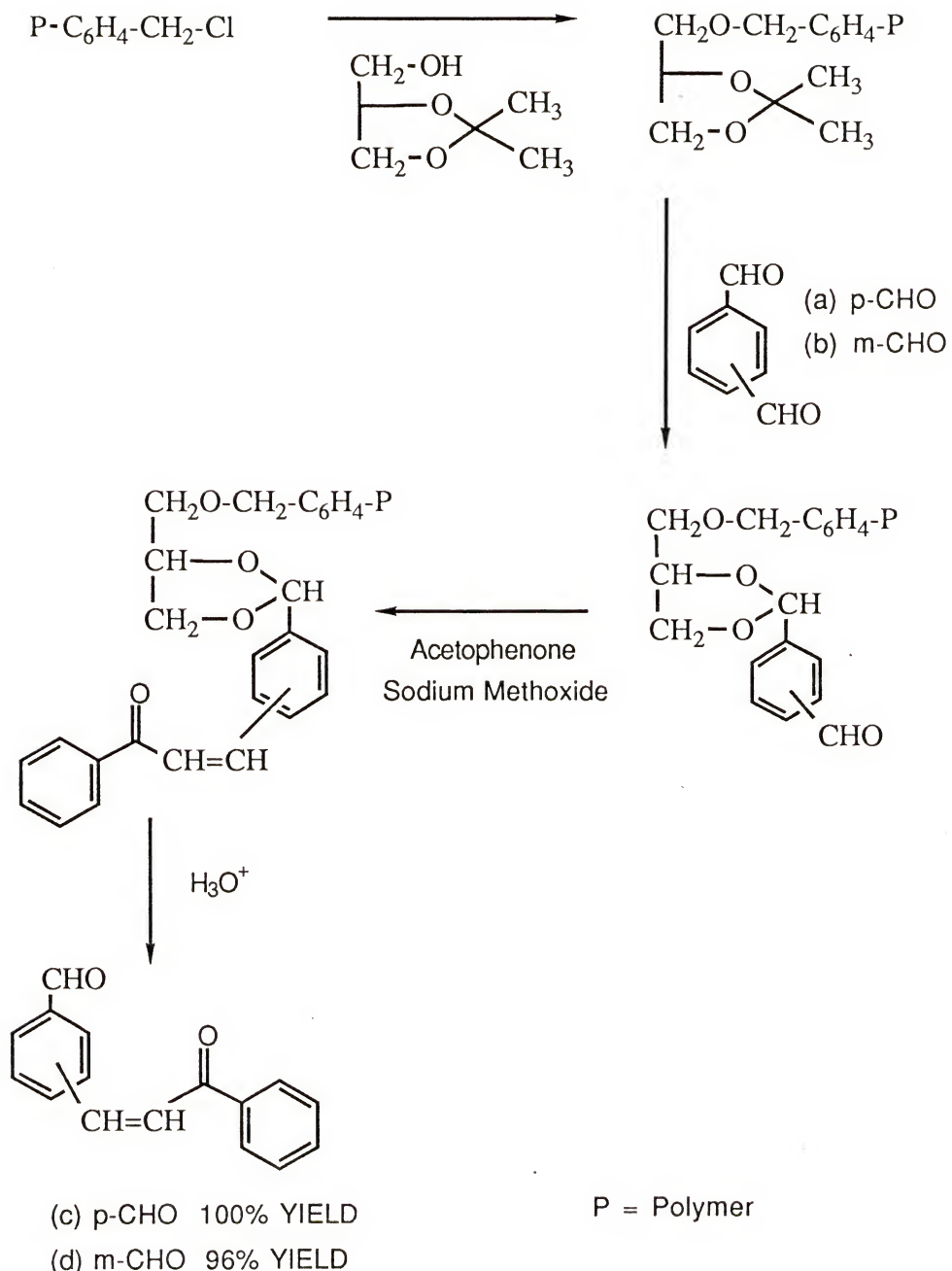


Figure 1-2 Polymer-supported Cross Aldol Reactions

bound to the polystyrene matrix was unable to dimerize and was found to be 25-120 times more active for various olefin hydrogenation reactions than the corresponding reduced nonattached titanocene dichloride or benzyltitanocene dichloride. This observation strongly indicated that the titanocene species were isolated.

In a follow-up study, R.H. Grubbs et al. investigated hydrogenation of olefins as a function of loading of catalyst on 20% crosslinked macroporous polystyrene [77JA4517]. They found that the ratio of H_2 /(minute) (millimole of Ti) increased as the loading decreased, and that the rate in milliliters/(minute) (gram of polymer) reached a maximum at the loading of 0.14 millimole of Ti/gram of polymer (DF = 1.5%). Both of these observations are consistent with site isolation at low loadings. In contrast, Scott et al. [77JA625] have presented evidence that site-site interaction is significant in this same polymer (see section 1.2.3).

1.2.2 Claims of No Site Isolation

In 1964 Letsinger et al. [64JA5163] reported the preparation of "popcorn" polystyrene that had been copolymerized with 4-vinylbenzoic acid. The amounts of the comonomers used are shown in Table 1-2.

The copolymer showed two absorptions in the infrared spectrum for the carboxyl group. One appeared at $5.90\mu\text{m}$ (1695 cm^{-1}) (a hydrogen bonded carbonyl) and another at $5.79\mu\text{m}$ (1727

cm^{-1}) (a non-hydrogen bonded carbonyl). Though the relative areas of the two absorbances were not reported, apparently the major portions of carboxyl groups were hydrogen bonded indicating that substantial site isolation was not achieved in this system.

Table 1-2 Composition of 4-Vinylbenzoic Acid-Styrene (ST)-Divinylbenzene (DVB) Copolymer

COMPOUND	MASS(g)	MMOL	MOL%
4-vinylbenzoic acid	6.5	40	13.8
styrene	26	250	86.0
divinylbenzene	0.06	0.92	0.16

In 1972 Collman et al. [72JA1789], in an effort to prepare isolated rhodium and iridium species with open coordination sites, prepared resin-substituted triphenylphosphine on crosslinked polystyrene (Biobeads SX-2, 2% crosslinking). By using sequential bromination (Br_2 , FeBr_3), lithiation (BuLi, tetrahydrofuran (THF)), and treatment with $(\text{C}_6\text{H}_5)_2\text{PCl}$, the polystyrene resin contained 1.2 mmol of P/g polymer (DF= 12.6%). When this resin was treated with rhodium (I) or iridium (I) complexes, two $\text{P}(\text{C}_6\text{H}_5)_3$ were released per metal atom introduced into the polymer. The authors reported that "in these and similar cases, intermediate levels of coordination per metal atom in the polymer by resin-bound phosphine could not be achieved either

by varying the ratio of the starting complex to resin or the level of phosphine incorporated in the resin" [72JA1789]. Their efforts included the use of levels of phosphine substitution as low as 2% of the benzene rings with similar results being obtained. "Popcorn" polystyrene resin substituted at 10 mol% gave the same result. The authors concluded that there was sufficient mobility in the resin, especially when it was swollen with solvent, to allow individual phosphine units to migrate together. Efforts to use commercially available, more highly crosslinked resins were also unsuccessful in providing site isolation of the phosphine units.

The possibility of intramolecular cyclizations of diesters on copolystyrene-2% divinylbenzene was investigated. Crowley et al. [72MI1] attempted to perform a Dieckmann cyclization of a *tert*-butyl sebacyl resin ester, the formation of which is shown in Figure 1-3, using potassium alkoxide. The attempt yielded chiefly transesterification product, but a small yield of cyclic ketoesters was also formed.

Cyclization of the *tert*-butyl sebacyl resin ester occurred in two directions, yielding cleaved and retained ketoesters. The cleaved product was identified as 5 and the retained product as 6 after HBr cleavage in methylene chloride (CH_2Cl_2) (see Figure 1-4). None of the site isolated eight-membered ring product was reported.

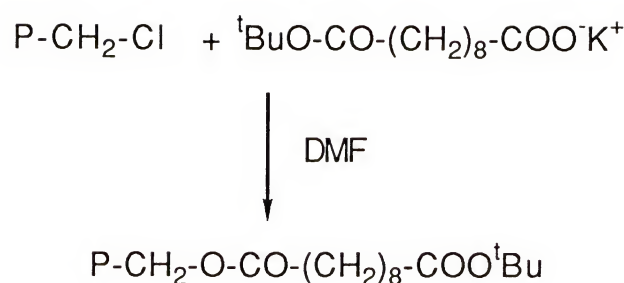


Figure 1-3 Formation of Polymer-bound Sebacyl Ester

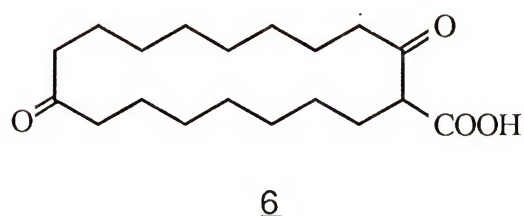
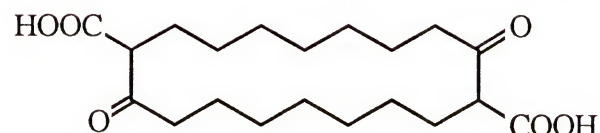


Figure 1-4 Products of the Attempted Cyclization of Polymer-bound Sebacyl Ester

After these disappointing results, the authors chose to prepare the resin bound ω -cyanopelargonyl thiol ester, since it would be more reactive toward cyclization and less labile to cleavage by Dieckmann conditions. The thiol resin ester was prepared by the reaction shown in Figure 1-5. With the hindered base, lithium bis-triethyldisilazide, cleavage of the thiol ester from the polymer was prevented. The cyclization product, obtained in 19% yield, was exclusively the diketodinitrile, $\underline{\mathcal{Z}}$, Figure 1-6.

Unreacted cyanothiol ester was cleaved from the resin after completion of the reaction in 75% yield. In stark contrast to the results of Kraus and Patchornik, the ester moieties evidently are not isolated from one another during reaction. Finally, the authors carried out detailed radiolabelling experiments to show that interpolymeric reactions were occurring.

The possibility that increasing the crosslinking might allow site isolation in the polymer was investigated [77JA625]. Polystyrene bound carboxylic acids were prepared by derivatizing commercially available polystyrenes. The polystyrenes were sequentially brominated ($\text{Br}_2/\text{Tl}(\text{OAc})_3/\text{CH}_2\text{Cl}_2$), lithiated (BuLi/THF) and carboxylated (CO_2 gas). Polystyrenes which could be produced by this method were the macroreticular 20% DVB-polystyrene and the "swellable" 1%, 2%, and 4% DVB-polystyrenes. But these methods failed with "swellable" 8% and 12% DVB-polystyrenes.

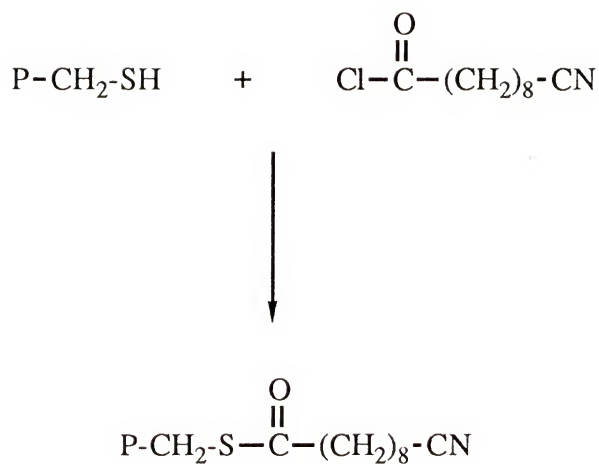
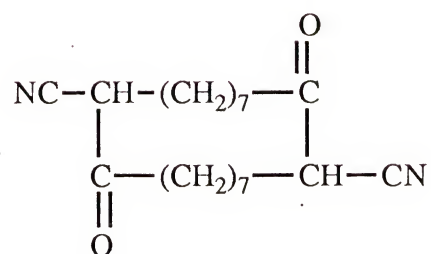


Figure 1-5 Formation of Polymer-bound ω -Cyanopelargonyl Thiol Ester



7

Figure 1-6 Product of Attempted Cyclization of Thiol Ester Using Lithium Bistriethyldisilazide

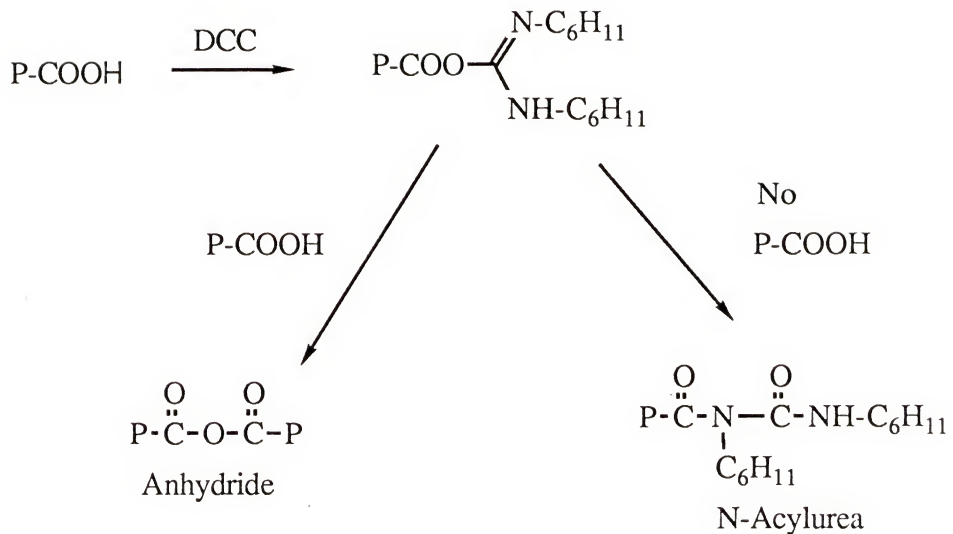


Figure 1-7 Reactions of Polymer-bound Carboxylic Acid with Dicyclohexylcarbodiimide (DCC)

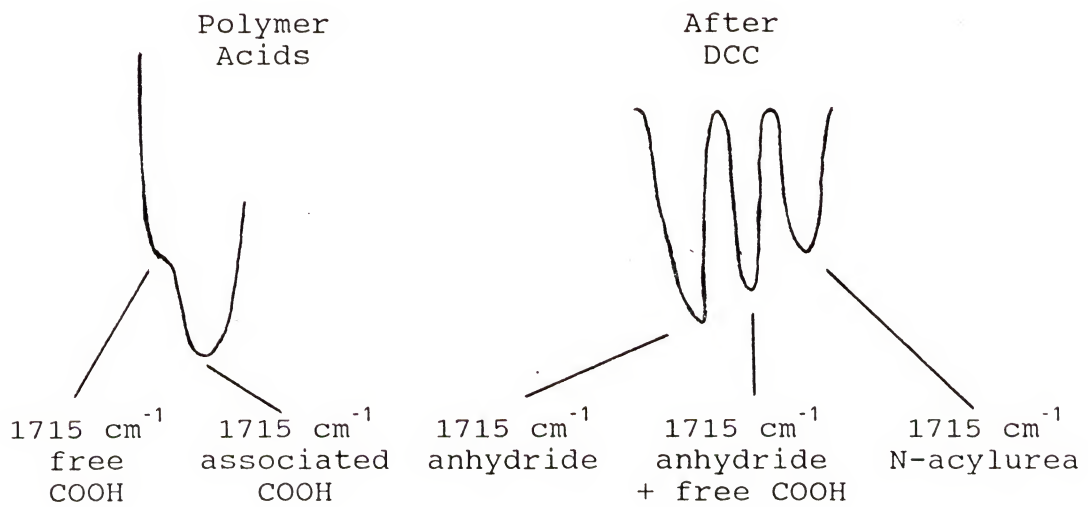


Figure 1-8 Spectra of the Carbonyl Region of a Carboxylated Polystyrene, before and after Reaction with DCC. The spectra pictured are for SX-2 (see Table 1-3) [77JA625]

The polystyrene bound carboxylic acids were then treated with excess dicyclohexylcarbodiimide (DCC) in methylene chloride at room temperature for 50 h. DCC reacts with a carboxyl group to produce an O-acylisourea intermediate. If the intermediate encounters another carboxyl group, then an anhydride and 1,3-dicyclohexylurea are formed. The O-acylisourea intermediate decomposes to a stable N-acylurea if it is not intercepted by another carboxylic acid (see Figure 1-7). The polymer samples were filtered, washed and dried, and then infrared spectra were taken. They are shown in Figure 1-8 below. The numerical values of the measurements are given in Table 1-3.

Table 1-3 Relative Intensities of Infrared Absorption Bands (KBr) for Various Carboxylated Polystyrenes, before and after Treatment with Dicyclohexylcarbodiimide (DCC) [77JA625]

SX1 = 1% crosslinked, "swellable" polystyrene					
SX2 = 2% crosslinked, "swellable" polystyrene					
SX4 = 4% crosslinked, "swellable" polystyrene					
SM2 = macroreticular 20% DVB-polystyrene					
	1715 cm^{-1} free COOH	1685 cm^{-1} associated COOH	1785 cm^{-1} anhydride	1720 cm^{-1} anhydride + free COOH	1660 cm^{-1} N- acylurea
SX1	0.7	1.0	1.0	0.9	0.9
SX2	0.7	1.0	1.0	0.9	0.8
SX4	0.7	1.0	1.0	3.7	3.7
SM2	0.8	1.0	1.0	1.5	1.6

While the above data do not give the concentrations of each species, they show that site-site interactions on more highly crosslinked polystyrene still remain significant, although they are less than those of lesser crosslinked polystyrene copolymers.

1.2.3 Efforts to Clarify the Claims about Site Isolation

The following viewpoint was expressed [77MI2]: "The question of site isolation in highly crosslinked polystyrene is an important one and one which has not been fully answered. Grubbs et al. [77JA4517] have presented compelling evidence that site isolation can be attained with a macroreticular 20% crosslinked polystyrene resin. In contrast, Scott et al. [77JA625] have reported data which suggest that site-site interaction is significant in this same copolymer. Unfortunately, in both studies a quantitative estimate of site-site interaction is not possible." In the study made by Scott et al., the solvent used was methylene chloride (a good swelling solvent), while Grubbs et al. used cyclohexane (a poor swelling solvent). In a study related to these results, Regan and Lee [77MI2] prepared a resin-bound cobalt complex using a 20% crosslinked macroreticular polystyryl-diphenylphosphine resin. When the resin was heated in excess *m*-xylene for 168 h at 70°C, only 35% of the cobalt remained as the 1:1 complex. When the resin was heated similarly in hexadecane, no formation of the 2:1 complex was indicated.

Thus, there are conditions under which even 20% crosslinked polystyrene has considerable mobility.

Mazur and Jayalekshmy helped to clarify some of the controversy about mobility in polymeric resins with their publication about the reactivity of polymer-bound *o*-benzyne [79JA677]. The authors performed experiments in which polymer-bound benzyne was generated, as shown in Figure 1-9. When the reactions were complete, the products of the benzyne intermediates were cleaved from the polymer and analyzed for identification. When the benzyne was generated using the reagent iodobenzene diacetate (IBD), products were formed which were likely derived from intrapolymeric reactions. In contrast, when the polymer-bound benzyne was generated using lead tetraacetate (LTA), only polymer-bound phenyl acetate was formed. By generating the benzyne using LTA in the presence of tetraphenylcyclopentadienone (TC), the expected Diels-Alder product was formed in high yield; thus the benzyne was formed with LTA but was not undergoing coupling.

By performing a series of time-delayed trapping experiments with TC, the authors established that polymer-bound benzyne has an extended lifetime and thus that the mobility of polymer-bound benzyne had been greatly reduced compared to benzyne in solution. The authors estimated that the frequency of encounter between the intermediates bound to a 2% crosslinked polystyrene resin lay between $2.6 \times 10^{-2} \text{ s}^{-1}$ and $1.1 \times 10^{-3} \text{ s}^{-1}$. This study showed that it was possible to have

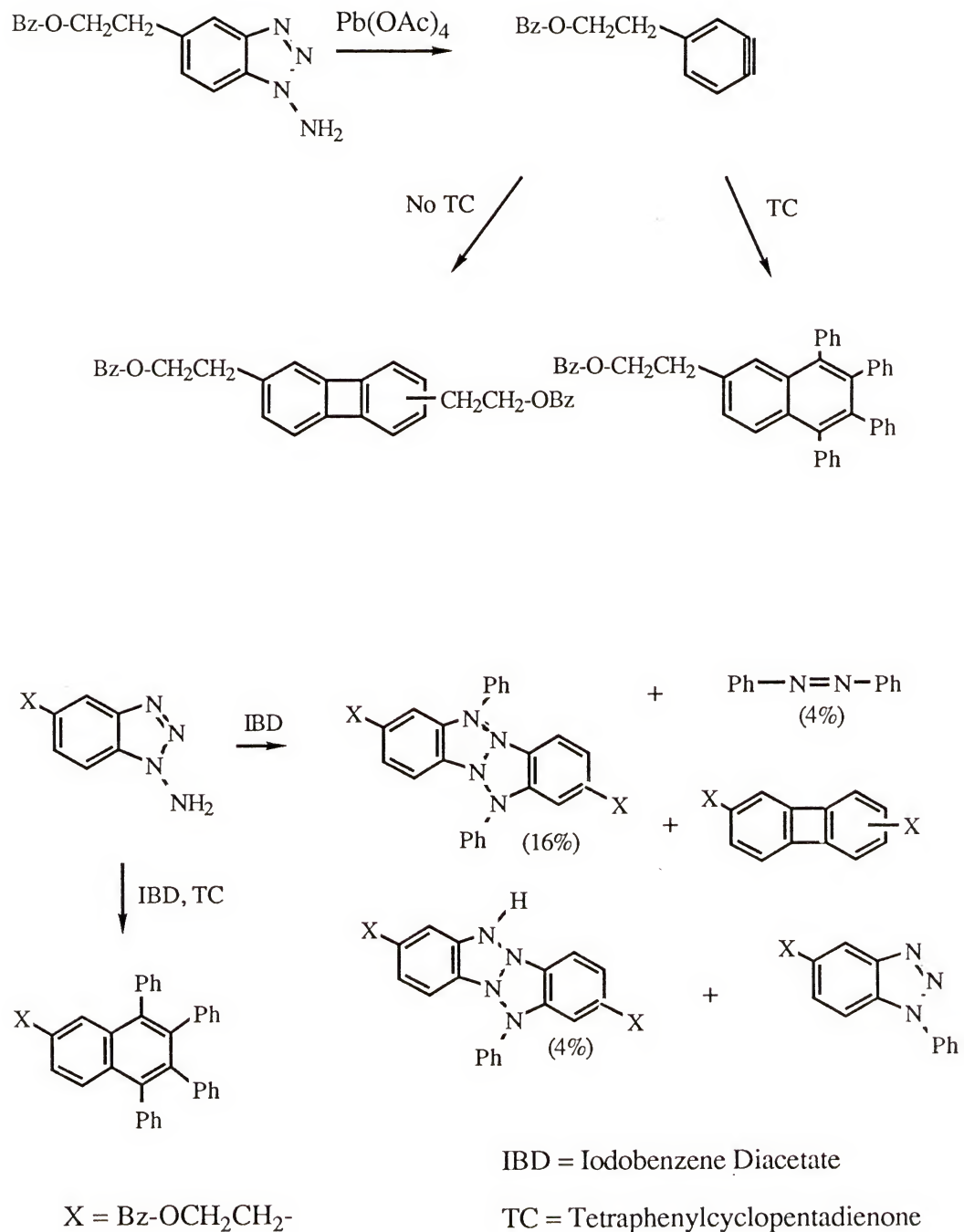


Figure 1-9 Reactions Forming and Consuming Monomeric Benzyne

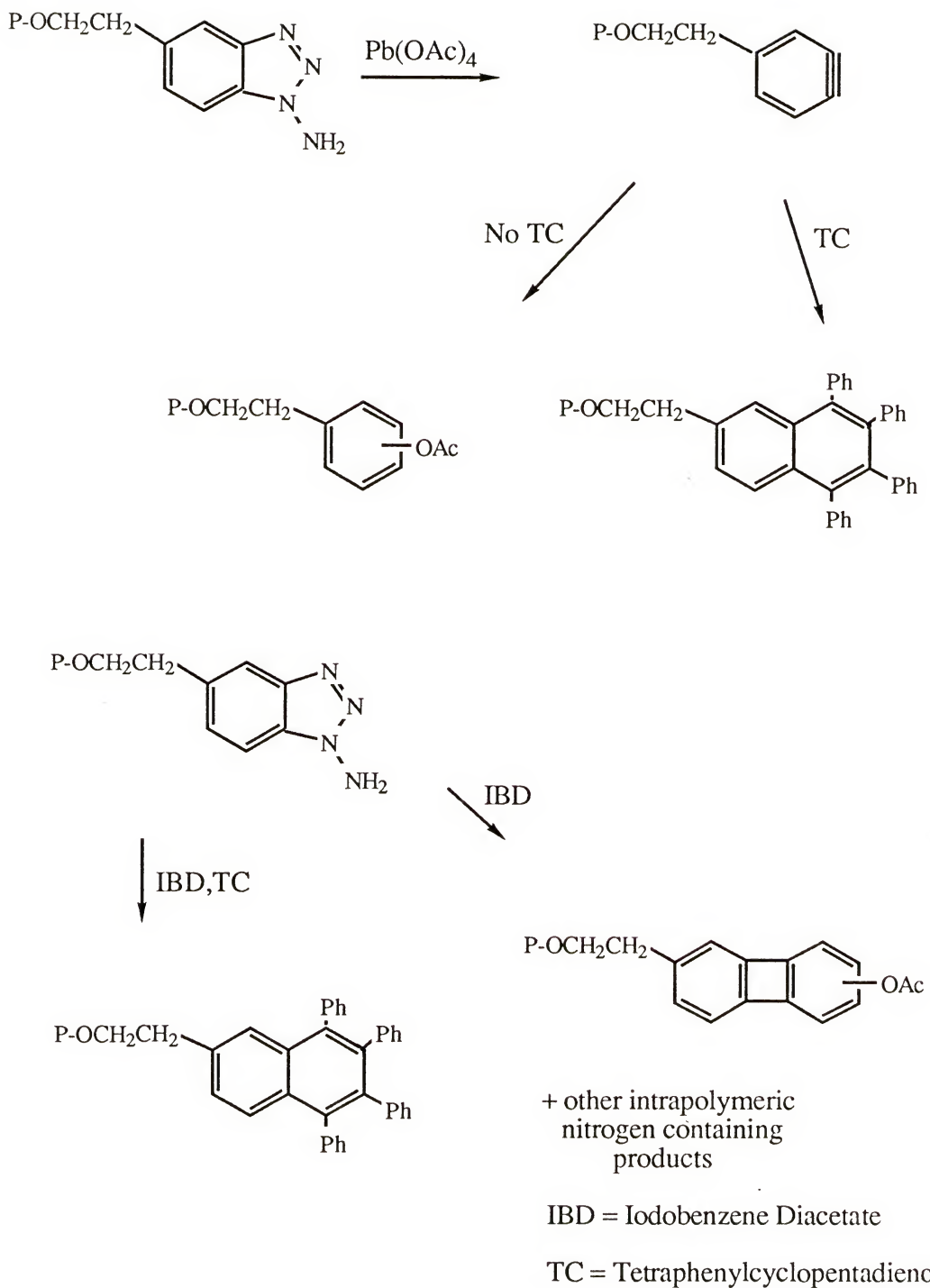


Figure 1-10 Reactions Forming and Consuming Polymer-bound Benzene

isolation of a species bound in polystyrene resins if reaction of the species proceeds faster than the rate of encounter between species within the polymer.

In 1981 Ford and Chang [81JOC5364] reported the generation and trapping of ester enolates at room temperature in high yields by using 10%-20% crosslinked polystyrenes and degrees of functionalization as high as 0.67 mmol/g (DF = 7.2%). Both microporous and macroporous polystyrenes were prepared and investigated. The starting material for all experiments was a copolymer of styrene and chloromethylstyrene (60/40 meta/para) crosslinked with divinylbenzene, which was prepared by suspension techniques in their laboratory. The chloromethyl groups were esterified by reaction with potassium phenyl propanoate. After a method for complete esterification was developed, some chloromethyl polymers were allowed to react for shorter times with potassium phenyl propanoate to afford partially esterified polymers which still contained residual chloromethyl groups to achieve lower loadings on polymers with otherwise the same properties. Ester enolates were formed at room temperature and consumed by quickly adding an electrophile with vigorous stirring, usually within one minute. The authors reported several conclusions from their experiments: "(1) With 2% crosslinked gel (microporous) polymer and with 20% crosslinked macroporous polymer the acylation yield decreases and the self-condensation yield increases as the concentration of ester bound to the polymer

increases.... (2) Increasing the crosslinking level of the gel polymer from 2% to 6% or of the macroporous polymer from 6% to 20% increases the acylation yield and decreases the self-condensation yield. (3) No self-condensation is detected with the 20% crosslinked macroporous polymer at an ester concentration of 0.55 mmol/g of polymer, and only 17% self-condensation occurs at 1.08 mmol of ester/g of polymer. (4) In all experiments with fully esterified polymers 33-44% of the polymer-bound ester failed to react" [81JOC5364].

The last two studies mentioned show that sites in polystyrene have less mobility than species in solution, but that most species bound to polymers will, given time, migrate and interact within the polymer. Lacking from the literature are credible studies which relate the amount of mobility to the degree of crosslinking.

An attempt at quantifying the relationship between mobility and degree of crosslinking was made by Wulff and Schulze [78AG(E)537]. These authors reported the preparation of polymers containing bound benzylthiol with both random and ordered distributions. Using the monomers bis(p-vinylbenzyl) disulfide and p-vinylbenzyl thioacetate, three series of polymers were prepared having as far as possible comparable polymeric properties and containing the same loadings of thiol groups. The compositions of the polymers are shown in Table 1-4.

Both the random and ordered copolymers were allowed to react with NaBH_4 and AlCl_3 in diglyme to reduce the S-S bonds and the thioacetate groups to produce polymers containing

Table 1-4 Characteristics of Random (R) and Ordered (NR) Polymers Containing Bound Benzylthiol Moieties

Polymer		Crosslinking		mmol Sulfur/g polymer	
NR	R	NR	R	NR	R
A1	A2	1%	-	1.62	1.30
B1	B2	40%	37%	1.36	1.28
C1	C2	45%	45%	0.154	0.15

ordered and random benzylthiol moieties, respectively. These polymers were then reacted with iodine in methanol to cause formation of S-S bonds. The amount of iodine consumed was quantified in order to determine the amount of S-S bond formation. The percentages of -SH bonds that were reduced and then reoxidized are shown in Table 1-5.

Table 1-5 Reduction and Reoxidation Yields of Polymer-bound Benzylthiol Polymers

Polymer Sample		%SH Groups		Degree of Reoxidation	
NR	R	NR	R	NR	R
A1	A2	97%	97%	99%	69%
B1	B2	68%	96%	98%	33%
C1	C2	95%	96%	95%	<5%

The results for polymers C strongly suggested that site isolation could be achieved with low loadings (approximately 1%) on polymers that are crosslinked at ca. 40%. But lacking from this study was an independent means of assessing the formation of S-S bonds or unreacted -SH bonds.

Interestingly, in this laboratory V.L. King, working with Dr. James A. Deyrup, developed reasons to question the results of Wulff and Schulze. Deyrup and King developed methods for the synthesis and analysis of thiols on macroporous polymers. They developed "a range of deprotection reactions along with reliable and convenient methods for directly determining thiol content" [84MI1]. They found that the analytical methods used by Wulff and Schulze gave erroneous estimates of thiol content in macroporous polymers, and thus the results of Wulff and Schulze were unreliable.

Thus from a review of the literature it is possible to see that there is still ambiguity in the understanding of mobility of groups in polystyrene. A systematic, quantitative study of the isolation of groups in polystyrene as a function of loading and crosslinking is needed.

1.3 Characteristics of Crosslinked Polymers

1.3.1 Difficulties in Studying Crosslinked Polymers

The characterization of crosslinked polymer networks is among the more difficult tasks of polymer analysis and analytical chemistry. In contrast to linear polymers,

crosslinked polymers have essentially infinite molecular weights. As a result of the crosslinked nature of these polymers, they are insoluble in all solvents, and thus many analytical techniques which depend on the solubilization of the substance for analysis cannot be used on crosslinked polymers. In addition, the analytical problem of crosslinked polymers is not only the determination of connections or sequences of monomers as it is in linear polymers, but it is also the determination of spatial relations among the constituents of the polymer.

Highly crosslinked polymers are amorphous solids which obviate the use of fractionation, solution nuclear magnetic resonance (NMR) and x-ray analysis. Among the limited techniques that can be used are infrared (IR)/Raman, visible (VIS), and ultraviolet (UV) spectroscopies and solid-state NMR. For aromatic polymers, such as polystyrenes, the use of UV spectroscopy is not possible because of the intense absorption of the UV radiation by the aromatic rings. Visible light spectroscopic characterization is possible with many polymers, but many functional groups do not absorb visible light. Those substances which do absorb visible light tend to be large molecules (or ions), which might not easily penetrate a crosslinked network.

IR and Raman spectroscopies are very important in the study of polymers because of the characteristic absorptions of organic functional groups. These techniques have become even

more important recently with the development of Fourier transform IR (FTIR) [83MI1]. The effective sensitivity of FTIR is 80-200 times higher than that of a standard dispersive instrument, depending on resolution [85MI1]. Furthermore the importance of IR analysis should increase as computerized data-processing software, for techniques such as difference spectroscopy (spectral subtraction), factor analysis, spectral deconvolution and least squares curve fitting, becomes more available. For further reading many sources of information about infrared analysis and computing techniques are available [66MI1, 66MI2, 75MI1, 80MI2, 83MI1, 84MI2, 87MI1, 87MI2].

1.3.2 Residual Vinyl Groups

As the polymerization of a styrene/divinylbenzene(St/DVB) mixtures proceeds, the viscosity of the mixture increases. In lightly crosslinked polymer mixtures, it is possible that the polystyrene chains remain well-solvated and the increase in viscosity is relatively small; however, for more highly crosslinked mixtures, the increase in viscosity can be very large, and the mobility of the aromatic groups can thus diminish greatly before the polymerization is complete. The lack of mobility of the growing chains increasingly results in the inability of the radical terminus and available vinyl groups of DVB to encounter one another. The radical termini increasingly must undergo disproportionation reactions and an increasing fraction of the initial vinyl groups remain

unreacted as the initial DVB content of the monomer mixture increases. And as the initial DVB content increases, the increasing fraction of unincorporated vinyl groups can be seen by IR and NMR spectroscopy [89MI1].

1.3.3 Polymeric Heterogeneity

The distribution of the crosslinks in polystyrene is not uniform [86MI3]. In fact, in the same polymer sample there are regions of high crosslinking density, regions of low crosslinking density and probably every variation in between. One reason for this is that the monomers in the initial mixture do not incorporate into the growing polymer chains at the same rate. The reactivity ratios of *p*-divinylbenzene (*p*-DVB) are ($r_1=0.260$, $r_2=1.180$) and of *m*-divinylbenzene are ($r_1=0.580$, $r_2=0.580$) [80MI3]. For *p*-DVB these ratios imply that styrene has about 4 times greater tendency to react with *p*-DVB than with itself while *p*-DVB has a slightly greater tendency to react with itself than with styrene. The result of this is that the polymer that is formed early in the sample will have higher than average incorporation of *p*-DVB and therefore higher crosslinking density. And since the *p*-DVB is consumed faster than the styrene, polymer that is formed late in the sample will incorporate less than average *p*-DVB and therefore exhibit lower crosslinking density.

The problem of increasing viscosity as the polymerization proceeds will result in more chain transfer reactions and

therefore in fewer crosslinks forming late in the polymerization, which implies that the late-forming polymer chains have even fewer crosslinks than would be predicted from consideration of the reactivity ratios alone.

Any amine monomer that is incorporated into this early formed polymer will be less accessible and have less than average mobility. Amine monomers that are incorporated into the late formed polymer chains will be more accessible and have greater than average mobility. Thus one may expect that a range of accessibilities and mobilities exists for the amines in such polymers.

1.3.4 Microporous and Macroporous Polymers

Typical polystyrene resins with a few mol% of divinylbenzene crosslinking agent swell substantially in good solvents, i.e., organic liquids of similar characteristics such as toluene, xylenes, etc. When the solvents are removed and the polymer is examined by electron microscopy, the polymer is found to be lacking any pores. This results because of the extensive mobility of the polystyrene chains to fold upon themselves to fill vacancies formed as the solvent is removed.

Polystyrene resins with more substantial crosslinking (typically greater than 20 mol%) are not able to collapse once the solvent present during the polymerization is removed. A means of obtaining an even more porous structure is to carry

out the polymerization in an inert solvent which is a good solvent for the comonomers and a poor solvent for the polymer chains. The precipitation of the polymer chains as they form causes the formation of greater porosity. Examination of these polymers reveals that the resins maintain their pore structure even in the absence of solvent. As a result, macroporous polymers have very large amounts of surface area per unit mass (e.g., $300 \text{ m}^2/\text{g}$ of polymer is not uncommon). Even solvents (such as methanol, water, and hexane), which normally have little affinity for aromatic hydrocarbon substances (such as polystyrene), are able to fill the voids and have access to most of the polymeric material.

1.4 Proposal of Research

The problems of site isolation found with the low cross-linked polystyrene resins and the problems of accessibility in more highly crosslinked resins mentioned in the introduction to this chapter have led to the suggestion that macroporous polymers might be useful for site isolation while maintaining good site accessibility. It was proposed for this research project that macroporous polymers be prepared which would allow the examination of this hypothesis for polymers of different degrees of crosslinking. Polymers which contain primary amine functions were chosen since it would be possible to examine site mobility by measuring urea formation from a coupling reaction and by examining hydrogen bonding that

occurs between acetamides that result from the acetylation of the amine functional groups in the polymers. An added benefit of these two approaches to the examination of site isolation (or mobility) is that the accessibility of the amine sites in the macroporous polymers could be examined by the same analytical technique, infrared spectroscopy.

Furthermore, it was decided that resins formed from comonomer solutions containing 20, 40, 60 and 80 mol% of the crosslinking agent divinylbenzene would be examined. For comparison the amine functional groups would be introduced into the resin with both random and non-random distributions for the examination of site isolation.

This dissertation reports on the preparation of polystyrene resins loaded with carbamate esters and silanediamines and their conversion into polystyrene resins containing amine functions with random and non-random distributions. The characteristics of the resins will then be examined by analysis of: 1) a reaction which couples the amine groups to form urea, 2) hydrogen bonding of acetamides formed from the amine groups and 3) the amine catalyzed aldol condensation of phenylacetaldehyde.

CHAPTER 2 SYNTHESIS OF MONOMERS AND POLYMERS

2.1 Introduction

This research depended on the comparison of polymers in which amine groups were placed in the polymer randomly and with those placed in an ordered manner. In order to incorporate a benzylamine derivative into a polystyrene matrix, the benzylamine derivative must be in the form of a polymerizable vinyl analog. Derivatives of 4-vinylbenzylamine were prepared that would allow the preparation of polymers in which the amine was distributed in two ways: 1) sites would be created in which two amine functional groups are placed in close proximity (these are called bifunctional amine sites), and 2) the amines would be distributed randomly throughout the polymer. The bifunctional sites were created by binding two amine monomers to a spacer group and then polymerizing the product.

The monomers were combined with styrene and commercial divinylbenzene-reagent using AIBN as the initiator. The divinylbenzene-reagent was 80 mol% divinylbenzene and 19 mol% ethylvinylbenzene according to the company analysis. The divinylbenzene fraction was a mixture of meta and para isomers

in the ratio m/p=2.2. The polymerization were carried out in anhydrous DMSO solvent at 100°C under an N₂ atmosphere for 24 hours. The monomer mixtures were prepared such that for a given loading of a functional group, the divinylbenzene constituted 20, 40, 60 or 80 mol% of the initial monomer composition. Polymers were prepared at the above degrees of crosslinking and at loadings such that the final amine concentration would be 3.0, 1.5, 0.5 and 0.1 mol% of the polymerized monomer moieties.

2.2 Preparation of Ordered Amine Polymers

2.2.1 Silanediamines of Pyrrolidine

Early in this research it was desired that the amines be secondary amines since secondary amines readily form enamines with aldehydes and ketones and are excellent catalysts for the aldol condensations of aldehydes and ketones [63JA209]. Furthermore it was desired that the amine be a cyclic amine rather than a primary amine so that there would be fewer degrees of freedom of movement for the amine (thus, movement would be more nearly restricted to movement with the polymer chain to which it was attached). And it was intended that the amine polymers that were created in this laboratory would be tested for the catalysis of aldol reactions. In order to investigate the preparation of polymers which contained secondary amine placed in ordered sites, it was necessary to

investigate the preparation of silanediamines of secondary amines.

Silanediamines are a useful class of compounds for the introduction of amines into a polystyrene matrix since they are easily cleaved with acid [60MI1]. In fact this property presents a difficulty in their purification since washing an organic phase with aqueous acid would have otherwise been an excellent means of removing the excess amine that was used in the synthesis of the silanediamines. But the ease of their cleavage with acid indicated that the polymers that would be loaded with silanediamines would be readily converted to the ordered bifunctional amine polymers under mild conditions.

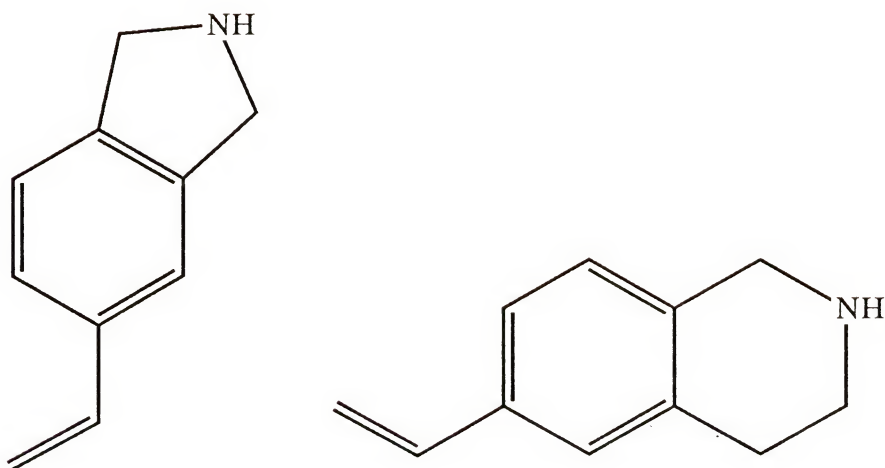
The results of the investigations of silanediamines formed from reactions with pyrrolidine are shown in Table 2-1 along with some characteristic measures of the stability of the silanediamines. As the bulkiness of the two hydrocarbon groups attached to silicon increases, the stability of the silanediamine increases. Even the compound *tert*-butylchlorosilylpyrrolidine 13 which has the good leaving group, chloride, can survive chromatography on neutral alumina. But because a practical method for the preparation of the vinyl analog of the compound isoindoline 8 or the compound 1,2,3,4-tetrahydroisoquinoline 9 (see Figure 2-1) could not be found in the course of this research, synthesis of the silanediamines of secondary amines was abandoned.

Table 2-1 Silanediamines of Pyrrolidine

$\text{R}^1\text{R}^2\text{SiCl}_2 + \text{HN} \begin{array}{c} \text{C}_5\text{H}_9 \\ \\ \text{N} \end{array} \longrightarrow \text{R}^1\text{R}^2\text{Si}(\text{N} \begin{array}{c} \text{C}_5\text{H}_9 \\ \\ \text{N} \end{array})_2 \text{ or } \text{R}^1\text{R}^2\text{Si} \begin{array}{c} \text{N} \begin{array}{c} \text{C}_5\text{H}_9 \\ \\ \text{N} \end{array} \\ \\ \text{Cl} \end{array}$				
		I	II	
R^1, R^2	REACTION CONDN.	PRODUCT	YIELD	HYDROLYSIS CONDITIONS
Ph, Ph	A	I, <u>10</u>	76%	C
$^i\text{Pr}, ^i\text{Pr}$	A	I, <u>11</u>	94%	C
$^t\text{Bu}, \text{Ph}$	A	I, <u>10</u>	87%	C
$^t\text{Bu}, ^t\text{Bu}$	A	II, <u>13</u>	95%	C

A = Excess Pyrrolidine, *n*-Butyllithium

C = Wash with Aqueous Acid



8

9

Figure 2-1 5-Vinylisoindoline 8 and 6-Vinyl-1,2,3,4-tetrahydroisoquinoline 9

2.2.2 Preparation of 4-Vinylbenzylamine

It was understood that the vinyl analog of the primary amine benzylamine, i.e. 4-vinylbenzylamine 16, could be and was prepared according to the scheme in Figure 2-2.

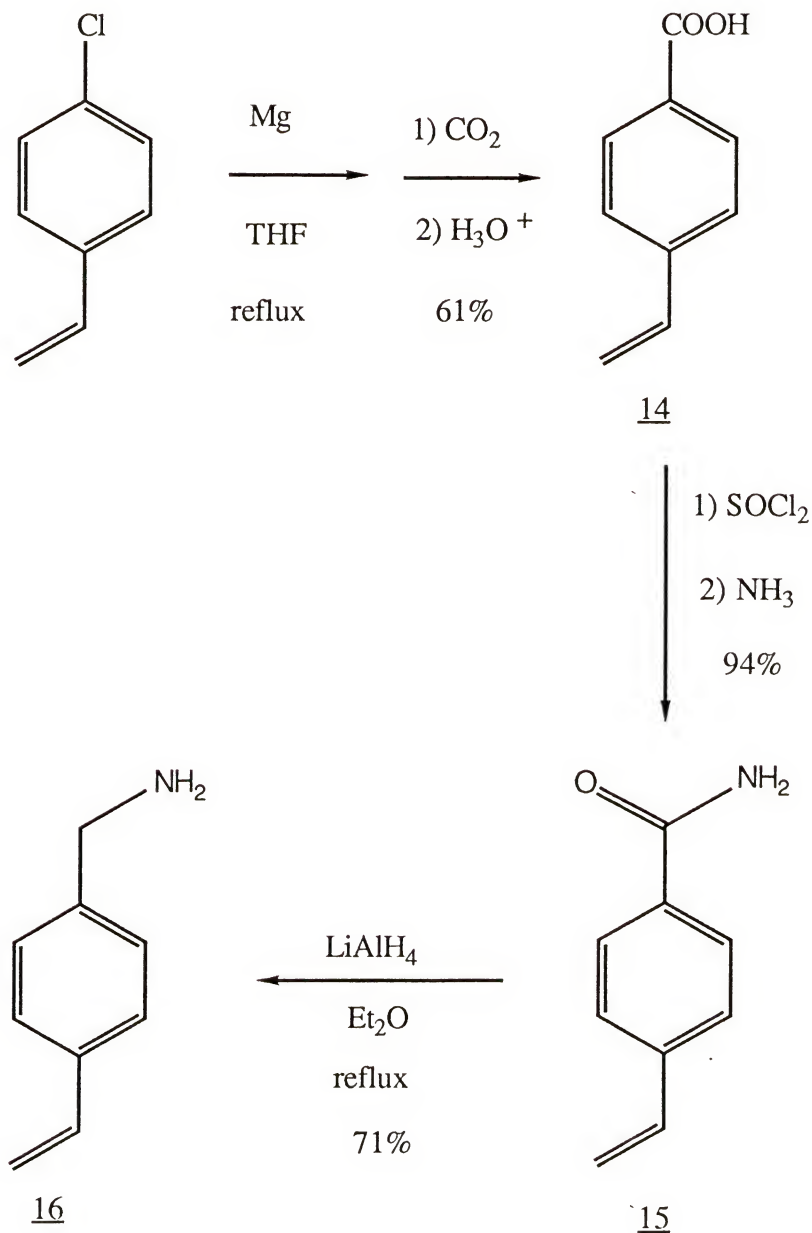


Figure 2-2 Preparation of 4-vinylbenzylamine 16

Interestingly, when THF was substituted for diethyl ether in the LiAlH_4 reduction step in Figure 2-2, not only was the amide function reduced to the amine but a significant fraction of the vinyl groups is also reduced. For the uses that were intended for the silanediamine the reduction of the vinyl group was an intolerable situation, and all future reductions involved the use of diethyl ether, although the reaction was much more easily performed with THF.

Table 2-2 Silanediamines of Benzylamine

$\text{R}^1\text{R}^2\text{SiX}_2 + 2 \text{ NH}_2 \text{--} \text{C}_6\text{H}_4\text{--CH}_2 \longrightarrow \text{R}^1\text{R}^2\text{Si}(\text{NH} \text{--} \text{C}_6\text{H}_4\text{--CH}_2)_2$				
R1, R2	X	REACTION CONDN.	PRODUCT, YIELD	HYDROLYSIS CONDITIONS
Ph, Ph	Cl	A	<u>17</u> , 45%	D, E, F
ⁱ Pr, ⁱ Pr	Cl	A	<u>18</u> , 99%	D, E, F
^t Bu, Ph	Cl	A, 4 Days	<u>19</u> , 75%	E, F
^t Bu, ^t Bu	Cl	B	<u>20</u> , 82%	F
^t Bu, ^t Bu	OTf	C	<u>20</u> , 89%	F

A = Excess Amine

B = Slight Excess Amine, 4 Days

C = 1.1 eq. Amine, Excess Triethylamine

D = Exposure to Atmosphere

E = Chromatography on Neutral Alumina (10% H_2O)

F = Wash with Aqueous Acid

2.2.3 Model Silanediamines of Benzylamine

Because of the choice of 4-vinylbenzylamine 16 for this research, it was necessary to investigate the preparation, purification and characterization of some silanediamines of benzylamine so that a stable vinyl analog could be prepared for incorporation into polystyrene. The results of the investigation are shown in Table 2-2.

As the size of the hydrocarbon substituents on silicon increases, the stability of the silanediamine also increases. In fact, the compound *1,1-di-tert-butyl-N,N'-dibenzylsilanedianime* 20 (see Table 2-2) has remained a clear, colorless liquid for over six months although it has been stored in a round bottom flask with just a rubber septum in Florida! The compound *1-tert-butyl-1-phenyl-N,N'-dibenzylsilanedianime* 19 lasted no more than two weeks under similar conditions without substantial color change, presumably from the oxidation of the hydrolyzed amine.

2.2.4 Silanedianime Monomers

Two starting materials were used for the synthesis of *1,1-di-tert-butyl-N,N'-bis(benzyl)silanedianime* 20, see Table 2-2. In order to synthesize the silanedianime from *1,1-di-tert-butylchlorosilane* it was necessary to react the dichlorosilane with the lithium amide of benzylamine in tetrahydrofuran for four days at room temperature. Such harsh conditions would have almost certainly failed to produce *1,1-*

di-*tert*-butyl-*N,N'*-bis(4-vinylbenzyl)silanediamine 21 from 4-vinylbenzylamine 16 because of the probable anionic polymerization of the vinyl group. So attempts were made to prepare the compounds 1,1-diphenyl-*N,N'*-bis(4-vinylbenzyl)silanediamine and 1-*tert*-butyl-1-phenyl-*N,N'*-bis(4-vinylbenzyl)silanediamine using triethylamine as the base. But both compounds decomposed too easily for use in the preparation of silanediamine-loaded polymers. A reference to the use of di-*tert*-butylsilyl ditriflate for the silylation of functional groups under extremely mild conditions [81TL3455, 82TL4871] provided the solution.

Indeed, with the use of di-*tert*-butylsilyl ditriflate it was possible to form 1,1-di-*tert*-butyl-*N,N'*-bis(4-vinylbenzyl)silanediamine 21 in very good yield using merely triethylamine as the base. The silanediamine was purified by column chromatography on neutral alumina and used as such for the preparation of silanediamine polymers. After two months in the laboratory freezer the viscous liquid crystallized and was subsequently recrystallized in petroleum ether.

2.2.5 Preparation of Silanediamine-loaded Polymers and the Removal of the Di-*tert*-butylsilyl Protecting Group

Polymers containing silanediamines were obtained by polymerizing monomer 21 with styrene and divinylbenzene. Polymers containing bifunctional amine sites were then prepared by treating the silanediamine-loaded polymers with

glacial acetic acid in tetrahydrofuran; the reaction is shown in Figure 2-3.

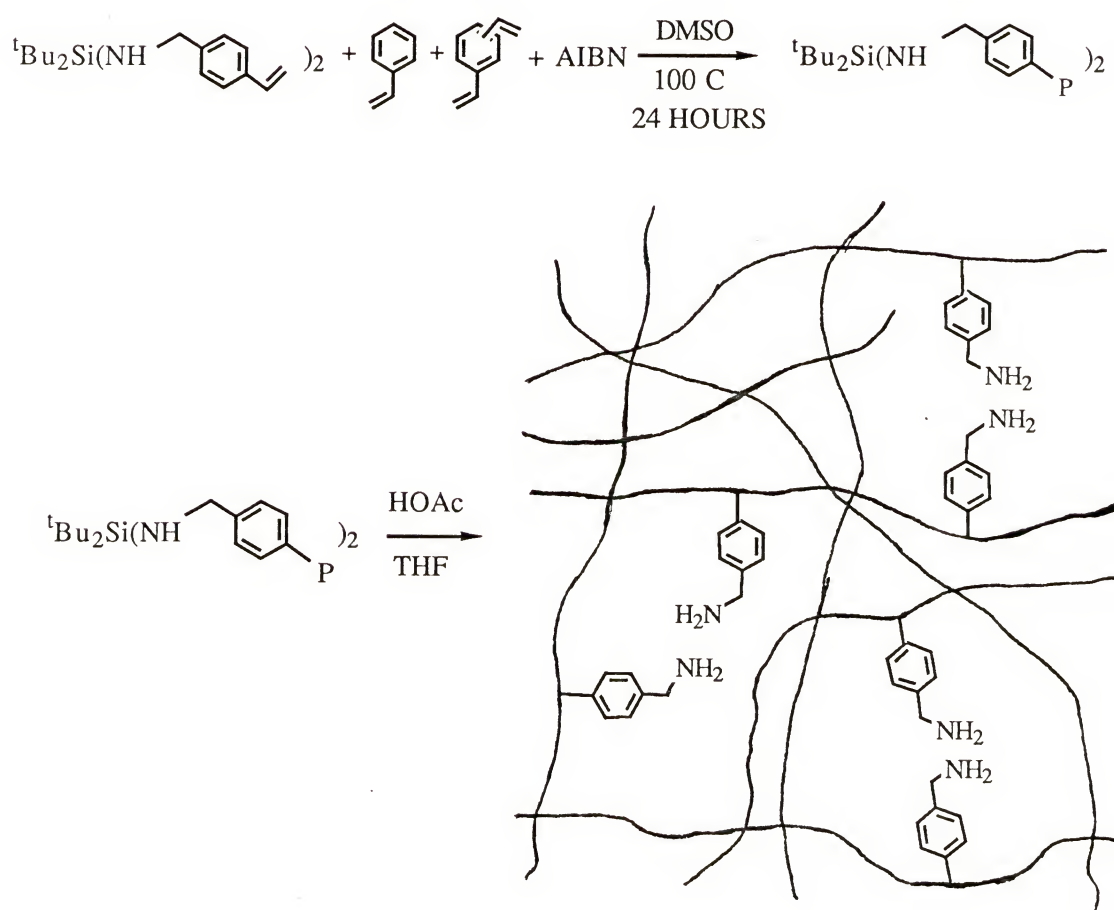


Figure 2-3 Preparation of Bifunctional Amine Sites in Crosslinked Polystyrene

2.3 Preparation of Random Amine Polymers

2.3.1 Selection and Preparation of a Monomer for the Preparation of the Random Amine Prepolymer

For comparison with the ordered polymers, it was necessary to prepare polymers with randomly distributed amine groups. The average spacing in randomly distributed groups is discussed in the next chapter, but at low loadings it is greater than that expected of bifunctional amine sites. And the spacing of the randomly distributed groups increases as the loading decreases.

It might have been possible to polymerize 4-vinylbenzyl-amine with styrene and divinylbenzene, but determination of the loading of the amine group in the polymer after the polymerization was complete could have been a serious problem. It was decided that the polymerization of the O-(*tert*-buty)-N-(4-vinylbenzyl)carbamate 22 would allow the introduction of an amine precursor whose loading could be determined by infrared analysis of the polymer sample. The preparation of the carbamate 22 monomer is shown in Figure 2-4.

A random distribution is expected because the carbamate monomer 22 should not show any greater tendency to associate with itself than with either styrene or divinylbenzene. In fact, when the IR spectra of the samples of carbamate polymers were taken, even very little hydrogen bonding (i.e., evidence of association) was found by IR to occur between the *tert*-butoxycarbonyl (BOC) groups. Furthermore because the

polymerization were carried out in the polar solvent DMSO, the carbamate monomer should be well solvated which should further insure a random distribution.

2.3.2 Removal of the *tert*-Butoxycarbonyl (BOC) Protecting Group

The carbamate polymers were then treated with hydrogen chloride generated in benzene to give the randomly distributed amine polymers as shown in Figure 2-5. The polymer samples were then analyzed by IR spectroscopy to determine that all of the BOC groups had been removed.

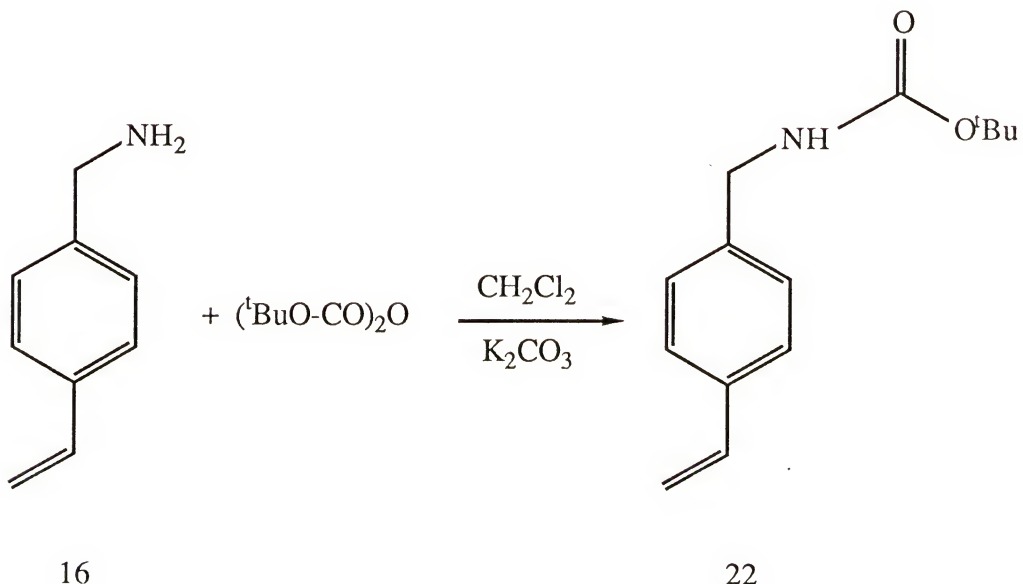


Figure 2-4 Preparation of O-(*tert*-butyl)-N-(4-vinylbenzyl)carbamate 22

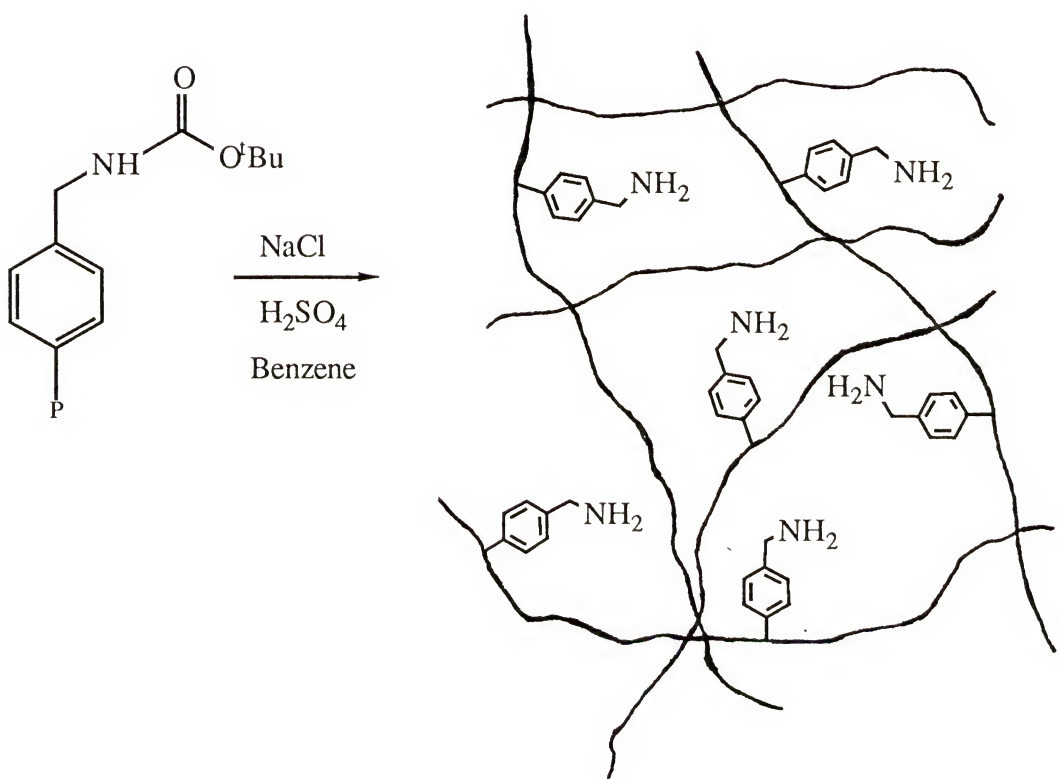
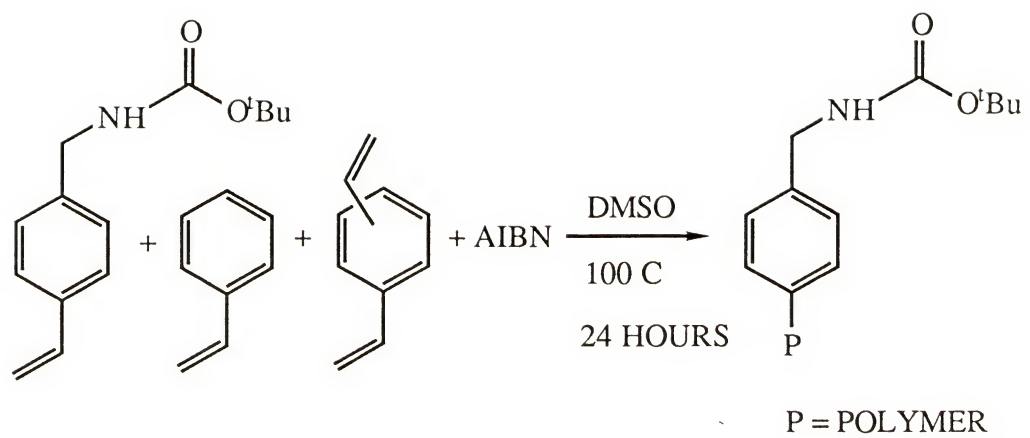


Figure 2-5 Preparation of Randomly Distributed Amine Copolymers

2.4 Preparation of N-(4-Vinylbenzyl)acetamide Calibration Curves for the Spectroscopic Quantification of Amine Groups in Polymers

2.4.1 Justification for the Use of Infrared Spectroscopy

The determination of the amount of nitrogen incorporated into the ordered polymers was a serious difficulty. Analysis by carbon, hydrogen and nitrogen (CHN) combustion has an uncertainty of $\pm 0.4\%$; however, polymers loaded at 3 mol% with bound benzylamine have a nitrogen content of about 0.4% by mass. Thus the exclusive use of CHN analysis would have left large uncertainties in this determination. Another method was needed for the determination of amine nitrogen at lower loadings. The method used was to treat the amine polymers acetylimidazole and pyridine. The amount of acetamide which formed was determined by infrared spectroscopy but the method required the preparation of a calibration curve for which concentration of amine could be determined by measuring the IR absorbance of the amide group. Another use of the acetamide calibration curve was that it could be used to calibrate the concentrations of other carbonyl compounds (i.e., ureas and urethanes) once the relative molar absorbtivities of the carbonyl groups of amides, ureas and urethanes were determined.

2.4.2 Preparation of 4-Vinylbenzylacetamide and its Polymers for Calibration Curves

A mixture of the monomer 16 and its polymer was treated with acetic anhydride and pyridine. The amine starting

material was not purified because the product of the reaction was easier to purify from the polymeric materials than was the monomeric 4-vinylbenzylamine 16. The product of the reaction, N-(4-vinylbenzyl)acetamide 23, was purified by extraction and by chromatography. Monomer 23 was then polymerized with styrene and divinylbenzene in DMSO to produce samples for the calibration curves for 20X (20 mol% DVB) and 80X (80 mol% DVB) polystyrene in which the ratio of the areas of the acetamide peak over the aromatic peak was plotted versus its concentration in the starting mixture. The reaction is shown in Figure 2-6. The calibration curves are shown in Figures 2-7 and 2-8.

2.4.3 Analysis of the Calibration Data

The data used for the preparation of the 20X and 80X calibration curves are presented in Tables 2-3 and 2-5. The least squares analysis of the calibration data for the 20X and 80X calibration curves is presented in Tables 2-4 and 2-6, respectively. The calculations and the statistical analysis were made using Lotus 1-2-3 software, copyright 1985, release 2.

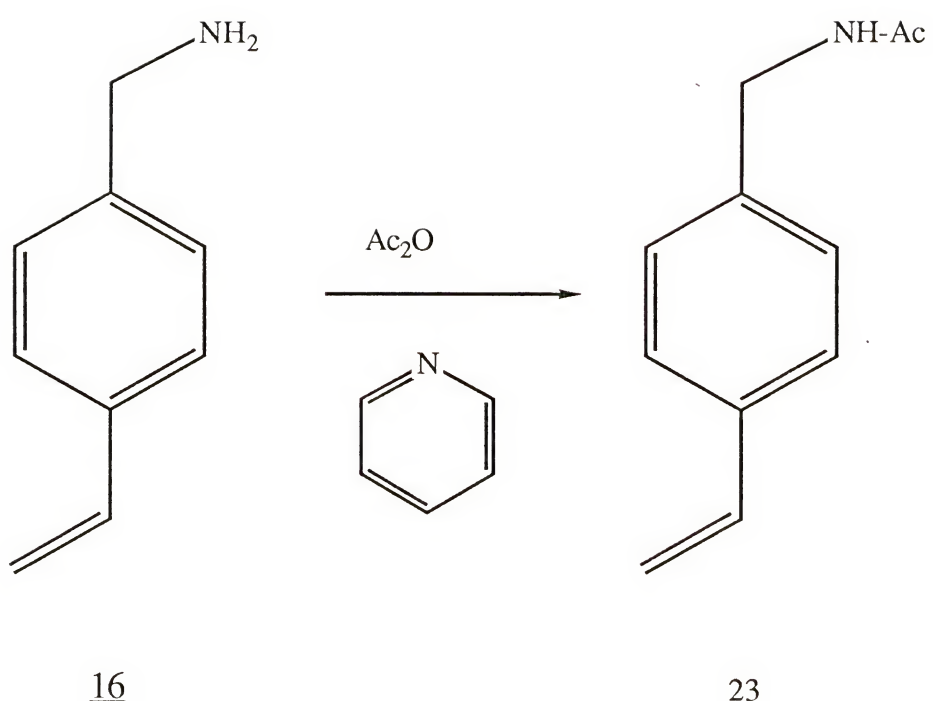


Figure 2-6 Preparation of $\text{N}-(4\text{-Vinylbenzyl})\text{acetamide}$ 23

Table 2-3 Calibration Curve Data of N-(4-Vinylbenzyl)acetamide ²³ versus its Concentration in 20X Comonomer Solutions

SAMPLE	CONCN MOL% (Based on the Masses of the Comonomers)	RATIO OF AREAS
		<u>AMIDE</u> <u>AROMATIC</u>
I40-A	0.506	0.1261
I40-F	0.966	0.2517
I39-E	1.52	0.4222
I41-A	1.92	0.5332
I41-A	1.93	0.5039
I39-D	2.02	0.5386
I39-C	2.44	0.6935
I39-B	2.79	0.7703
I39-A	3.26	1.016
I40-B	3.31	0.9242
I40-B	3.31	0.8956
I38-F	3.71	1.168
I41-B	3.76	1.005
I38-E	4.16	1.209
I40-E	4.53	1.410
I40-E	4.53	1.266
I41-C	4.54	1.222
I41-C	4.54	1.217
I38-D	4.56	1.493
I38-C	5.09	1.629
I40-D	5.54	1.799
I40-D	5.54	1.740
I38-B	5.54	1.811
I38-A	6.02	1.903
I40-C	6.46	2.026
I40-C	6.46	2.034
I37-F	6.51	2.055
I37-E	6.90	2.354
I37-D	7.33	2.462

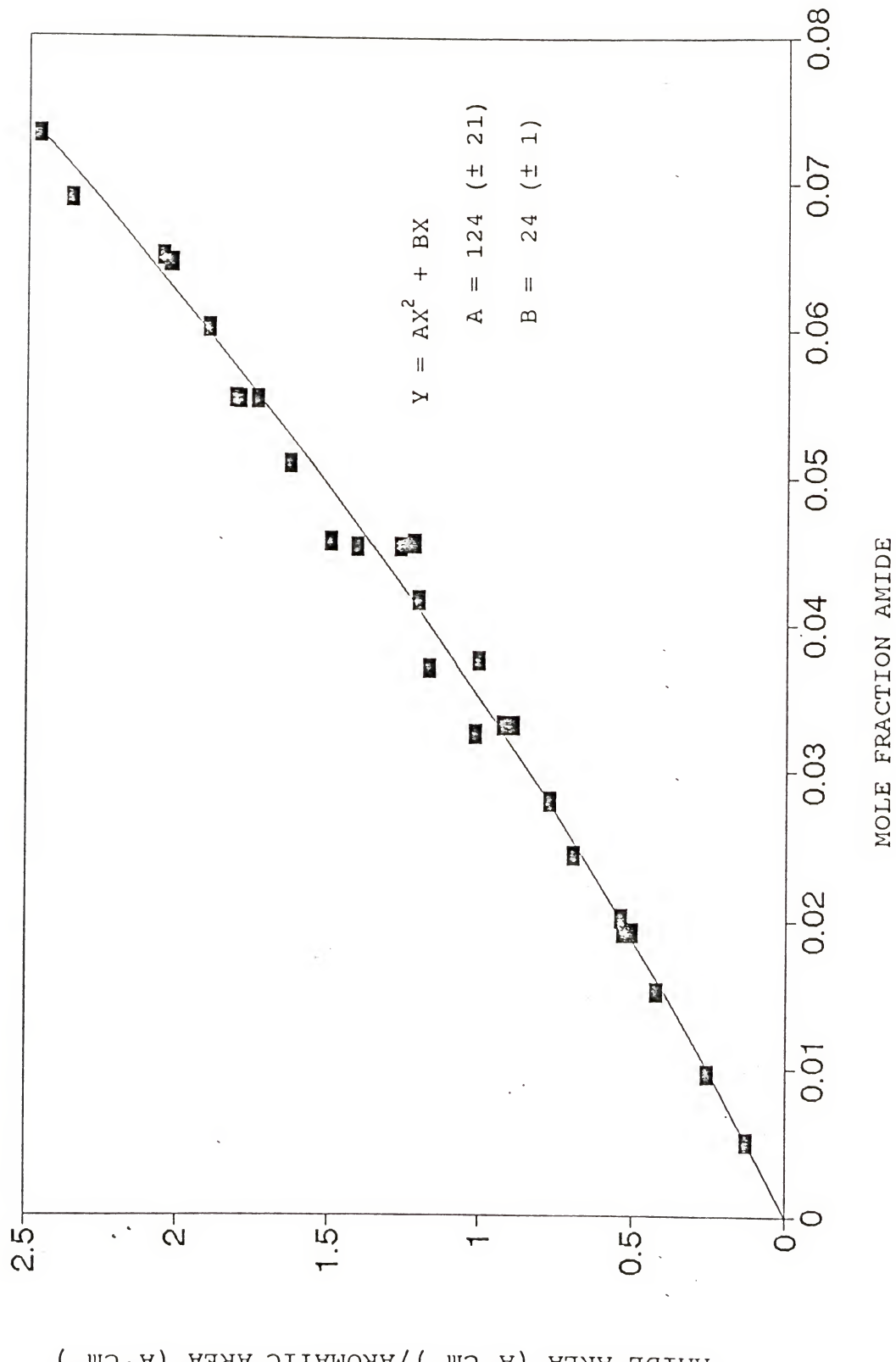


Figure 2-7 Calibration Curve of N-(4-Vinylbenzyl) acetamide 23 versus its Concentration in 20X Comonomer Solution

Table 2-4 Least Squares Analysis of the Calibration Data
of 20X N-(4-Vinylbenzyl)acetamide 23 (from the
Lotus program)

Y = AX ² + BX		
Regression Output:		
Constant		0
Std Err of Y Est		0.0697
R Squared		0.989
No. of Observations		29
Degrees of Freedom (df)		27
	B	A
X Coefficient(s)	24.3	124
Std Err of Coef.	1.2	21

Table 2-5 Calibration Data of N-(4-Vinylbenzyl)acetamide
23 versus its Concentration in 80X Comonomer
Solution

SAMPLE	CONCN (Based on the Masses of the Comonomers)	RATIO OF AREAS
		AMIDE AROMATIC
I113-G	0.890	0.2936
I113-F	1.69	0.4610
I113-E	2.48	0.6942
I113-D	3.24	1.184
I113-C	4.07	1.570
I113-B	4.54	2.045
I113-A	5.21	1.980

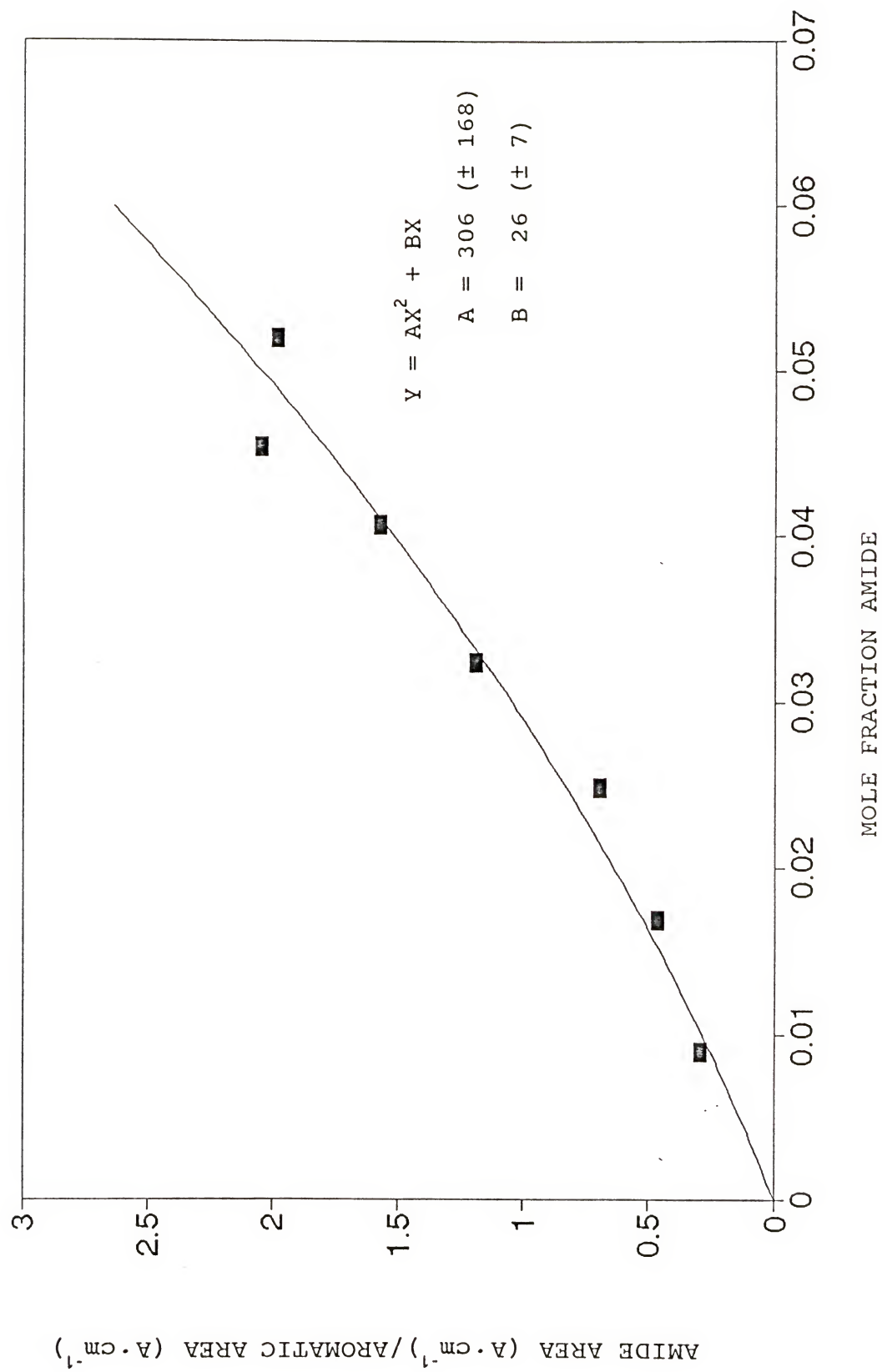


Figure 2-8 Calibration Curve of N-(4-Vinylbenzyl) acetamide $\underline{2.3}$ Versus its Concentration in 80X Comonomer Solution

Table 2-6 Least Square Analysis of the 80X Calibration
 Curve Data of N-(4-Vinylbenzyl)acetamide 23
 (from Lotus program)

$Y = AX^2 + BX$		
Regression Output:		
Constant		0
Std Err of Y Est		0.155
R Squared		0.961
No. of Observations		7
Degrees of Freedom (df)		5
	B	A
X Coefficient(s)	25.6	306
Std Err of Coef.	7.3	168

CHAPTER 3
MEASURE OF PROXIMITY AND MOVEMENT OF
AMINE GROUPS IN POLYMERS

3.1 Introduction

The investigation of the stability of bifunctional amine sites in polystyrene requires some standard against which the ordered polymer can be compared. Perhaps the ideal characteristic of such a standard would be a polymer in which the amine groups were distributed equally-spaced throughout the polymer. Since such a polymer cannot at present be prepared, another choice of a standard is necessitated. Another approach to the problem is to use a polymer standard whose distribution of amine groups is not controlled but rather can be reasonably predicted.

One such distribution is a random distribution of amine functions where the placement of the amine groups might be modeled as a simple binomial distribution of spheres. While the amine groups are not likely to be spherical, when it is realized that the groups have some motional freedom about the point of their attachment to the polymer chain, then perhaps the immediate neighborhood of the amine groups can be reasonably approximated as a sphere (although the dimension of the sphere may be unknown). For this research the random distribution of amine groups was prepared by the two-step

Table 3-1 Probability of Proximity of Spherical Groups

LAYER#	1	2	3	
#SPHERES PER LAYER	12	64	108	
LOADING	P	P	P	PROBABILITY
6 mol%	0.524	0.981	0.996	PER LAYER
	0.524	0.991	1.0000	CUMULATIVE
3 mol%	0.306	0.858	0.963	PER LAYER
	0.306	0.901	0.996	CUMULATIVE
2 mol%	0.215	0.725	0.887	PER LAYER
	0.215	0.725	0.976	CUMULATIVE
1 mol%	0.114	0.474	0.602	PER LAYER
	0.114	0.534	0.843	CUMULATIVE
0.5 mol%	0.058	0.274	0.418	PER LAYER
	0.058	0.317	0.602	CUMULATIVE
0.1 mol%	0.0119	0.0620	0.168	PER LAYER
	0.0119	0.0732	0.168	CUMULATIVE
0.01 mol%	0.00120	0.00638	0.0107	PER LAYER
	0.00120	0.00757	0.0182	CUMULATIVE
P = PROBABILITY				

process of forming carbamate copolymers followed by the removal of the BOC group as discussed in chapter 2.

The approximation of the amines as spheres allows the calculation of the probabilities of proximity of the amines based on the random (binomial) distribution of spheres as concentric layers of spheres. Some of the characteristics of the random distribution of spheres are shown in Table 3-1.

The development of this model and more detailed, calculated results are shown in the Appendix A.

3.1.1 Quantitative Infrared (IR) Spectroscopy

Infrared spectroscopy was the major analytical method used in this project in order to assess the results of events that occurred in the polymer samples. Three types of interactions were investigated in order to "measure" the proximity of the amine functional groups that were incorporated into the polymer. The interactions were: 1) the coupling of amine groups to form urea, 2) the observation of hydrogen bonding of amine groups that had been converted to the corresponding acetamides, and 3) the catalysis of the aldol condensation of phenylacetaldehyde. Infrared spectroscopy was chosen as the analytical technique since it can be used quantitatively and each sample can be analyzed in a reasonable amount of time.

In order to be used quantitatively, the infrared spectrum must be evaluated as its absorbance spectrum. The absorbance of each functional group can then be related to its concentration by Beer's law: $A = abc$, where A is the absorbance of the functional group, a is the molar absorptivity of the functional group, b is the path length of the sample, and c is the molar concentration of the functional group [66MI1]. But it was not possible to maintain a constant path length for the samples used in this project so an

internal standard was used for the analyses. The internal standard was the polystyrene matrix itself. In terms of Beer's law the appropriate equation for the use of an internal standard is:

$$A_1/A_2 = a_1 b_1 c_1 / a_2 b_2 c_2 = (a_1/a_2) \times (c_1/c_2) \quad \text{eqn (3-1)}$$

since $b_1 = b_2$, where the subscripts 1 and 2 refer to functional groups 1 and 2, respectively. Functional group 2 was always the aromatic groups of the polystyrene matrix in this research. The term (a_1/a_2) is the ratio of the molar absorptivities of the functional groups 1 and 2. For a linear calibration curve this is the only datum that is needed in order to determine the mol% of a functional group in the polymer as a mole fraction of the aromatic units in the polymer. Once the relative molar absorptivities are determined, the concentrations of the various species is then given by equation 3-2:

$$(c_1/c_2) = (a_2/a_1) \times (A_1/A_2) \quad \text{eqn (3-2)}$$

The determination of the concentration of the other functional groups that were studied in this research, i.e., ureas and urethanes, would have required the preparation of separate calibration curves for each in order to determine the relative molar absorptivities of each. But an alternative

approach was used. The method required the determination of the molar absorptivity of the urethane and urea groups of appropriate model compounds relative to the molar absorptivity of the acetamide group of an appropriate model compound, i.e., the determination of the ratio (a_2/a_1) . These ratios and the monomeric and polymeric acetamide calibration curves could allow the determination of urethane and urea concentrations in polymer samples.

Table 3-2 Calibration Curve Data of the N-Benzylacetamide 26/Toluene Solutions

SAMPLE	MOL% CONCN	AROMATIC AREA	AMIDE AREA	<u>AMIDE AREA</u> AROMATIC AREA
I115-A	0.53	13.74	6.44	0.469
I115-B	1.1	13.74	13.06	0.9512
I115-C	2.1	13.63	25.59	1.877
I115-D	3.1	13.35	38.29	2.868
I115-E	4.1	13.10	51.83	3.956
I115-F	5.3	12.91	65.14	5.046
I115-G	6.1	12.73	75.43	5.925
I115-H	7.3	12.46	91.77	7.365
I115-I	8.5	12.21	106.53	8.725

The ratios were obtained by preparing solutions of model compounds in toluene and then determining the molar absorptivities of the urea, urethane and acetamide groups

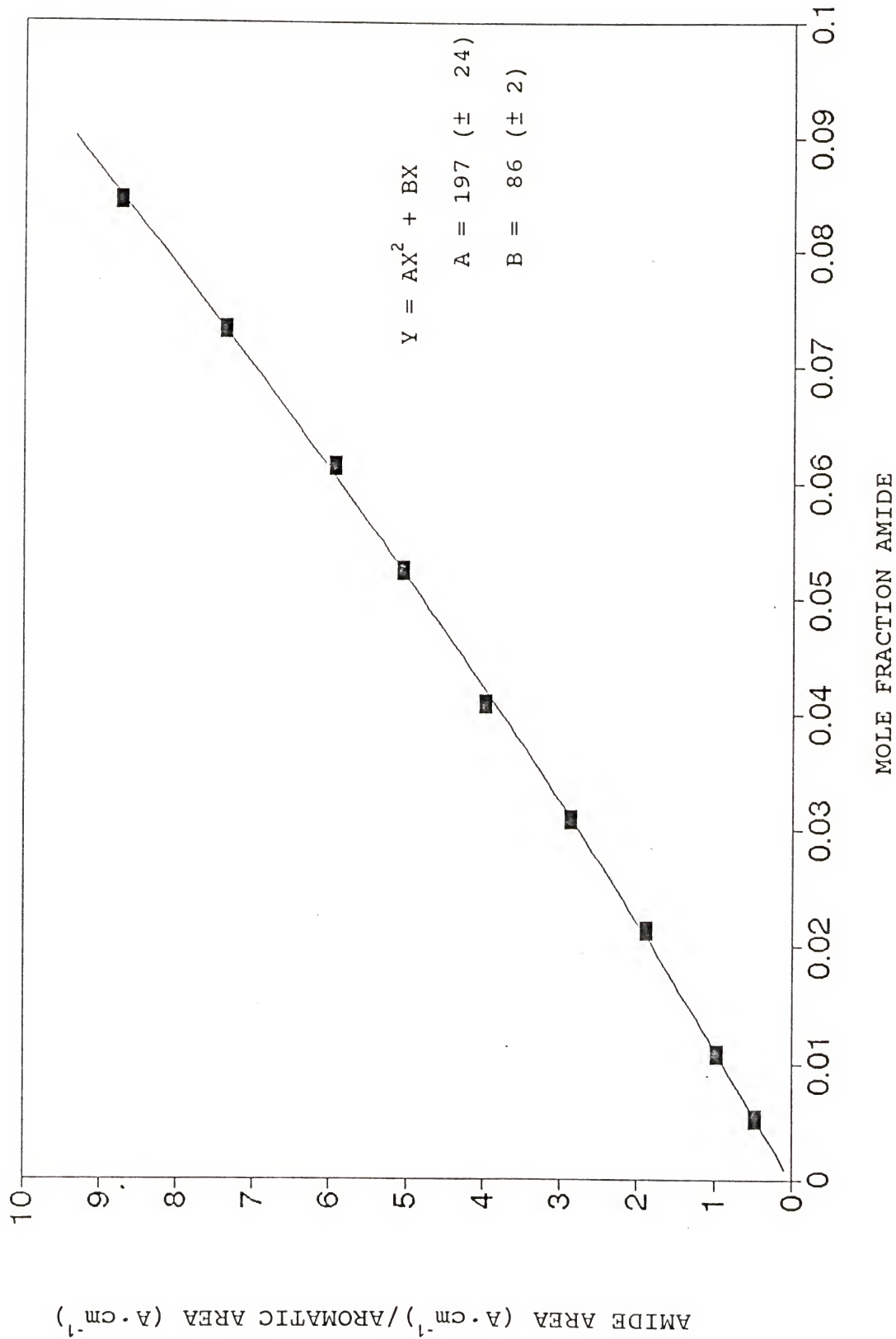


Figure 3-1

N-benzylacetamide/Toluene Calibration Curve

Table 3-3 Least Squares Analysis of the N-Benzylacetamide 26/Toluene Calibration Curve Data

Regression Output: $Y = AX^2 + BX$		
Constant		0
Std Err of Y Est		0.0635
R Squared		0.9996
No. of Observations		9
Degrees of Freedom (df)		7
X Coefficient(s)	B	A
	86.01	197
Std Err of Coef.	1.66	24

relative to aromatic absorption of toluene. By comparing the calibration curves of N-benzylacetamide/toluene with that of $P-C_6H_4CH_2-NH-Ac$ /polystyrene, it was possible to determine the conversion factor for relating the results of the urethane/toluene and urea/toluene calibration measurements to the hypothetical urethane/polystyrene and urea/polystyrene calibration curves. The results of the N-benzylacetamide/toluene calibration data are given in Table 3-2 and a graphical presentation of the results is given in Figure 3-1. The least squares analysis of the data shown in Table 3-2 is presented in Table 3-3. The results of the determination of the relative molar absorptivities of two acetamides, two urethanes and N,N-dibenzylurea in toluene are shown in Table 3-4.

Table 3-4 Relative Molar Absorptivities of Model Carbonyl Compounds (versus Toluene)

Compound	Average Relative Molar Absorptivity Versus Toluene ± Uncertainty	Peak Position cm ⁻¹
<u>26</u> , NHB	86.0 ± 1.7*	1686
<u>27</u> , NHB	95.9 ± 2.2**	1683
<u>27</u> , HB	94.2 ± 12.4**	1669
<u>28</u> , NHB	58.3 ± 4.4**	1669
<u>28</u> , HB	76.0 ± 5.5**	1671
<u>24</u> , NHB	111.9 ± 9.4**	1720
<u>28</u> , HB	106.7 ± 3.0**	1709
<u>25</u> , NHB	114 ± 13**	1720
<u>25</u> , HB	124.1 ± 8.3**	1720
<u>26</u> = Ph-CH ₂ -NH-Ac		
<u>27</u> = 4-MeC ₆ H ₄ -CH ₂ -NH-Ac		
<u>28</u> = (Ph-CH ₂ -NH) ₂ CO		
<u>24</u> = Ph-CH ₂ -NH-BOC		
<u>25</u> = 4-MeC ₆ H ₄ -CH ₂ -NH-BOC		
* Based on the uncertainty of the coefficient of the calibration curve		
** Based on two measurements.		

Table 3-5 Molar Absorptivities of Model Carbonyl Compounds Relative to Polymer-bound Benzylacetamide

Compound	Average Relative Molar Absorptivity Versus Toluene	Average Relative Molar Absorptivity Versus Polystyrene	Ratio of Molar Absorptivities (Relative to P-C ₆ H ₄ CH ₂ NHAc)
<u>26</u> , NHB	86.0 ± 1.7*	24.3 ± 1.2	1.11
<u>28</u> , NHB	95.9 ± 2.2**	"27.1"	1.11
<u>27</u> , HB	94.2 ± 12.4**	"26.6"	1.10
<u>28</u> , NHB	58.3 ± 4.4**	"16.5"	0.678
<u>28</u> , HB	76.0 ± 5.5**	"21.5"	0.884
<u>24</u> , NHB	111.9 ± 9.4**	"31.6"	1.30
<u>24</u> , HB	106.7 ± 3.0**	"30.2"	1.24
<u>25</u> , NHB	114. ± 13.**	"32.2"	1.30
<u>25</u> , HB	124.1 ± 8.3**	"35.1"	1.44
<u>26</u> = Ph-CH ₂ -NH-Ac			
<u>27</u> = 4-MeC ₆ H ₄ -CH ₂ -NH-Ac			
<u>28</u> = (Ph-CH ₂ -NH) ₂ CO			
<u>24</u> = Ph-CH ₂ -NH-BOC			
<u>25</u> = 4-MeC ₆ H ₄ -CH ₂ -NH-BOC			
* Based on the standard deviation of the calibration curve.			
** Based on the average of the measurements of two solutions.			
The numbers in quotations are the values of the "Relative Molar Absorptivity" that would be expected for a polystyrene calibration curve for the functional group indicated.			

Thus the equations which may be obtained from the data in Table 3-5 and the initial slope of the polymer-bound benzylacetamide calibration curve are:

$$\text{Acetamide (NHB) mol\%} = \left(\frac{100\%}{24.3} \right) \left(\frac{\text{Acetamide Area}}{\text{Aromatic Area}} \right) \text{ eqn (3-3A)}$$

$$\text{Acetamide (NHB) mol\%} = (4.12\%) \left(\frac{\text{Acetamide Area}}{\text{Aromatic Area}} \right) \text{ eqn (3-3B)}$$

Using the Molar Absorptivity Ratios of the hydrogen bonded forms of compounds 28 and 25 allows the following equations to be obtained:

$$\text{Urethane (NHB) mol\%} = \left(\frac{4.12\%}{1.44} \right) \left(\frac{\text{Urethane Area}}{\text{Aromatic Area}} \right) \text{ eqn (3-4A)}$$

$$\text{Urethane (NHB) mol\%} = (2.86\%) \left(\frac{\text{Urethane Area}}{\text{Aromatic Area}} \right) \text{ eqn (3-4B)}$$

$$\text{Urea (NHB) mol\%} = \left(\frac{4.12\%}{0.884} \right) \left(\frac{\text{Urea Area}}{\text{Aromatic Area}} \right) \text{ eqn (3-5A)}$$

$$\text{Urea (NHB) mol\%} = (4.66\%) \left(\frac{\text{Urea Area}}{\text{Aromatic Area}} \right) \text{ eqn (3-5B)}$$

The validity of this method is demonstrated in Table 3-6 where the term "Spectral Concn/Mass Concn" is very close to unity for the 40X polymers. In addition the CHN analyses of the carbamate and acetamide polymers agree with the

Table 3-6 Results of IR Measurements on the Carbamate-loaded Polymers

SAMPLE	INITIAL MASS CONCN (mol%)	AROMATIC AREA	BOC AREA	BOC SPECTRAL CONCN (mol%)	SPECTRAL CONCN	
					MASS CONCN	
G26 (20)	2.99	6.91	10.78	4.3	1.4	
G61 (20)	2.39	14.64	15.50	2.9	1.2	
H1 (20)	2.86	2.43	2.39	2.7	0.94	
I50-A	0.44	19.25	3.65	0.52	1.2	
I91-A	1.71	24.27	19.12	2.2	1.3	
J8-A-3	2.89	19.01	24.44	3.5	1.2	
J10-A-3	1.49	21.60	13.06	1.7	1.1	
J10-E-3	1.49	29.90	21.45	2.0	1.3	
J106-A-2	2.74	26.67	35.63	3.7	1.3	
G62 (40)	2.97	28.90	31.42	3.0	1.0	
H2 (40)	2.86	13.01	14.41	3.0	1.1	
H5 (40)	2.86	1.46	1.97	3.7	1.3	
I50-B	0.39	6.96	0.35	0.14	0.35	
I91-B	1.53	35.94	18.31	1.4	0.91	
J8-B-3	2.92	16.72	17.87	2.9	1.0	
J10-B-3	1.42	28.57	14.72	1.4	0.99	
J106-B-2	2.80	25.65	24.35	2.6	0.93	
G63 (60)	3.14	22.95	21.30	2.5	0.81	
H3 (60)	3.01	21.99	15.76	2.0	0.65	
I50-C	0.399	30.88	2.79	0.25	0.62	
I91-C	1.60	31.73	12.08	1.0	0.65	
J8-C-3	2.88	23.70	21.88	2.5	0.88	
J10-C-3	1.40	43.64	13.16	0.82	0.59	
J106-C-2	2.75	17.17	14.18	2.3	0.82	
G64 (80)	3.03	37.71	28.22	2.0	0.67	
H4 (80)	2.93	16.27	9.93	1.7	0.57	
I50-D	0.47	43.84	3.41	0.21	0.45	
I91-D	1.47	42.74	11.53	0.74	0.50	
J8-D-3	2.94	42.41	33.26	2.1	0.73	
J10-D-3	1.46	29.22	12.15	1.1	0.78	
J106-D-2	2.64	24.57	15.53	1.7	0.65	

concentration determined from the initial masses of the comonomers, assuming complete incorporation of the comonomers.

While IR spectroscopy can be used for quantitative results, the technique does have its limitations. One of the major limitations of IR spectroscopy is the presence of

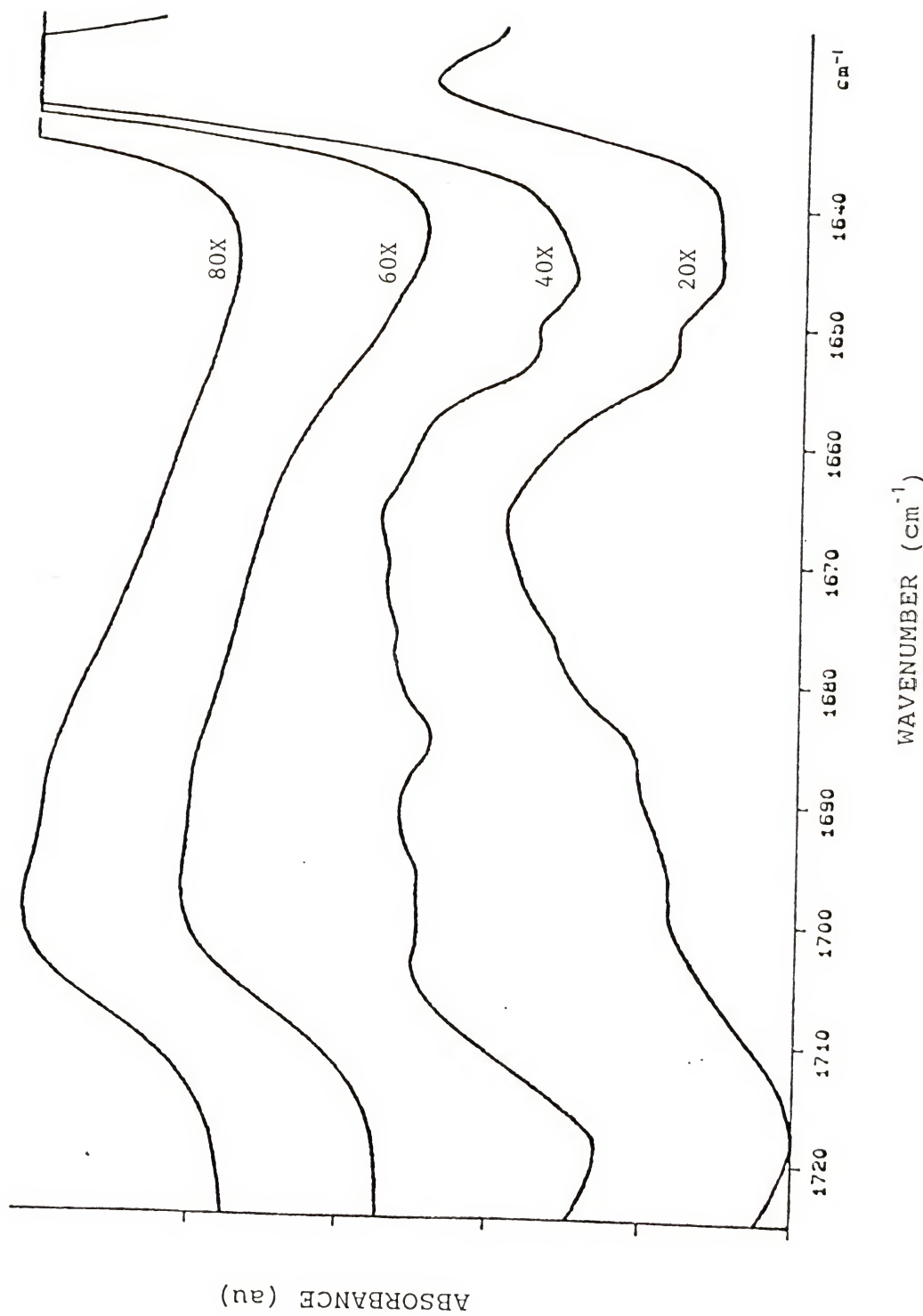


Figure 3-2 IR Spectra of "Blank" 20X, 40X, 60X and 80X Polystyrene

overlapping bands. The positions of the maximum absorbance for the various groups that were investigated in this research are shown in Table 3-4. Figure 3-2 shows the spectra of polystyrene for each degree of crosslinking studied in this research, i.e., 20X, 40X, 60X and 80X. One can see that the aromatic overtone peaks of the polystyrene overlap with the peaks of the carbonyl groups investigated. Although the carbonyl groups of organic compounds absorb IR radiation strongly compared with the aromatic overtones, because the carbonyl groups loaded into the polymers spectra are, at most, present at 3 mol% of the aromatic groups, the absorbances of the carbonyl and the aromatic groups strongly interfere.

3.1.2 Extraction of Data from IR Spectra

In order to more clearly assess the contribution to the area of the functional groups that were being investigated, the polystyrene absorption was subtracted from the spectrum of each polymer sample using the spectral subtraction feature of the IR instrument. Otherwise a separate calibration curve would have been needed for each series of crosslinked polymers because of the changes in the pattern of the aromatic overtones (see Figure 3-2 above). A typical result that may be obtained from the subtraction of spectra is shown in Figure 3-3. The peaks of each group were then integrated, using the integration feature of the IR instrument, to get that group's contribution to the area under the peak in the original

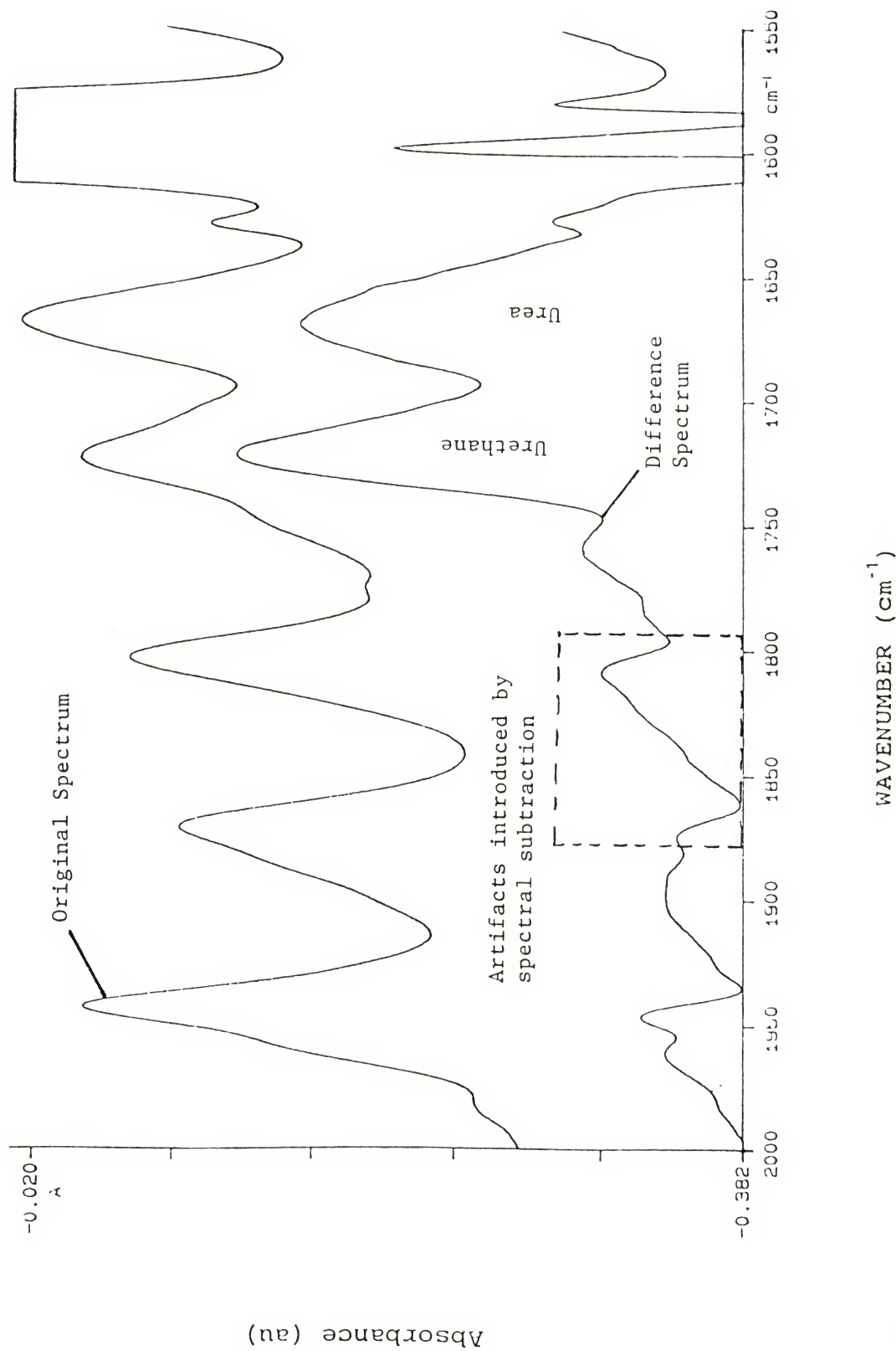


Figure 3-3 Typical Results Obtained from the Subtraction of Spectra

spectrum. Examples of this process are given in Appendix C. While the subtraction program definitely extended the lower limits of concentration that could be studied, it was found that the coupled samples from polymers loaded at less than 1.0 mol% could not be reliably analyzed. The noise from various bands and possibly from impurities in the polymer samples swamped the signals from the urethane and urea bands.

A problem that may be associated with the subtraction program is that the peaks of the IR spectra are not calibrated with an internal standard as NMR spectra typically are. The result is that the possible shifting of the sample spectral peaks relative to the spectral peaks of the blank polystyrene decreases the effectiveness of the subtraction process. In fact, artifacts are introduced which have the appearance of peaks. These false peaks are labelled in Figure 3-3. It is my opinion that the artifacts and possibly impurities were the major problems encountered in the analysis of polymers loaded at 0.5 mol% that were coupled with carbonyldiimidazole.

3.2 Measure of Proximity by Formation of Urea and Urethane Moieties

3.2.1 Coupling of Amines to Form Urea and Urethane Moieties

There is a possible advantage to "measuring" proximity and mobility by coupling amine groups to form urea. Because the formation of urea is very favorable energetically, it is possible that the amine nitrogens are "trapped" on polymer

chains in a non-relaxed conformation (i.e., the polymer chains have moved, perhaps substantially, from their original or equilibrium positions). Thus the use of a chemical reaction to measure proximity offers the possibility of insight into the magnitude of the distance that polymer chains are capable of moving.

3.2.2 Coupling Reaction

Amines (2 moles = 1 eq.) react with the compound 1,1'-carbonyldiimidazole (1 mole = 1 eq.) to form a urea when the reagents are in solution. This reaction is shown in Figure 3-4. If the urea is then mixed with ethanol, no further reaction occurs. But when this reaction is carried out with amines that are bound in a polystyrene matrix, intermediates may be more easily observed. These possibilities are illustrated in Figure 3-5.

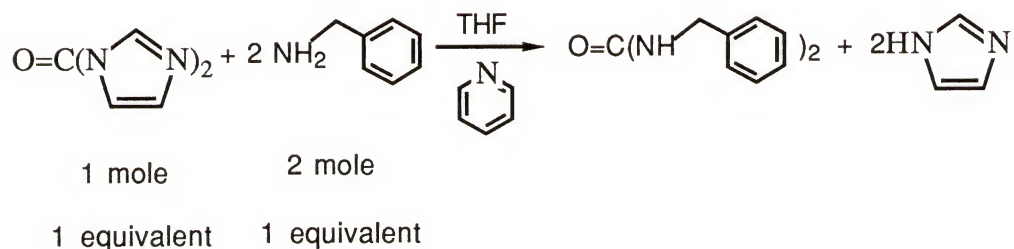


Figure 3-4

Reaction for the Coupling of Monomeric Amines with 1,1'-Carbonyldiimidazole

A noteworthy feature of Figure 3-5 is that a "semi-urea" forms in addition to the urea that is typically observed. Evidence obtained in the course of this research supports the idea that formation of the semi-urea is essentially irreversible for the reaction conditions used. In other words once an amine has reacted to form a semi-urea, it cannot react with another semi-urea to form a molecule of urea for the reaction conditions used. Only those semi-urea molecules that are in the proximity of a free amine with which it can react can form urea. Thus all of the amines that are "trapped" as semi-urea molecules react with ethanol that is added later to convert them to urethanes.

The formation of urea or semi-urea is a kinetic measure of the average mobility of the amine groups in the polymer. The experiment is a kinetic measurement since there is a competition between the diffusion of carbonyldiimidazole into the polymer to react with each free amine group and the rate at which the free amine groups are able to migrate to react with a semi-urea that has already formed in their proximity. If two amine groups are in close proximity, they are more likely to encounter each other or will encounter each other more frequently, and are more likely to form a moiety of urea rather than two moieties of semi-urea.

3.2.3 Analysis of Polymer Samples Containing Urea and Urethane Moieties

A problem occurs with the IR analysis of polymer samples which contain urethane and urea groups. The urethane and urea

groups in the polymer sample occur in both their hydrogen-bonded (HB) and non-hydrogen-bonded (NHB) forms. The HB form is generally about 15 cm^{-1} wavenumbers below that of the NHB form (see Table 3-4). While the peak positions of the HB urethane and NHB urea do not coincide, some of their peaks do overlap extensively. And because the mixing of molar absorptivities corresponding to the HB and NHB forms would complicate the calculation of concentrations of the urethane and urea species, it would have been better if a single peak were present for each. It was possible to obtain a single peak for the urethane and urea groups by taking the IR spectra of bromoform (CHBr_3) mulls of the polymer samples. Bromoform was used as a mulling material because its refractive index is comparable to that of polystyrene and thus causes the mull, though composed of an insoluble solid suspended in the bromoform, to be transparent. The transparency allowed the samples to be analyzed at the limits of the linearity of the IR instrument. Apparently the bromoform hydrogen bonds to the carbonyl groups of the urethane and urea moieties. Thus all carbonyl species in the polymer were converted to their HB form, and thus the urethane and urea were more thoroughly, though not completely, resolved.

The appropriate polystyrene background (i.e., either 20X, 40X, 60X or 80X) was subtracted from the spectrum of the polymer sample. The areas of the urethane and urea peaks were then integrated and recorded. The ratio of these areas to the

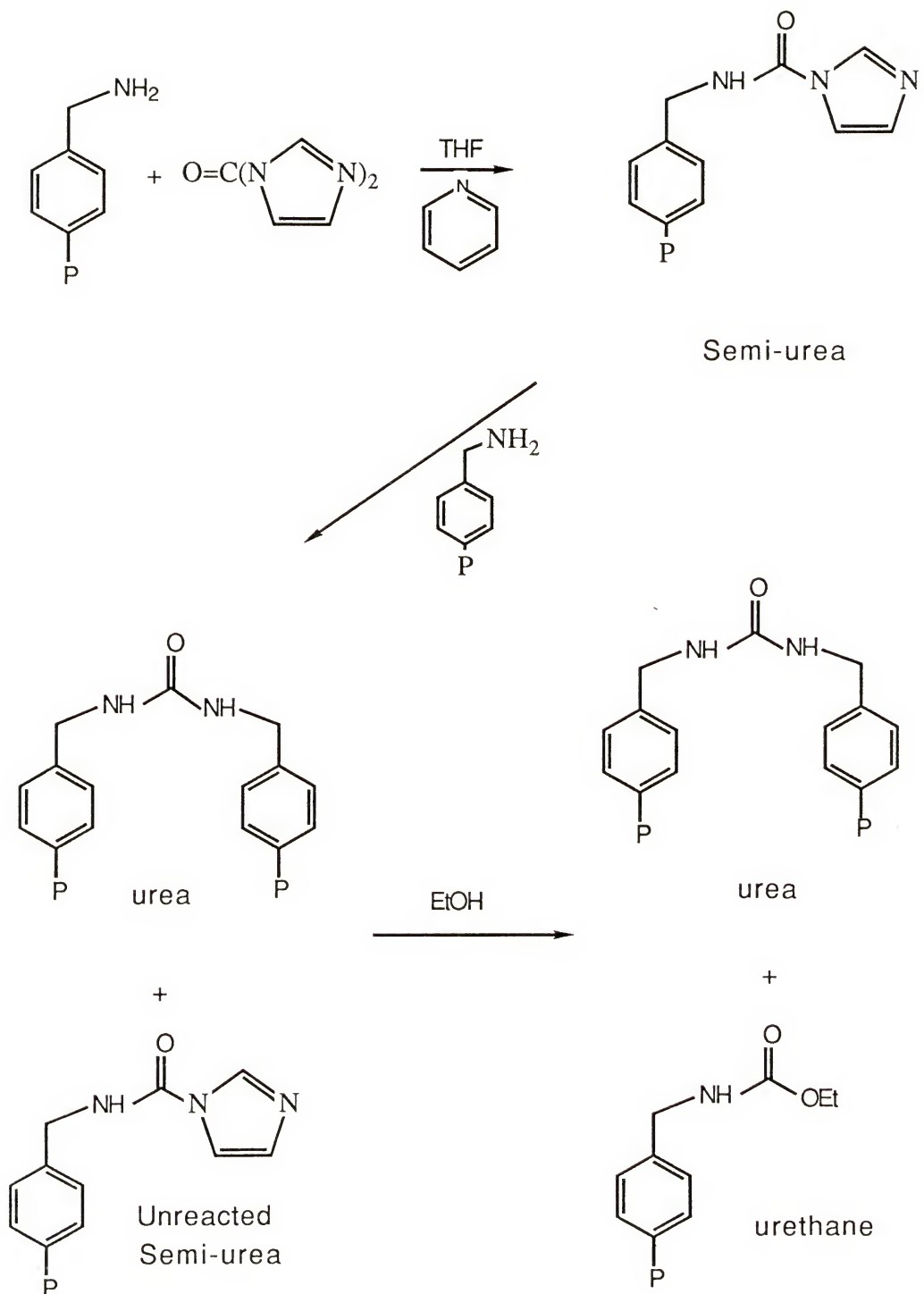


Figure 3-5 Coupling of Polymer-bound Amines with 1,1'-Carbonyldiimidazole

area of the aromatic absorption at 1600 cm^{-1} allowed the calculation of the urethane and urea concentrations in the polymer samples.

3.2.4 Conditions and Results of the Coupling Reaction

Random and ordered polymers in tetrahydrofuran were treated with equivalent amounts of carbonyldiimidazole over the period of one week until the amount of carbonyldiimidazole amounted to 20 equivalents for the reaction written as shown in Figure 3-4. The carbonyldiimidazole was added slowly so that any water that was inadvertently present would have been consumed, and the remaining carbonyldiimidazole would couple the amines under the same conditions as an initially dry polymer sample. At the end of eight days the samples were treated with a large excess of ethanol. After some days the polymer samples were filtered, dried and analyzed by infrared spectroscopy.

The mol%'s of the urea and urethane functional groups were determined from calibration curves. The results of the investigation are shown in Table 3-7. Graphical presentations of the data given in Table 3-7 is presented in Figures 3-6 through 3-11. In Figures 3-6 through 3-9, the data is presented for samples for which the degree of crosslinking was held constant as indicated in each figure.

In appendix A a theoretical curve is derived which may be applied to the coupling of the random amine-polymers results

Table 3-7 Results of the Coupling of Polymer-bound Amines to Form Urea and Urethane

	INITIAL CONCN AMINE	URETHANE CONCN (mol%)	UREA CONCN (mol%)	RATIO OF CONCNS <u>URETHANE</u> UREA	YIELD %
R 20	1.7	0.80	0.50	1.6	109
	2.2	0.31	0.69	0.45	79
	2.9	0.63	0.89	0.71	84
	3.5	1.8	1.3	1.5	124
NR 20	1.4	0.23	0.39	0.59	73
	1.5	0.15	0.94	0.15	134
	2.8	0.68	1.0	0.68	95
	2.9	0.39	1.4	0.29	107
R 40	1.4	0.25	0.27	0.93	56
	1.4	0.58	0.26	2.3	78
	2.9	0.93	0.63	1.5	75
	3.0	0.58	0.90	0.64	80
NR 40	1.4	0.098	0.21	0.47	36
	1.5	0.095	0.44	0.22	65
	2.9	0.46	0.97	0.48	84
	3.1	0.14	0.70	0.21	49
R 60	0.82	0.41	0.18	2.3	93
	1.0	0.38	0.24	1.6	84
	2.5	1.2	0.59	2.1	96
	3.0	0.48	0.28	1.7	34
NR 60	1.4	0.067	0.14	0.49	24
	1.5	0.074	0.37	0.20	54
	2.8	0.20	0.55	0.36	46
	3.3	0.17	0.71	0.24	48
R 80	0.74	0.29	0.11	2.8	69
	2.0	0.37	0.083	4.4	27
	2.1	1.0	0.36	2.8	80
	2.9	0.60	0.25	2.4	38
NR 80	1.4	0.10	0.23	0.46	40
	1.8	0.11	0.31	0.36	42
	2.8	0.22	0.28	0.78	27
	3.4	0.15	0.72	0.21	46

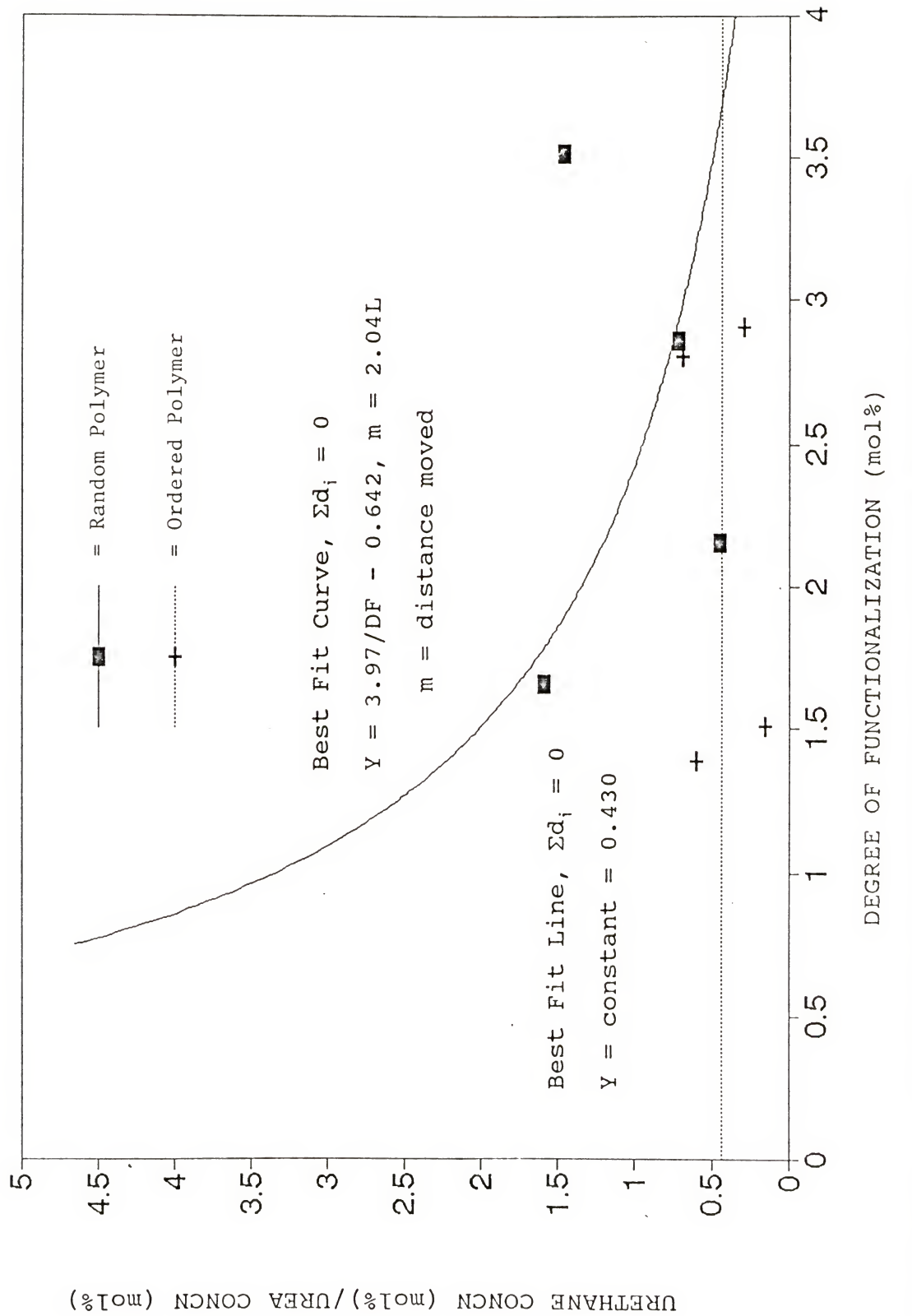


Figure 3-6

Graphical Presentation of the Coupling Reaction Data (20X)

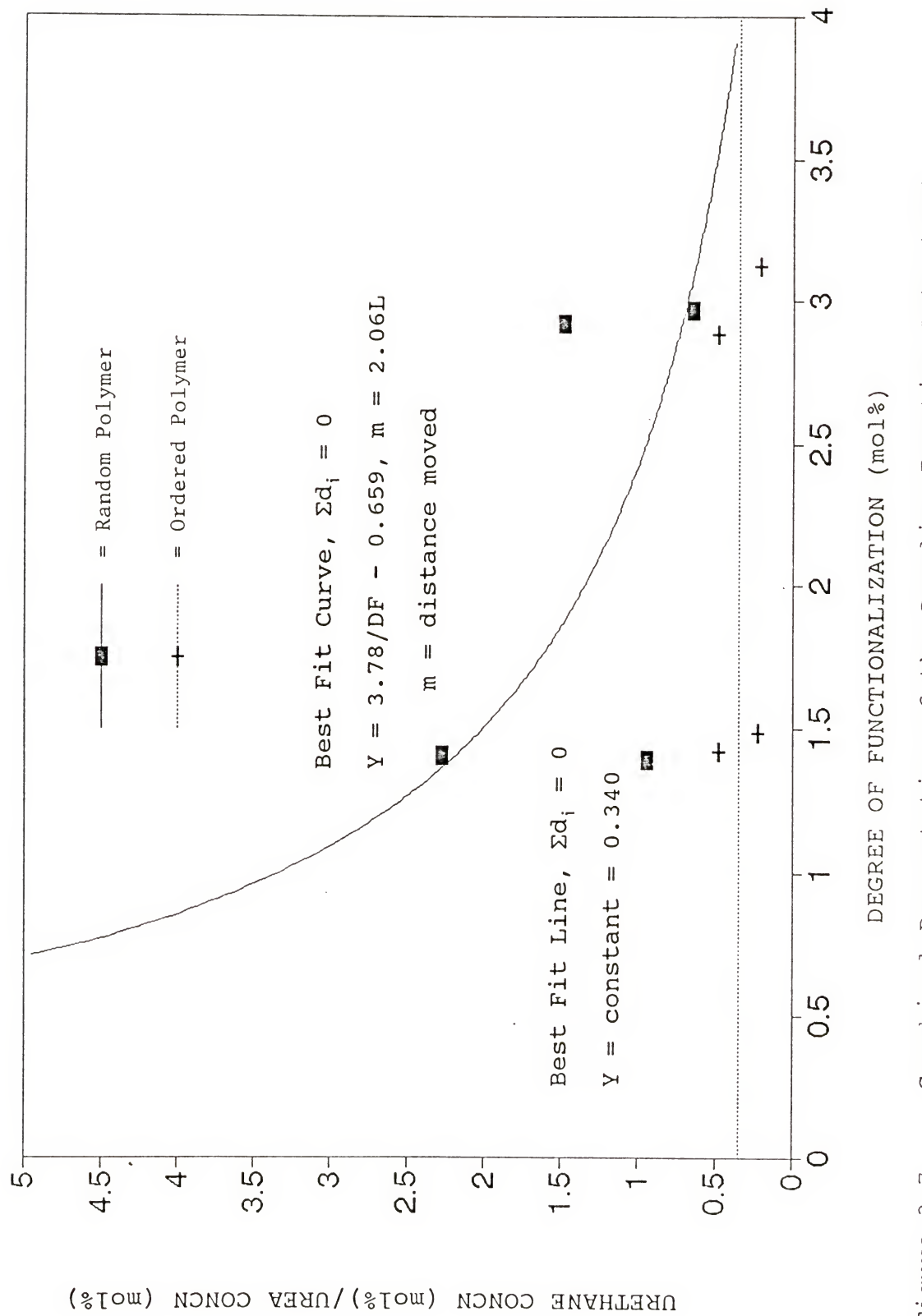


Figure 3-7

Graphical Presentation of the Coupling Reaction Data (40X)

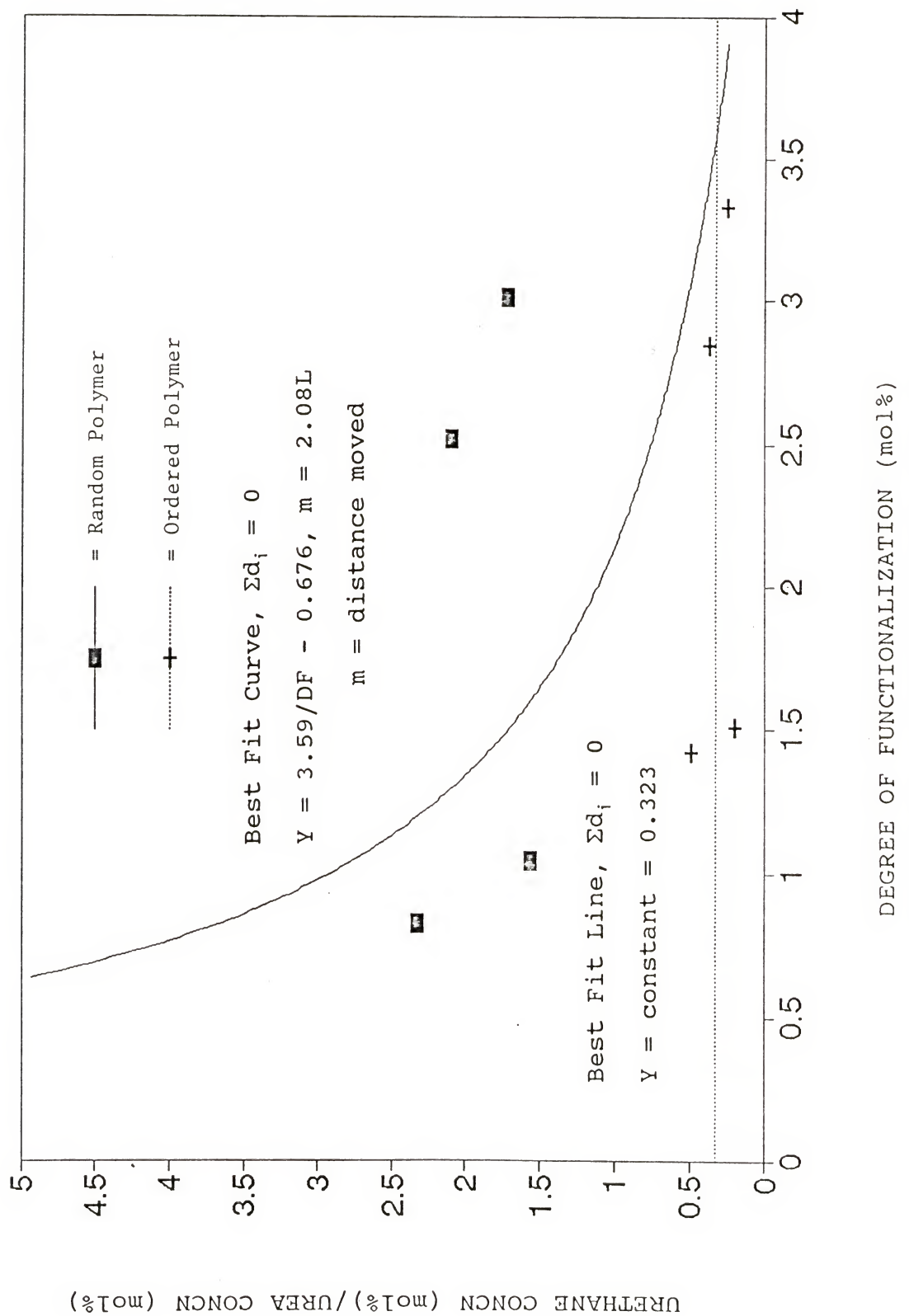


Figure 3-8

Graphical presentation of the Coupling Reaction Data (60X)

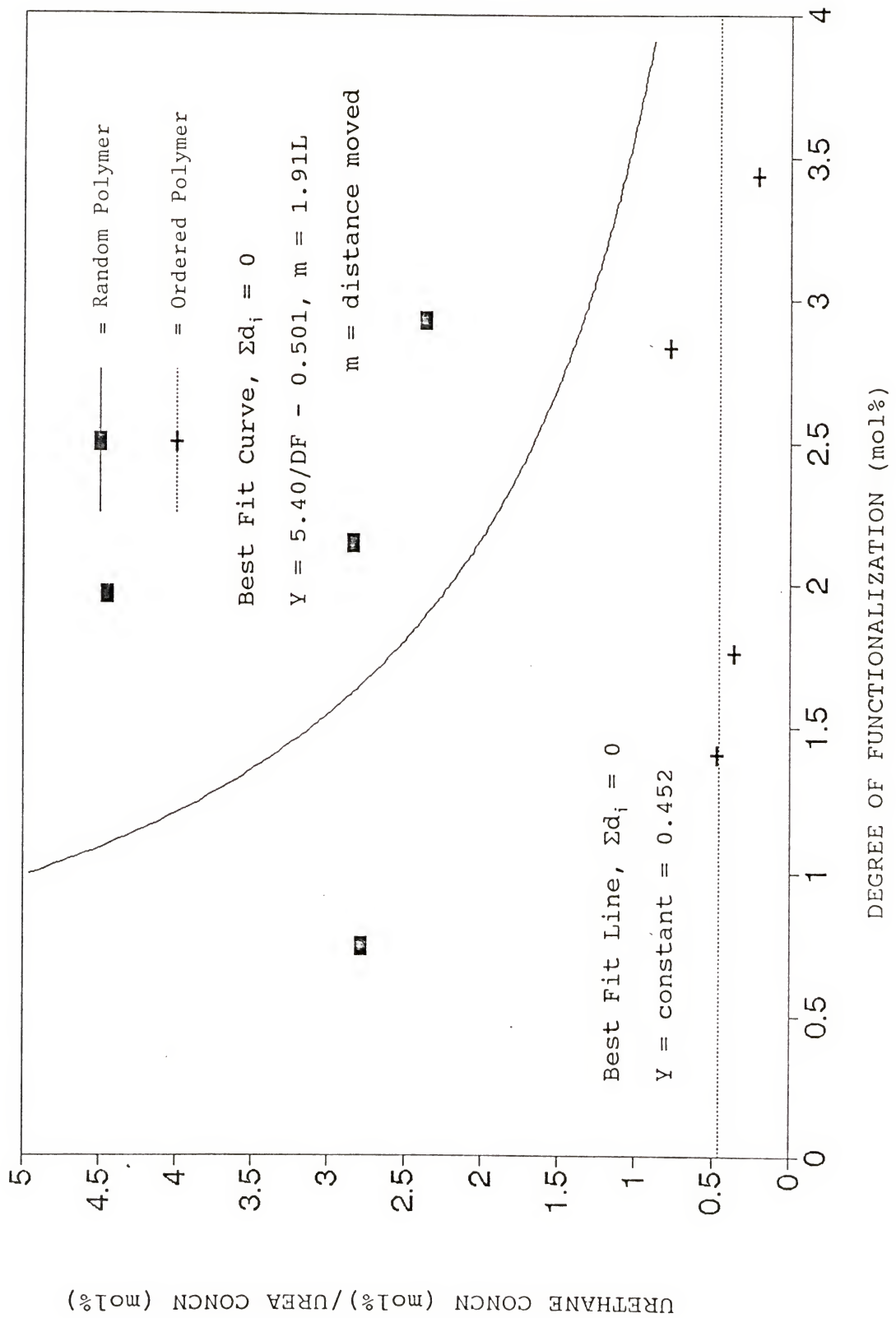
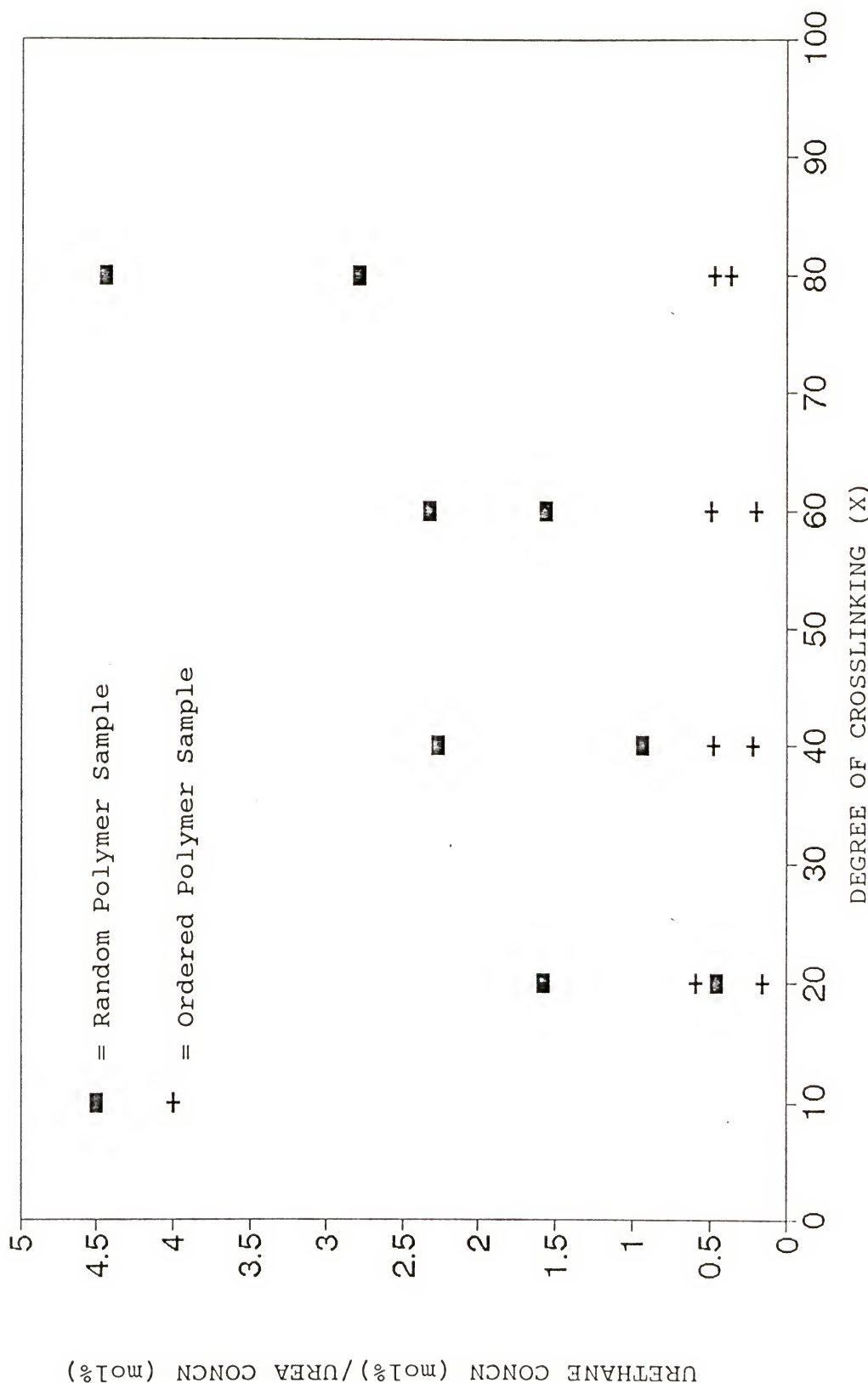


Figure 3-9

Graphical Presentation of the Coupling Reaction Data (80X)



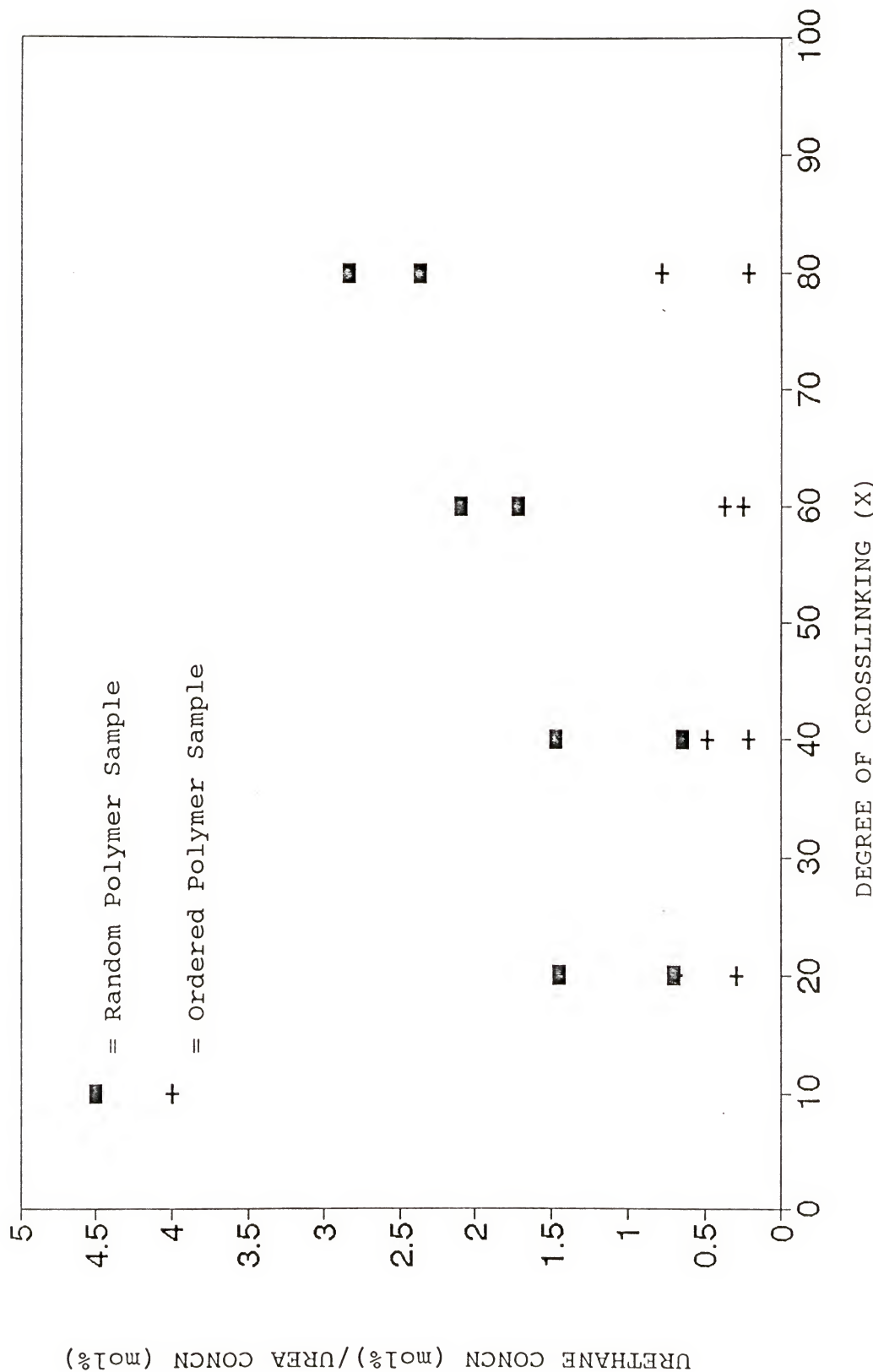


Figure 3-11 Graphical Presentation of the Coupling Data as a Function of Crosslinking (nominally 3.0 mol% Random and Ordered Polymers)

shown in Figures 3-6 through 3-9. The curve obtained in appendix A has the form:

$$R_m = \frac{(7.470290m^2 - 40.3777m + 55.21749)}{DF} + (1.141942m^2 - 5.58031 + 5.986803) \quad \text{eqn (3-6)}$$

where R_m = predicted ratio of the urethane concn/urea concn, m = mobility (i.e. distance moved) of the amine groups (in terms of the unit sphere diameter, L --see appendix A),

and DF = the degree of functionalization of the polymer.

Applying eqn (3-6) to the data of the coupling of the random polymers in Table 3-7, it is possible to calculate values for m which gives the best fit of the curve (i.e. eqn 3-6) where the sum of the deviation is equal to zero. Other statistical quantities characterizing the random-polymer couplings were then calculated and shown in Table 3-9.

The best lines ($y = \text{constant}$, the sum of the deviations equal to zero) were fitted to the results of the coupling of the ordered amines since the urethane/urea ratio may be expected to be invariant (constant) with concentration. The constancy may be expected since the distance between the amine groups formed from the silanediamine moieties does not depend on the loading of the silanediamine groups in the polystyrene matrix.

In Figures 3-10 and 3-11, the urethane/urea ratios are presented as a function of crosslinking for samples which were substituted (as closely as possible) at 1.5 mol% and 3.0 mol%.

These figures give one a visual impression of the differences of the coupling results for polymers of different degrees of crosslinking and between the random and ordered polymers.

3.2.5 Discussion of the Results of the Coupling Reaction

The data in Table 3-7 permit the summary of characteristics shown in Table 3-8.

Table 3-8 Results of Analysis of Figures 3-6 through 3-9

Regression Output: $y = k(m)/DF + c(m)$	R20	R 40	R 60	R 80
Mobility, m	2.04	2.05	2.08	1.91
k	3.97	3.78	3.59	5.40
c	-0.642	-0.659	-0.676	-0.501
Std Err of Y Est (Uncertainty)	1.33	1.53	2.76	5.14
No. of Observations	4	4	4	4
Degrees of Freedom (df)	2	2	2	2
$k(m) = (7.470290m^2 - 40.3777m + 55.21749)$				
$c(m) = (1.141942m^2 - 5.58031 + 5.986803)$				
Regression Output: $y = \text{constant}$	NR 20	NR 40	NR 60	NR 80
Constant B	0.430	0.344	0.323	0.452
Std Err of Y Est (Uncertainty)	0.343	0.209	0.180	0.331
No. of Observations	4	4	4	4
Degrees of Freedom (df)	3	3	3	3

The (std err of Y est) for the ordered polymers was calculated using the best line, $y = \text{constant}$, where the sum of the deviations is equal to zero. The standard deviation for the four data points and equation (3-7) gave the uncertainties shown in Table 3-8 ($df = 3$, $t = 3.18$) [86MI4].

The (std err of Y est) for the random polymers was calculated using the best fit theoretical curve (eqn A-15) discussed in Appendix A where the sum of the deviations is equal to zero. The standard deviation for the four data points and equation (3-7) gave the uncertainties shown in Table 3-8 ($df = 2$, $t = 4.30$) [86MI4].

$$\text{Uncertainty} = \pm t * (\text{S.D.} / \sqrt{n}) \quad \text{eqn (3-7)}$$

where t = Value of "Student's" distribution for the given degrees of freedom,

S.D. = Standard deviation of the data, and

n = number of data points.

Using the best fit theoretical curve for the random polymers and using the best lines ($y = \text{constant}$) for the ordered polymers, in order to see the trends more clearly it is possible to calculate the hypothetical values (and uncertainties) of the urethane/urea ratios that would be obtained for samples of the concentrations shown in the Table 3-9.

The results shown in Table 3-9 show very little distinction for the average values of the urethane concn/urea concn for the ordered polymers as the crosslinking changes.

For the ordered polymers, the lack of distinction might have been expected since the spacing between the amine groups is independent of the concentration of the silanediamine that was used to load the polymer. However, the large uncertainties associated with the urethane/urea ratios in Table 3-9 do not give much certainty to this conclusion.

Table 3-9 Hypothetical Urethane/Urea Ratios Based on the Best Lines (and Curves) for the Data in Table 3-8

		URETHANE CONCN/UREA CONCN		
RANDOM		1.5M	2.25M	3.0M
20X		2.0 \pm 1.3	1.1 \pm 1.3	0.7 \pm 1.3
40X		1.9 \pm 1.5	1.0 \pm 1.5	0.6 \pm 1.5
60X		1.7 \pm 2.8	0.9 \pm 2.8	0.5 \pm 2.8
80X		3.1 \pm 5.1	1.9 \pm 5.1	1.3 \pm 5.1
ORDERED		1.5M	2.25M	3.0M
20X		0.43 \pm 0.34	0.43 \pm 0.34	0.43 \pm 0.34
40X		0.34 \pm 0.21	0.34 \pm 0.21	0.34 \pm 0.21
60X		0.32 \pm 0.18	0.32 \pm 0.18	0.32 \pm 0.18
80X		0.45 \pm 0.33	0.45 \pm 0.33	0.45 \pm 0.33

Likewise there is no significant distinction in the average values in Table 3-9 for the random polymers as a group for the different degrees of crosslinking. However, it is possible to see that the amount of site isolation may be a strong function of the loading. The theoretical model (see

Appendix A, Figures A-3 and A-4), which predicts the amount of urethane and urea that may be expected under various conditions, shows that the amount of urethane that can form (because of site isolation) increases dramatically at low loadings of the amine groups in the polystyrene matrix. Nevertheless, the large uncertainties that are present in the data leave this observation to be confirmed by further experimentation.

Table 3-10 Average Site Accessibility Data Obtained from the Coupling of Amine Polymers with 1,1'-Carbonyldiimidazole

	AVERAGE YIELD (%)	# of OBSERVATIONS	AVERAGE DEVIATION (%)
R 20	99	4	17
NR 20	102	4	18
R 40	72	4	9
NR 40	58	4	16
R 60	77	4	21
NR 60	43	4	9
R 80	53	4	21
NR 80	39	4	6

Because the experiments are a kinetic measure (for the reasons discussed above) of site isolation (or mobility, depending on one's perspective), it is only possible to draw conclusions regarding the isolation in terms of relative rates. The coupling results support the idea that as the degree of crosslinking in the polystyrene increases, the mobility (relative to the rate of diffusion of materials into the polymer) of the chains remains roughly constant. Nevertheless it is not possible to say that there is any difference in the distance that the amine groups were able to move for all polymers, regardless of the degree of crosslinking.

Site accessibility decreases as the crosslinking increases for both the ordered and the random polymers, but the accessibility decreases more rapidly for the ordered polymers. The accessibility to ordered polymers is less than that of the random polymer for 40X, 60X and 80X crosslinking. It is concluded (based on the IR analyses of the carbamate polymers and repeated CHN analyses of some of the silanediamine-loaded polymers) that the carbamate monomer is incorporated into the growing polymer chains slowly while the silanediamine monomer is incorporated quickly. As discussed in chapter 1, the result is that the carbamate monomers are more likely to be incorporated into lightly crosslinked regions while the silanediamine monomers are more likely to be incorporated into more heavily crosslinked regions.

3.2.6 Conclusions

No significant difference was found in the mobility (i.e. distance moved) of the amine groups for the 20X, 40X, 60X and 80X crosslinked random polystyrene polymers. No conclusions are drawn from the results of the coupling reactions that were performed on the 20X, 40X, 60X and 80X crosslink ordered polymers.

The method of coupling the random and ordered polymers with carbonyldiimidazole followed by analysis by IR spectroscopy gave accessibilities to the amine groups for the various degrees of crosslinking.

3.3 Measure of Proximity by Hydrogen Bonding

3.3.1 Advantages for the Use of Hydrogen Bonding to Measure Proximity

A second method of measuring proximity is that of assessing the amount of hydrogen bonding. If a majority of both amines of the bifunctional sites were to undergo acetylation, then the acetamide groups that formed should have a greater than random chance of being proximate, and greater amounts of hydrogen bonding should be observed in the ordered polymers than that observed for the random polymers, both being at the same loading. In fact, it is possible that the ratios of the various forms of association of the acetamide groups may be different for the ordered and random amine

polymers and for acetamides in toluene solution, evidence of which will be shown below.

The advantage of this measure of proximity is that hydrogen bonding involves small amounts of energy in contrast to the coupling of amines to form urea. Because of the small amounts of energy involved, hydrogen bonding is an easily reversible interaction. Thus, hydrogen bonding should provide a measure of proximity of functional groups that are attached to chains that are very close to their equilibrium (or relaxed) conformations.

3.3.2 Acetylation Reaction

Amine polymers were treated with acetylimidazole and pyridine; the reaction is shown in Figure 3-12. The amount of acetamide which formed was determined by infrared spectroscopy using the calibration curve that was described in the previous chapter. Another use of the calibration curve was that hydrogen bonding in randomly distributed acetamides could be studied as a function of concentration since it is reasonable to expect that the acetamide groups were randomly distributed for the same reasons discussed for the carbamate polymers. If both amine groups of the ordered bifunctional sites could be acetylated, then greater than random hydrogen bonding might be expected.

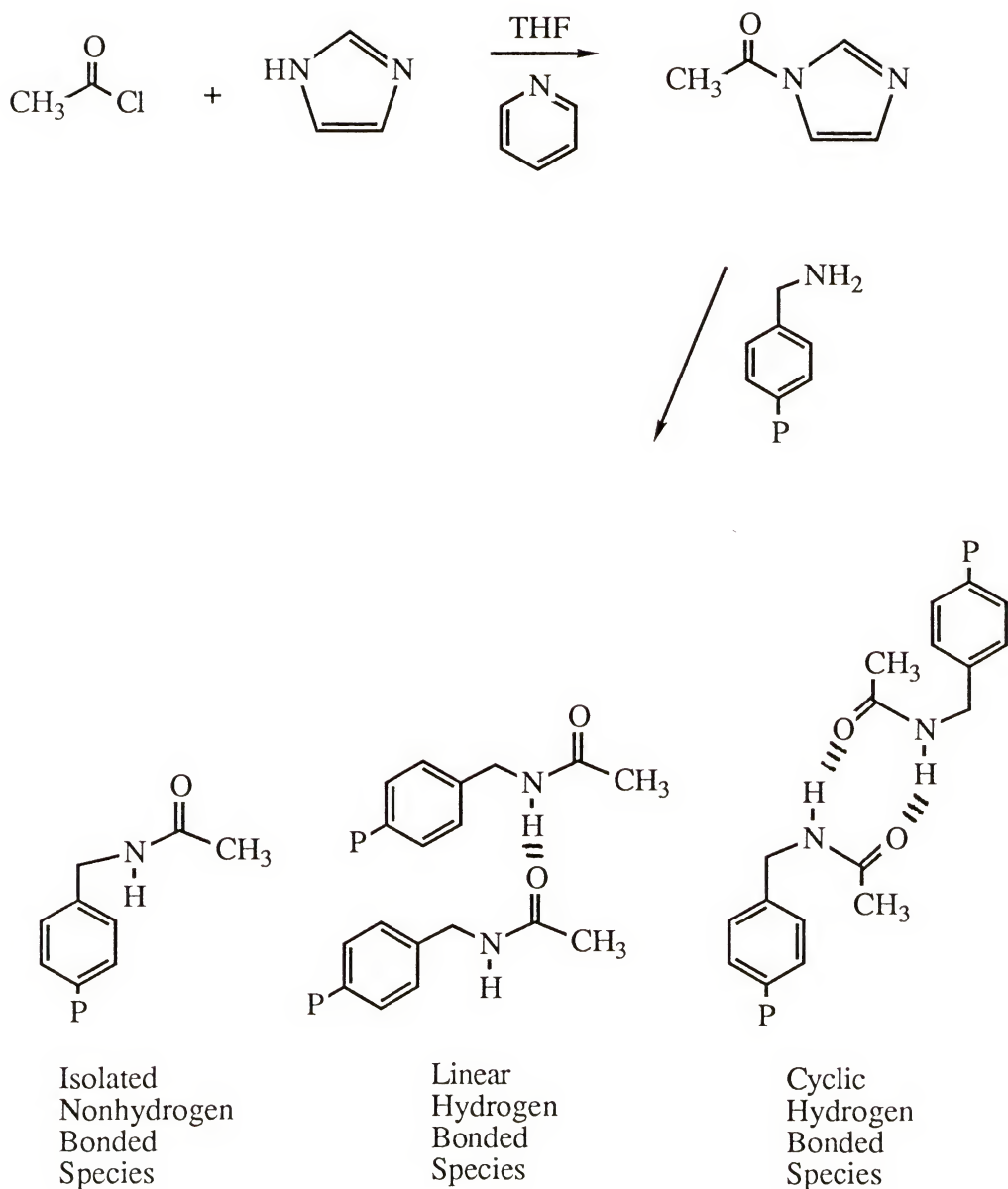


Figure 3-12 Reaction of Polymer-bound Amines with Acetylimidazole

Table 3-11 Results of the Acetylation of Amine Polymers

SAMPLE	TIME OF REACTION	AMIDE AREA	AMIDE CALIB CONCN	INITIAL AMINE CONCN	YIELD %
		AROMATIC AREA			
R20					
G83-A-2	2 days	0.693	2.4	2.9	83
G83-C	2 months	0.727	2.5	2.9	86
I99-A-2	2 days	0.456	1.6	2.1	75
I99-A-3	2 months	0.579	2.0	2.1	94
J33-A-1-A	2 days	1.026	3.4	3.5	97
J33-A-1-A	2 days	0.963	3.2	3.5	92
NR20					
I59-A-2	2 days	0.909	3.1	2.9	106
I59-A-3	3 months	0.904	3.1	2.9	105
I100-A-2	2 days	0.414	1.5	1.5	98
I100-A-3	2 months	0.477	1.7	1.5	112
J29-A-1	2 days	0.793	2.7	2.8	97
J31-A-1	2 days	0.353	1.3	1.4	91
J31-A-1	2 days	0.331	1.2	1.4	86
J35-A-1	2 days	0.470	1.7	1.6	101
R40					
G84-A-2	2 days	0.582	2.0	3.0	68
G84-C	2 months	0.605	2.1	3.0	71
I99-B-2	2 days	0.347	1.2	1.4	89
I99-B-3	2 months	0.337	1.2	1.4	87
J33-B-1	2 days	0.753	2.6	2.9	88
J33-B-1	2 days	0.697	2.4	2.9	82
J35-B-1	2 days	0.292	1.1	1.4	75
NR40					
I59-B-2	2 days	0.611	2.1	3.1	68
I59-B-3	3 months	0.883	3.0	3.1	96
I100-B-2	2 days	0.293	1.1	1.5	71
I100-B-3	2 months	0.253	0.92	1.5	62
J29-B-1	2 days	0.397	1.4	2.9	49
J31-B-1	2 days	0.176	0.64	1.4	45

Table 3-11--continued

SAMPLE	TIME OF REACTION	AMIDE AREA	AMIDE CALIB CONCN	INITIAL AMINE CONCN	YIELD %
		AROMATIC AREA			
R60					
G85-A-2	2 days	0.407	1.4	2.5	57
G85-C	2 months	0.445	1.6	2.5	62
I99-C-2	2 days	0.213	0.78	1.0	75
I99-C-3	2 months	0.242	0.88	1.0	85
J33-C-1	2 days	0.541	1.9	2.5	75
J33-C-1	2 days	0.480	1.7	2.5	67
J35-C-1	2 days	0.197	0.72	0.82	87
NR60					
I59-C-2	2 days	0.535	1.9	3.3	56
I59-C-3	3 months	0.585	2.0	3.3	61
I100-C-2	2 days	0.135	0.50	1.5	33
I100-C-3	2 months	0.178	0.65	1.5	43
J29-C-1	2 days	0.269	0.97	2.8	34
J31-C-1	2 days	0.0994	0.37	1.4	26
R80					
G86-A-2	2 days	0.346	1.2	2.0	61
G86-C	2 months	0.455	1.6	2.0	79
I99-D-2	2 days	0.140	0.52	0.74	70
I99-D-3	2 months	0.159	0.58	0.74	79
J33-D-1	2 days	0.480	1.7	2.1	79
J33-D-1	2 days	0.471	1.7	2.1	78
J35-D-1	2 days	0.200	0.73	1.1	64
NR80					
I59-D-2	2 days	0.453	1.6	3.4	47
I59-D-3	3 months	0.505	1.8	3.4	52
I100-D-2	2 days	0.121	0.45	1.8	25
I100-D-3	2 months	0.136	0.50	1.8	28
J29-D-1	2 days	0.325	1.2	2.8	41
J31-D-1	2 days	0.0929	0.34	1.4	24

Table 3-12 Summary of Accessibility Data Obtained from the Acetylation Reaction

	2 DAY AVERAGE YIELD (%)	# OF OBSERVATIONS	AVERAGE DEVIATION
R20	96.3	4	7.9
NR20	96.3	4	5.2
R30	80.7	5	7.2
NR40	58.4	4	11.2
R60	70.4	5	8.1
NR80	37.4	4	6.5
R80	70.4	5	6.5
NR80	34.5	4	9.6
	2 MONTH AVERAGE YIELD %	# OF OBSERVATIONS	AVERAGE DEVIATION
R20	90.2	2	3.7
NR20	108.4	2	3.3
R30	79.0	2	8.0
NR40	78.8	2	17.0
R60	73.5	2	11.2
NR60	52.2	2	9.1
R80	79.0	2	0.2
NR80	40.1	2	11.7

3.3.3 Analysis of Hydrogen Bonding in Polymer Samples

The polymer samples were analyzed by IR spectroscopy as their Nujol mulls. Nujol is a high boiling hydrocarbon and should provide a very nonpolar medium for the acetamide

groups. A nonpolar medium should most favor the occurrence of hydrogen bonding, and thus, was chosen for the investigation of hydrogen bonding.

3.3.4 Conditions and Results of the Acetylation Reaction

Polymer samples in THF were treated with excess pyridine, imidazole and acetyl chloride. After two days and again after at least two months, portions of the acetylation reaction were taken, washed, dried and analyzed by IR spectroscopy (Nujol mull). The results of the acetylation reactions are shown in Table 3-10. The accessibilities to the amine sites are summarized in Table 3-11.

3.3.5 Discussion of the Acetylation Results

Figures 3-13 through 3-15 show the carbonyl regions of the IR spectra of acetylated random (R) and ordered (NR) amine polymer. The random polymer spectra show a strong non-hydrogen bonded (NHB) peak at 1685 cm^{-1} and only very limited absorption in the hydrogen bonded (HB) region for 3 mol% polymers. In contrast, the ordered polymer samples show the non-hydrogen bonded peak at 1685 cm^{-1} plus a substantial HB peak, even loaded at 1.5 mol%.

Interestingly, the HB peak shown in Figures 3-14 and 3-15 is only about 15 cm^{-1} below that of the NHB peak. In contrast, the HB peak of copolymerized 4-vinylbenzylacetamide at approximately 7 mol%, shown in Figure 3-16, is about 20 to 25

cm^{-1} below that of the NHB peak and is much broader than the HB peaks shown in Figures 3-14 and 3-15. The spectrum of the acetylated 80X, 3 mol% ordered polymer is superimposed upon that of the 7 mol% copolymerized 4-vinylbenzylacetamide in Figure 3-17 in order to show the placement and width of the peaks more clearly. The HB peak of the acetylated ordered (NR) polymers also appears in the IR spectra of the carbonyl region of N-benzylacetamide in toluene as shown in region E of Figure 3-18. This middle HB peak might be correlated with the small broad peak (Region C) located at about 3230 cm^{-1} in Figure 3-19. The hydrogen and non-hydrogen bonded NH peaks of amides has been studied in the laboratory of Dr. Willis Person and correlated with various forms of hydrogen bonding of amides (personal communication, October 25, 1990). Region C of Figure 3-19 is associated with amides which hydrogen bond via a cyclic structure whereas the much larger peak (Region B) of Figure 3-19 is characteristics of amides which hydrogen bond in a linear fashion. To more certainly show that these effects are occurring would require resolution of the carbonyl and the NH peaks into their various component peaks and the determination of the magnitude of the contribution of each to the various spectra in Figures 3-18 and 3-19. The resolution of the peaks shown in Figures 3-18 and 3-19 probably awaits further availability of computer software for this purpose.

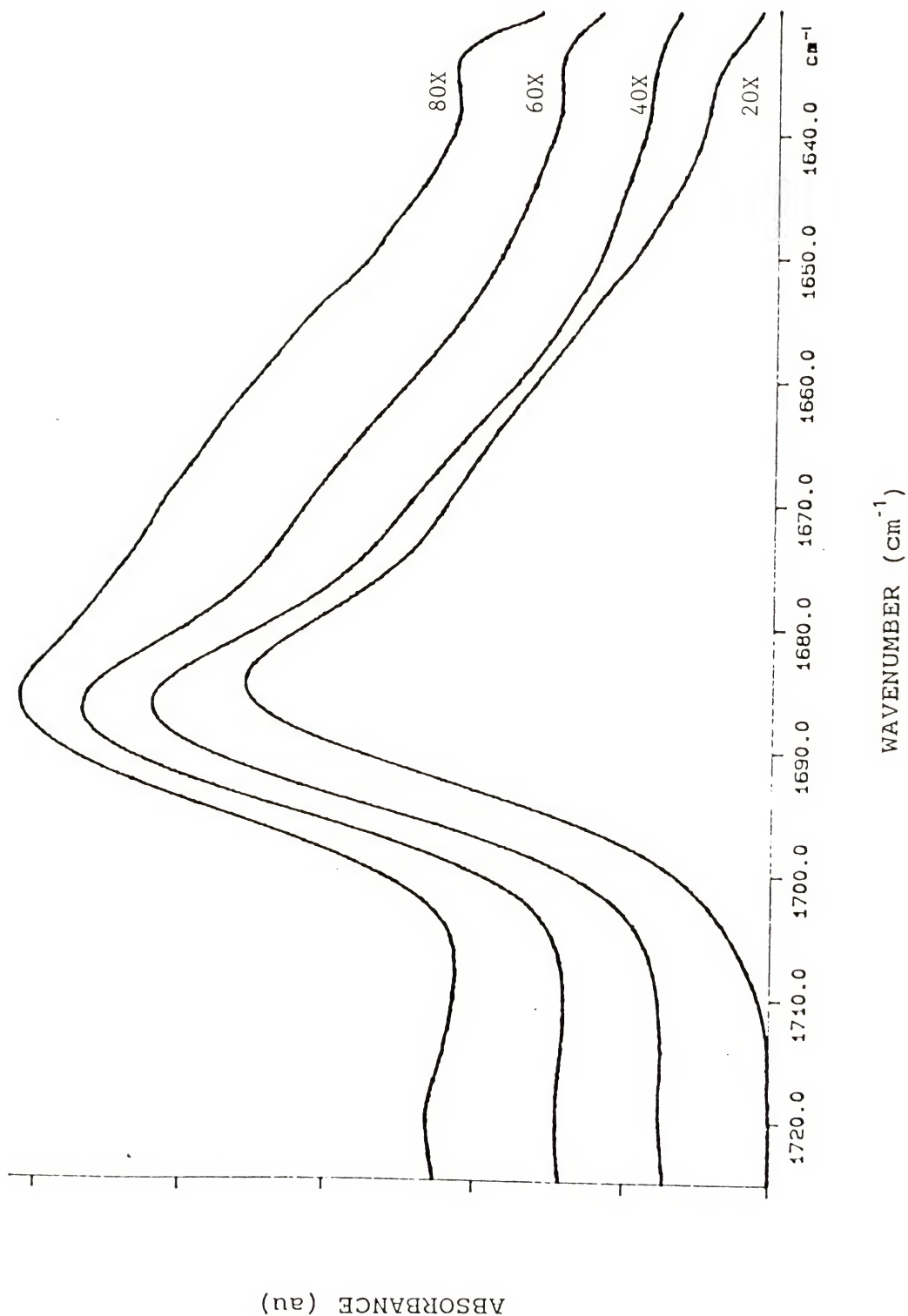


Figure 3-13 Spectra of the Carbonyl Region of Acetylated Random Polymer Samples (3%; 20X, 40X, 60X and 80X) (Polystyrene Subtracted) (Nujol Mulls)

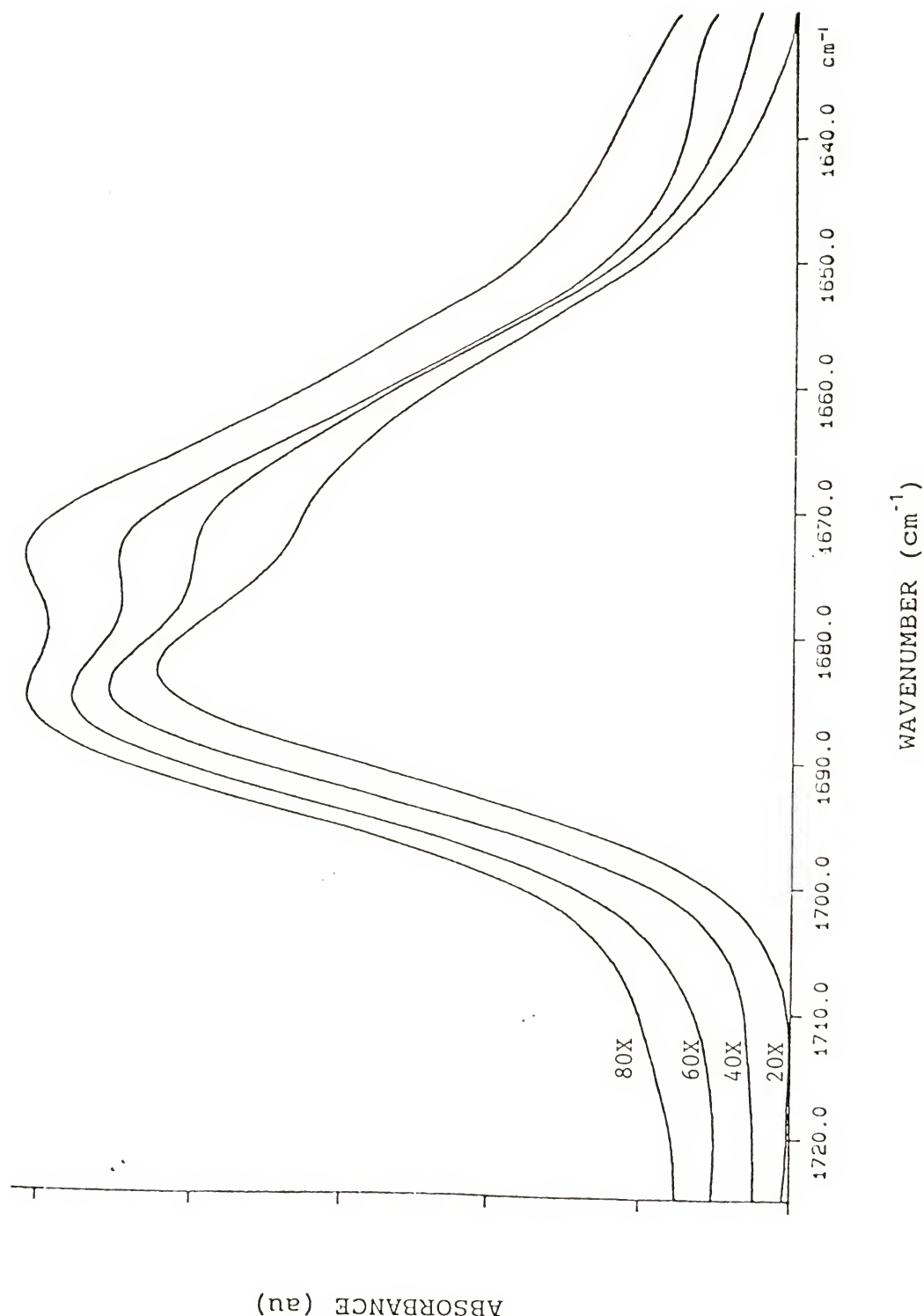


Figure 3-14 Spectra of the Carbonyl Region of Acetylated Ordered Polymer Samples (3%; 20X, 40X, 60X and 80X) (Polystyrene subtracted) (Nujol Mulls)

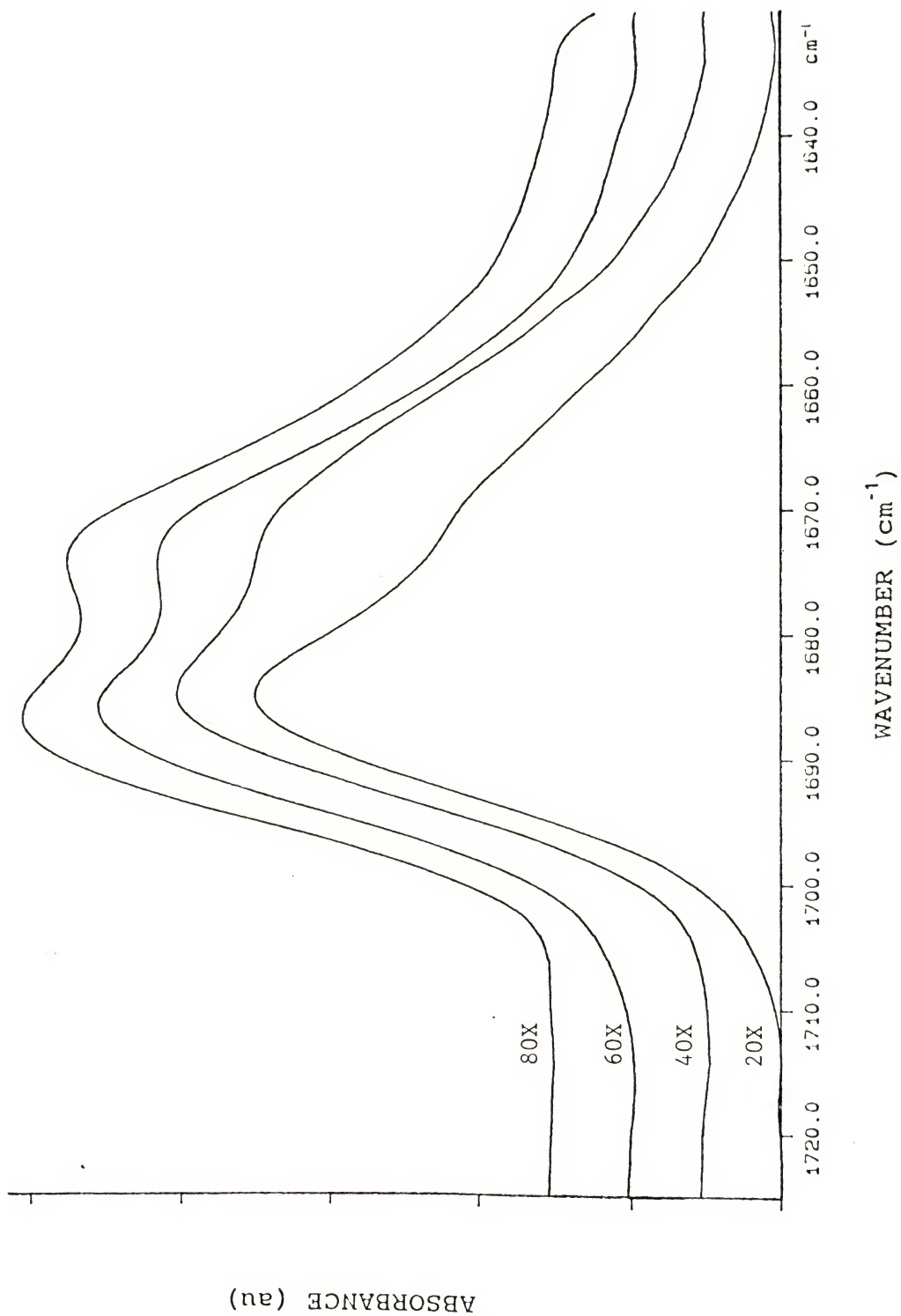


Figure 3-15 Spectra of the Carbonyl Region of Acetylated Ordered Polymer Samples (1.5%; 20X, 40X, 60X and 80X) (Polystyrene subtracted) (Nujol Mulls)

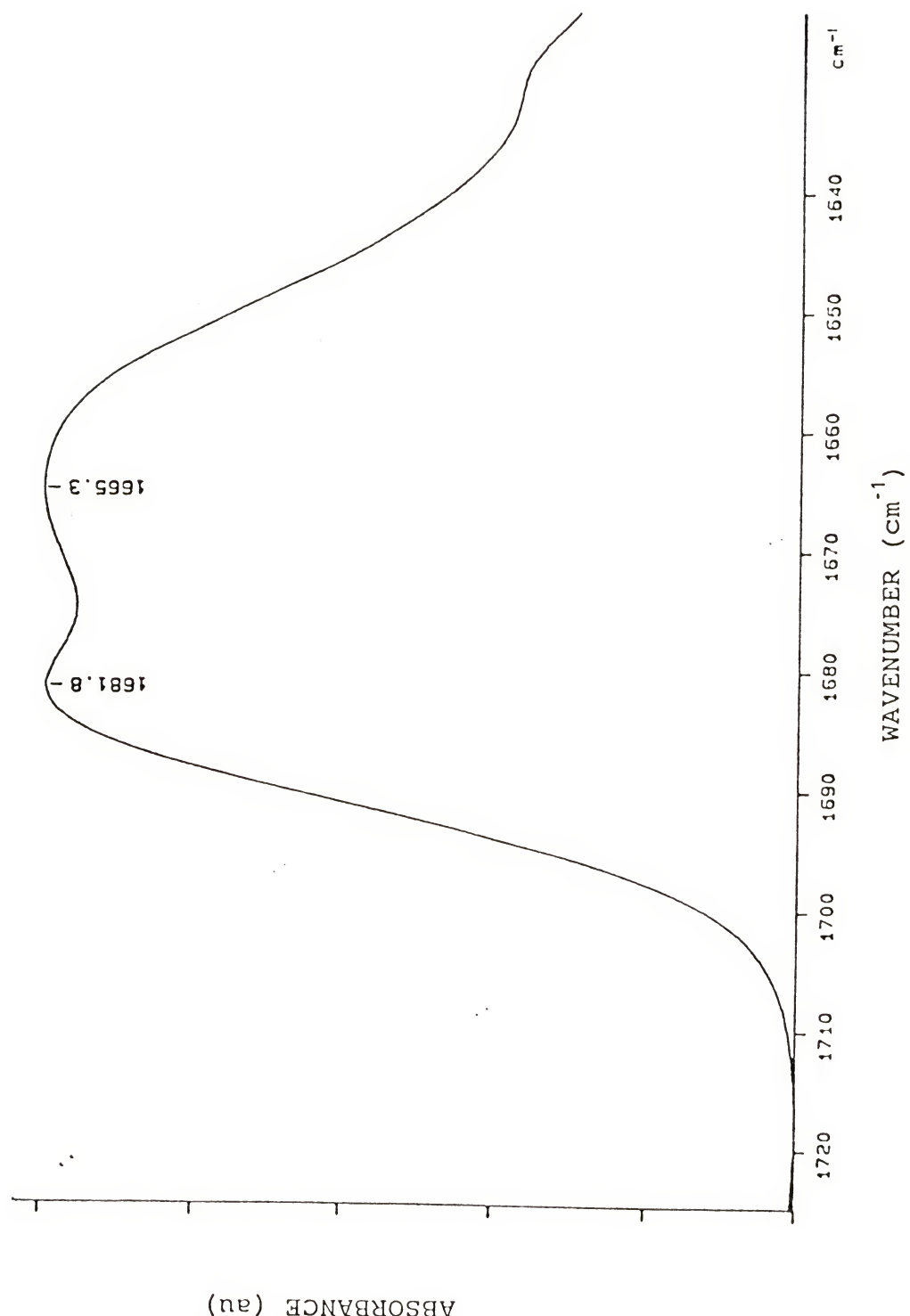


Figure 3-16 Spectrum of 7.3 mol% Polymer-bound Benzylamine

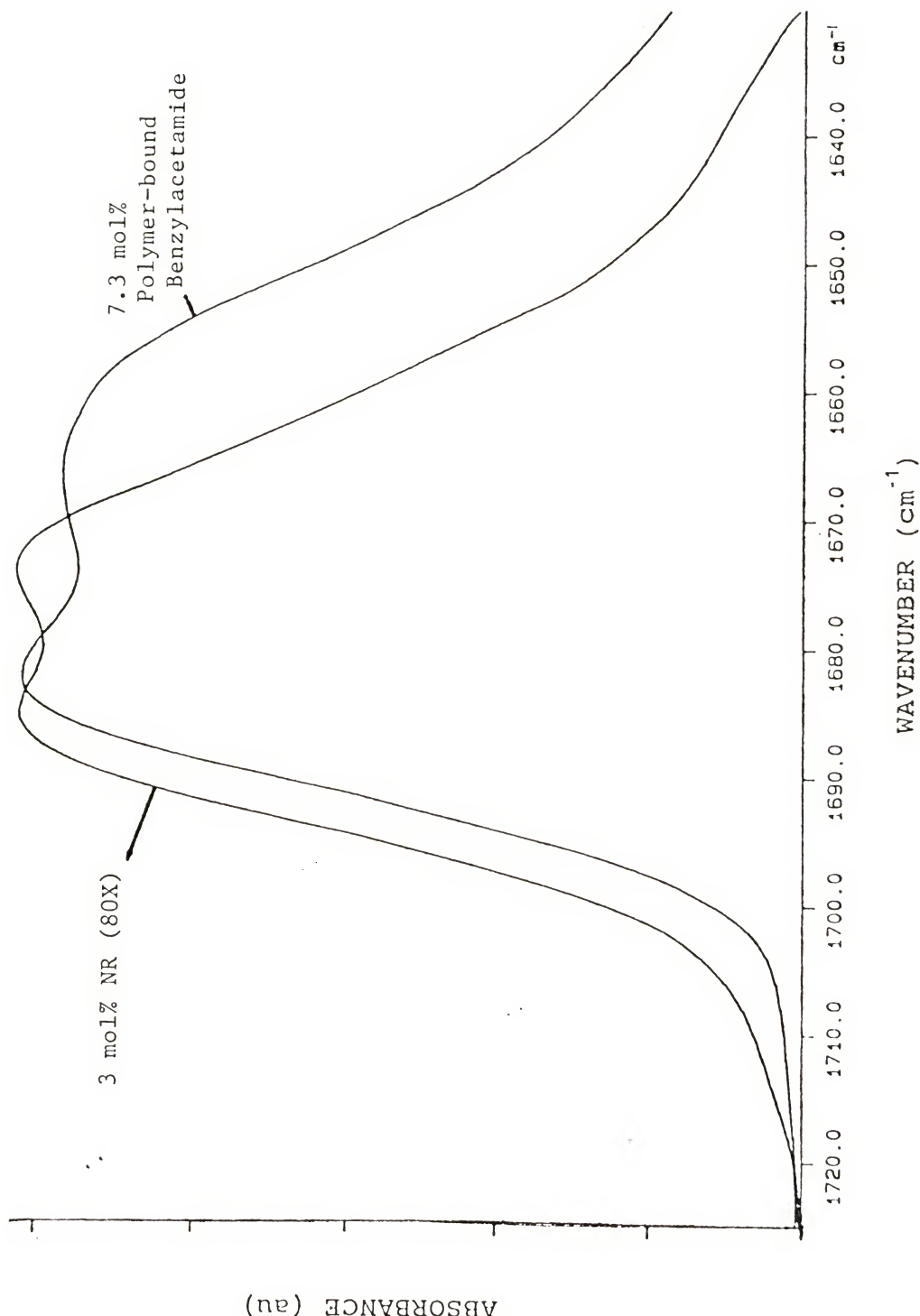


Figure 3-17 Spectrum of 7.3 mol% Polymer-bound Benzylacetamide Superimposed with the 3 mol% NR (80X) Carbonyl Spectrum

Figure 3-17

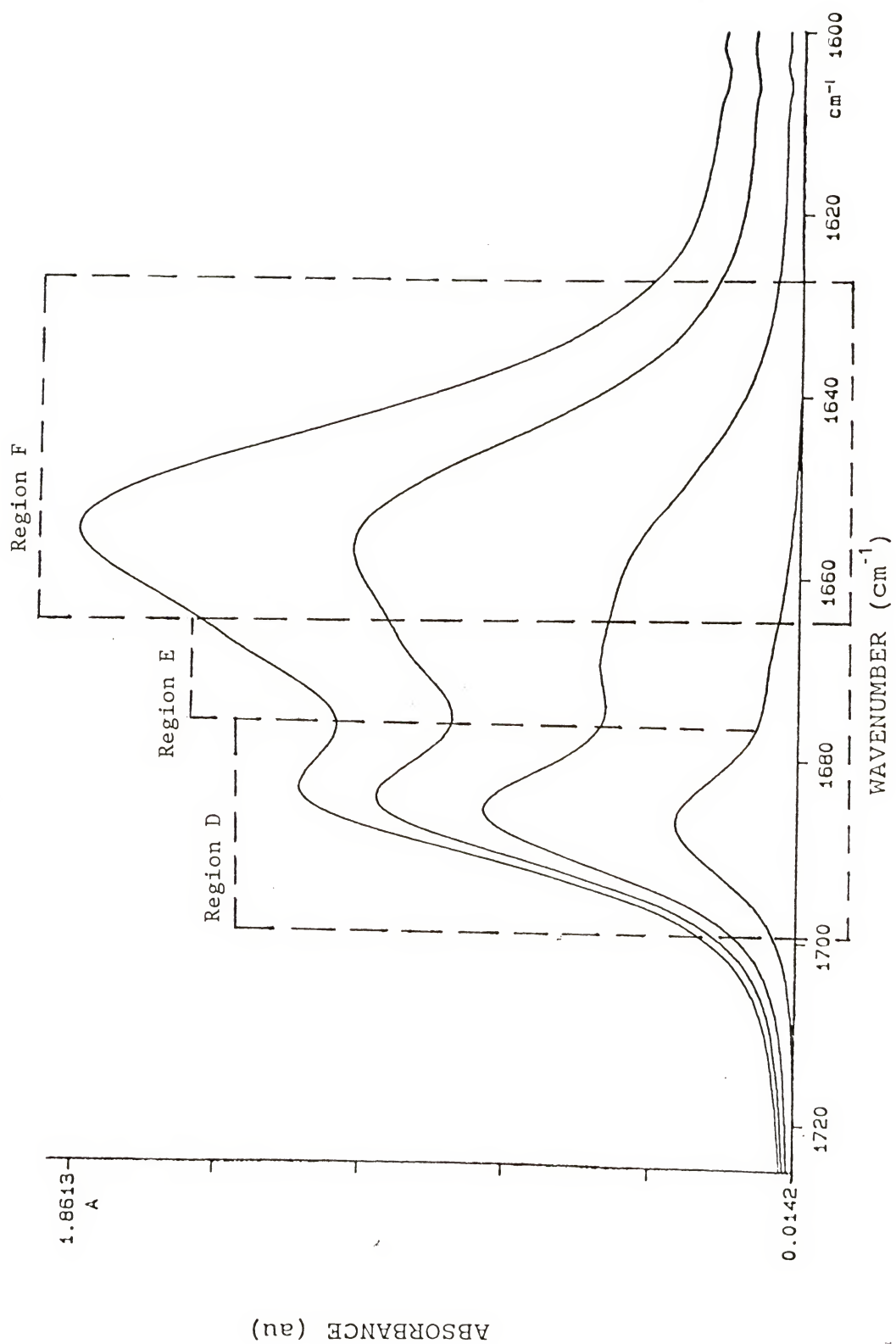


Figure 3-18 IR Spectra of the Carbonyl Region of Various Concentrations of N-Benzylacetamide in Toluene (Toluene Subtracted)

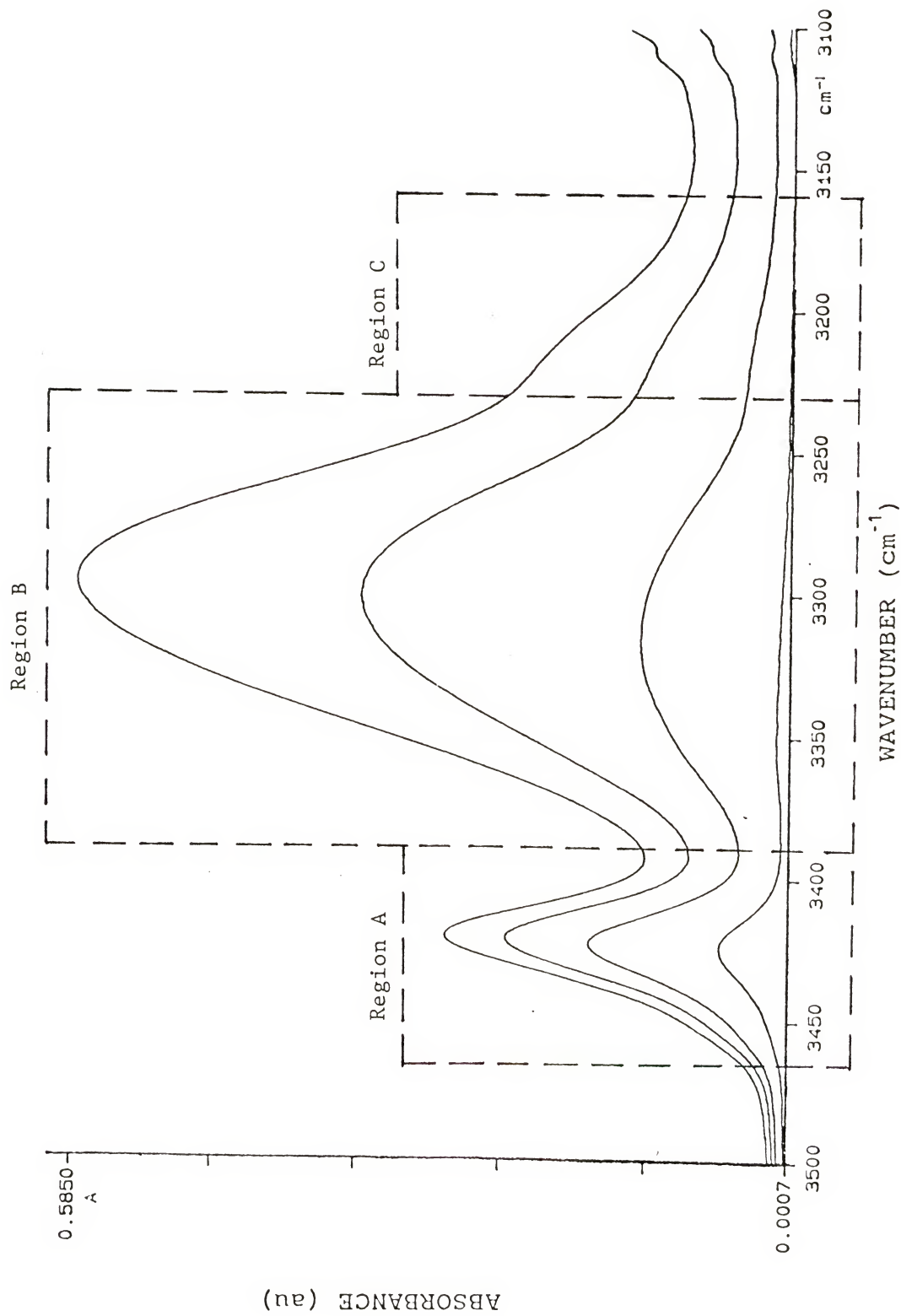


Figure 3-19 IR Spectra of the NH Region of Various Concentrations of N-Benzylacetamide in Toluene (Toluene Subtracted)

Figure 3-19

3.3.6 Conclusions

As the cross-linking increases, the fraction of the total carbonyl absorption area attributable to hydrogen bonding in the ordered polymer increases. Clearly this indicates that the amine groups of the ordered polymers remain in closer proximity than those of the random polymer, and as the degree of cross-linking increases, an increasing fraction the amine groups remain in close proximity. No trend was discerned from the examination of hydrogen bonding in the random polymer samples.

Site accessibility decreases as the crosslinking increases for both the ordered and the random polymers, but the accessibility decreases more rapidly for the ordered polymers. The accessibility to ordered polymers is less than that of the random polymers for 40X, 60X and 80X crosslinking. It is concluded that the carbamate monomer is incorporated into the growing polymer chains slowly while the silanediamine monomer is incorporated quickly. As discussed in chapter 1, the result is that the carbamate monomers are more likely to be incorporated into lightly crosslinked regions while the silanediamine monomers are more likely to be incorporated into more heavily crosslinked regions.

The fact the yield of the acetylation of the 20X ordered polymers is higher than the yield for the 20X random polymers in spite of the expected heavier crosslinking suggests that the actual amine concentration is higher than the

concentration calculated from the initial masses of monomers used in each sample. This is consistent with the idea that the silanediamine monomer has a relatively high reactivity. Because no polymerization can go to completion, the fraction of silanediamine monomers left unincorporated should be small compared to the fraction of unincorporated styrene monomers.

3.4 Measure of Proximity by the Amine-catalyzed Aldol Condensation of Phenylacetaldehyde

3.4.1 The Rationale for the Use of the Amine-catalyzed Aldol Condensation of Phenylacetaldehyde for the Measure of Proximity

If a reaction is catalyzed by amine intermediates, then it is possible that a polymer in which the amine groups are bound in close proximity during its preparation (i.e., the silanediamine-loaded polymers) might show greater activity for catalysis of that reaction than the randomly loaded amine polymers or than amines in solution.

3.4.2 The Amine-catalyzed Aldol Condensation of Phenylacetaldehyde

The condensation reaction is shown in Figure 3-20; a possible mechanism is shown in Figure 3-21. Notice that in Figure 3-21, a key step in the amine-catalyzed reaction is the reaction of an enamine intermediate with an imine. This step is the justification for the expectation of catalysis since the enamine is known to be a better nucleophile than the corresponding enol and the imine is a better electrophile than

the corresponding carbonyl compound. Support for this mechanism comes from studies in which the concentrations of enamines was shown to be similar in magnitude to the concentrations of enols even for relatively small concentrations of primary amines [82MI1]. Furthermore "the equilibrium between carbonyl compounds and imines is known to be established rapidly under relatively mild conditions" [71MI1].

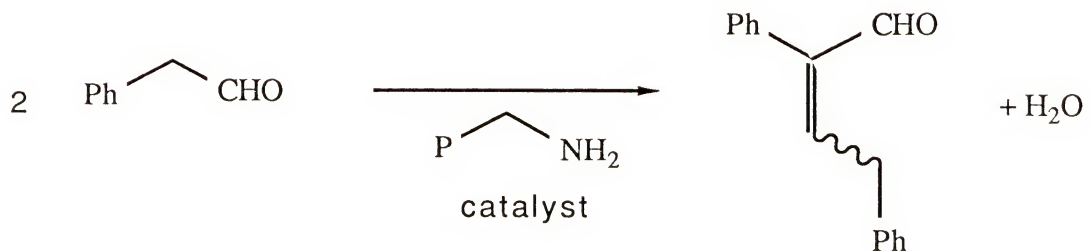


Figure 3-20 Stoichiometry of the Amine-catalyzed Aldol Condensation of Phenylacetaldehyde

3.4.3 Conditions, Analysis and Results of the Condensation Reaction

The reactions were set up in screw cap vials containing weighed quantities of 20X, 40X, 60X and 80X random and ordered polymers loaded at approximated 3.0, 1.5, 0.5 and 0.1 mol%. Triethylamine (NEt_3) and acetic acid were chosen to buffer the

reaction in order to insure the presence of at least some of the amine groups in the polymers were in their neutral (non-protonated) forms, and because tertiary amines are poor catalysts for amine-catalyzed aldol reactions [68MI1].

The reaction was allowed to proceed for one week, at which time 10.0 ml of methylene chloride was added to each vial. Typically after one week the color of the the more highly loaded polymers solids (i.e., 3 and 1.5 mol%, both random and ordered) had changed from white to a yellowish-green. This color development was characteristic of the reactions of phenylacetaldehyde using benzylamine and tertiary amine buffer solutions that were investigated before attempting the polymer catalyzed reactions. The methylene chloride was added to each vial to insure extraction of the products of the reaction. Then, 24 hours after the addition of the methylene chloride, aliquots of each reaction mixture were taken, diluted and analyzed by GC/MS. A typical gas chromatogram is shown in Figure 3-22 in which peaks 225, 587, 608 and 623 were obtained. Peak 225 is phenylacetaldehyde, peaks 587 and 623 are cis- and trans-crotanaldehyde [54JA5466], but peak 608 is an unknown substance with a parent mass of about 209. The total ion current of peaks 225, 587, 608 and 623 of each sample were integrated, and the ratios of the peaks that are shown in Tables 3-10 and 3-11 were calculated.

3.4.4 Discussion of the Condensation Results

The data in Tables 3-13 and 3-14 show that there is no advantage to catalysis of the aldol reaction by amine polymers (whether random or ordered) over that of the tertiary amine buffer solution. In fact, the data for the 20X random polymer show some possibility for catalysis, but the effect does not seem to be substantial and could simply be the appearance of randomness in the data.

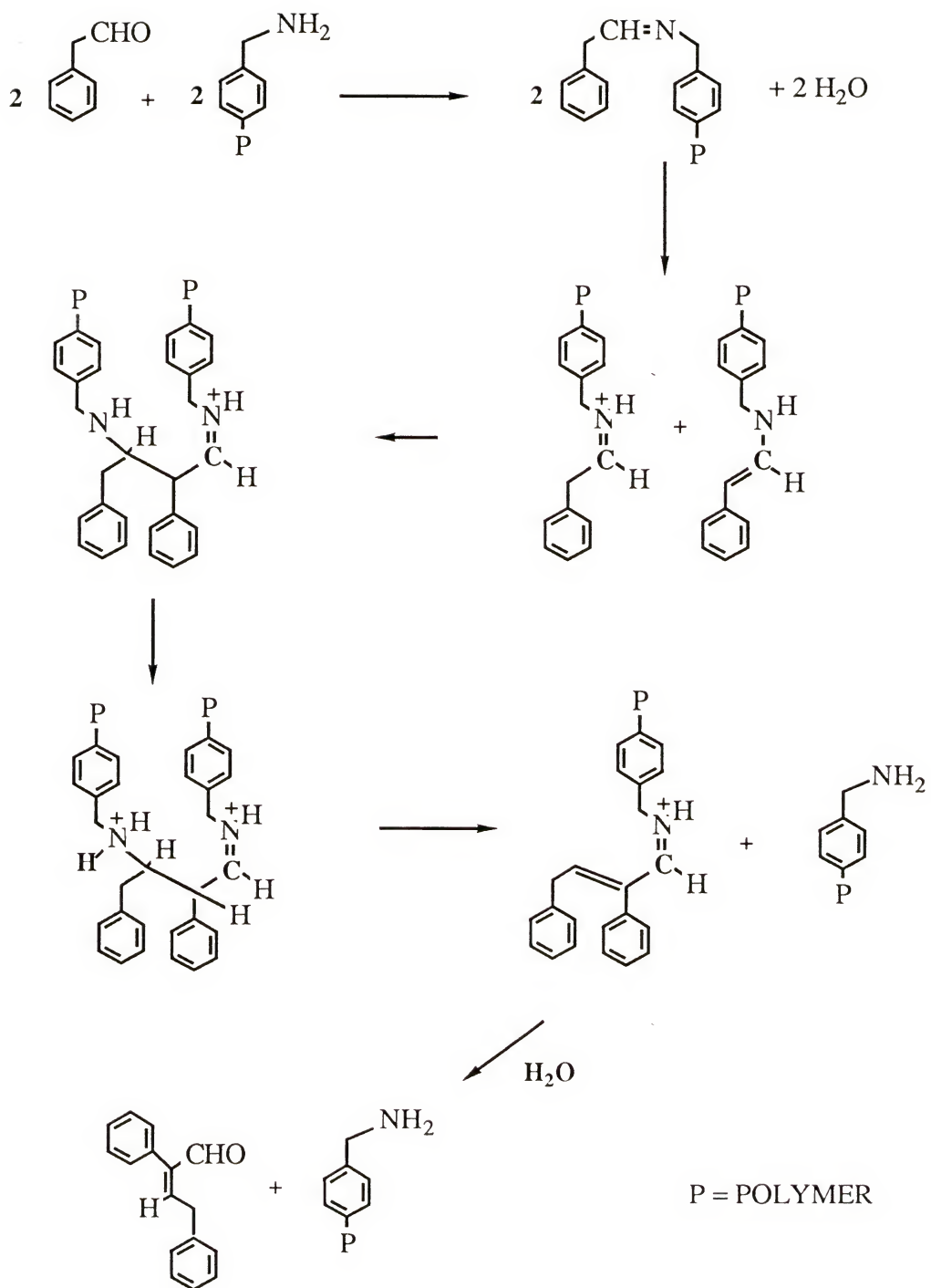
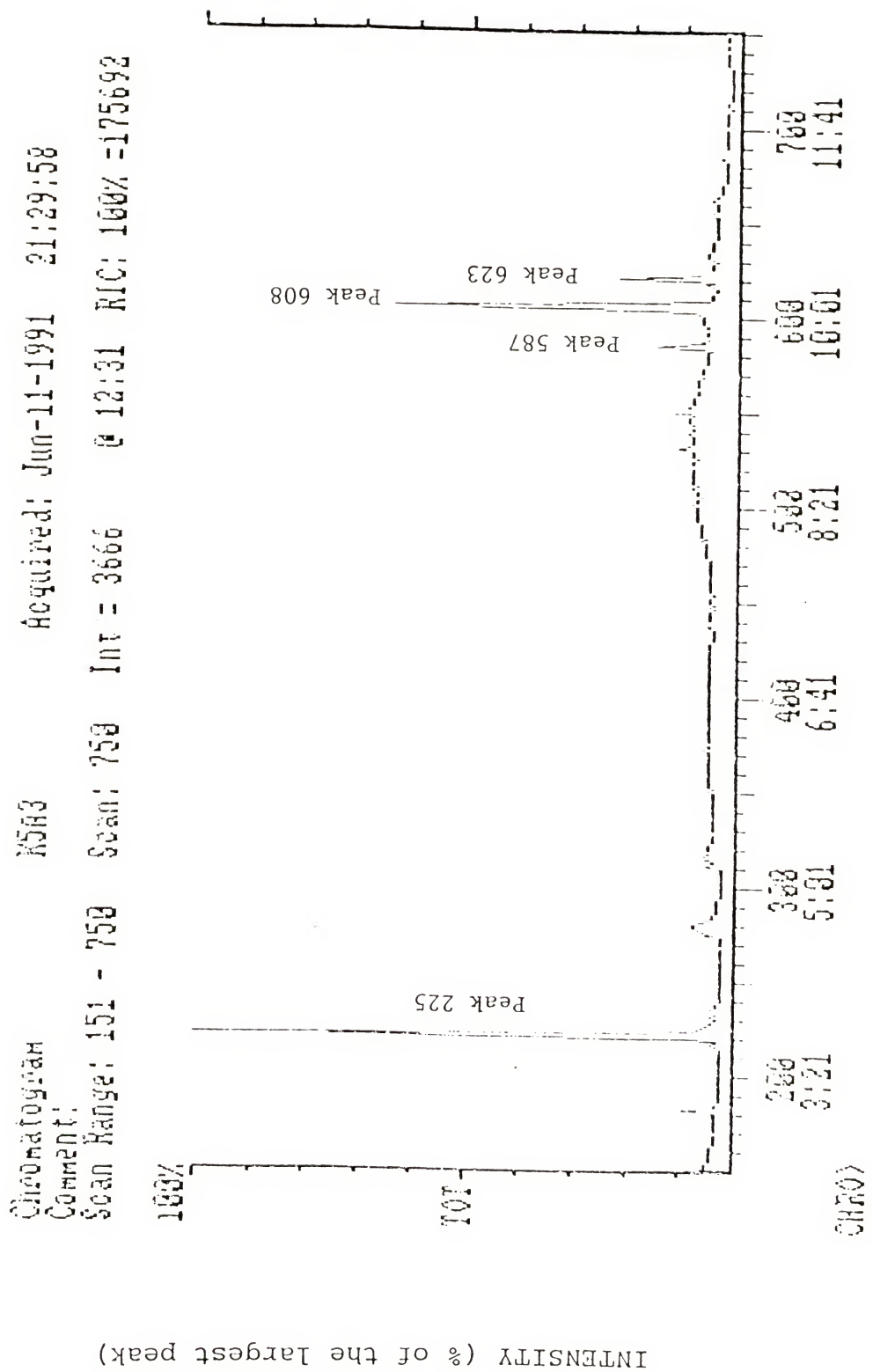


Figure 3-21 Possible Mechanism of the Amine-catalyzed Aldol Condensation of Phenylacetaldehyde



RETENTION TIME (upper scale--seconds; lower scale--minutes:seconds)

Figure 3-22 GC Trace of an Extract of the Aldol Reaction

Table 3-13 Results of Amine-catalyzed Aldol Condensation
of Phenylacetaldehyde

	AMINE CONCN MOL%	PEAK AREA 587/225	PEAK AREA 608/225	PEAK AREA 623/225
BLANK	0.00	0.1455	0.2293	0.0848
20X RANDOM	3.6	0.0549	0.0883	0.0373
	1.6	0.0828	0.0904	0.0352
	0.44	0.1202	0.9096	0.2336
	0.11	0.1174	0.3660	0.1360
20X ORDERED	2.9	0.1178	0.3147	0.1257
	1.5	0.0963	0.3406	0.1100
	0.53	0.0946	0.2521	0.1198
	0.11	0.1709	0.1379	0.0413
40X RANDOM	2.6	0.0969	0.2597	0.0996
	1.4	0.0726	0.2093	0.0855
	0.39	0.1070	0.3040	0.1300
	0.10	0.0906	0.3534	0.1034
40X ORDERED	3.1	0.0997	0.2785	0.1123
	1.5	0.0968	0.2911	0.0882
	0.53	0.0592	0.1826	0.0863
	0.11	0.1194	0.1170	0.0317
60X RANDOM	2.3	0.1325	0.5912	0.2768
	0.82	0.0742	0.2316	0.0925
	0.40	0.0755	0.2634	0.0805
	0.10	0.0934	0.6948	0.1660
60X ORDERED	3.3	0.0874	0.2720	0.0788
	1.5	0.0889	0.3048	0.0938
	0.58	0.1580	0.2033	0.0714
	0.10	0.1435	0.1843	0.0597
80X RANDOM	1.7	0.0865	0.2295	0.1191
	1.1	0.0603	0.2006	0.0749
	0.47	0.0871	0.2963	0.0622
	0.11	0.1007	0.3050	0.0867
80X ORDERED	3.4	0.0864	0.2818	0.0962
	1.8	0.1206	0.9094	0.2153
	0.49	0.0974	0.2440	0.1314
	0.10	0.1293	0.1505	0.0486

Table 3-14 Results of Amine-catalyzed Aldol Condensation
of Phenylacetalddehyde (On an equivalent basis)

	AMINE CONCN MOL%	EQ AMINE X 10 ³	PEAK AREA 587/225 PER EQ. AMINE	PEAK AREA 608/225 PER EQ AMINE	PEAK AREA 623/225 PER EQ AMINE
RANDOM 20X	3.7	9.4	5.8	9.4	4.0
	1.7	8.6	9.6	10	4.1
	0.44	5.8	21	160	41
	0.11	1.6	72	220	83
	2.9	6.5	18	48	19
	1.5	11	8.8	31	10
ORDERED 20X	0.53	7.5	13	33	16
	0.11	3.7	46	37	11
	2.6	6.6	15	40	15
	1.4	6.5	11	32	213
	0.39	5.5	19	55	24
	0.10	2.2	41	160	47
RANDOM 40X	3.12	8.6	12	32	13
	1.5	7.6	13	38	12
	0.53	8.1	7.3	23	11
	0.11	3.1	39	38	10
	2.3	4.7	28	130	59
	0.82	3.3	23	71	28
ORDERED 60X	0.40	8.2	9.2	32	9.8
	0.10	2.3	41	310	73
	3.3	9.4	9.3	29	8.4
	1.5	6.9	13	44	14
	0.58	7.3	22	28	9.7
	0.10	3.3	44	57	18
RANDOM 80X	1.7	4.0	22	57	30
	1.1	4.4	14	45	17
	0.47	6.9	13	43	9.1
	0.11	2.4	42	130	36
	3.4	7.6	11	37	13
	1.8	7.9	15	110	27
ORDERED 80X	0.49	9.7	10	25	14
	0.10	3.3	39	46	15

CHAPTER 4 CONCLUSIONS

No significant difference was found in the mobility (i.e. distance moved) of the amine groups for the 20X, 40X, 60X and 80X crosslinked random polystyrene polymers. No conclusions are drawn from the results of the coupling reactions that were performed on the 20X, 40X, 60X and 80X crosslinked ordered polymers.

The method of coupling the random and ordered polymers with carbonyldiimidazole followed by analysis by IR spectroscopy gave accessibilities to the amine groups for the various degrees of crosslinking.

A theoretical model whose development is given in Appendix A can be used to convert the coupling of the amine groups of the random polymers into measurements of the distances that at some time the amine groups must have moved in order to form urea. The theoretical model of the amine groups in the random polymers was developed because it was not possible to measure the distribution and because it is not possible to prepare a polymer in which the amine groups are spaced with well defined distances in the sample. The model treats the amine groups as a random distribution of spheres in the presence of other similar sized spheres. The coupling

results when interpreted by the theoretical model show little difference between the distance that the amine groups can move (see Table A-4) for the different degrees of crosslinking.

From the theoretical model and the results of this research, it is possible to conclude that site isolation in crosslinked polystyrene can be achieved only with low loadings and not by increasing the degree of crosslinking.

In contrast to the above results, the study of hydrogen bonding of the acetylated amine polymers showed that the mobility of the amine groups increases as the crosslinking decreases; however it is not possible to affix numerical values to the distances between the acetamide groups. Even if it were possible, the results of the hydrogen bonding study do not contradict the findings of the coupling experiments. In the coupling experiments it is possible to "trap" the amine groups that are attached to polymer chains that are in a non-relaxed conformations since the formation of urea from the two amine groups releases a substantial amount of free energy on formation. The amount of energy involved in hydrogen bonding, however, is much less than that of the formation of urea so that the observation of the effects of hydrogen bonding implies that the polymer chains are not deformed from their relaxed conformation by the occurrence of the hydrogen bond.

There is another substantial distinction between the experiments. The coupling of the amine groups is an essentially irreversible event while hydrogen bonding is a

very reversible phenomenon. While both the formation of urea and acetamide occur in the presence of the solvent THF (which is a good solvent for polystyrene) so that the amine groups should have added mobility due to the solvent assisting the movement of the bound monomer units, it was necessary to wash and dry all samples for analysis by IR spectroscopy. The removal of the solvent from the acetylated samples allowed the polymer chains to return to their relaxed conformations, while the polymer sample on which the irreversible coupling reactions had been carried out, need not nor should return to their original or relaxed conformations.

Accessibility to the amine groups is given by both the coupling and the acetylation reactions, and both methods give comparable results. The average results are given in Table 3-8 for the reactions with carbonyldiimidazole and in Table 3-11 for the acetylation reaction. In general the accessibility of the sites decreases as the degree of crosslinking increases. Access to the amines in the ordered polymers decreases with increasing crosslinking more rapidly than access in the random polymers.

It is concluded (based on the IR analyses of the BOC polymers and repeated CHN analyses of the silanediamine-loaded polymers) that the BOC monomer is incorporated into the growing polymer chains slowly while the silanediamine monomer is incorporated quickly. As discussed in chapter 1, the result is that the BOC monomers are more likely to be

incorporated into lightly crosslinked regions and the silanediamine monomers are more likely to be incorporated into more heavily crosslinked regions.

The fact the yield of the acetylation of the 20X ordered polymers is higher than the yield for the 20X random polymers, in spite of the expected heavier crosslinking, suggests that the actual amine concentration is higher than the concentration calculated from the initial masses of monomers used in each sample. This is consistent with idea that the silanediamine monomer has a relatively high reactivity. Because no polymerization can go to completion, the fraction of silanediamine monomers left unincorporated should be small compared to the fraction of unincorporated styrene monomers.

No evidence of catalysis of the aldol condensation of phenylacetaldehyde was found for either the random or the ordered amine polymers at any of the concentrations studied.

CHAPTER 5 EXPERIMENTAL SECTION

5.1 Introduction

Melting points are recorded in degrees Centigrade (°C) and are uncorrected. Melting points were determined with a Thomas-Hoover Unimelt capillary melting apparatus. Infrared spectra were recorded on a Perkin-Elmer model 1600 infrared spectrophotometer. Nuclear magnetic resonance spectra were recorded on the Varian VXR-300 and/or the General Electric QE-300 spectrometers. All chemical shifts (δ) are recorded in parts per million (ppm) downfield from tetramethylsilane as an internal reference. Multiplicities of proton resonances are designated as singlet (s), doublet (d), triplet (t), doublet of doublets (dd), multiplet (m) or broad (br). The composition of vaporizable compounds was checked by GC/MS in the departmental analytical laboratory under the supervision of Dr. David H. Powell. CHN analyses were also performed in the departmental analytical laboratory under the supervision of Mr. Mel Courtney. Solvent removal was performed at reduced pressure on a Buchi Rotavapor-R which was equipped with either a water aspirator or a mechanical vacuum pump.

5.2 Syntheses

5.2.1 Silanediamine Compounds

Silanamine compounds in which the amine group is a pyrrolidyl moiety are named by Chemical Abstracts as derivatives of pyrrolidine. Those silanediamines compounds which contain two pyrrolidyl moieties (attached to silicon) are named 1,1'-(R¹R²silylene)bis(pyrrolidine).

5.2.2 1,1'-(Diphenylsilylene)bis(pyrrolidine), 10

To a round bottom flask were added anhydrous diethyl ether (5 ml) and 2.5M n-butyllithium in hexane (4.6 ml, 11.4 mmol, 1.2 eq.). The round bottom flask was ice cooled while freshly distilled pyrrolidine (1.19 ml, 14.3 mmol, 1.5 eq.) was slowly added. Dichlorodiphenylsilane (1.00 ml, 4.76 mmol, 1.0 eq.) was then slowly added. A white precipitate immediately formed. After 30 minutes, the mixture was filtered through glass wool. The solvent was removed from the filtrate in vacuo and hexane was added. The resulting mixture was again filtered through glass wool, and the solvent was removed from the filtrate in vacuo. The residue was purified by chromatography on neutral alumina with hexane. The final product was a clear colorless liquid: 1.16 g (76%); ¹H-NMR (CDCl₃) δ1.74 (m, 8H), 3.075 (t, 8H), 7.35 (m, 4H), 7.57 (m, 6H); ¹³C-NMR (CDCl₃) δ26.9, 47.6, 127.5, 129.0, 134.4, 135.3. MS: m/z (% relative intensity) 322 (M⁺, 25.00), 252 (46.15), 251 (76.81), 183 (100.00), 182 (10.19), 181 (46.33), 176

(12.02). MS (HR) for $C_{20}H_{26}N_2Si$ calcd. 322.1865; found: 322.1855.

5.2.3 1,1'-(Bis(1-methylethyl)silylene)bis(pyrrolidine), 11

A round bottom flask was flame-dried. After the flask was cooled, tetrahydrofuran (10 ml) and 2.5M n-butyllithium in hexanes (4.43 ml, 11.1 mmol, 5.0 eq.) were added to the flask. While the flask was being ice-cooled, freshly distilled pyrrolidine was slowly added. After a few minutes bis(1-methylethyl)-dichlorosilane (0.411g, 2.22 mmol, 1.0 eq.) was added to the round bottom flask. After 3 days the contents of the flask were partitioned between hexane and water. The hexane layer was dried with anhydrous sodium sulfate, after which the solvent was removed in vacuo. The residue was a clear colorless liquid: 0.268g (94%); 1H -NMR ($CDCl_3$) δ 1.00 (d and m, 28H), 1.665 (q, 8H), 3.008 (t, 8H); ^{13}C -NMR ($CDCl_3$) δ 13.5, 18.1, 26.6, 47.4. Mass spectrum: m/z (% relative intensity) 255 ($[M + 1]^+$, 16.39), 254 (M^+ , 27.32), 253 (39.60), 211 (100.00), 184 (11.75), 142 (69.42), 114 (17.74). MS (HR) for $C_{14}H_{30}N_2Si$ calcd. 254.2178; found: 254.2166.

5.2.4 1,1'-(1,1-Dimethylethyl)phenylsilylene)bis-(pyrrolidine), 12

Tetrahydrofuran (10 ml) and 2.5M n-butyllithium in hexanes (3.80 ml, 9.49 mmol, 5.0 eq.) were added to a flame dried round bottom flask. The flask was chilled to $-78^{\circ}C$, and then freshly distilled pyrrolidine (1.58ml, 19.0 mmol,

10.0 eq.) was added slowly. After the solution was allowed to warm up to room temperature, *tert*-butylphenyldichlorosilane (0.20 ml, 0.949 mmol, 1.0 eq.) was added to the flask. After 4 days the solution was partitioned between hexane and water. The organic layer was dried with anhydrous sodium sulfate, and the solvent was removed in vacuo. The product was purified by chromatography on a column of neutral alumina (deactivated by 10% H₂O) with hexane eluent. The solvent was removed in vacuo to leave a clear, colorless liquid: 0.25g (87%); ¹H-NMR (CDCl₃) δ0.998 (s, 9H), 1.73 (m, 8H), 3.09 (m, 4H), 7.33 (m, 3H), 7.60 (m, 2H); ¹³C-NMR (CDCl₃) δ20.1, 26.8, 27.9, 40.1, 127.3, 128.6, 135.4, 137.0. MS: m/z (% relative intensity) 302 (M⁺, 1.56), 245 (100.00), 232 (1.72), 177 (11.67), 176 (69.55), 175 (2.40). MS (HR) for C₁₈H₃₀N₂Si calcd. 302.2178; found: 302.2172.

5.2.5 Bis(1,1-dimethylethyl)chlorosilylpyrrolidine, 13

To a flame dried round bottom flask were added n-butyllithium in hexanes (0.946 ml, 2.37 mmol, 5.0 eq.) and 10 ml tetrahydrofuran. The flask was chilled to -78°C. Pyrrolidine (0.395 ml, 4.732 mmol, 10 eq.) was added slowly. After the flask was allowed to warm to room temperature, bis(1,1-dimethylethyl)dichlorosilane (0.10 ml, 0.473 mmol, 1.0 eq.) was added to the flask. After 6 days the solution was partitioned between hexane and water. The organic layer was dried with anhydrous sodium sulfate, and the solvent was

removed in vacuo. The product was purified by chromatography on a column of neutral alumina (deactivated by 10% H₂O) with hexane as an eluent. The eluent was removed in vacuo, leaving a clear, colorless liquid: 0.112g (95%); ¹H-NMR (CDCl₃) δ1.09 (s, 18H), 1.716 (m, 4H), 3.17 (t, 4H); ¹³C-NMR (CDCl₃) δ24.3, 26.6, 28.2, 49.0. MS: m/z (% relative intensity) 248 ([M + 1]⁺, 32.71), 247 (M⁺, 30.74), 212 (100.00), 192 (4.76), 190 (11.72). MS (HR) for C₁₂H₂₆ClNSi calcd. 247.1523; found: 247.1516.

5.2.6 4-Vinylbenzoic acid, 14

A round bottom flask was flame dried and connected to a reflux condenser. Magnesium (1.45 g, 59.8 mmol) was slightly ground and added to the flask with 40 ml of anhydrous tetrahydrofuran. The magnesium was refluxed with methyl iodide (0.52 ml, 8.30 mmol). After 30 minutes 4-chlorostyrene (5.0 ml, 41.5 mmol) was added to the reaction mixture, and the refluxing was continued for another five hours. The mixture was allowed to cool to room temperature, and then was poured onto crushed dry ice. After the dry ice had sublimed, the resulting solid was mixed with dilute sodium hydroxide. The resulting mixture was filtered through celite, and the filtrate was extracted with chloroform. The aqueous phase was acidified and again extracted with chloroform. The latter chloroform extract was dried with anhydrous sodium sulfate, and the solvent was removed in vacuo yielding a white solid:

4.44 g (72%), mp 140-142°C (lit 140-142°C [84MI3]); $^1\text{H-NMR}$ (CDCl_3) δ 5.42 (d, 1H), 5.90 (d, 1H), 6.78 (dd, 1H), 7.50 (d, 2H), 8.08 (d, 2H), 12.63 (br s, 1H); $^{13}\text{C-NMR}$ (CDCl_3) δ 116.9, 126.2, 128.5, 130.5, 135.9, 142.7, 171.4. MS(EI): m/z (% relative intensity) 149 ($[\text{M} + 1]^+$, 8.40), 148 (M^+ , 100.00), 132 (8.27), 131 (75.36), 103 (36.49). MS (HR) for $\text{C}_9\text{H}_8\text{O}_2$ calcd. 148.0524; found: 148.0521.

5.2.7 4-Vinylbenzamide, 15

4-Vinylbenzoic acid (4.44 g, 30.0 mmol) and recently distilled thionyl chloride (7.56 ml, 12.5 g, 104.5 mmol) were gently refluxed in a 250 ml round bottom flask. After one hour excess thionyl chloride was distilled off. Anhydrous ether (25 ml) was added to the round bottom flask, and anhydrous ammonia was admitted to the flask until it stopped being absorbed. The contents of the flask were poured into cold, concentrated ammonium hydroxide. The organic material was extracted into a solution of tetrahydrofuran and chloroform, and then dried with anhydrous magnesium sulfate. The solvent was removed in vacuo. To insure the complete removal of tetrahydrofuran, toluene (25 ml) was added to the flask, and much of the solvent was distilled at atmospheric pressure. The remaining toluene was removed in vacuo to give a white solid: 7.67g (84%); mp 167-169°C (lit. 169-170°C [83MI2]); $^1\text{H-NMR}$ (CDCl_3) δ 5.38 (d, 1H), 5.86 (d, 1H), 6.75 (dd, 1H), 7.48 (d, 2H), 7.78 (d, 2H); $^{13}\text{C-NMR}$ (DMSO-d_6) δ 116.4,

126.4, 127.8, 128.1, 131.9, 135.8, 169.1. The NH peaks were very broad and highly variable in location. MS(EI): m/z (% relative intensity) 148 ($[M + 1]^+$, 7.97), 147 (M^+ , 26.81), 131 (34.78), 105 (28.26), 104 (35.87), 103 (83.33), 44 (100.00). MS (HR) for C_9H_9NO calcd. 147.0684; found: 147.0689.

5.2.8 4-Vinylbenzylamine, 16

A 500 ml round bottom flask was flame dried. Diethyl ether (200 ml) and 4-vinylbenzamide (7.67 g, 52.14 mmol) were added and stirred with a magnetic stirrer. Lithium aluminum hydride (7.72 g, 203.3 mmol) was added in small bits in order to keep the foaming under control. After the addition was complete, the mixture was gently refluxed for two hours. The excess $LiAlH_4$ was then neutralized by the careful addition of water, followed by concentrated sodium hydroxide. The ether layer was decanted, and the solvent was removed in vacuo. The residue was dissolved in a solution of chloroform and tetrahydrofuran. This solution was extracted three times with 1 M hydrochloric acid. The combined aqueous acid extracts were made basic and extracted with methylene chloride. The combined methylene chloride layers were dried with anhydrous sodium sulfate, and the solvent was removed in vacuo leaving a clear, yellow liquid: 4.575 g (71%). When pure samples of 4-vinylbenzylamine were needed for further syntheses, portions of this crude product were distilled bulb to bulb in a kugelrohr tube to yield a clear, colorless liquid: mp 0-3°C;

¹H-NMR (CDCl₃) 1.60 (location and breadth were highly variable, s, 2H), 3.85 (s, 2H), 5.20 (d, 1H), 5.75 (d, 1H), 6.70 (dd, 1H), 7.30, 7.40 (m, m, 4H); ¹³C-NMR (CDCl₃) δ 45.8, 113.0, 126.0, 126.9, 135.8, 136.2, 142.7. MS(EI): m/z (% relative intensity) 134 ([M + 1]⁺, 12.50), 133 (M⁺, 100.00), 117 (37.92), 116 (45.41), 105 (87.08), 44 (97.51). MS (HR) for C₉H₁₁N calcd. 133.0891; found: 133.0888.

5.2.9 1,1-Diphenyl-N,N'-dibenzylsilanediamine, 17

A 50 ml round bottom flask was flame dried. Diphenyl-dichlorosilane (5.0ml, 6.02g, 23.8 mmol), toluene (20 ml), triethylamine (7.3 ml, 5.3 g, 52.3 mmol, 2.2 eq.), and benzylamine (6.0 ml, 5.90 g, 52.3 mmol, 1.1 eq.) were added to the flask. A copious amount of white precipitate formed immediately. After eighteen hours the mixture was filtered, and the solid was washed with toluene. The solvent was removed from the combined filtrates in vacuo. The liquid residue was distilled bulb to bulb in a kugelrohr tube at 0.1 torr and 180-270°C. The distilled material formed a solid which was recrystallized from hexane: 4.25 g (45%), mp 55-72 (lit. no mp reported [53JA995, 79MI]); ¹H-NMR (CDCl₃) δ 1.62 (t, 2H), 4.12 (d, 4H), 7.30 and 7.70 (m and m, 20H); ¹³C-NMR (CDCl₃) δ 45.6, 126.4, 127.0, 127.8, 128.3, 129.6, 134.7, 134.9, 143.7. MS (HR) for C₂₆H₂₇N₂Si [M + 1]⁺ calcd. 395.1944; found: 395.1941.

5.2.10 1,1-Bis(1-methylethyl)-N,N'-dibenzylsilanediamine, 18

A round bottom flask was flame dried. Toluene (5 ml), distilled benzylamine (0.67 ml, 6.09 mmol), and 1,1-bis(1-methylethyl)dichlorosilane (0.25 ml, 1.385 mmol) were added. A copious amount of white precipitate formed immediately. After 24 hours, the mixture was filtered, and the solvent was removed in vacuo. The remaining solvent and excess benzylamine were removed at 0.5 torr and 90-100°C leaving a clear liquid: 0.44 g (99%); $^1\text{H-NMR}$ (CDCl_3) δ 0.90 (t, 2H), 1.05 (d and m, 14H), 4.07 (d, 4H), 7.28 (m, 10H); $^{13}\text{C-NMR}$ (CDCl_3) δ 12.9, 18.2, 45.7, 126.3, 126.8, 128.2, 144.5. MS: m/z (% relative intensity) 283 (43.86), 220 (3.24), 178 (12.01), 177 (15.98), 176 (100.00). MS (HR) for $\text{C}_{20}\text{H}_{30}\text{N}_2\text{Si}$ $[\text{M} + 1]^+$ calcd. 327.2257; found: 327.2256.

5.2.11 1-tert-Butyl-1-phenyl-N,N'-dibenzylsilanediamine, 19

A round bottom flask was flame dried. n-Butyllithium in hexanes (2.5 M, 1.10 ml, 2.2 eq.) was added to the flask, which was then cooled to -78°C. Benzylamine (1.30 ml, 11.86 mmol, 10 eq.) was added and the flask was allowed to warm up to room temperature. Upon addition of the benzylamine to the flask a deep red solution was formed. (1,1-Dimethyl-ethyl)phenyldichlorosilane (0.25 ml, 1.19 mmol, 1.0 eq.) was added to the flask. After three days the solvent was removed in vacuo, and diethyl ether was added to the round bottom flask. A white solid was present which did not dissolve in the

diethyl ether. The mixture was filtered, and the solvent of the filtrate was removed in vacuo. A bulb to bulb transfer in a kugelrohr tube was made at 170°C and 0.1 torr. The excess benzylamine was removed from the distillate at 100°C and 0.1 torr leaving a clear, colorless liquid: 0.426g (96%); ¹H-NMR (CDCl₃) δ1.00 (s, 9H), 1.30 (t, 2H), 4.10 (d, 4H), 7.30, 7.68, 7.80 (m, m, m, 15H); ¹³C-NMR (CDCl₃) δ18.7, 27.5, 46.0, 126.6, 127.1, 128.3, 128.5, 128.8, 135.4, 144.5. MS: m/z (% relative intensity) 318 (11.21), 317 (41.67), 211 (18.92), 210 (100.00). MS (HR) for C₂₄H₃₁N₂Si [M + 1]⁺ calcd. 375.2256; found: 375.2267.

5.2.12 1,1-Di-tert-butyl-N,N'-dibenzylsilanediamine, 20

5.2.12.1 First method

A solution of lithium benzylamide in THF was prepared in a flame dried round bottom flask by the addition of n-butyl-lithium (3.52 ml, 8.80 mmol, 5.0 eq.) to freshly distilled benzylamine (1.92 ml, 1.89 g, 17.6 mmol, 10.0 eq.) in THF at -78°C. This solution was allowed to warm up to room temperature and di-tert-butyldichlorosilane (0.373 ml, 0.376 g, 1.76 mmol, 1.0 eq.) was added. At the end of four days the reaction mixture was extracted between hexane and water. The organic phase was dried with anhydrous sodium sulfate, and the solvent was removed in vacuo. The residue was chromatographed on neutral alumina (deactivated by 10% water by weight). The column, prepared in hexane, was eluted with hexane. The

appropriate fractions were combined, and the solvent was removed in vacuo, yielding a clear, colorless liquid: 0.51 g (82%); $^1\text{H-NMR}$ (CDCl_3) δ 0.90 (t, 2H), 1.07 (s, 18H), 4.12 (d, 4H), 7.30 (m, 10H).

5.2.12.2 Second method

A round bottom flask was flame dried. Benzene (10 ml), freshly distilled triethylamine (0.20 ml, 1.435 mmol, 2.3 eq.), and benzylamine (0.20 ml, 1.85 mmol, 3.0 eq.) were added to the flask. The flask was moved to a dry box and di-tert-butylsilyl ditriflate (0.20 ml, 0.617 mmol, 1.0 eq.) was added. After 36 hours the benzene solvent was removed in vacuo, and hexane was added. The hexane solution was filtered, and the solvent was removed from the filtrate in vacuo leaving a clear, colorless, viscous liquid: 0.214 g (98%); $^1\text{H-NMR}$ (CDCl_3) δ 0.90 (t, 2H), 1.07 (s, 18H), 4.12 (d, 4H), 7.30 (m, 10H); $^{13}\text{C-NMR}$ (CDCl_3) δ 21.7, 28.9, 46.3, 126.2, 126.5, 128.2, 144.4. MS (CI): m/z (% relative intensity) 356 ($[\text{M} + 2]^+$, 27.66), 355 ($[\text{M} + 1]^+$, 100.00), 354 (M^+ , 0.42), 298 (68.93), 297 (15.94), 248 (38.02). MS (HR) for $\text{C}_{22}\text{H}_{34}\text{N}_2\text{Si}$ calcd. 354.2491; found: 354.2494. MS (HR) for the ion [tert -Bu-Si(NH-CH₂-Ph)₂]⁺ calcd. 297.1787; found: 297.1791.

5.2.13 1,1-Di-*tert*-butyl-N,N'-bis(4-vinylbenzyl)silane-diamine, 21

Freshly kugelrohr distilled 4-vinylbenzylamine (0.5463 g, 4.10 mmol, 2.20 eq.) was added to a flame dried round bottom flask. This was followed by 10 ml of dry benzene and freshly

distilled triethylamine (0.57 ml, 0.415 g, 4.10 mmol, 2.20 eq.). This solution and di-*tert*-butylsilyl ditriflate were transferred to a dry box where the ditriflate (0.605ml, 0.821 g, 1.86 mmol, 1.0 eq.) was added to the flask. The flask was left in the lab freezer overnight and warmed up the next morning. The benzene solvent was removed in vacuo. The residue was partitioned between ether and aqueous sodium bicarbonate. The ether was removed in vacuo, and methylene chloride was added to dissolve the residue. The solution was dried with anhydrous sodium sulfate, filtered, and the solvent was removed from the filtrate in vacuo. The residue was chromatographed on a column of neutral alumina (deactivated by 10% H₂O) prepared in hexane. The residue was eluted with hexane, the appropriate fractions were combined, and the solvent was removed in vacuo leaving a clear, colorless liquid: 1.04 g (77%); ¹H-NMR (CDCl₃) δ 0.90 (t, 2H), 1.06 (s, 18H), 4.10 (d, 4H), 5.20 (d, 2H), 5.72 (d, 2H), 6.70 (dd, 2H), 7.30 (m, 8H); ¹³C-NMR (CDCl₃) δ 21.7, 28.9, 46.0, 113.0, 126.1, 126.6, 135.7, 136.7, 141.1. The viscous liquid crystallized after two months; the solid was recrystallized from petroleum ether: mp 53-55°C. MS(CI): m/z (% relative intensity) 408 ([M + 2]⁺, 14.77), 407 ([M + 1]⁺, 77.81), 349 (6.15), 274 (1.94), 54 (100.00). MS (HR) C₂₆H₃₉N₂Si [M+1]⁺ calcd. 407.2883; found: 407.2880.

Anal. for $C_{26}H_{38}N_2Si$:

Calcd: C, 76.25; H, 10.01; N, 6.87.

Found: C, 76.29; H, 9.61; N, 6.75.

5.2.14 O-(tert-Butyl)-N-(4-vinylbenzyl)carbamate, 22

4-Vinylbenzylamine (0.133 g, 0.998 mmol) which had not been kugelrohr distilled, methylene chloride (5 ml), di-*tert*-butyl dicarbonate (0.275 ml, 0.26 g, 1.20 mmol), and potassium carbonate (0.276 g, 1.99 mmol) were placed in a flame dried round bottom flask. After 24 hours the mixture was filtered and the solvent was removed in vacuo leaving a clear, colorless liquid. A column of neutral alumina (10% water by weight) in hexane was prepared. The residue was eluted with hexane. The appropriate fractions were combined and the solvent was removed in vacuo leaving a white solid. The solid was recrystallized from petroleum ether, and the solid was filtered. The solvent remaining on the solid was removed in vacuo: 0.14 g (59%), mp 58.5-59.5°C; 1H -NMR ($CDCl_3$) δ 1.46 (s, 9H), 4.28 (d, 2H), 4.95 (br s, 1H), 5.74 (d, 1H), 6.70 (dd, 1H), 7.25 (d, 2H), 7.38 (d, 2H); ^{13}C -NMR ($CDCl_3$) δ 28.3, 44.4, 79.4, 113.7, 126.3, 127.6, 136.3, 136.6, 138.5, 155.8. The relatively low yield resulted from the use of starting material which contains some polymeric impurities. MS(EI): m/z (% relative intensity) 234 ($[M + 1]^+$, 2.99), 233 (M^+ , 4.85), 179 (25.37), 178 (62.31), 177 (16.79), 133 (49.63), 132 (100.00), 117 (58.21), 116 (29.10), 59 (16.79), 58 (53.73), 42

(52.61). MS (HR) for $C_{14}H_{19}NO_2$ calcd. 233.1416; found: 233.1422.

Anal. for $C_{11}H_{19}NO_2$:

Calcd: C, 71.64; H, 8.74; N, 5.99.

Found: C, 71.79; H, 8.40; N, 5.93.

5.2.15 N-(4-Vinylbenzyl)acetamide, 23

4-Vinylbenzylamine (0.585 g, 4.39 mmol) which had not been kugelrohr distilled, acetic anhydride (2.0 ml, 20.0 mmol), and anhydrous pyridine (4.0 ml, 49.5 mmol) were added to a round bottom flask. After several hours, the liquid was extracted into diethyl ether; the ether was washed with aqueous acid and base. The ether solvent was dried with anhydrous magnesium sulfate, filtered, and the solvent was removed in vacuo. The remaining solid was chromatographed on column of neutral alumina in methylene chloride using methylene chloride as the eluent. The appropriate fractions were combined, and the solvent was removed in vacuo. The remaining solid was recrystallized from a mixture of hexane and methylene chloride: 0.37 g (48%); mp 90-93°C; 1H -NMR ($CDCl_3$) δ 1.985 (s, 3H), 4.37 (d, 2H), 5.24 (d, 1H), 5.73 (d, 1H), 6.16 (Broad s, 1H), 7.24 (d, 2H), 7.35 (d, 2H); ^{13}C -NMR ($CDCl_3$) δ 23.3, 43.5, 114.0, 126.5, 128.1, 136.3, 136.6, 138.5, 155.8. MS(EI): m/z (% relative intensity) 176 ($[M + 1]^+$, 95.80), 175 (M^+ , 19.87), 133 (50.24), 132 (100.00), 117 (66.88), 106 (56.38), 105 (35.70). MS (HR) for $C_{11}H_{13}NO$ calcd. 175.0997; found: 175.0995.

Anal. for $C_{11}H_{13}NO$:

Calcd: C, 74.97; H, 7.96; N, 7.98.

Found: C, 75.11; H, 7.60; N, 7.91.

5.2.16 O-(tert-Butyl)-N-benzylcarbamate, 24

Benzylamine (1.11 g, 10.36 mmol), methylene chloride (5 ml), di-*tert*-butyl dicarbonate (3.00 ml, 2.85 g, 13.06 mmol), and potassium carbonate (2.76 g, 20.0 mmol) were placed in a flame dried round bottom flask. After 24 hours the mixture was filtered and the solvent was removed in vacuo leaving a clear, colorless liquid. A column of neutral alumina (10% water by weight) in hexane was prepared and the liquid was added to it. The column was eluted with hexane. The appropriate fractions were combined and the solvent was removed in vacuo leaving a white solid. The solid was recrystallized from petroleum ether to give 24: 2.77 g (70%), mp 53.5-54.5°C, lit 53°C [82JOC2697]; 1H -NMR ($CDCl_3$) δ 1.46 (s, 9H), 4.31 (d, 2H), 4.88 (br s, 1H), 7.29 (m, 5H); ^{13}C -NMR ($CDCl_3$) δ 28.4, 44.6, 79.4, 127.3, 127.4, 128.5, 138.9, 155.9. MS: m/z (% relative intensity) 208 ($[M + 1]^+$, 4.00), 152 (100.00), 108 (19.64), 106 (100.00), 58 (57.09), 57 (17.82), 42 (29.82). A gas chromatogram of the final product is shown in Figure 5-1.

Anal. for $C_{12}H_{17}NO_2$:

Calcd: C, 69.11; H, 8.80; N, 6.75.

Found: C, 69.17; H, 8.25; N, 6.56.

5.2.17 O-(tert-Butyl)-N-(4-methylbenzyl)carbamate, 25

4-Methylbenzylamine (0.495 g, 4.088 mmol), methylene chloride (5 ml), di-*tert*-butyl dicarbonate (1.14 ml, 1.08 g, 4.95 mmol), and potassium carbonate (1.38 g, 10.0 mmol) were placed in a flame dried round bottom flask. After 16 hours the mixture was filtered and the solvent was removed in vacuo leaving a clear, colorless liquid. A column of neutral alumina (10% water by weight) in hexane was prepared. The residue was eluted with hexane. The appropriate fractions were combined, and the solvent was removed in vacuo leaving a white solid. The solid was crystallized from hexane and dried in vacuo to give 25: 0.735 g (81%); mp 71-72°C; $^1\text{H-NMR}$ (CDCl_3) δ 1.46 (s, 9H), 2.33 (s, 3H), 4.27 (d, 2H), 4.79 (br s, 1H), 7.16 (m, 4H); $^{13}\text{C-NMR}$ (CDCl_3) δ 21.1, 28.2, 28.4, 44.4, 127.5, 129.2, 135.9, 136.9, 155.8. MS: m/z (% relative intensity) 222 ($[\text{M} + 1]^+$, 5.94), 166 (100.00), 165 (13.37), 121 (44.55), 120 (96.04), 106 (91.58), 105 (75.25). MS (HR) for $\text{C}_{13}\text{H}_{19}\text{NO}_2$ calcd. 221.1416; found: 221.1396. A gas chromatogram of the final product is shown in Figure 5-1.

Anal. for $\text{C}_{13}\text{H}_{19}\text{NO}_2$:

Calcd: C, 70.11; H, 9.21; N, 6.32.

Found: C, 70.31; H, 8.90; N, 6.25.

5.2.18 N-Benzylacetamide, 26

Benzylamine (15.4 g, 144 mmol), acetic anhydride (28.8 ml, 288 mmol), and anhydrous pyridine (46.6 ml, 576 mmol) were added to a round bottom flask. After several hours the liquid was extracted into diethyl ether; the ether was washed with aqueous acid and base. The ether was dried with anhydrous magnesium sulfate, filtered, and the solvent was removed in vacuo: 19.3 g (90%); mp 60-61°C (lit 61°C [38JA657]); ¹H-NMR (CDCl₃) δ 2.01 (s, 3H), 4.42 (d, 2H), 5.87 (br s, 1H), 7.30 (m, 5H); ¹³C-NMR (CDCl₃) δ 23.2, 43.7, 127.5, 127.8, 128.7, 138.2, 169.8. MS: m/z (% relative intensity) 150 ([M + 1]⁺, 11.48), 149 (M⁺, 60.93), 107 (50.55), 106 (100.00), 91 (53.86). A gas chromatogram of the final product is shown in Figure 5-1.

Anal. for C₉H₁₁NO:

Calcd: C, 72.05; H, 7.92; N, 9.38.

Found: C, 72.59; H, 7.60; N, 9.31.

5.2.19 N-(4-Methylbenzyl)acetamide, 27

4-Methylbenzylamine (0.482 g, 3.27 mmol), acetic anhydride (0.70 ml, 7.03 mmol), and anhydrous pyridine (1.4 ml, 17.3 mmol) were added to a round bottom flask. After several hours the liquid was extracted into diethyl ether; the ether was washed with aqueous acid and base. The ether solvent was dried with anhydrous magnesium sulfate, filtered, and the solvent was removed in vacuo. The solid was crystallized from hexane to give 27: 0.446 g (72%); mp 110-

111°C (lit 111-112°C [25JA3055]); $^1\text{H-NMR}$ (CDCl_3) δ 1.99 (s, 3H), 2.33 (s, 3H), 4.36 (d, 2H), 5.89 (br s, 1H), 7.15 (m, 4H); $^{13}\text{C-NMR}$ (CDCl_3) δ 21.0, 23.2, 43.5, 127.8, 129.3, 135.2, 137.2, 169.8. The relatively low yield results from the use of starting material which contains some polymeric impurities. MS: m/z (% relative intensity) 164 ($[\text{M} + 1]^+$, 16.00), 163 (M^+ , 53.41), 148 (16.00), 120 (45.88), 106 (100.00), 105 (48.47). A gas chromatogram of the final product is shown in Figure 5-2.

Anal. for $\text{C}_8\text{H}_{13}\text{NO}$:

Calcd: C, 73.14; H, 8.55; N, 8.57.

Found: C, 73.36; H, 8.15; N, 8.43.

5.2.20 N,N'-Dibenzylurea, 28

Freshly distilled benzylamine (4.9 g, 46 mmol, 5 ml) was refluxed with dimethylcarbonate overnight. The next day the low boiling components were removed by distillation. The contents of the flask were crystallized from toluene, then CHCl_3 , and finally EtOH to give white crystals, mp 166-167°C (lit. 169°C [34JA144]); $^1\text{H-NMR}$ (DMSO-d_6) δ 4.23 (d, 4H), 6.46 (t, 2H), 7.27 (m, 10H); $^{13}\text{C-NMR}$ (DMSO-d_6) δ 42.9, 126.4, 126.9, 128.1, 140.8, 158.0. MS: m/z (% relative intensity) 241 ($[\text{M} + 1]^+$, 7.97), 240 (M^+ , 17.23), 134 (2.93), 107 (51.93), 106 (100.00), 79 (61.08), 77 (26.03). A gas chromatogram of the final product is shown in Figure 5-2.

Anal. for $C_{15}H_{16}N_2O$:

Calcd: C, 74.58; H, 7.15; N, 11.65.

Found: C, 74.75; H, 6.68; N, 11.61.

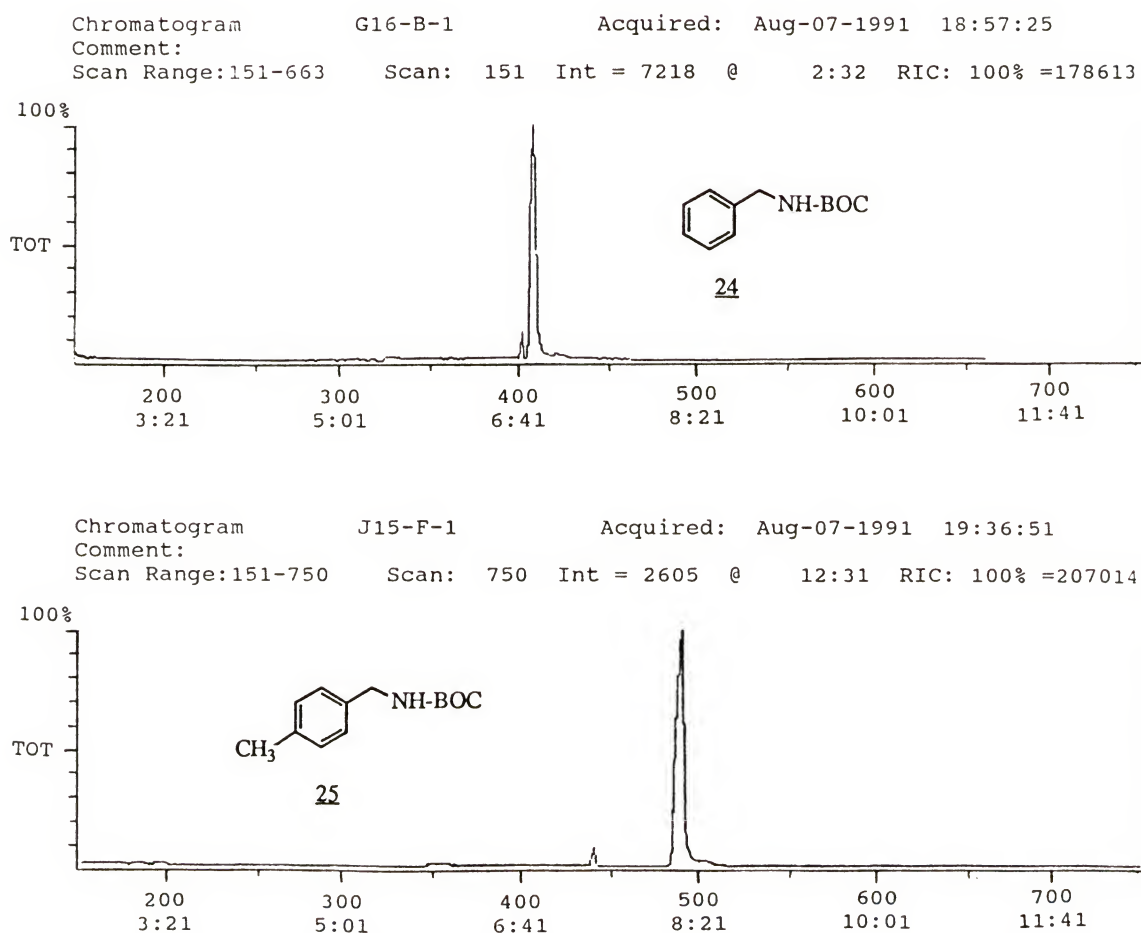


Figure 5-1 Gas chromatograms of compounds 24 and 25

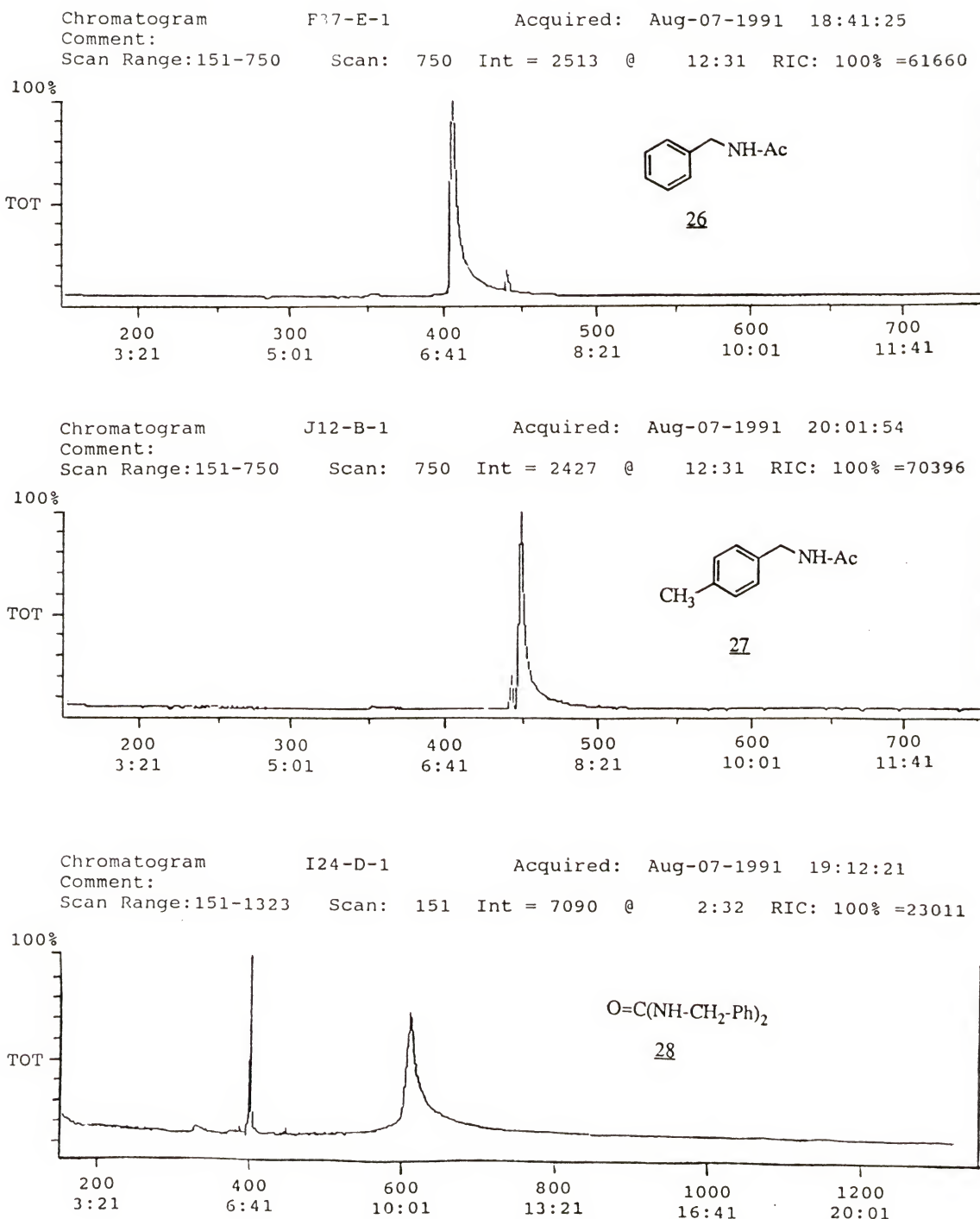


Figure 5-2 Gas chromatograms of compounds 26, 27 and 28

5.3 Polymer Preparation

5.3.1 General Synthetic Method for the Preparation of Polymers (Known to be Macroporous)

The monomers were combined with styrene and a commercial divinylbenzene reagent using AIBN as the initiator. The divinylbenzene was 81 mol% divinylbenzene and 19 mol% ethylvinylbenzene. The divinylbenzene fraction was a mixture of meta and para isomers in the ratio m/p=2.2. The polymerization were carried out in anhydrous DMSO solvent at 100°C under an N₂ atmosphere for 24 hours. The monomer mixtures were prepared such that for a given loading of functional group the divinylbenzene constituted 20, 40, 60 or 80 mol% of the total monomer composition. Polymers were prepared at the above degrees of crosslinking and at loadings such that the final amine concentration would be 3.0, 1.5, 0.5 and 0.1 mol%. The quantity of DMSO varied from 1.2 to 1.4 times the combined massed of the comonomers of the samples.

5.3.2 Preparation of N-(4-Vinylbenzyl)acetamide Copolymers

5.3.2.1 Preparation of 20 mol% Crosslinked Polymers

The solutions I37-A and I37-B, whose compositions are given in Table 5-1, were prepared and mixed. Vials were then labelled, tared and various amounts of I37-A and I37-B were added to the tared vials with each addition being weighed and the masses recorded.

The masses of I37-A and I37-B were then used to calculate the concentrations of each component of each pre-polymer sample. Assuming complete incorporation of the monomers, the mol% of the loading of the acetamide monomer as a percentage of the aromatic moieties is given by the equation:

Table 5-1 Composition of Reagents Used for the Preparation of 20X N-(4-Vinylbenzyl)acetamide 23 Copolymer Calibration Samples

I37-A = 20X comonomer blank solution			
I37-B = 7.333 mol% acetamide, 20X comonomer solution			
I37-B = 0.1898 g acetamide + 3.9225 g of I37-A			
	I37-A	I37-B	
AMIDE	---	0.1898	GRAMS
	---	1.083	MMOL
STYRENE	3.2883	1.0286	GRAMS
	31.573	9.876	MMOL
DVB	1.5854	0.4959	GRAMS
	12.178	3.809	MMOL
DMSO	7.5927	2.3751	GRAMS
AIBN	0.0728	0.0228	GRAMS
	0.443	0.139	MMOL

mol% N-(4-Vinylbenzyl)acetamide =

$$(13.64 + (\frac{\text{mass of I37-A}}{\text{mass of I37-B}} * 13.25))^{-1} \quad \text{eqn (5-1)}$$

The samples in each vial were degassed, sealed under nitrogen and then polymerized at 100°C for 24 hours. The samples were then crushed and extracted with H₂O and CH₂Cl₂,

with the extracting solvents being changed periodically. After a few days the samples were washed with anhydrous ethanol, anhydrous methylene chloride and dried under a stream of nitrogen. Each sample was analyzed by IR as its nujol mull. The results of the IR measurements are shown in Table 5-2.

Table 5-2 Data from IR Measurements of 20X N-(4-Vinylbenzyl)acetamide 23 Calibration Samples

SAMPLE	INITIAL MASS CONCN MOL%	AMIDE AREA	AROMATIC AREA
I40-A	0.51	4.31	34.18
I40-F	0.97	8.07	32.06
I39-E	1.5	10.91	25.84
I41-A	1.9	17.69	33.18
I41-A	1.9	9.03	17.92
I39-D	2.0	9.77	18.14
I39-C	2.4	14.57	21.01
I39-B	2.8	9.66	12.54
I39-A	3.3	28.58	28.13
I40-B	3.3	30.73	33.25
I40-B	3.3	25.38	28.34
I38-F	3.7	27.21	23.30
I41-B	3.8	22.55	22.43
I38-E	4.2	12.10	10.01
I40-E	4.5	42.29	29.99
I40-E	4.5	32.59	25.75
I41-C	4.5	31.63	25.89
I41-C	4.5	22.45	18.44
I38-D	4.6	18.07	12.10
I38-C	5.1	27.75	17.04
I40-D	5.5	49.99	27.79
I40-D	5.5	43.27	24.87
I38-B	5.5	51.97	28.70
I38-A	6.0	43.02	22.61
I40-C	6.5	67.62	33.37
I40-C	6.5	42.93	21.11
I37-F	6.5	31.65	15.40
I37-E	6.9	43.51	18.48
I37-D	7.3	26.69	10.84

Table 5-3 Composition of Reagents used for the Preparation of 80X N-(4-Vinylbenzyl)acetamide
23 Calibration Curve Samples

I109-A = 0.1253 g amide + 1.0998 g DMSO			
I110-D = 0.4250 g I109-D + 0.4850 g DVB + 0.0101 g AIBN = 5.813 mol% N-(4-Vinylbenzyl)acetamide in 80X comonomer solution			
80X Comonomer Solutions			
I109-A		I110-D	
Amide	---	0.04347	grams
		0.2481	mmol
DVB REAGENT	0.9282	0.4850	grams
	8.995	4.700	mmol
DMSO	1.1039	0.6312	grams
			mmol
AIBN	0.0219	0.0101	grams
	0.133	0.062	mmol

5.3.2.2 Preparation of 80 mol% Crosslinked Polymers

The solutions I109-D and I110-D, whose compositions are given in Table 5-3, were prepared and thoroughly mixed. Vials were then labelled, tared and various amounts of I109-D and I110-D were added to the tared vials with each addition being weighed and the masses recorded. The samples in the vials were degassed of oxygen and sealed under nitrogen. The samples were then polymerized at 100°C for 24 hours. The masses of I109-D and I110-D were then used to calculate the theoretical concentrations of each polymer sample. Assuming complete incorporation of the monomers, the mol% of the loading of the acetamide monomer is given by the equation:

mol% N-(4-Vinylbenzyl)acetamide =

$$(17.20 + (\frac{\text{mass of I109-D}}{\text{mass of I110-D}} * 13.42))^{-1} \quad \text{eqn (5-2)}$$

The results of the measurements by IR spectroscopy of the 80X samples are shown in Table 5-4.

Table 5-4 Data from IR Measurements on 80X N-(4-Vinylbenzyl)acetamide 23 Calibration Curve Samples

Sample	Concn mol%	Aromatic Area	Amide Area
I113-G	0.89	42.30	12.42
I113-F	1.7	50.54	23.30
I113-E	2.5	44.60	30.96
I113-D	3.2	43.78	51.85
I113-C	4.1	37.83	59.37
I113-B	4.5	16.34	33.41
I113-A	5.2	15.24	30.18

CHN Analysis: Sample I38-A (see Table 5-2 and Appendix B)

Estimated (w/AIBN): C, 90.28; H, 7.71; N, 1.18

Estimated (wo/AIBN): C, 90.71; H, 7.72; N, 0.73

Found: C, 90.49; H, 7.91; N, 0.81

5.3.3 Preparation of Silanediamine-loaded Copolymers

A typical set of polymers loaded with 1,1-di-*tert*-butyl-*N,N'*-bis(4-vinylbenzyl)silanediamine (SiN₂) at crosslinking percentages of 20%, 40%, 60% and 80% is shown in Table 5-6.

Solutions J1-X, X = A,B,C,D and I118-B shown in Table 5-5 were prepared and used to prepare the final comonomer mixtures. The above reagents and DMSO were combined to make the samples J3-A, J3-B, J3-C and J3-D. The solutions were thoroughly mixed, degassed, sealed under an N₂ atmosphere and polymerized at 100°C for 24 hours.

The masses of solutions given in Table 5-6 permit the calculation of the reagents shown in Table 5-7.

At the end of 24 hours the polymer samples were crushed, extracted with CH₂Cl₂ and H₂O over one to several days. The mixture was filtered and the polymer was washed with anhydrous ethanol and anhydrous methylene chloride. The polymers were dried under a stream of nitrogen.

CHN Analysis: Sample J4-D-3 (from J3-D) (see above)

Estimated (w/AIBN): C, 91.03; H, 8.10; N, 0.55

Estimated (wo/AIBN): C, 91.24; H, 8.09; N, 0.33

Found: C, 90.76; H, 8.08; N, 0.35

The dried silanediamine containing polymers were placed in a vial with enough glacial acetic acid and anhydrous tetrahydrofuran to cover the polymer solid. After 24 hours the mixtures were filtered, the solid was washed with anhydrous ethanol and dried under a stream of nitrogen.

Table 5-5 Composition of Reagents Used for the Preparation of Silanediamine-loaded Polymers

J1-A, J1-B, J1-C and J1-D = Comonomer solutions of 20X, 40X, 60X and 80X ST, DVB reagent and AIBN, resp.					
I118-B = Solution of Silanediamine and DMSO					
	J1-A	J1-B	J1-C	J1-D	
STYRENE	2.0784	1.4574	0.7543	0.0000	GRAMS
	19.956	13.993	7.242	0.000	MMOL
DVB	0.9099	1.7225	2.6187	3.5419	GRAMS
	6.989	13.231	20.114	27.206	MMOL
AIBN	0.0454	0.0523	0.0529	0.0482	GRAMS
	0.276	0.318	0.322	0.294	MMOL
SOLUTION I118-B			SiN ₂ = Silanediamine monomer <u>21</u>		
SiN ₂	0.1639	GRAMS			
	0.403	MMOL			
DMSO	3.584	GRAMS			

Table 5-6 Amounts of Reagents used for the Preparation of Silanediamine-loaded Polymers

I118-B (see Table 5-5)				
J1-A, J1-B, J1-C and J1-D (see Table 5-5)				
	Silanediamine Copolymer Samples			
	J3-A	J3-B	J3-C	J3-D
Comonomer Solution	grams	grams	grams	grams
J1-A	0.3567			
J1-B		0.3758		
J1-C			0.4001	
J1-D				0.4207
I118-B	0.4317	0.4439	0.4422	0.4387

Table 5-7 Calculated Composition of the Silanediamine-loaded Polymers

All mol% are calculated as a percentage of the sum of the monomers styrene, DVB and the silanediamine					
The DVB reagent is about 80% m,p-divinylbenzene and 20% m,p-ethylvinylbenzene					
J3-A, J3-B, J3-C and J3-D (See Table 5-4)					
	Silanediamine Copolymer Sample				
	J3-A	J3-B	J3-C	J3-D	
STYRENE	0.2444 2.346 72.99	0.1694 1.627 50.64	0.0881 0.846 26.09	0.0000 0.000 0.00	GRAM MMOL MOL%
DVB	0.1070	0.2003	0.3058	0.4151	GRAM
REAGENT	0.822 25.56 20.5	1.538 47.88 38.3	2.349 72.45 58.0	3.188 98.54 78.8	MMOL MOL% MOL% X
AIBN	0.0053 0.0325 1.01	0.0061 0.0370 1.15	0.0062 0.0376 1.16	0.0056 0.0344 1.06	GRAM MMOL MOL%
SiN ₂	0.01888 0.04642 1.444	0.01941 0.04773 1.486	0.01934 0.04755 1.466	0.01918 0.04717 1.458	GRAM MMOL MOL%
DMSO	0.4128	0.4245	0.4229	0.4195	GRAM

5.3.4 Preparation of Carbamate-loaded Copolymers

A typical sample for the preparation of polymers loaded with O-(*tert*-butyl)-N-(4-vinylbenzyl)carbamate (BOC) is shown in Table 5-8. The samples were prepared by first making solutions of a) O-(*tert*-butyl)-N-(4-vinylbenzyl)carbamate in dimethylsulfoxide solution (I96-B) and, b) solutions of styrene, divinylbenzene reagent and AIBN (J1-A, J1-B, J1-C or

Table 5-8 Amounts of Reagents Used for the Preparation of Carbamate-loaded Polymers

I96-B = 0.2018 g O-(t-Butyl)-N-(4-Vinylbenzyl)-carbamate (BOC) + 4.0188 g DMSO				
J1-A, J1-B, J1-C and J1-D (see Table 5-5) = (Styrene, DVB, AIBN solutions)				
Comonomer Solutions	BOC Copolymer Samples			
	J7-A	J7-B	J7-C	J7-D
	grams	grams	grams	grams
J1-A	0.3300			
J1-B		0.3427		
J1-C			0.3694	
J1-D				0.3795
I96-B	0.4255	0.4242	0.4272	0.4255

J1-D). These solutions were then added to tared vials, and the mass of each added solution determined. The vials were degassed of oxygen and sealed under an atmosphere of nitrogen. The polymerizations were carried out at 100°C for 24 hours. The amounts of reagents used to prepare samples of carbamate-loaded polymers are shown in the Table 5-8. IR spectra of the carbamate-loaded polymers were taken to determine the actual concentration of carbamate group in the polymer.

The masses of solutions shown in Table 5-8 permitted the calculation of the reagents shown in Table 5-9. At the completion of the polymerization, the polymers were crushed into fine particles, and analyzed by IR spectroscopy as their Nujol mulls. The results of the analyses are shown in Table 5-10.

Table 5-9 Calculated Composition of the Carbamate-loaded Polymers

The DVB reagent is about 80% <i>m,p</i> -divinylbenzene and 20% <i>m,p</i> -ethylvinylbenzene					
All mol% are calculated as a percentage of the sum of the monomers styrene, DVB and BOC					
J7-A, J7-B, J7-C and J7-D (See Table 5-8)					
Carbamate Copolymer Sample					
	J7-A	J7-B	J7-C	J7-D	
STYRENE	0.2261 2.171 72.82	0.1545 1.484 50.53	0.0813 0.781 26.03	0.0000 0.000 0.00	GRAM MMOL MOL%
DVB	0.0990	0.1826	0.2824	0.3744	GRAM
REAGENT	0.760 25.50 20.4	1.403 47.77 38.2	2.169 72.30 57.8	2.876 98.29 78.6	MMOL MOL% MOL%
AIBN	0.0049 0.0301 1.01	0.0055 0.0338 1.15	0.0057 0.0347 1.16	0.0051 0.0310 1.06	GRAM MMOL MOL%
BOC	0.02034 0.05003 1.678	0.02028 0.04987 1.698	0.02043 0.05023 1.674	0.02034 0.05003 1.710	GRAM MMOL MOL%
DMSO	0.40516	0.40392	0.40677	0.40516	GRAM

Note that the samples I50-X, X = A,B,C,D typically depart in their values of (mass concn/spectral concn) from the other polymers in each series. This probably occurs in part due to the difficulties incurred in the IR analyses.

Table 5-10 Results of IR Measurements of the Carbamate-loaded Polymers

SAMPLE	INITIAL MASS CONCN (mol%)	AROMATIC AREA	BOC AREA	BOC SPECTRAL CONCN (mol%)	SPECTRAL CONCN MASS CONCN
20X					
G61(20)	2.4	14.64	15.50	2.894	1.2
H1(20)	2.9	2.43	2.39	2.689	0.94
I50-A	0.44	19.25	3.65	0.518	1.2
I91-A	1.7	24.27	19.12	2.154	1.3
J8-A-3	2.9	19.01	24.44	3.515	1.2
J10-A-3	1.5	21.60	13.06	1.653	1.1
J10-E-3	1.5	29.90	21.45	1.961	1.3
J106-A-2	2.7	26.67	35.63	3.652	1.3
40X					
G62(40)	3.0	28.90	31.42	2.972	1.0
H2(40)	2.9	13.01	14.41	3.028	1.1
H5(40)	2.9	1.46	1.97	3.689	1.3
I50-B	0.39	6.96	0.35	0.137	0.35
I91-B	1.5	35.94	18.31	1.393	0.91
J8-B-3	2.9	16.72	17.87	2.922	1.0
J10-B-3	1.4	28.57	14.72	1.408	0.99
J106-B-2	2.8	25.65	24.35	2.595	0.93
60X					
G63(60)	3.1	22.95	21.30	2.537	0.81
H3(60)	3.0	21.99	15.76	1.959	0.65
I50-C	0.40	30.88	2.79	0.247	0.62
I91-C	1.6	31.73	12.08	1.041	0.65
J8-C-3	2.9	23.70	21.88	2.524	0.88
J10-C-3	1.4	43.64	13.16	0.824	0.59
J106-C-2	2.7	17.17	14.18	2.258	0.82
80X					
G64(80)	3.0	37.71	28.22	2.046	0.67
H4(80)	2.9	16.27	9.93	1.668	0.57
I50-D	0.47	43.84	3.41	0.213	0.45
I91-D	1.47	42.74	11.53	0.737	0.50
J8-D-3	2.9	42.41	33.26	2.144	0.73
J10-D-3	1.5	29.22	12.15	1.137	0.78
J106-D-2	2.6	24.57	15.53	1.728	0.65

CHN Analysis: Sample J8-A-3 (from sample J7-A) (see Table 5-8 and Appendix B). The CHN estimations below are made from the concentration of the BOC group determined by IR spectroscopy.

Estimated (w/AIBN): C, 90.65; H, 7.73; N, 0.66

Estimated (wo/AIBN): C, 90.88; H, 7.71; N, 0.43

Found*: C, 90.20; H, 7.98; N, 0.46

*Average of 2 Analyses

The washed and dried BOC loaded polymers were placed in vials with granular NaCl, enough anhydrous benzene to cover the polymer solid, and concentrated H_2SO_4 . When the sulfuric acid was added to the vials, hydrogen chloride began forming. Each vial was immediately closed before the foaming mixture could escape from the vials. The mixtures was left in the closed vials from one to several days. When the samples were opened the polymer solids were washed with H_2O , EtOH and CH_2Cl_2 , and then dried under a stream of N_2 . The samples were analyzed by IR to insure that the carbamate groups had been completely cleaved.

5.4 Infrared Analysis Methods

5.4.1 Determination of Relative Molar Absorptivities

Solutions were prepared of model compounds in toluene and were analyzed by IR spectroscopy. The data were then used to determine the molar components of the solutions. To the

solutions were added either CHBr_3 or THF in order to insure that the carbonyl compound in solution was either hydrogen bonded or not hydrogen bonded, respectively.

5.4.2 Extraction of Data from IR spectra

Various copolymers were analyzed by IR. Because of the different degrees of cross-linking of the samples, it was necessary to subtract the polystyrene contribution to the spectrum in order to assess the area of the peaks due the absorbances of the acetamide, urethane and urea groups in each sample. Before subtraction of the polystyrene contribution to the IR spectrum, the aromatic peak at 1600 cm^{-1} was integrated. Then the aromatic overtone peaks in the region from 2000 cm^{-1} to about 1770 cm^{-1} of a blank polystyrene sample were subtracted from the sample spectrum using the auto-subtraction function of the Perkin-Elmer Model 1600 IR spectrometer to obtain the best result. The areas of the various peaks, i.e., acetamide, urethane or urea, were then integrated using the peak integration integration feature of the instrument in order to determine the concentration of species of interest. Examples of this process are given in Appendix C.

5.5 Reactions on Polymers

5.5.1 Conditions Used for the Coupling of Amine Groups with Carbonyldiimidazole

The reaction for the formation of urea moieties from amines in the polymer samples is shown in Figure 5-1.

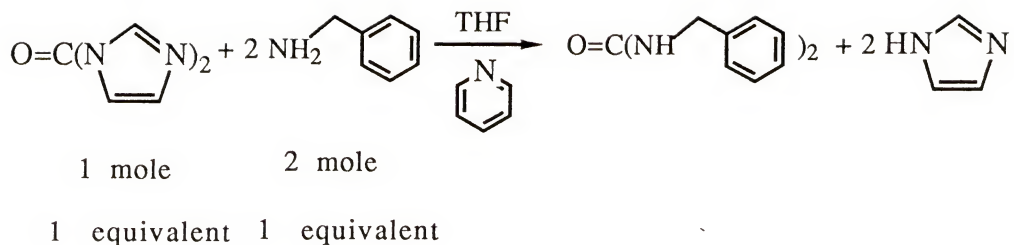


Figure 5-3 Stoichiometry of Reaction for the Formation of Urea from Amine-loaded Copolymers with Carbonyldiimidazole

Equivalents of carbonyldiimidazole were added to each polymer sample according to the schedule that is shown in Table 5-11.

Table 5-11 Schedule for the Addition of Carbonyldiimidazole to Amine Copolymers

day	1	2	3	4	5	6	7
Equivs.	2	2	2	2	4	4	4

At the end of eight days a large excess of anhydrous ethanol was added to each sample. Each sample was again allowed to remain undisturbed for a few days. The samples were then filtered, washed with ethanol and CH_2Cl_2 , and then dried under a stream of nitrogen. The samples were analyzed

by IR spectroscopy as their CHBr_3 mulls. The results of IR analyses are presented in Table 5-12.

5.5.2 Conditions Used for the Acetylation of Random and Ordered Polymers

A typical acetylation reaction is explained below. About 0.1 g (0.027 mmol amine, 1 eq.) of the washed and dried polymer samples, J29-A (3% NR, 20X), J29-B (3% NR, 40X), J29-C (3% NR, 60X) and J29-D (3% NR, 80X) were added to separate vials. To each vial was then added 0.5 ml of a solution consisting of 0.40 ml pyridine (0.39 g, 4.9 mmol, 180 eq.) and 0.10 g imidazole (1.47 mmol, 54 eq.). Each vial then received 0.10 ml acetyl chloride (0.10 g, 1.27 mmol, 47 eq.). Thus the acetyl imidazole which was formed in situ was present in about 47 equivalents.

Portions were taken from the above mixtures for IR analysis at the end of two days. The portions taken were washed and dried and analyzed as their nujol mulls. Other polymer samples that were treated in the same manner as described above were sampled after two days and then again later with the time elasped being from two to three months. The results of the IR measurements is shown in Table 5-13.

5.5.3 Amine-catalyzed Reactions of Phenylacetaldehyde

The reaction shown in Figure 5-1 was setup in screw cap vials on 20X, 40X, 60X and 80X random and ordered polymers loaded at approximated 3.0, 1.5, 0.5 and 0.1 mol%. The

Table 5-12 Results of the IR Measurements on the Amine-polymer Samples Coupled with 1,1'-Carbonyldiimidazole

POLYMER	SAMPLE	AROMATIC AREA	URETHANE AREA	UREA AREA
R 20	J27-A-8-A	32.28	8.47	3.71
	I105-A-7-B	40.06	4.09	6.36
	I60-A-8-B	27.66	5.75	5.66
	J25-A-8-A	29.58	17.95	8.57
NR 20	J23-A-8-A	25.50	1.95	2.29
	I104-A-7-B	34.93	1.68	7.53
	J21-A-8-A	28.83	6.47	6.58
	I61-A-8-B	33.91	4.38	10.56
R 40	I105-B-7-B	59.92	4.95	3.68
	J27-B-8-A	48.67	9.32	2.86
	J25-B-8-A	41.31	12.64	5.95
	I65-B-8-B	29.18	5.59	6.05
NR 40	J23-B-8-A	64.64	2.08	3.07
	I104-B-7-B	55.75	1.75	5.60
	J21-B-8-A	23.67	3.63	5.27
	I61-B-8-B	48.33	2.31	7.73
R 60	J27-C-8-A	47.51	6.49	1.94
	I105-C-7-B	68.11	8.58	3.81
	J25-C-8-A	30.32	12.39	4.10
	I60-C-8-B	34.91	5.52	2.23
NR 60	J23-C-8-A	42.81	0.94	1.34
	I104-C-7-B	68.87	1.67	5.88
	J21-C-8-A	41.18	2.72	5.18
	I61-C-8-B	51.85	2.93	8.44
R 80	I105-D-7-B	59.92	5.81	1.45
	J27-D-8-A	59.05	7.17	1.12
	J25-D-8-A	28.45	9.46	2.32
	I60-D-8-B	34.86	6.95	2.04
NR 80	J23-D-8-A	63.30	2.19	3.29
	I104-D-7-B	72.30	2.65	5.14
	J21-D-8-A	54.52	3.89	3.48
	I61-D-8-B	62.32	3.11	10.33

Table 5-13 Results of the IR Measurements on the Acetylated Amine-polymer Samples

Sample	Time of Reaction	Aromatic Area	Total Amide Area
R20			
G83-A-2	2 days	6.36	4.41
G83-C-3	2 months	14.45	10.51
I99-A-2	2 days	19.94	9.10
I99-A-3	2 months	33.60	19.44
J33-A-1-A	2 days	38.91	39.92
J33-A-1-A	2 days	38.10	36.69
NR20			
I59-A-2	2 days	33.85	30.78
I59-A-3-A	3 months	34.10	30.84
I100-A-2	2 days	31.58	13.09
I100-A-3	2 months	32.74	15.62
J29-A-1-A	2 days	43.49	34.48
J31-A-1-A	2 days	66.43	23.48
J31-A-1-A	2 days	41.68	13.78
J35-A-1-A	2 days	39.20	18.44
R40			
G84-A-2	2 days	2.87	1.67
G84-C-3	2 months	19.85	12.01
I99-B-2	2 days	15.42	5.35
I99-B-3	2 months	39.87	13.44
J33-B-1-A	2 days	53.09	39.98
J33-B-1-A	2 days	37.30	26.01
J35-B-1-A	2 days	41.86	12.23
NR40			
I59-B-2	2 days	11.15	6.81
I59-B-3-A	3 months	34.11	30.12
I100-B-2	2 days	30.36	8.89
I100-B-3	2 months	38.77	9.82
J29-B-1-A	2 days	36.90	14.64
J31-B-1-A	2 days	40.23	7.07

Table 5-13--continued

Sample	Time of Reaction	Aromatic Area	Total Amide Area
R60			
G85-A-2	2 days	2.75	1.12
G85-C-3	2 months	34.79	15.48
I99-C-2	2 days	27.78	5.92
I99-C-3	2 months	35.23	8.54
J33-C-1-A	2 days	62.01	33.56
J33-C-1-A	2 days	38.68	18.57
J35-C-1-A	2 days	33.83	6.67
NR60			
I59-C-2	2 days	21.79	11.66
I59-C-3-A	3 months	29.07	17.00
I100-C-2	2 days	47.01	6.37
I100-C-3	2 months	33.97	6.04
J29-C-1-A	2 days	47.12	12.66
J31-C-1-A	2 days	48.11	4.78
R80			
G86-A-2	2 days	1.59	0.55
G86-C-3	2 months	14.33	6.52
I99-D-2	2 days	32.94	4.61
I99-D-3	2 months	41.62	6.61
J33-D-1-A	2 days	52.69	25.29
J33-D-1-A	2 days	37.64	17.73
J35-D-1-A	2 days	34.12	6.83
NR80			
I59-D-2	2 days	16.68	7.56
I59-D-3-A	3 months	41.24	20.84
I100-D-2	2 days	54.01	6.54
I100-D-3	2 months	46.40	6.29
J29-D-1-A	2 days	46.37	15.06
J31-D-1-A	2 days	48.45	4.50

Table 5-14

Characteristics of Reactions of Amine-polymer-catalyzed Aldol Condensation of Phenylacetaldehyde

SAMPLE	AMINE CONCN MOL%	μ MOLES AMINE PER GRAM (X 1000)	MASS OF POLYMER (G)	μ MOLES AMINE	MILLI EQS. AMINE
RANDOM 20X	3.7	330	0.0244	8.0	9.4
	1.6	150	0.0493	7.4	8.6
	0.44	40	0.1246	4.9	5.8
	0.11	9.9	0.1409	1.4	1.6
ORDERED 20X	2.9	260	0.0213	5.6	6.5
	1.5	140	0.0687	9.4	11
	0.53	48	0.1342	6.4	7.5
	0.11	9.6	0.3332	3.2	3.7
RANDOM 40X	2.6	220	0.0253	5.6	6.6
	1.4	120	0.0462	5.6	6.5
	0.39	34	0.1396	4.7	5.5
	0.10	8.8	0.2122	1.9	2.2
ORDERED 40X	3.1	270	0.0276	7.4	8.6
	1.5	130	0.0511	6.5	7.6
	0.53	45	0.1525	6.9	8.1
	0.11	9.2	0.2852	2.6	3.1
RANDOM 60X	2.3	180	0.0219	4.0	4.7
	0.82	67	0.0418	2.8	3.3
	0.40	32	0.2174	7.0	8.2
	0.10	8.3	0.2345	1.9	2.3
ORDERED 60X	3.3	270	0.0298	8.1	9.4
	1.5	120	0.0482	5.9	6.9
	0.58	47	0.1341	6.3	7.3
	0.10	8.4	0.3305	2.8	3.3
RANDOM 80X	1.7	130	0.0258	3.4	4.0
	1.1	88	0.0431	3.8	4.4
	0.47	36	0.1611	5.9	6.9
	0.11	8.2	0.2504	2.0	2.4
ORDERED 80X	3.4	260	0.0244	6.5	7.6
	1.8	140	0.0500	6.8	7.9
	0.49	37	0.2216	8.3	9.7
	0.10	7.9	0.3570	2.8	3.3

Table 5-15 Results of Analyses on the Amine-polymer-catalyzed Reaction Mixtures

SAMPLE	AMINE CONCN MOL%	AREA PEAK 225	AREA PEAK 587	AREA PEAK 608	AREA PEAK 623
NO POLYMER		1663544	242074	381390	141067
RANDOM 20X	3.65	1425872	78350	125964	53241
	1.65	1415162	117154	127871	49759
	0.438	302673	36388	275304	70718
	0.110	501754	58921	183665	68245
ORDERED 20X	2.91	890223	104825	280187	111867
	1.51	669187	64435	227910	73633
	0.531	734239	69495	185132	87987
	0.106	2052390	350701	282993	84745
RANDOM 40X	2.60	3946172	382556	1024729	393135
	1.41	808338	58699	169224	69105
	0.395	535277	57293	162728	69602
	0.103	625979	56690	221215	64725
ORDERED 40X	3.12	1402032	139844	390481	157489
	1.49	698584	67603	203351	61610
	0.531	1037934	61487	189543	89545
	0.107	1889200	225573	221101	59939
RANDOM 60X	2.26	2357426	312385	1393692	652589
	0.824	676866	50248	156786	62601
	0.399	624663	47145	164533	50277
	0.102	345006	32217	239721	57271
ORDERED 60X	3.33	787770	68867	214244	62104
	1.51	597580	53142	182132	56025
	0.577	2015648	318459	409865	143906
	0.104	2294910	329271	422874	137069
RANDOM 80X	1.73	659239	57054	151267	78492
	1.14	1110100	66923	222681	83141
	0.472	433734	37797	128499	26994
	0.106	373672	37617	113984	32411
ORDERED 80X	3.44	703534	60800	198228	67698
	1.76	440013	53044	400157	94720
	0.486	623599	60745	152171	81924
	0.102	2035677	263117	306448	98967

characteristics of each reaction are shown in Table 5-14. The reaction was allowed to proceed for one week, at which time 10.0 ml of methylene chloride was added to each vial. After another 24 hours, aliquots of each reaction mixture were taken, diluted and analyzed by GC/MS. The results of the analyses are shown in Table 5-15.

APPENDIX A
THEORETICAL MODEL FOR RANDOMLY DISTRIBUTED AMINES

Because a model for the random placement of groups in a polymer sample was not found in the literature, one is developed in this appendix. One such model has the polymer-bound benzylamine, styrene and divinylbenzene moieties approximated as spheres (of equal size) distributed randomly in concentric layers.

A close pack arrangement of spheres places twelve spheres around a single central sphere. The cross-sectional area of each sphere is given by

$$\text{Area} = \pi r_o^2 \quad \text{eqn (A-1)}$$

where r_o is the radius of the spheres.

The area of a concentric shell which would pass through the centers of the twelve spheres ($r = 2r_o$) is given by

$$\text{Area} = 4\pi(2r_o)^2 = 16\pi r_o^2 \quad \text{eqn (A-2)}$$

If the spheres were able to pack so as to cover the entire area of the concentric shell at $r = 2r_o$, then the number of spheres could be calculated by the area of the

concentric shell divided by the cross-sectional area of each sphere, i.e.,

$$16\pi r_o^2 / \pi r_o^2 = 16 \quad \text{eqn (A-3)}$$

Because the spheres can apparently occupy only 75% of the area of the concentric shell, and because at $2r_o$, the layer number, L , is $L = 1$, and L increments by one for every increase of r by $2r_o$, a convenient formula for describing the number of spheres in each concentric layer is

$$n_L = \text{number of spheres in a given layer} = 12 \cdot L^2 \quad \text{eqn (A-4)}$$

Since this model is being developed to model the reaction of amines with carbonyldiimidazole, subsequent language will refer to the placement and reaction of the amine group.

After one amine group has reacted with carbonyldiimidazole to form a semi-urea, it is probably the nearest amine group in the polymer matrix that then reacts with the semi-urea when a moiety of urea is formed. Thus, a distribution is needed which describes the probability of finding an amine group in a given layer away from a central sphere (assumed to be the amine which has first reacted with carbonyldiimidazole). The derivation of this distribution is described below.

The probability that the first layer is the nearest occupied layer is the probability of finding one (or more) amine spheres in the layer, thus

$$P_{N,L} = P(\geq 1, 1) = 1 - P(0, 1) \quad \text{eqn (A-5)}$$

where the second number (whether the second subscript or the second number in the parentheses) refers to the layer number.

Using the law of conditional probability [70MI1], the probability that the second layer is the nearest occupied layer is given by the equation

$$P_{N,2} = P(0, 1) \cdot P(\geq 1, 2) \quad \text{eqn (A-6)}$$

and the probability that the L^{th} layer is the nearest occupied layer is given by

$$P_{N,L} = \left[\prod_{i=1}^{L-1} P(0, i) \right] \cdot P(\geq 1, L) \quad \text{eqn (A-7)}$$

But it is not sufficient to simply determine the distribution of nearest occupied layers since the nearest occupied layer may have multiple occupancy of amines. Rather, the distribution of nearest neighbors depends on the product of the probability of a given layer being the nearest occupied layer and the probable occupancy (excluding the possibility of

zero occupancy). The probable occupancy, K_L , of a layer when the layer is the nearest occupied layer is given by

$$K_L = \frac{1 \cdot P(1, L) + 2 \cdot P(2, L) + \dots + n_L \cdot P(n_L, L)}{P(\geq 1, L)} \quad \text{eqn (A-8)}$$

which is equivalent to

$$K_L = \frac{n_L \cdot DF}{P(\geq 1, L)} = \frac{n_L \cdot DF}{1 - P(0, L)} \quad \text{eqn (A-9)}$$

Thus, the product, S_L , of eqns (A-7) and (A-9) gives

$$S_L = \left[\prod_{i=1}^{L-1} P(0, i) \right] \cdot (n_L \cdot DF) \quad \text{eqn (A-10)}$$

In order to convert S into the fraction of nearest amines, Y , found in each layer, it is necessary to divide each term S_L by the sum $\sum_{L=1}^{\infty} S_L$. Fortunately $\sum_{L=1}^{\infty} S_L$ quickly converges as is shown in Table A-1 below. The cumulative distribution, Z , may then be obtained by forming the cumulative sum of the terms of Y ; again the terms are shown in Table A-1 below. For purposes of the calculation, it may be easily shown that

$$\left[\prod_{i=1}^{L-1} P(0, i) \right] = (1 - DF)^{\sum_{i=1}^{L-1} n_i} \quad \text{eqn (A-11)}$$

The results of the equations (1) through (11) are shown in detail in Table A-1 (6% DF and 0.1% DF). In order to have a better description of the distribution of the amine

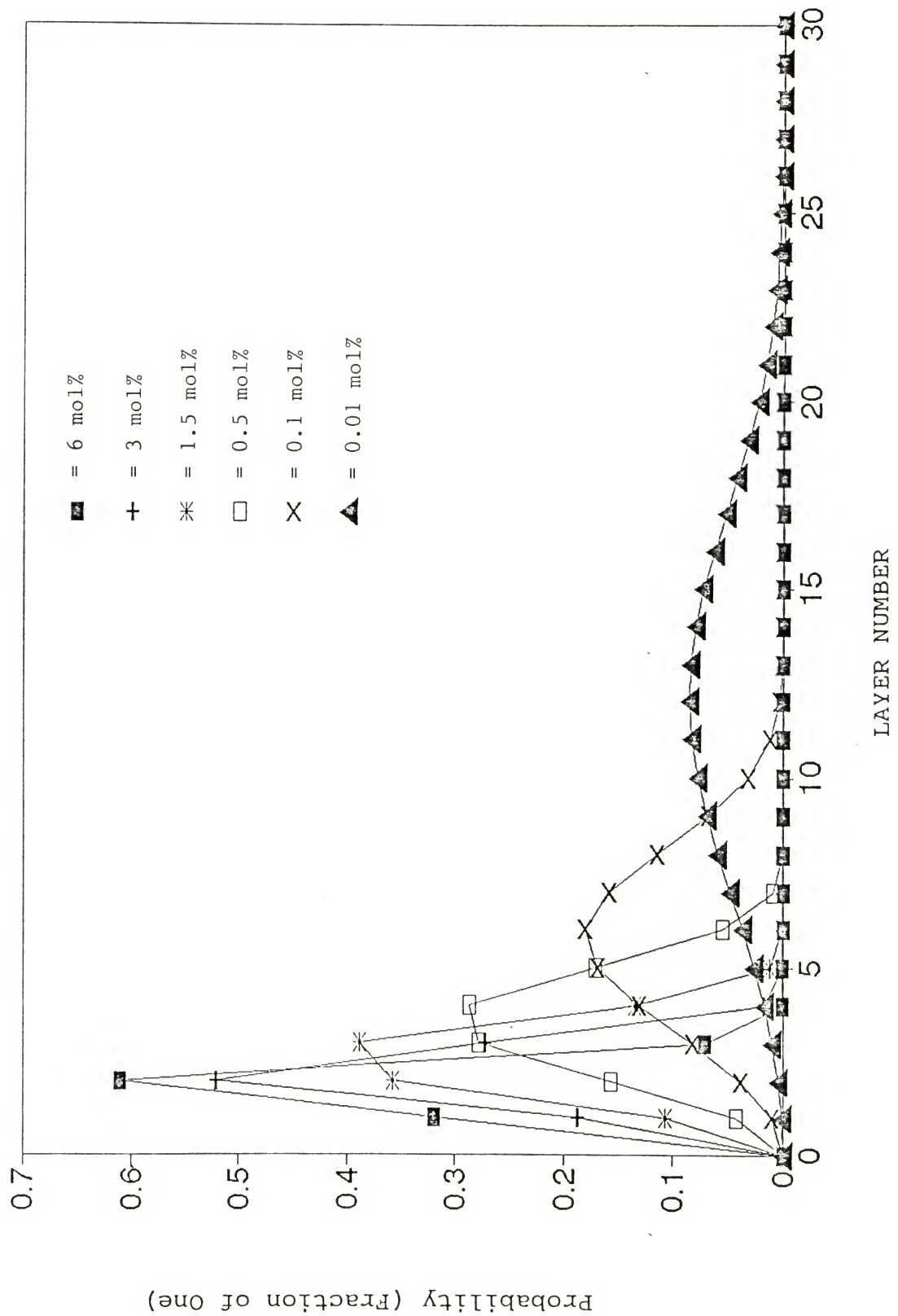


Figure A-1 Graphical Presentation of the Values of the Function Y

Table A-1 Values for Various Quantities Related to the Random Distribution of Spheres

DF=6%	P(0, L)	P _{N,L}	K	S	Y	Z
0	0	0.476	0.524	1.374	0.7200	0.3201
1	12	0.0513	0.4515	3.035	1.3706	0.6094
2	48	0.0012	0.0244	6.488	0.1582	0.0703
3	108	0.0000	0.0000	11.52	0.0003	0.0002
4	192	0.0000	0.0000	2.12E-10	0.0000	1.0000
5	300	0	1.84E-18	26	0	1.0000
6	432	0	4.52E-30	35	0	1.0000
7	588	0	7.16E-46	46	0	1.0000
8	768	0	1.65E-66	58	0	1.0000
9	972	0	0	72	0	1.0000
10	1200	0				
SUM OF TERMS =		1.0000		2.2492	1.0000	

Table A-1--contd.

DF=0.01%	LAYER	n	P(0,L)	P _{N,L}	K	S	Y	Z
	1	12	0.988	0.0119	1.005	0.0120	0.0097	0.0097
	2	48	0.953	0.0463	1.024	0.0474	0.0383	0.0480
	3	108	0.898	0.0964	1.054	0.1017	0.0821	0.1301
	4	192	0.825	0.1477	1.098	0.1623	0.1310	0.2612
	5	300	0.741	0.1809	1.157	0.2093	0.1690	0.4301
	6	432	0.649	0.1813	1.231	0.2232	0.1802	0.6104
	7	588	0.555	0.1491	1.322	0.1972	0.1592	0.7696
	8	768	0.464	0.0999	1.432	0.1430	0.1155	0.8851
	9	972	0.378	0.0537	1.563	0.0839	0.0678	0.9528
	10	1200	0.301	0.0228	1.717	0.0392	0.0316	0.9845
	11	1452	0.234	0.00753	1.895	0.0143	0.0115	0.9960
	12	1728	0.177	0.00189	2.101	0.0040	0.0032	0.9992
	13	2028	0.131	0.00035	2.335	0.0008	0.0007	0.9999
	14	2352	0.095	0.00005	2.599	0.0001	0.0001	1.0000
	15	2700	0.067	0.00000	2.894	0.0000	0.0000	1.0000
	16	3072	0.046	0.00000	3.221	0.0000	0.0000	1.0000
	17	3468	0.031	0.00000	3.579	0.0000	0.0000	1.0000
	18	3888	0.020	0.00000	3.969	0.0000	0.0000	1.0000
	19	4332	0.013	9.95e-12	4.390	0	0	1.0000
	20	4800	0.0082	1.31e-13	4.840	0	0	1.0000
SUM OF TERMS =				1.0000		1.2384	1.0000	

groups, perhaps it is better to develop a distribution in which the placement of the nearest amines are broken down in divisions finer than layers. This may be accomplished by fitting a continuous mathematical function to Z . A graph of Z for various values of DF is shown in Figure A-1. A function which models Z very well (found by trial and error search) is

$$Z \approx 1 - \exp \{ D(L) \} \quad \text{eqn (A-12)}$$

where $D(L)$ is a polynomial of the form

$$D(L) = aL^3 + bL^2 + cL \quad \text{eqn (A-13)}$$

where L now refers to integral and non-integral layer numbers. The values of the coefficients a , b and c for various values of DF are given in Table A-2. The values of Z which may then be generated from eqn (A-12) for various values of DF are shown in Table A-3.

Table A-2 Values of the Coefficients in Equation A-13

LOADING	a	b	c
6.0%	-0.327	0.0410	-0.0997
3.5%	-0.186	0.0713	-0.124
3.0%	-0.154	0.0520	-0.106
2.5%	-0.122	0.0299	-0.0851
2.0%	-0.0919	0.00938	-0.0632
1.5%	-0.0858	0.105	-0.0698
1.0%	-0.0398	-0.0136	-0.0257
0.5%	-0.0214	0.00431	-0.0364
0.1%	-0.00387	-0.00203	-0.00553

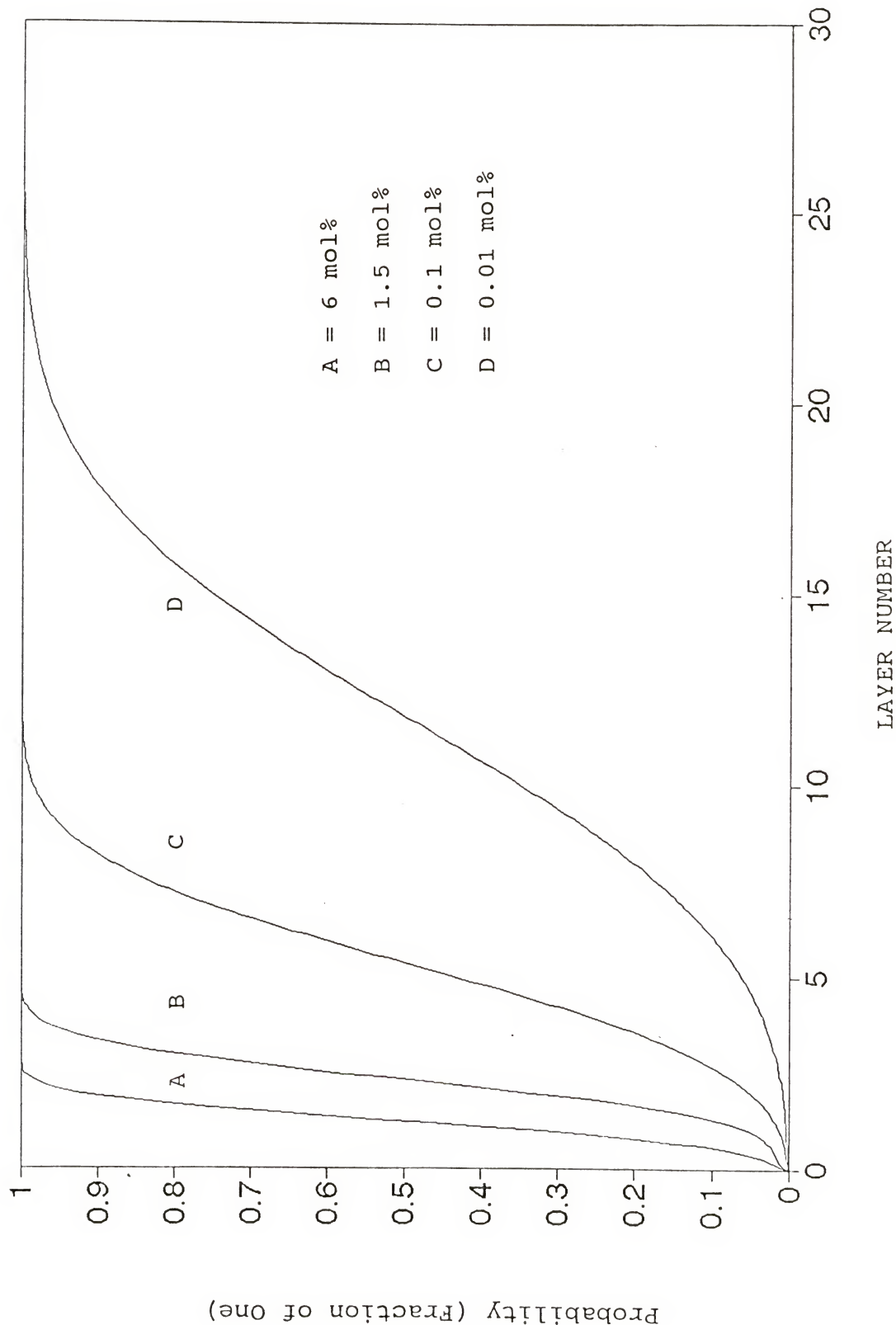


Figure A-2

Plot of the Values of Z for Various Degrees of Functionalization versus L

Table A-3 Estimations of the Values of Z at Various Distances (L) from a Central Sphere for Various Degrees of Functionalization

DISTANCE (L)	6%	3.5%	3%	2.5%
	Z	Z	Z	Z
	ESTIMATE	ESTIMATE	ESTIMATE	ESTIMATE
0	0	0	0	0
0.1	0.00984	0.01176	0.01020	0.00829
0.2	0.02071	0.02309	0.02018	0.01665
0.3	0.03446	0.03506	0.03084	0.02579
0.4	0.05283	0.04873	0.04305	0.03639
0.5	0.07735	0.06505	0.05761	0.04909
0.6	0.10929	0.08491	0.07528	0.06450
0.7	0.14949	0.10907	0.09669	0.08315
0.8	0.19830	0.13813	0.12238	0.10550
0.9	0.25547	0.17249	0.15275	0.13189
1.0	0.32011	0.21231	0.18801	0.16254
1.1	0.39071	0.25749	0.22815	0.19753
1.2	0.46519	0.30765	0.27298	0.23678
1.3	0.54113	0.36211	0.32206	0.28003
1.4	0.61588	0.41995	0.37473	0.32688
1.5	0.68691	0.48000	0.43013	0.37673
1.6	0.75201	0.54092	0.48724	0.42886
1.7	0.80949	0.60133	0.54494	0.48243
1.8	0.85833	0.65983	0.60202	0.53650
1.9	0.89822	0.71511	0.65733	0.59013
2.0	0.92950	0.76610	0.70980	0.64235
2.1	0.95301	0.81194	0.75848	0.69227
2.2	0.96992	0.85209	0.80265	0.73912
2.3	0.98154	0.88634	0.84183	0.78224
2.4	0.98916	0.91475	0.87577	0.82117
2.5	0.99393	0.93767	0.90447	0.85561
2.6	0.99676	0.95561	0.92814	0.88547
2.7	0.99835	0.96926	0.94718	0.91082
2.8	0.99921	0.97931	0.96209	0.93187
2.9	0.99964	0.98648	0.97346	0.94899
3.0	0.99984	0.99144	0.98189	0.96258
3.2		0.99689	0.99223	0.98113
3.4		0.99901	0.99702	0.99132
3.6		0.99973	0.99899	0.99638
3.8		0.99994	0.99970	0.99864
4.0		0.99999	0.99992	0.99954
4.5				
5.0				
5.5				
6.0				
6.5				
7.0				

Table A-3--continued

DISTANCE (L)	2.0%	1.5%	1.0%	0.5%
	Z	Z	Z	Z
	ESTIMATE	ESTIMATE	ESTIMATE	ESTIMATE
0	0	0	0	0
0.1	0.00630	0.00442	0.00274	0.00361
0.2	0.01293	0.00932	0.00598	0.00724
0.3	0.02040	0.01507	0.00995	0.01104
0.4	0.02925	0.02203	0.01489	0.01511
0.5	0.03995	0.03055	0.02100	0.01958
0.6	0.05297	0.04097	0.02850	0.02458
0.7	0.06873	0.05357	0.03758	0.03021
0.8	0.08758	0.06864	0.04844	0.03660
0.9	0.10982	0.08639	0.06122	0.04384
1.0	0.13566	0.10702	0.07607	0.05204
1.1	0.16520	0.13065	0.09310	0.06129
1.2	0.19847	0.15733	0.11240	0.07169
1.3	0.23534	0.18706	0.13400	0.08330
1.4	0.27559	0.21975	0.15793	0.09620
1.5	0.31887	0.25525	0.18416	0.11044
1.6	0.36472	0.29332	0.21260	0.12606
1.7	0.41258	0.33365	0.24316	0.14310
1.8	0.46181	0.37586	0.27568	0.16156
1.9	0.51168	0.41950	0.30996	0.18145
2.0	0.56148	0.46410	0.34578	0.20274
2.1	0.61044	0.50914	0.38286	0.22540
2.2	0.65785	0.55406	0.42090	0.24938
2.3	0.70307	0.59835	0.45960	0.27460
2.4	0.74551	0.64148	0.49860	0.30098
2.5	0.78471	0.68296	0.53758	0.32841
2.6	0.82033	0.72236	0.57618	0.35678
2.7	0.85217	0.75933	0.61407	0.38595
2.8	0.88014	0.79355	0.65092	0.41578
2.9	0.90429	0.82484	0.68645	0.44610
3.0	0.92477	0.85305	0.72037	0.47675
3.2	0.95577	0.90018	0.78257	0.53836
3.4	0.97575	0.93549	0.83620	0.59921
3.6	0.98766	0.96046	0.88068	0.65794
3.8	0.99419	0.97708	0.91611	0.71331
4.0	0.99749	0.98748	0.94318	0.76428
4.5		0.99791	0.98201	0.86801
5.0		0.99977	0.99568	0.93589
5.5			0.99923	0.97342
6.0			0.99990	0.99074
6.5				0.99733
7.0				0.99938

Table A-3--continued

DISTANCE (L)	DF=0.1%		DF=0.01%
	Z		Z
	ESTIMATE	LAYER	CALCULATED
0	0	0	0
0.5	0.00375	1	0.00109
1.0	0.01137	2	0.00543
1.5	0.02560	3	0.01514
2.0	0.04891	4	0.03223
2.5	0.08333	5	0.05843
3.0	0.13011	6	0.09504
3.5	0.18959	7	0.14276
4.0	0.26094	8	0.20153
4.5	0.34215	9	0.27041
5.0	0.43013	10	0.34757
5.5	0.52095	11	0.43038
6.0	0.61036	12	0.51561
6.5	0.69424	13	0.59976
7.0	0.76919	14	0.67944
7.5	0.83288	15	0.75173
8.0	0.88427	16	0.81453
8.5	0.92357	17	0.86667
9.0	0.95201	18	0.90799
9.5	0.97143	19	0.93920
10.0	0.98392	20	0.96162
10.5	0.99147	21	0.97691
11.0	0.99575	22	0.98680
11.5	0.99801	23	0.99285
12.0	0.99913	24	0.99634
		25	0.99824
		26	0.99921
		27	0.99967
		28	0.99988
		29	0.99997
		30	1.00000

It is possible to obtain an approximation to a function which describes how the urethane/urea ratio should change with concentration. One such functions is obtained by assuming

that all amines within the distance $m \cdot L$ (where m is the distance moved in terms of the unit diameter of the spheres, L , in the random distribution of spheres model) of another amine couple to form urea, and all of the remaining amines ultimately form urethane. Values of this function for the loadings given in Table A-4 may be calculated by the equation:

$$R_m = (1-Z) / (0.5 \cdot Z) \quad \text{eqn (A-14)}$$

for any given layer. The results of this calculation are shown in Table A-4. The results in Table A-4 are presented graphically in Figure A-3.

Table A-4 Theoretical Values Expected for the Urethane
Concn/Urea Concn Ratios (assuming different
mobilities, i.e. distances moved)

Degree of Functional- ization of Polymer	Distance Moved by the Amine Groups ($n \cdot L$)		
	1L	2L	3L
DF=0.01%	1839	366.6	130.1
DF=0.1%	204.4	39.68	13.37
DF=0.5%	45.94	8.059	2.195
DF=1.0%	24.29	3.784	0.7763
DF=1.5%	16.69	2.309	0.3445
DF=2.0%	12.74	1.562	0.1627
DF=2.5%	10.30	1.114	0.07774
DF=3.0%	8.638	0.8177	0.03689
DF=3.5%	7.420	0.6106	0.01726
DF=6.0%	4.248	0.1517	0.000313

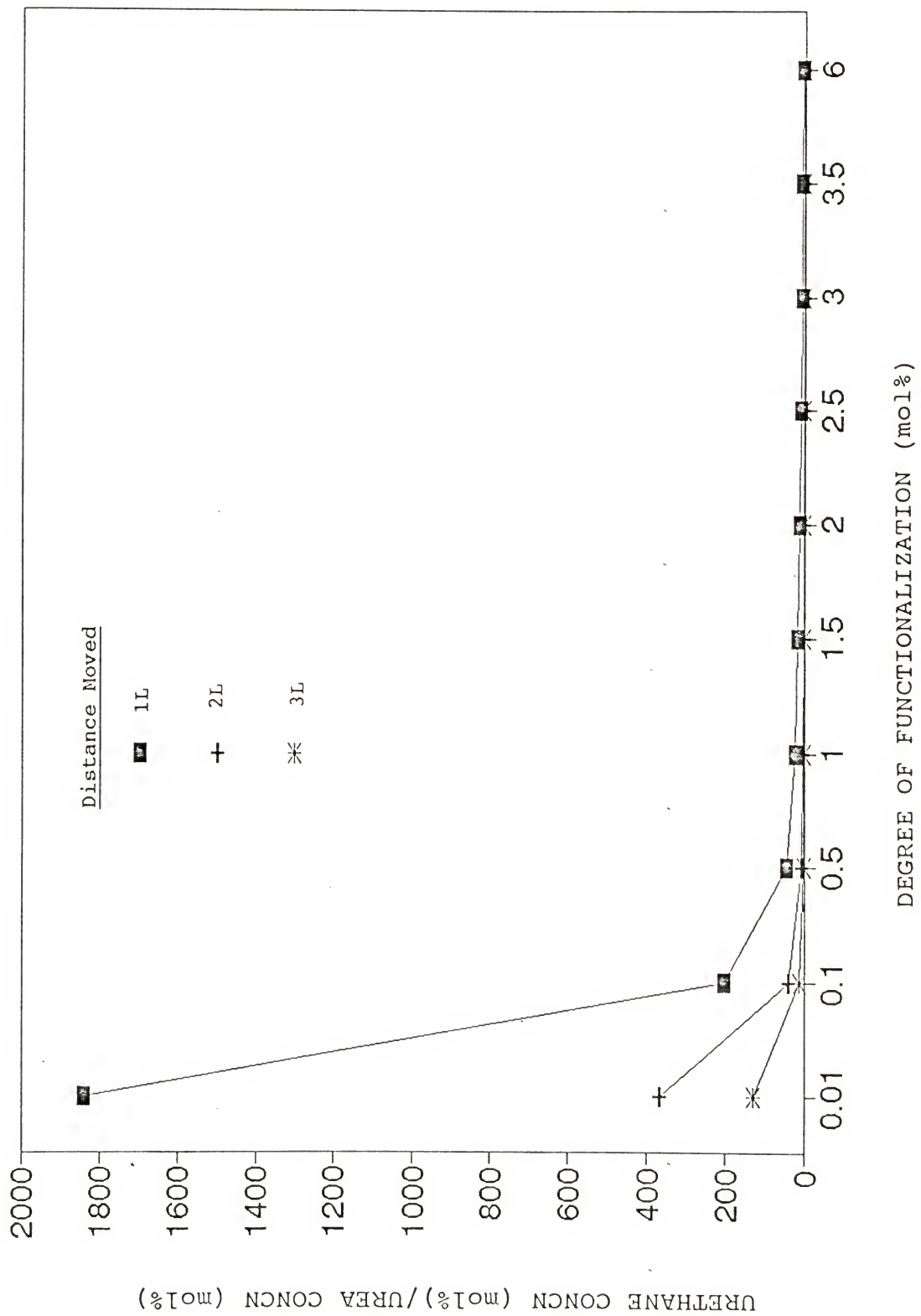


Figure A-3 Graphical Presentation of the Theoretical R_m Values.

Because the concentration of amines in polymers for this study varied over the range bounded by 0.5 mol% and 3.0 mol%, the theoretical R_m values of this range were fitted by an equation of the form:

$$R_m = k/DF + c \quad \text{eqn (A-15)}$$

where k and c are constants to be determined for $m = 1L$, $2L$ or $3L$; m is a variable describing the distance that the amine groups move in terms of the unit distance L . The results of this fitting procedure are shown graphically in Figure A-4. The values for k and c obtained by least squares fitting are shown in Table A-5.

Table A-5 Values of the Constants k and c for Integral Values of the Mobility Parameter m

m	k	c
1L	22.31	1.5484
2L	4.343	0.60605
3L	1.317	0.47665

These values of k and c may be fitted by a parabola so that a generalized equation for R_m may be approximated which may be used to fit the experimental coupling data to non-integral values of m , i.e. distance moved. The equation fitting k is:

$$k = 7.47029m^2 - 40.3777m + 55.21749 \quad \text{eqn (A-16)}$$

and the equation fitting c is:

$$c = 1.141942m^2 - 5.58031m + 5.986803. \quad \text{eqn (A-17)}$$

The merit of this fitting of k and c to a parabola is that the experimental data may now be fitted by an equation of the form of that in eqn (A-15) for nonintegral values of m , i.e. mobility or the distance moved. The best values of m were found by two methods. The first was the method of minimizing the sum of the squares of the deviations of the experimental points from that of the theoretical curve. The second was to make the sum of the deviations of the experimental points above the theoretical curve equal to the sum of the deviation of the points below the curve. The values of m obtained by these two methods is shown in Table A-6.

Table A-6 Values of m Obtained by Best Fits of the Theoretical R_m Curve to the Experimental Data for the Random Polymers

Random Polymer	Mobility, m , by $\sum d_i = 0$	Mobility, m , by $\sum d_i^2 = \text{minimum}$
20X	2.04	2.06
40X	2.06	2.09
60X	2.08	2.09
80X	1.91	1.79

d_i = the deviation between the experimental value and the calculated value of the urethane concn/urea concn.

The results of this fitting is shown graphically in Figures A-5 through A-8. For the cases of the 20X, 40X and the 60X polymers, the differences between the two methods is small, perhaps insignificant. But for the 80X polymer samples shown in Figure A-8, the least square fit, i.e. curve D, gives

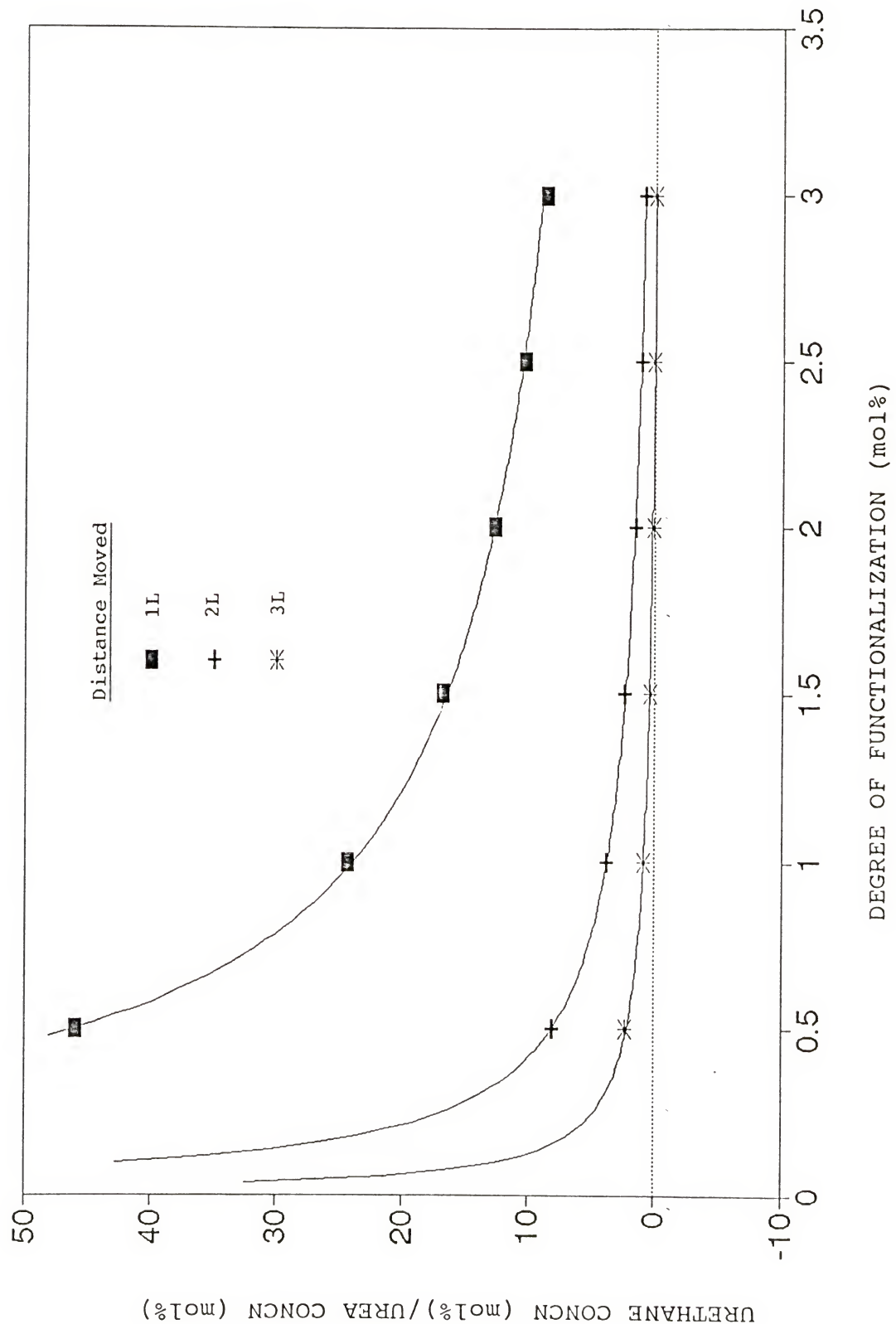


Figure A-4

Theoretical R_m Values along with the Fitted Curves of the Form:

$$Y = \frac{k}{DF + C}$$

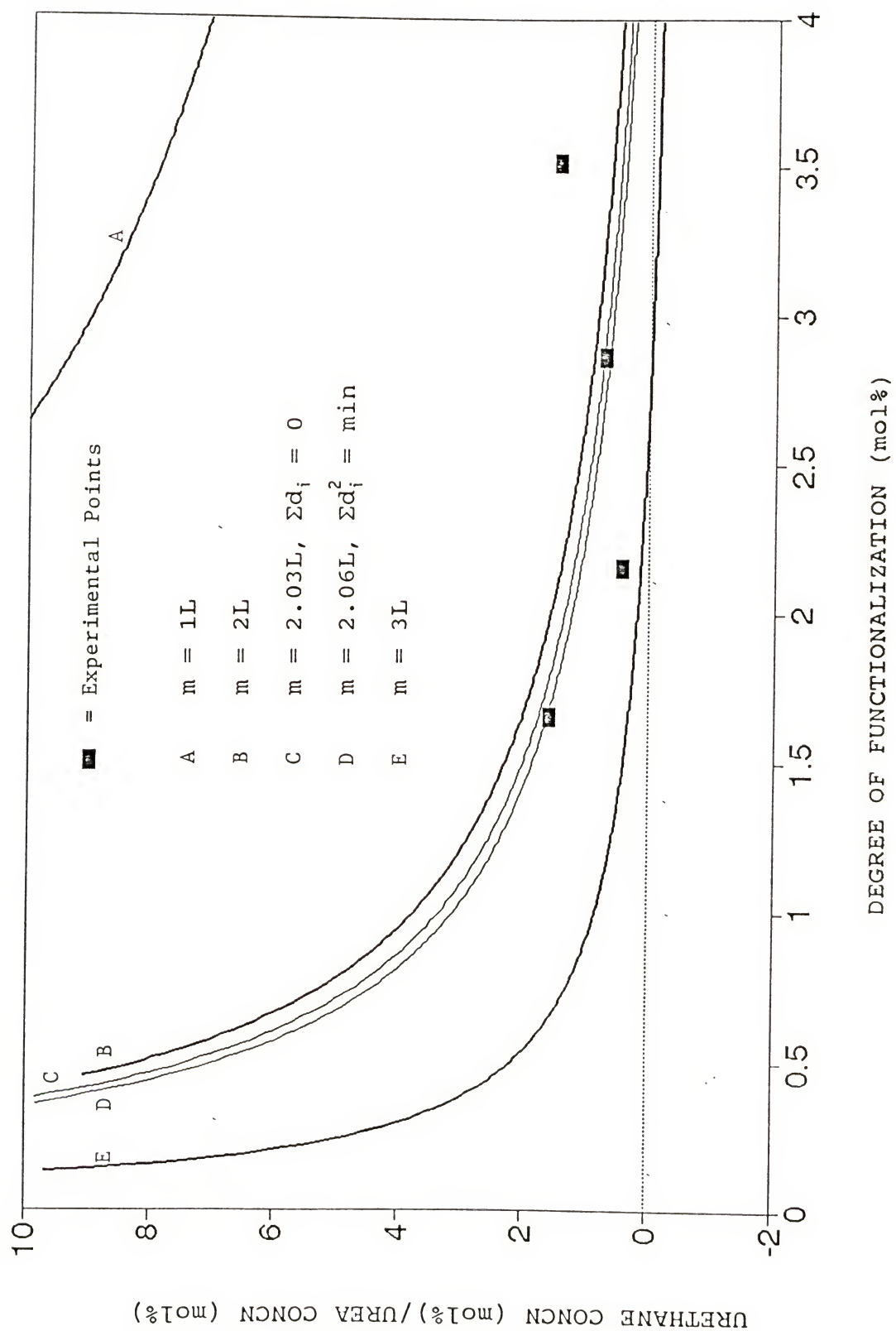


Figure A-5

Graphical Presentation of the Fitting of the Theoretical R_m Curves to the Experimental Data for the 20X Random Polymer

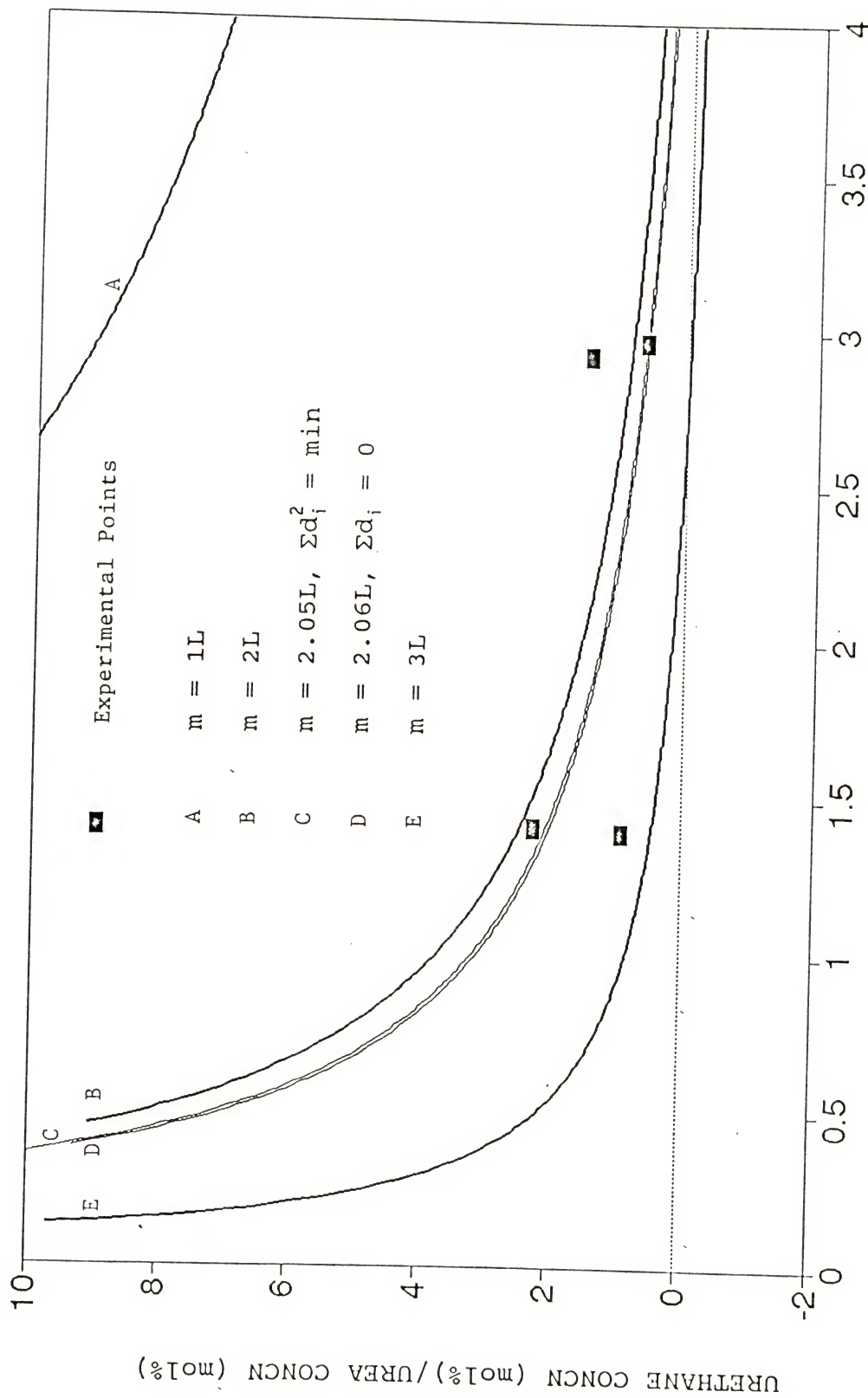


Figure A-6 Graphical Presentation of the Fitting of the Theoretical R_m Curves to the Experimental Data for the 40X Random Polymer

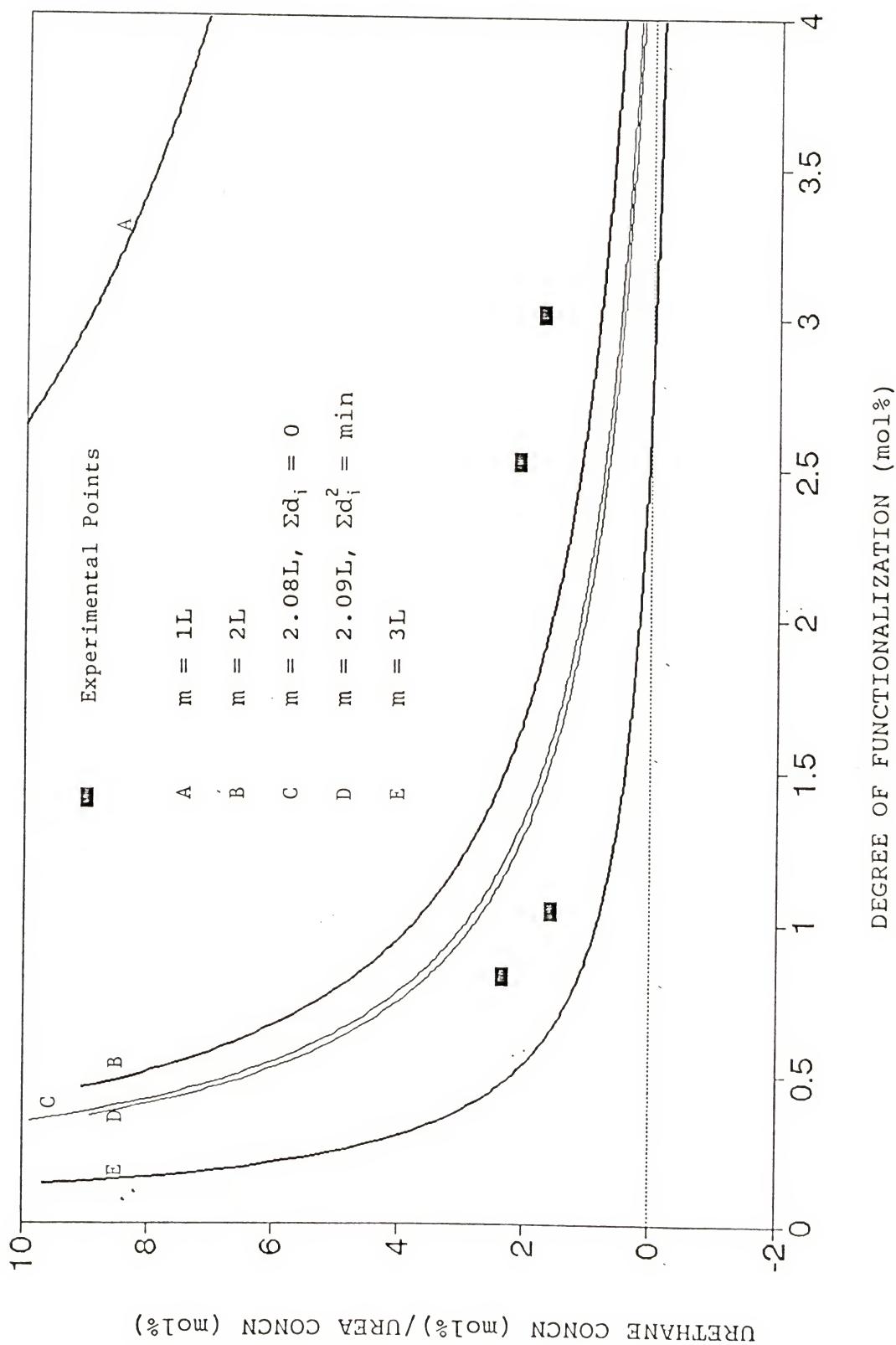


Figure A-7

Graphical Presentation of the Fitting of the Theoretical R_m Curves to the Experimental Data for the 60X Random Polymer

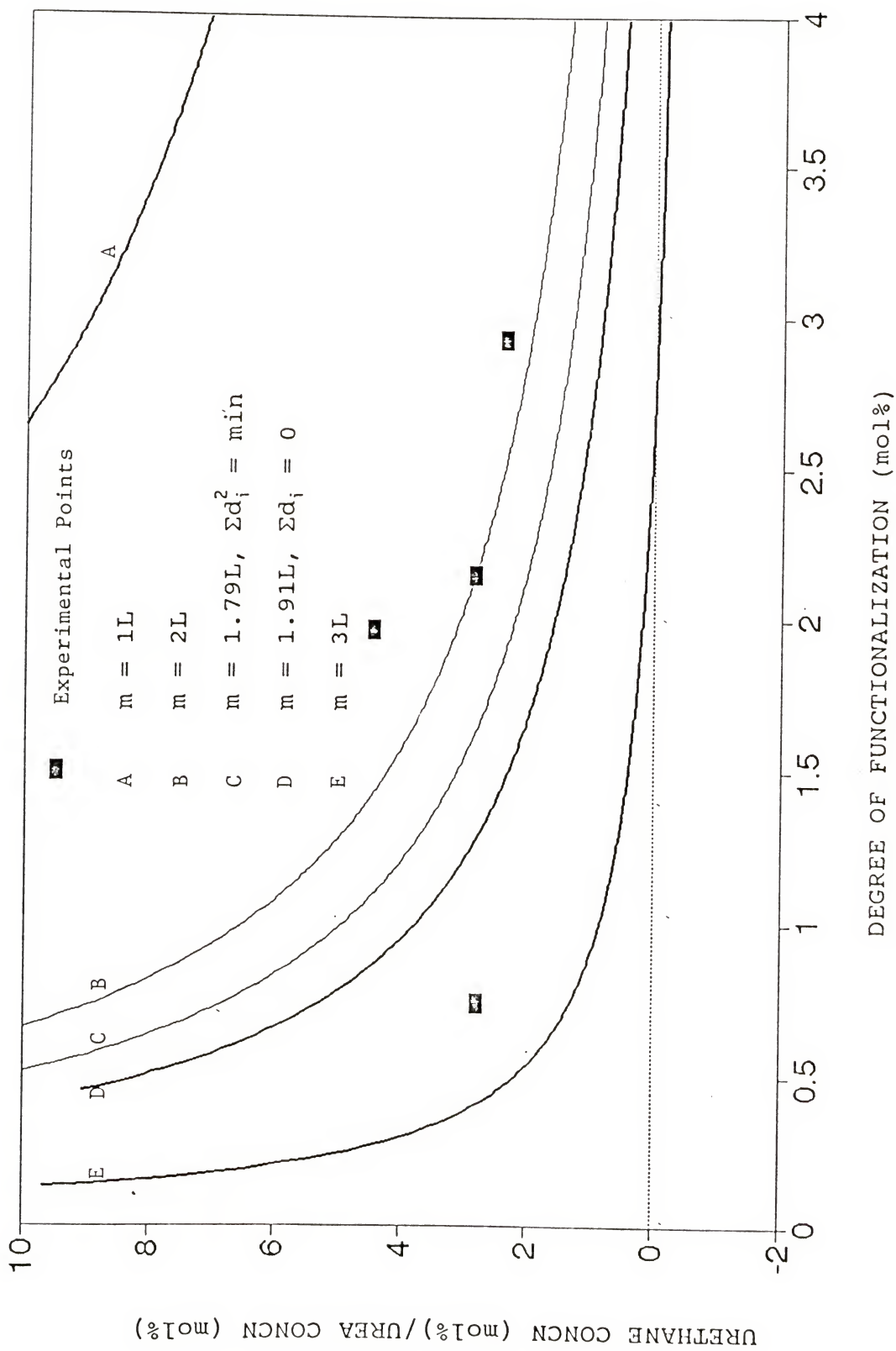


Figure A-8

Graphical Presentation of the Fitting of the Theoretical R_m Curves to the Experimental Data for the 80X Random Polymer

a fit which is not esthetically pleasing. The fit by the second method, i.e. curve C, is more pleasing to the eye and for that reason is believed to weigh the sample points more equally than the method of least squares. Also shown in Figure A-5 through A-8 are heavy lines which represent the theoretical curves that are obtained for $m = 1L$, $2L$ and $3L$.

The Z values in Table A-3 may be used to determine the amount of movement the amines must undergo in order to form urea when the polymer is reacted with carbonyldiimidazole. As each amine reacts with carbonyldiimidazole to form a semi-urea intermediate, the intermediate can form a moiety of urea most often by reacting with the nearest neighboring amine. Then the fraction of the amines which did form urea moieties allows one to look up from the appropriate column of Table A-3 the distance, in terms of the unit L, that at least some of the amines must have moved.

The results for the coupling of the random amine polymers are shown in Table A-7. The data of Table A-7 suggest a slightly greater mobility for the 20X polymers but this may be an artifact of the large variations of urea fractions that were obtained from the different samples that were coupled with carbonyldiimidazole. Although the model reveals that much clearer results about the measurement of mobility may be obtained at loadings lower than 1 mol%, the presently available instrumentation and methodologies do not allow that possibility.

Table A-7 Conversion of Urea Fractions into Distance Moved

INITIAL CONCN AMINE	UREA FRACTION	MAXIMUM DISTANCE MOVED (Multiples of L)
R 20		
1.7	0.61	2.5
2.2	0.64	2.2
2.9	0.62	1.9
3.0	0.72	1.9
R 60		
1.4	0.47	2.1
1.4	0.36	2.05
2.9	0.18	1.0
3.0	0.61	1.7
R 60		
0.82	0.43	2.2
1.0	0.47	2.3
2.5	0.47	1.75
3.0	0.18	1.0
R 80		
0.74	0.29	2.1
2.0	0.084	1.8
2.0	0.33	1.8
2.9	0.17	1.1
		$L = 1.0 \times 10^{-7}$ cm.

Finally it is possible to obtain a rough estimate of the value of L . By making the following assumptions:

- 1) the true density of macroporous polystyrene is 1 g/ml,
- 2) 110 g of polystyrene = 1 mole of aromatic units.

$$\text{Volume of one sphere} = \frac{(\text{mass of 1 mole of aromatic units})}{(p) (N_A)}$$

$$= (1/6) (\pi) (L^3) \quad \text{eqn (A-18)}$$

Solving these terms for L yields: $L = 1.0 \times 10^{-7}$ cm.

APPENDIX B CHN CALCULATIONS

Examples of the calculation of the atomic mass balances of some of the polymer samples are given in this appendix. The calculations are somewhat complicated by the reported result, "Results of these experiments show, for example, that azo-isobutyronitrile yields only 65 percent of the potential radicals as free scavengable radicals in solution," [62JA2596]. Thus this report reveals yet another unknown parameter in the design of these experiments.

Tables B-1 and B-2 are examples of the calculation of 20X and 80X silanediamine-loaded polymers. Tables B-3 and B-4 are examples of the calculation of 20X and 80X carbamate-loaded polymers. Table B-5 is an example of the calculation of a polymer loaded with 4-vinylbenzylacetamide.

Table B-1 Calculation of the Atomic Mass Balance of a Silanediamine-loaded Polymer (J4-A) (20X)

SiN_2 = Silanediamine monomer 21

SOLUTION	MASS	
	MASS (g)	FRACTION
J1-A		
AIBN	0.0454	0.0150
ST	2.0784	0.68510
DVB	<u>0.9099</u>	0.29993
SUM	3.0337	

SOLUTION	MASS	
	MASS (g)	FRACTION
I118-B		
SiN_2	0.1639	0.04373
DMSO	<u>3.5840</u>	0.95627
SUM	3.7479	

Solutions J4-A (0.3567g) and I118-B (0.4317g) were used to prepare sample J4-A.

SAMPLE J4-A

I118-B 0.4317 g	COMPONENTS	MASS (g)	MMOL
	SiN_2	0.0189	0.04642
	DMSO	0.4128	
J1-A 0.3567 g	COMPONENTS	MASS (g)	MMOL
	ST	0.2444	2.346
	DVB	0.1070	0.8218
	AIBN	0.00534	0.0325

Combining the reagents SiN_2 , ST, DVB and AIBN allows the following calculations:

C MMOL	H MMOL	N MMOL	Si MMOL	
1.207	1.764	0.09284	0.04642	SiN_2
18.77	18.77			ST
8.218	8.546			DVB
0.260	0.390	0.0650		AIBN - N_2
C	H	N	Si	
28.46	29.47	0.1579	0.04642	MMOL W/AIBN
28.20	29.08	0.09284	0.04642	MMOL WO/AIBN
341.8	29.70	2.212	1.304	MASS (mg) W/AIBN
338.7	29.31	1.300	0.7427	MASS (mg) WO/AIBN

MASS PERCENTAGES				
C	H	N	Si	
91.14	7.92	0.59	0.35	WITH AIBN
91.39	7.91	0.35	0.35	WITHOUT AIBN
90.29	7.86	0.47		FOUND (AVERAGE OF 4 ANALYSES)

Table B-2 Calculation of the Atomic Mass Balance of a Silanediamine-loaded Polymer (J4-D) (80X)

SiN_2 = Silanediamine monomer 21

SOLUTION	MASS	
<u>J1-D</u>	<u>MASS(g)</u>	<u>FRACTION</u>
AIBN	0.0482	0.0134
ST	0	0
DVB	<u>3.5419</u>	0.98657
SUM	3.5901	

SOLUTION	MASS	
<u>I118-B</u>	<u>MASS(g)</u>	<u>FRACTION</u>
SiN_2	0.2018	0.04781
DMSO	<u>4.0188</u>	0.95219
SUM	4.2206	

Solution J1-D (0.4207g) and I118-B (0.4387g) were used to prepare sample J4-D.

SAMPLE J4-D

I118-B (0.4387g)

	<u>MASS(g)</u>	<u>MMOL</u>
SiN_2	0.02098	0.05158
DMSO	0.4177	

J1-D (0.4207g)

	<u>MASS(g)</u>	<u>MMOL</u>
ST	0	0
DVB	0.4150	3.188
AIBN	0.00565	0.0344

<u>C MMOL</u>	<u>H MMOL</u>	<u>N MMOL</u>	<u>Si MMOL</u>	SiN_2 MMOL
1.341	1.960	0.1032	0.05158	ST MMOL
0.0000	0.0000			DVB MMOL
31.88	33.16			AIBN - N_2 MMOL
0.275	0.413	0.0688		

<u>C</u>	<u>H</u>	<u>N</u>	<u>Si</u>	
33.50	35.53	0.1719	0.05158	MMOL WITH AIBN
33.22	35.11	0.1032	0.05158	MMOL WITHOUT AIBN
402.3	35.81	2.408	1.449	MASS(mg) W/AIBN
399.0	35.39	1.445	1.449	MASS(mg) WO/AIBN

MASS PERCENTAGES

<u>C</u>	<u>H</u>	<u>N</u>	<u>Si</u>	
91.03	8.102	0.545	0.3277	WITH AIBN
91.24	8.093	0.330	0.3312	WITHOUT AIBN
90.70	8.10	0.41		FOUND (AVERAGE OF 4 ANALYSES)

Table B-3 Calculation of the Atomic Mass Balance of a Carbamate-loaded Polymer (20X)-Sample (J8-A)

CARB = O-(*tert*-Butyl)-N-(4-Vinylbenzyl)carbamate 22

MASS		
<u>J1-A</u>	<u>MASS(g)</u>	<u>FRACTION</u>
AIBN	0.0454	0.0150
ST	2.0784	0.68510
DVB	<u>0.9099</u>	0.2999
	3.0337	

MASS		
<u>I96-B</u>	<u>MASS(g)</u>	<u>FRACTION</u>
CARB	0.2018	0.04781
DMSO	<u>4.0188</u>	0.95219
	4.2206	

Solutions J1-A and I96-B were used to prepare sample J7-A.

<u>SAMPLE J7-A</u>	<u>MASS(g)</u>
I96-B	0.8184g
J1-A	0.6541g

	<u>MASS(g)</u>	<u>MMOL</u>
CARB	0.03913	0.1677
ST	0.44813	4.3027
DVB	0.19618	1.507
AIBN	0.00979	0.0596
DMSO	0.7793	

<u>C MMOL</u>	<u>H MMOL</u>	<u>N MMOL</u>	<u>O MMOL</u>	
2.348	2.348	0.1677	0.3354	CARB
34.42	34.42			ST
15.07	15.67			DVB
0.477	0.715	0.119		AIBN

<u>C MMOL</u>	<u>H MMOL</u>	<u>N MMOL</u>	<u>O MMOL</u>	
52.32	53.16	0.287	0.3354	MMOL W/AIBN
51.84	52.44	0.1677	0.3354	MMOL WO/AIBN
0.6284	0.05358	0.00402	0.005367	MASS (g) W/AIBN
0.6226	0.05286	0.002349	0.005367	MASS (g) WO/AIBN

<u>MASS PERCENTAGES</u>				
<u>C</u>	<u>H</u>	<u>N</u>	<u>O</u>	
90.89	7.750	0.581	0.7763	CALCD W/AIBN
91.13	7.736	0.3438	0.7855	CALCD WO/AIBN

But the CHN calculations for the carbamate-loaded polymers can also be based on the concentration of carbamate in the polymer based on the IR spectral analysis.

Table B-3--continued

Assumption: The styrene and divinylbenzene are incorporated in the same fraction in the final polymer as they are present in the initial mixture.

CARBAMATE SPECTRAL CONCN = 3.5 MOL%.
THEREFORE ST+DVB = 96.5 MOL%

ST+DVB = 5.81 MMOL
THEREFORE CARB = 0.212 MMOL

C MMOL	H MMOL	N MMOL	O MMOL	
2.963	2.963	0.2116	0.4232	CARB
34.42	34.42			ST
15.07	15.67			DVB
0.477	0.715	0.119		AIBN
<hr/>				
C	H	N	O	
52.93	53.77	0.331	0.4232	TOTAL MMOL W/AIBN
52.45	53.06	0.2116	0.4232	TOTAL MMOL WO/AIBN
635.7	54.20	4.63	6.771	MASS (mg) W/AIBN
0.6300	53.48	2.964	6.771	MASS (mg) WO/AIBN
<hr/>				
MASS PERCENTAGES				
C	H	N	O	
90.65	7.727	0.661	0.9655	W/AIBN
90.88	7.714	0.4276	0.9768	WO/AIBN
90.205	7.98	0.455		FOUND (AVERAGE OF 2 ANALYSES)

Based on the spectral concentration of the carbamate monomer.

Table B-4 Calculation of the Atomic Mass Balance of a Carbamate-loaded Polymer (80X)-Sample (J8-D)

CARB = O-(*tert*-Butyl)-N-(4-Vinylbenzyl)carbamate 22

J1-D	MASS	
	MASS (g)	FRACTION
AIBN	0.0482	0.0134
ST	0	0
DVB	<u>3.5419</u>	0.98657
	3.5901	

I96-B	MASS	
	MASS (g)	FRACTION
CARB	0.2018	0.047813
DMSO	<u>4.0188</u>	0.952187
	4.2206	

Solutions J1-D and I96-B were used to prepare sample J7-D.

SAMPLE J7-D		MASS (g)	MMOL	
I96-B	0.4255	CARB	0.02034	0.087199
J1-D	0.3795	ST	0.000000	0.000000
		DVB	0.374405	2.875835
		AIBN	0.005095	0.031028
		DMSO	0.405156	
C MMOL	H MMOL	N MMOL	O MMOL	
1.2208	1.2208	0.087199	0.17440	CARB
0	0			ST
28.76	29.91			DVB
0.248	0.372	0.0621		AIBN
C	H	N	O	
30.23	31.50	0.1493	0.1744	MMOL W/AIBN
29.97914	31.12947	0.087199	0.174399	MMOL WO/AIBN
0.363061	0.031751	0.002091	0.002790	MASS (g) W/AIBN
0.360079	0.031375	0.001221	0.002790	MASS (g) WO/AIBN

MASS PERCENTAGES (BASED ON THE INITIAL MASSES OF THE MONOMER SOLUTIONS)

C	H	N	O	
90.84	7.944	0.5230	0.6981	W/AIBN
91.05	7.934	0.3088	0.7056	WO/AIBN

But the CHN calculations for the carbamate-loaded polymers can also be based on the concentration of carbamate in the polymer based on the IR spectral analysis.

Table B-4--continued

CARB SPECTRAL CONCN = 2.14 MOL%
 THEREFORE ST + DVB = 97.9 MOL%

ST+DVB = 2.91 MMOL
 THEREFORE CARB = 0.0637 MMOL

<u>C MMOL</u>	<u>H MMOL</u>	<u>N MMOL</u>	<u>O MMOL</u>	
0.8916	0.8916	0.06369	0.1274	CARB
23.01	23.01			ST
0.3103	0.3227			DVB
0.248	0.372	0.0621		AIBN

SUM OF TERMS

<u>C</u>	<u>H</u>	<u>N</u>	<u>O</u>	
24.46	24.59	0.1257	0.1274	MMOL W/AIBN
23.91	23.90	0.06369	0.1274	MMOL WO/AIBN
293.7	24.79	1.76	2.038	MASS (mg) W/AIBN
0.287042	0.024087	0.892	2.038	MASS (mg) WO/AIBN

MASS PERCENTAGES (BASED ON THE SPECTRAL ANALYSIS OF THE POLYMER SAMPLE)

<u>C</u>	<u>H</u>	<u>N</u>	<u>O</u>	
91.13	7.690	0.5464	0.6322	CALCD W/AIBN
91.40	7.670	0.2840	0.6489	CALCD WO/AIBN
90.265	8.175	0.405		FOUND (AVERAGE OF 2 ANALYSES)

Table B-5 Calculation of the Atomic Mass Balance of a Acetamide-loaded Polymer (20X)-Sample (I38-A)

AMIDE = N-(4-Vinylbenzyl)acetamide 23

SOLUTION	MASS	I37-A	I37-A
<u>I37-A</u>	<u>MASS (g)</u>	<u>FRACTION</u>	<u>MMOL</u>
AMIDE	0	0	0
ST	3.2883	0.26224	31.573
DVB	1.5854	0.12643	12.178
AIBN	0.0728	0.00581	0.443
DMSO	<u>7.5927</u>	0.60552	97.177
	12.5392		

I37-B = 3.9225G I37-A + 0.1898G AMIDE

SOLUTION	MASS	I37-B'	I37-B'
<u>I37-B'</u>	<u>MASS (g)</u>	<u>FRACTION</u>	<u>MMOL</u>
AMIDE	0.1898	0.04615	1.083
ST	1.0286	0.25014	9.8765
DVB	0.49594	0.12060	3.8094
AIBN	0.0228	0.00554	0.139
DMSO	<u>2.3751</u>	0.57757	30.399
	4.1123		

Sample I38-A consisted of 0.0475g I37-A and 0.2110g I37-B' solutions. Using the above quantities it is possible to calculate the following composition of sample I38-A:

SAMPLE	MASS	MMOL		
<u>I38-A</u>	<u>MASS (g)</u>	<u>MMOL</u>		
AMIDE	0.009739	0.055576		
ST	0.065236	0.626362		
DVB	0.031452	0.241588		
AIBN	0.00144	0.008795		
DMSO	0.150629	1.927858		
C MMOL	H MMOL	N MMOL	O MMOL	
0.61133	0.72248	0.05558	0.05558	AMIDE
5.01090	5.01090	0	0	ST
2.41588	2.41588	0	0	DVB
0.0704	0.1055	0.0352	0	AIBN
C	H	N	O	
8.1085	8.2548	0.0908	0.05558	MMOL WITH AIBN
8.0381	8.1493	0.05558	0.05558	MMOL WITHOUT AIBN
97.391	8.320	1.27	0.8892	MASS (mg) W/AIBN
96.546	8.214	0.7784	0.8892	MASS (mg) WO/AIBN
MASS PERCENTAGES				
C	H	N	O	
90.28	7.713	1.18	0.8243	CALCD W/AIBN
90.71	7.718	0.7314	0.8355	CALCD WO/AIBN
90.49	7.91	0.81		FOUND (1 ANALYSIS)

APPENDIX C
TREATMENT OF SPECTRA FOR THE DETERMINATION
OF URETHANE AND UREA CONCENTRATIONS

In Figure C-1 is shown the region of the IR spectrum which contains the urethane, urea and aromatic overtone absorption bands for the random-polymer sample J27-A-8-A. Figure C-2 presents a magnified view of the same region. The spectra are of a sample which was analyzed as its CHBr_3 mull.

The aromatic overtones were removed by using the auto-subtraction of the Perkin-Elmer Model 1600 Series Infrared Spectrometer. The region extending from 1775 cm^{-1} to 2000 cm^{-1} was used as the reference for the subtraction process. The baseline for the urethane and urea peaks in the spectrum shown in Figure C-3 and an expanded view in Figure C-4 extends from 1756 cm^{-1} to 1636 cm^{-1} .

The urethane area was then determined by integrating the urethane peak from 1756 cm^{-1} to 1690 cm^{-1} . This is analogous to dropping a vertical line from the point on the curve at 1691 cm^{-1} to the baseline and measuring the area that is enclosed. The urea area was determined by integrating the urea peak from 1690 cm^{-1} to 1636 cm^{-1} . The areas that were found were $8.47 \text{ A} \cdot \text{cm}^{-1}$ and $3.71 \text{ A} \cdot \text{cm}^{-1}$ for the urethane and urea peaks, respectively. The aromatic peak in Figure C-1 was integrated from 1632.1 cm^{-1} to 1562.4 cm^{-1} , and the area found was $32.28 \text{ A} \cdot \text{cm}^{-1}$.

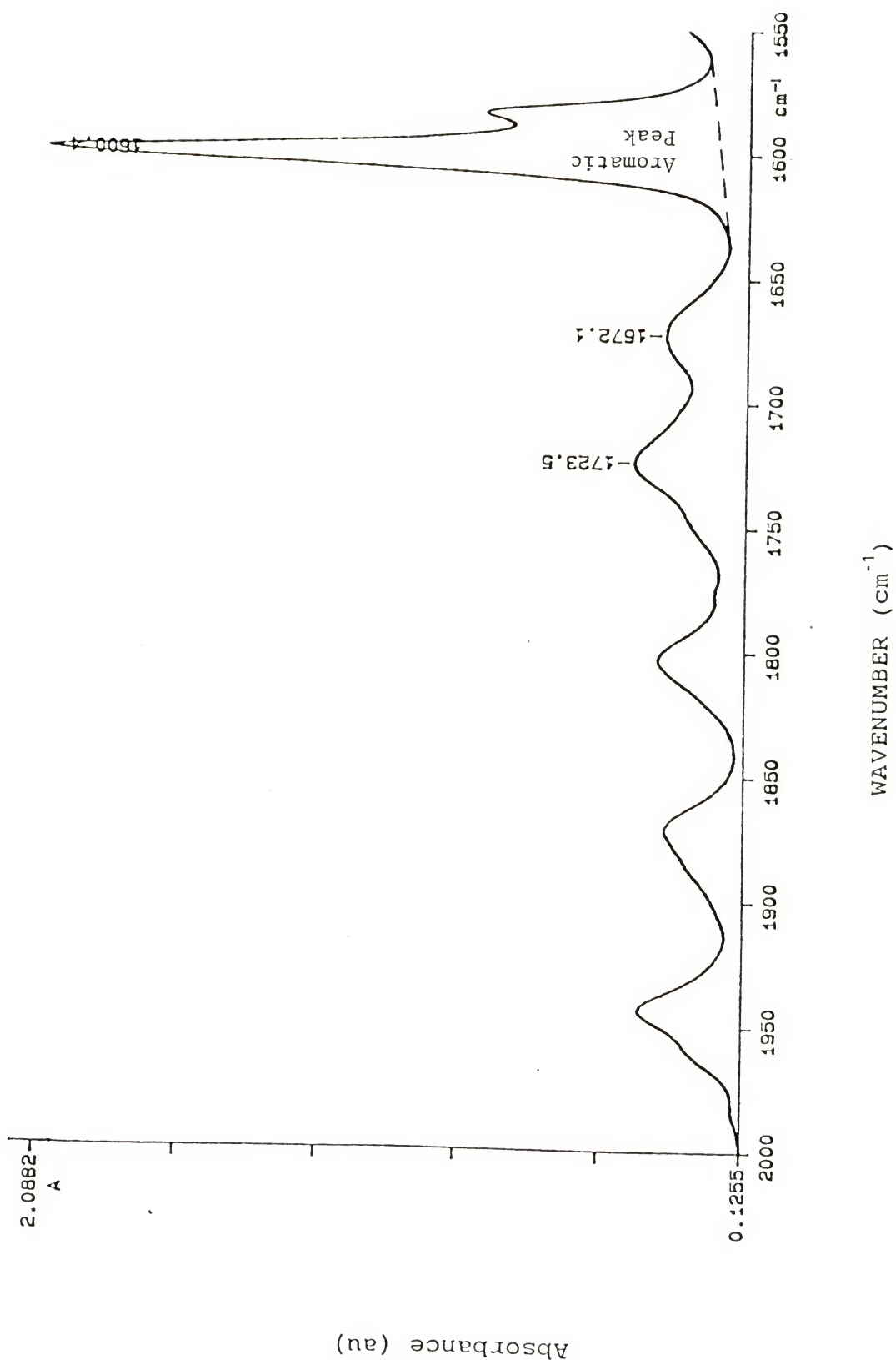


Figure C-1 IR Spectrum of a Random Polymer Sample after Coupling with Carbonyldiimidazole (CHBr₃, Mull)

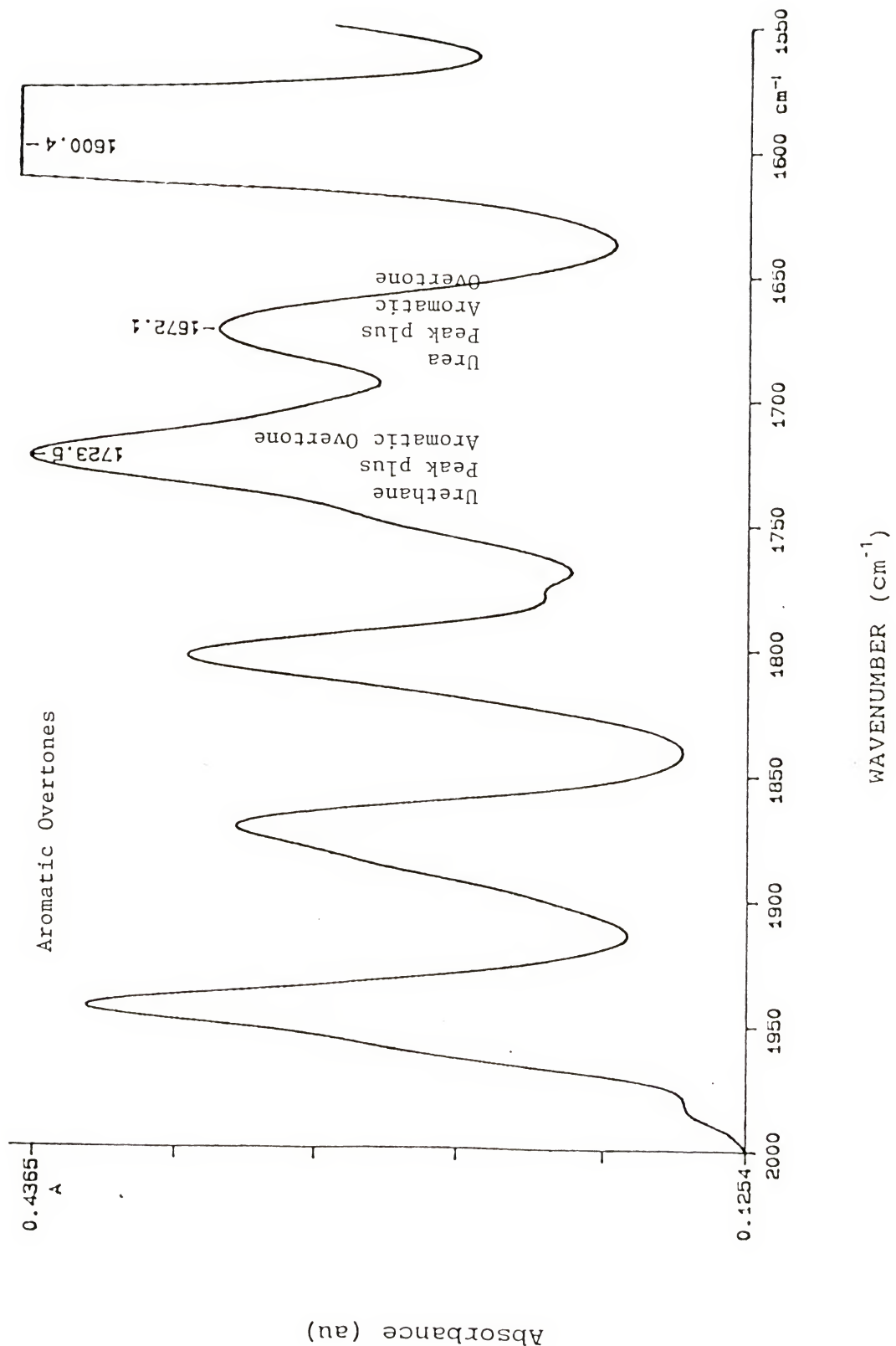


Figure C-2

Magnified view of the IR Spectrum shown in Figure C-1 (CHBr_3 Mull)

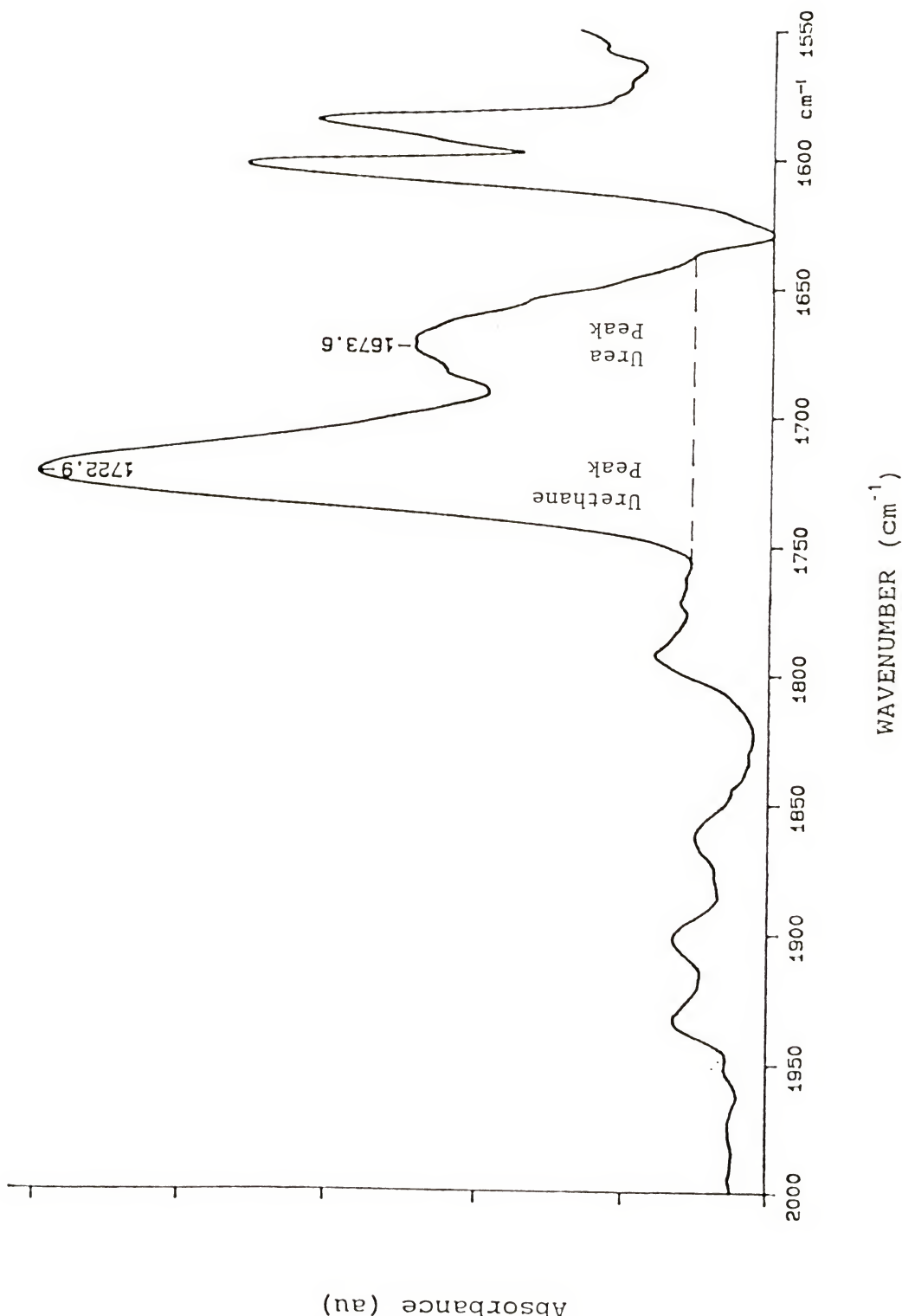


Figure C-3

IR Spectrum of the Carbonyl Region of a Coupled Ordered Polymer after the Aromatic Overtones have been Subtracted

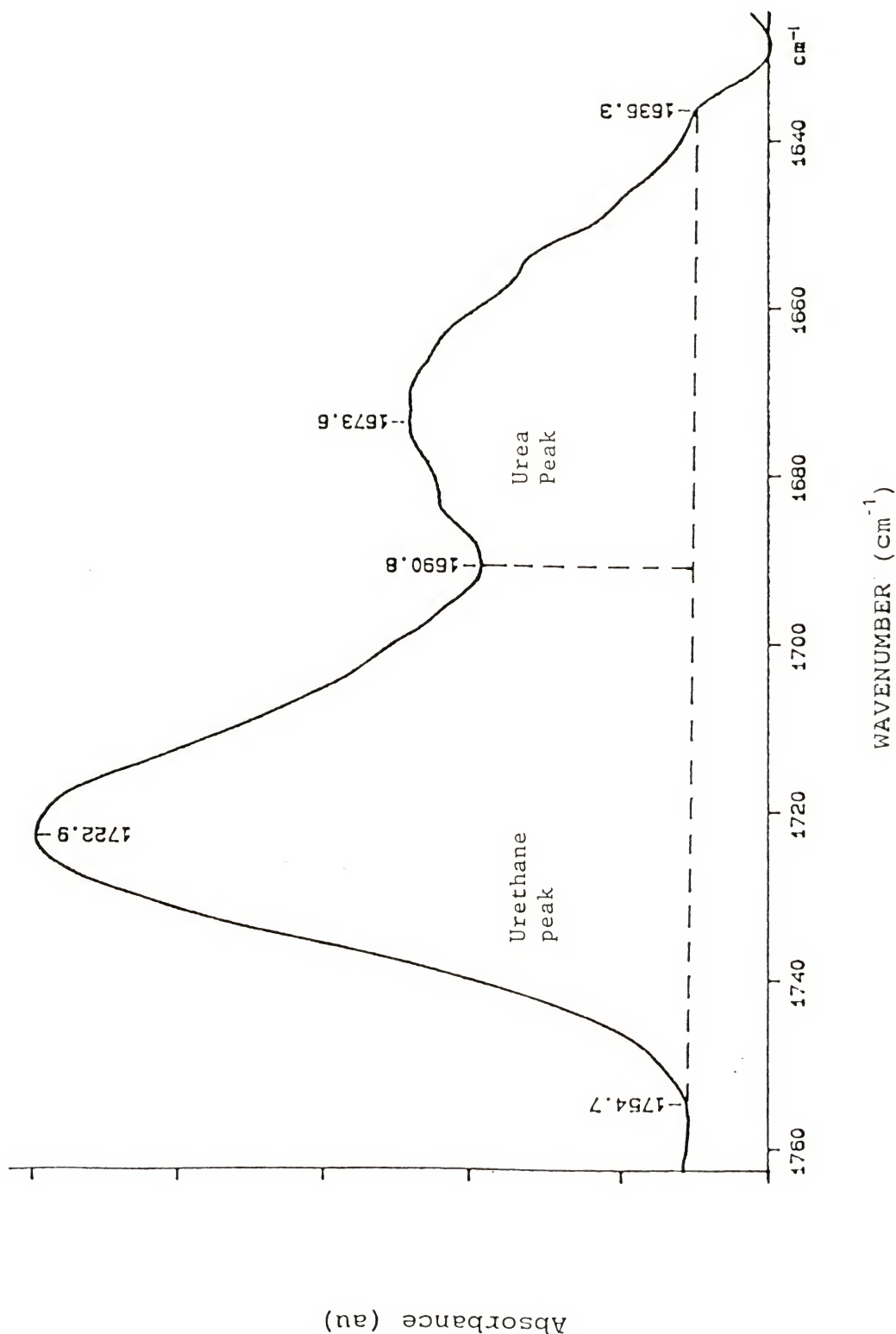


Figure C-4

An Expanded View of the IR Spectrum in Figure C-3 with the Baseline and Integration Bounds

Thus, the (urethane area)/(aromatic area) term is equal to 0.262, which gives that the urethane concentration is 0.80 mol%. The (urea area)/(aromatic area) term is equal to 0.115, which gives that the urea concentration is 0.50 mol%. The (urethane concn)/(urea concn) term is equal to 1.6.

Another example set of spectra is shown in Figures C-5 through C-8 for the ordered-polymer sample J21-A-8-A. The aromatic peak in Figure C-5 was integrated from 1637.4 cm^{-1} to 1562.5 cm^{-1} . Because this area included the small peak due to the carbon-carbon double bond absorbance at 1629.3 cm^{-1} , the small peak was integrated separately and subtracted from the former-integrated area to give an aromatic area of $28.83\text{ A}\cdot\text{cm}^{-1}$.

The urethane and urea peaks (shown in expanded form in Figure C-8) were integrated using the baseline and bounds shown in Figure C-8. The urethane and the urea areas were $6.47\text{ A}\cdot\text{cm}^{-1}$ and $6.58\text{ A}\cdot\text{cm}^{-1}$, respectively.

Thus, the (urethane area)/(aromatic area) term is equal to 0.224, which gives that the urethane concentration is 0.68 mol%. The (urea area)/(aromatic area) term is equal to 0.228, which gives that the urea concentration is 1.0 mol%. The (urethane concn)/(urea concn) term is equal to 0.68.

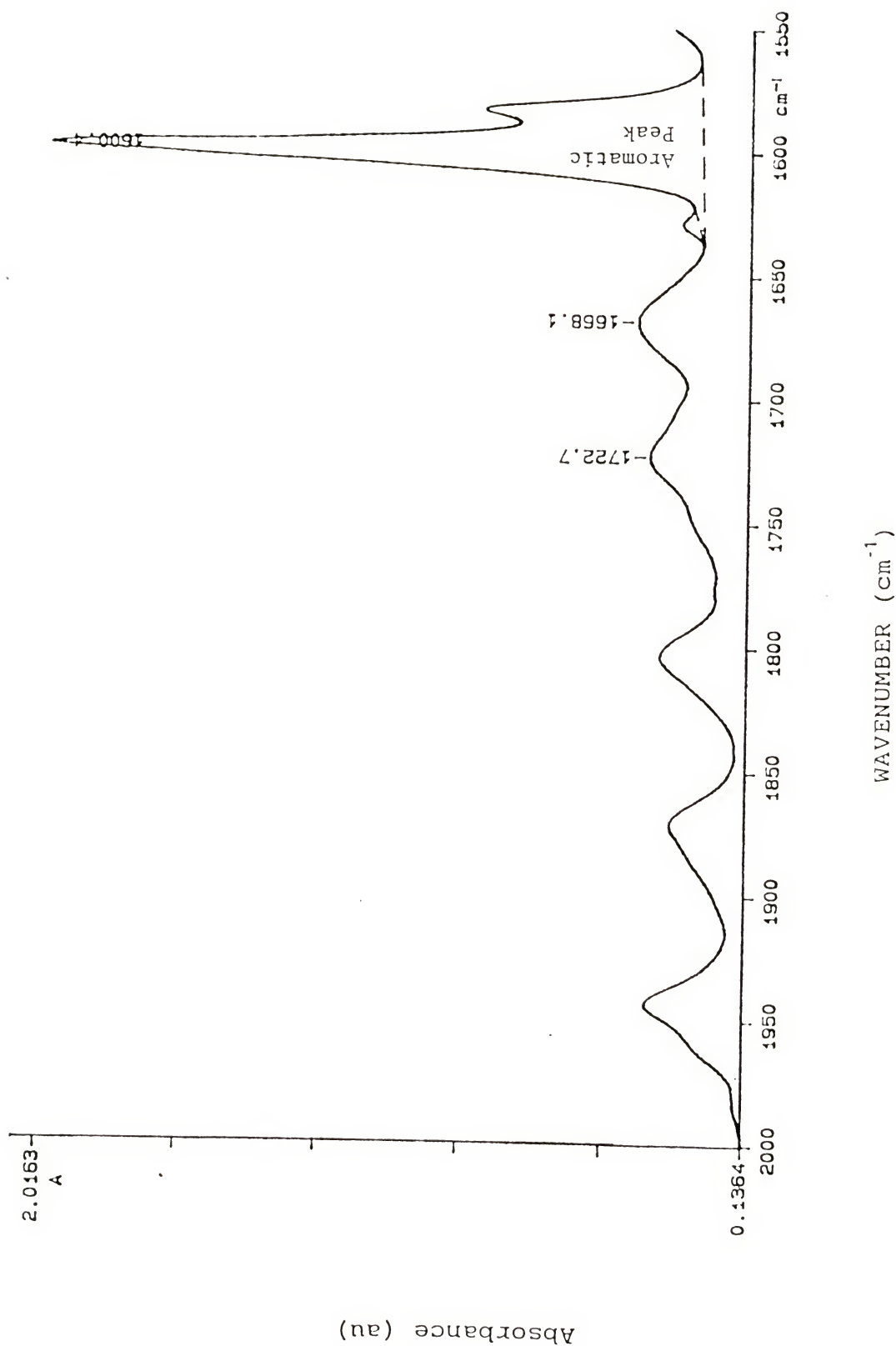


Figure C-5 IR Spectrum of an Ordered Polymer Sample after Coupling with Carbonyldiimidazole (CHBr₃ Mull)

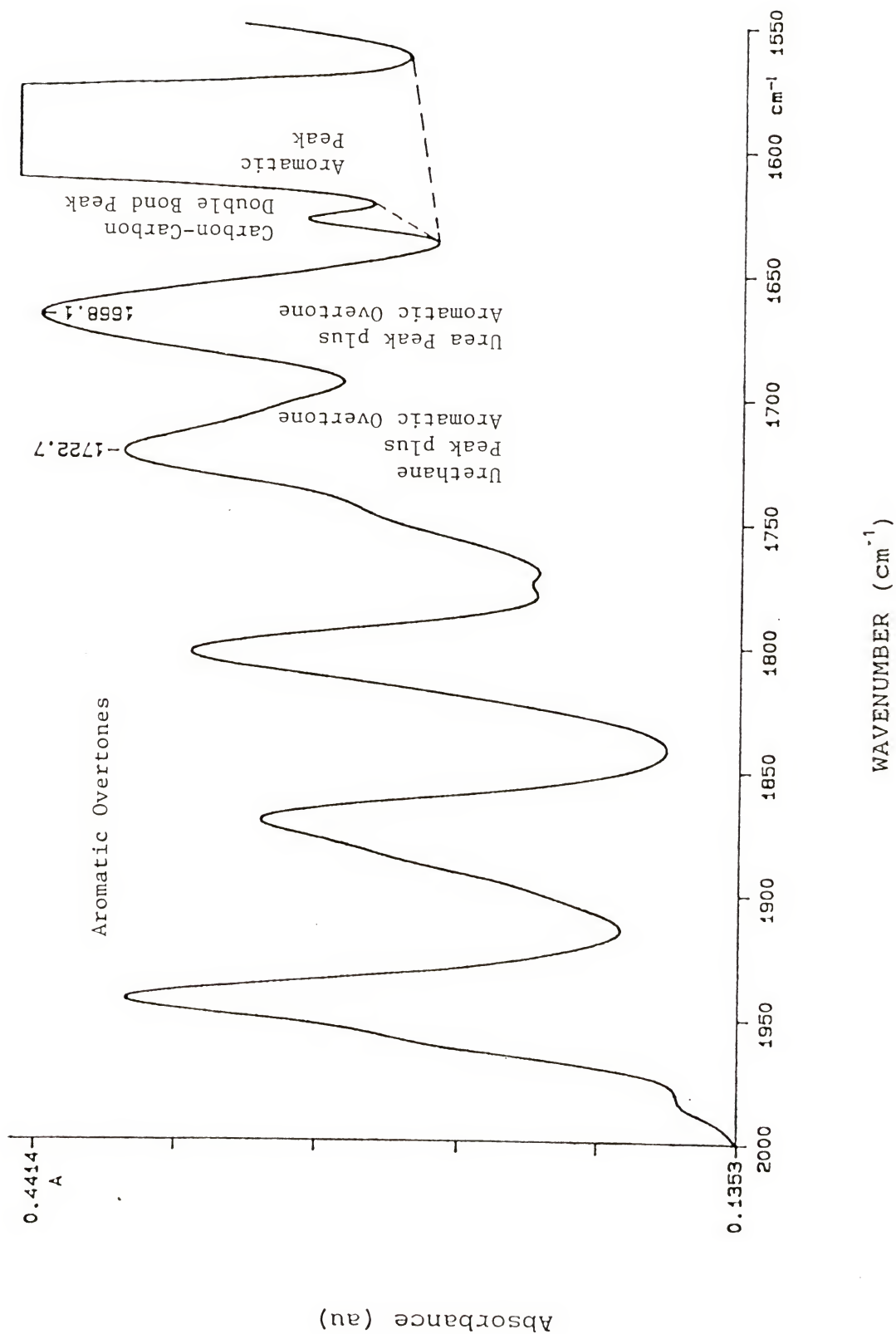


Figure C-6 Magnified view of the IR Spectrum shown in Figure C-5 (CHBr₃ Mull)

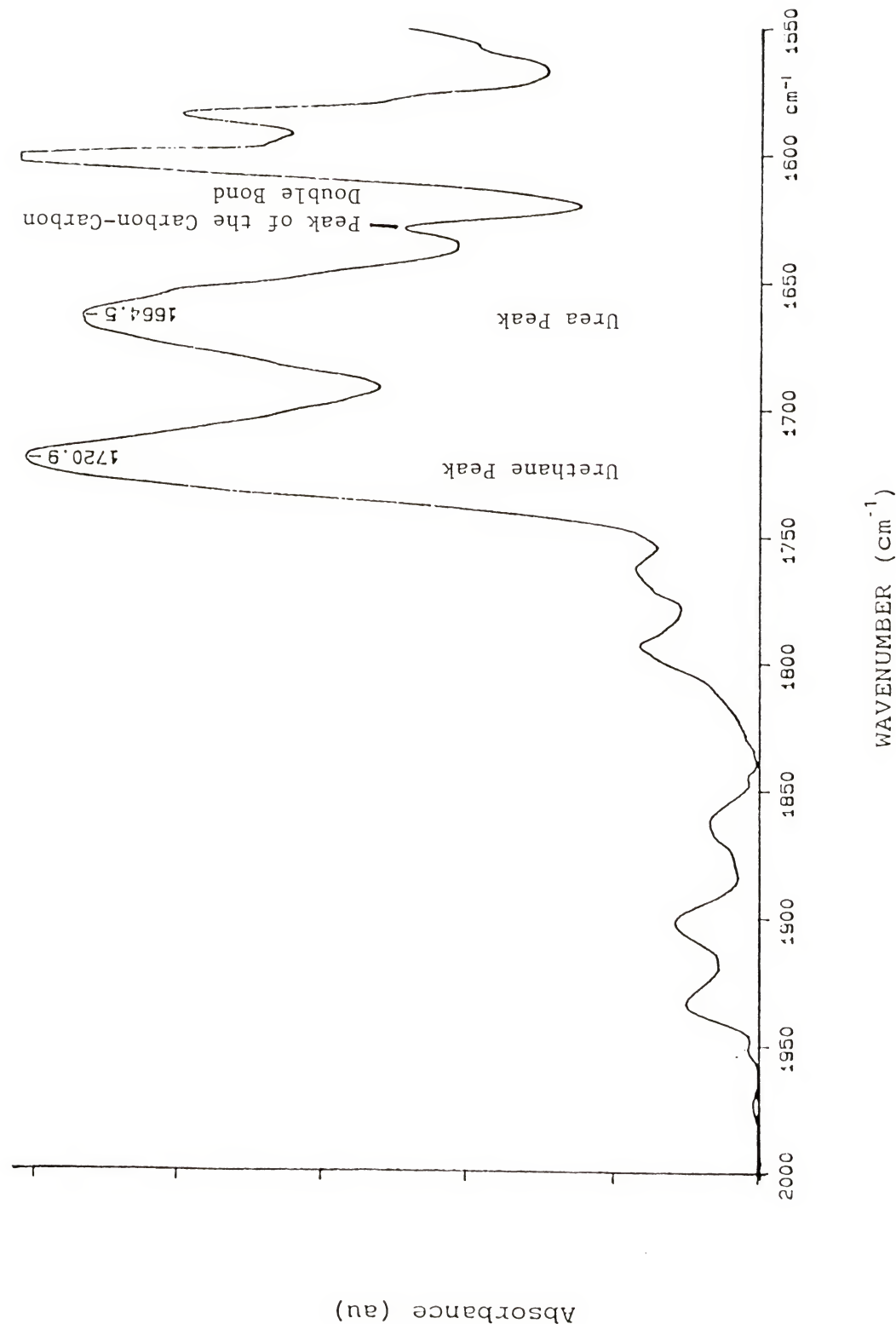


Figure C-7

IR Spectrum of the Carbonyl Region of a Coupled Ordered Polymer after the Aromatic Overtones have been Subtracted

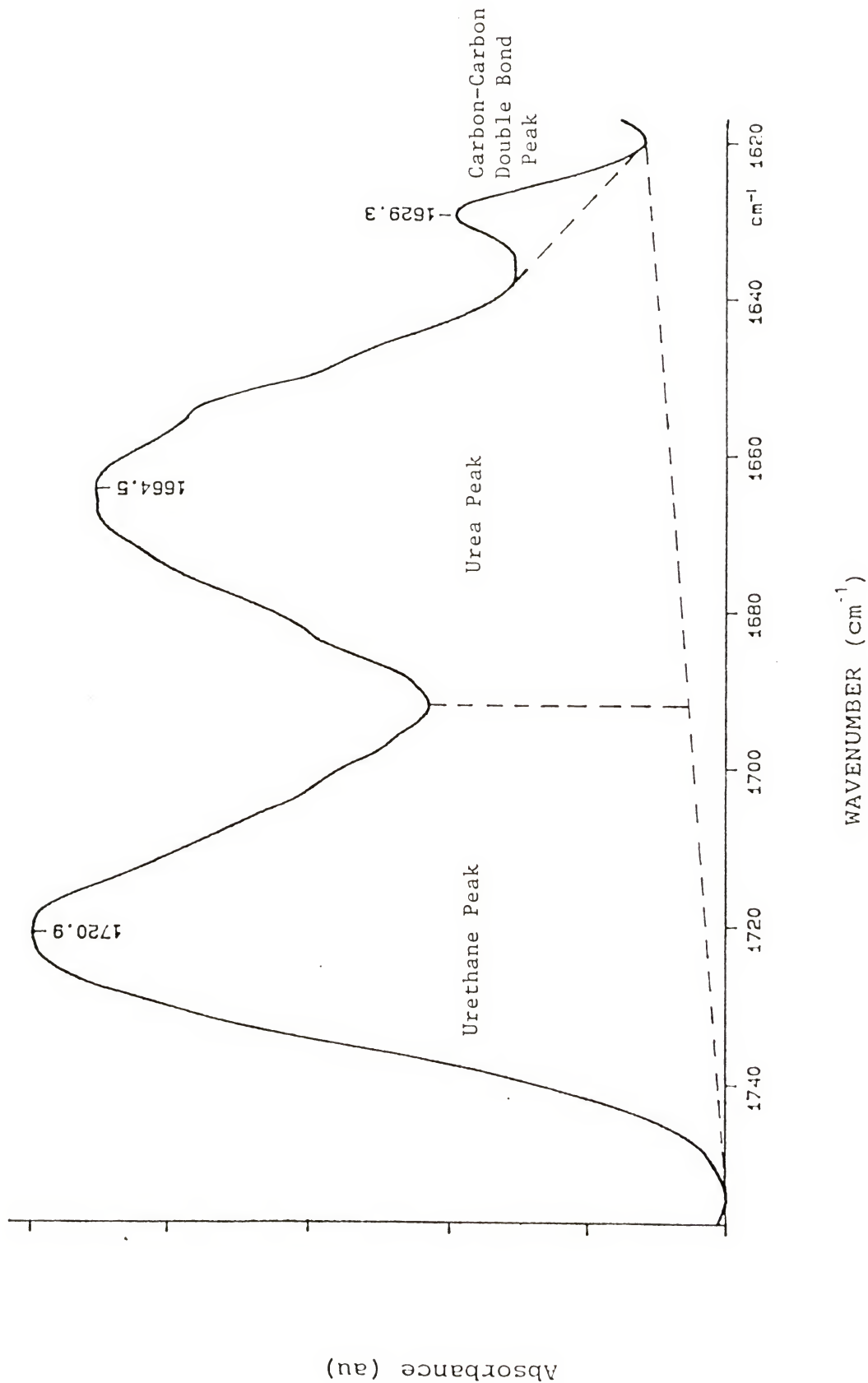


Figure C-8

An Expanded View of the IR Spectrum in Figure C-7 with the Baseline and Integration Bounds shown

BIBLIOGRAPHY

The system adopted here for references is one created by Katritzky and Rees in "Comprehensive Heterocyclic Chemistry", Pergamon Press, New York, 1984, vol. 4, p. 1085. References are designated by a number-letter code of which the first two digits (or first four digits for references before 1900) denote the year of publication, the next one or two letters the journal, and the final digits the page number. Books and all other sources are coded MI (miscellaneous) and are listed under the relevant year of publication.

Letter Codes for Journal Titles

<u>Code</u>	<u>Journal Abbreviation</u>
ACR	Acc. Chem. Res.
AG(E)	Angew. Chem., Int. Ed. Engl.
CJC	Can. J. Chem.
JA	J. Am. Chem. Soc.
JOC	J. Org. Chem.
M	Monatsch. Chem.
MI	Miscellaneous
PAC	Pure Appl. Chem.
TL	Tetr. Lett.

REFERENCES

[06M969] H. V. Lendenfeld, *Monatsch. Chem.*, 27, 969, 1906.

[23CB769] B. Helferich, P. E. Speidel and W. Toeldte, *Chemische Berichte*, 56, 769, 1923.

[25JA3055] W. H. Carothers and G. A. Jones, *J. Am. Chem. Soc.*, 47, 3055, 1925.

[34JA144] J. A. Murray and F. B. Dains, *J. Am. Chem. Soc.*, 56, 144, 1934.

[38JA657] T. B. Dorris, F. J. Sowa and J. A. Nieuwland, *J. Am. Chem. Soc.* 60, 657, 1938.

[53JA995] E. Larsson and L. Bjellerup, *J. Am. Chem. Soc.*, 75, 995, 1953.

[54JA5466] J. L. E. Erickson and G. N. Grammer, *J. Am. Chem. Soc.*, 80, 5466, 1958.

[60MI1] C. Eaborn; "Organosilicon Compounds", Academic Press, New York, 1960, p.345.

[62JA2596] P. D. Bartlett and T. Funahashi, *J. Am. Chem. Soc.*, 84, 2596, 1962.

[63JA209] G. Stork, A. Brizzolara, H. Landesman, J. Szmuszkovicz and R. Terrell, *J. Am. Chem. Soc.*, 85, 209, 1963.

[63JA2149] R. B. Merrifield, *J. Am. Chem. Soc.*, 85, 2149, 1963.

[64JA5163] R. L. Letsinger, M. J. Kornet, V. Mahadevan and D. M. Jerina, *J. Am. Chem. Soc.* 86, 5163, 1964.

[66MI1] L. J. Bellamy; "The Infra-red Spectra of Complex Molecules", Methuen & Co. Ltd., London, 1966.

[66MI2] R. T. Conley; "Infrared Spectroscopy", Allyn and Bacon, Boston, 1966, p.206.

[68MI1] A. T. Nielson and W. J. Houlihan in; "Organic Reactions", vol. 16, eds. R. Adams, A. H. Blatt, V. Boekelheide, T. L. Cairns, D. J. Cram and H. O. House, Wiley, Inc., New York, 1968.

[70JA7587] A. Patchornik and M. A. Kraus, J. Am. Chem. Soc. 92, 7587, 1970.

[70MI1] C. L. Perrin; "Mathematics for Chemists", Wiley-Interscience, New York, 1970, p.111.

[71MI1] M. L. Bender; "Mechanisms of Homogeneous Catalysis from Protons to Proteins", Wiley-Interscience, New York, 1971, p.165.

[72JA1789] J. P. Collman, L. S. Hegedus, M. P. Cooke, J. R. Norton, G. Dolcetti and D. N. Marquardt, J. Am. Chem. Soc., 94, 1789, 1972.

[72CJC2892] C. C. Leznoff and J. Y. Wong, Can. J. Chem., 50, 2892, 1972.

[72MI1] J. I. Crowley, T. B. Harvey III and H. Rapoport, Polym. Prepr., Am. Chem. Soc., Div. Polym. Chem., 13, 958, 1972.

[73CJC3756] C. C. Leznoff and J. Y. Wong, Can. J. Chem., 51, 3756, 1973.

[75JA2128] W. D. Bonds, Jr., C. H. Brubaker, Jr., E. S. Chadrasekaran, C. Gibbons, R. H. Grubbs and L. C. Kroll, J. Am. Chem. Soc. 97, 2128, 1975.

[75MI1] J. L. Koenig, Applied Spectroscopy, 29, 293, 1975.

[75PAC503] A. Patchornik and M. A. Kraus, Pure and Applied Chemistry, 43, 503, 1975.

[76ACR135] J. I. Crowley and H. Rapoport, Accounts of Chemical Research, 9, 135, 1976.

[77JA625] L. T. Scott, J. Rebek, L. Ovsyanko and C. L. Sims, J. Am. Chem. Soc., 99, 625, 1977.

[77JA4517] R. Grubbs, C. P. Lau, R. Cukier and C. Brubaker, Jr. J. Am. Chem. Soc., 99, 4517, 1977.

[77MI1] G. Wulff, W. Vesper, R. Grobe-Einsler and A. Sarhan, Makromolekulare Chemie, 178, 2799, 1977.

[77MI2] S. L. Regan and D. P. Lee, Macromolecules, 10, 1418, 1977.

[78AG(E)537] I. Schulze and G. Wulff, *Angew. Chem., Int. Ed. Engl.*, 17, 537, 1978.

[79JA677] S. Mazur and P. Jayalekshmy, *J. Am. Chem. Soc.*, 101, 677, 1979.

[79MI1] U. Wanagat, *Monatshefte fur Chemie*, 1979, 110(5), 1077.

[80MI1] "Polymer-Supported Reactions in Organic Synthesis", eds. P. Hodge and D. C. Sherrington, Wiley, New York, 1980.

[80MI2] H. W. Siesler and K. Holland-Moritz, "Infrared and Raman Spectroscopy of Polymers", Marcel Dekker, New York, 1980, Vol.4 of Practical Spectroscopy Series.

[80MI3] "Polymer Handbook", 3rd. ed., eds. J. Brandrup and E. H. Immergut, Wiley-Interscience, New York, 1980, p.II/218.

[81JOC5364] Y. H. Chang and W. T. Ford, *J. Org. Chem.*, 46, 5364, 1981.

[81TL3455] E. J. Corey, H. Cho, C. Rucker and D. H. Hua, *Tetr. Lett.* 22, 3455, 1981.

[82JOC2697] Y. Kita, J. Haruta, H. Yasuda, K. Fukunaga, Y. Shirouchi and Y. Tamura, *J. Org. Chem.*, 47, 2697, 1982.

[82MI1] J. Toullec in: "Advances in Physical Organic Chemistry", vol 18, eds. V. Gold and D. Bethell, Academic Press, New York, 1982, p.70.

[82TL4871] E. J. Corey and P. B. Hopkins, *Tetr. Lett.*, 23, 4871, 1982.

[83MI1] P. R. Griffiths, *Science*, 222, 297, 1983.

[83MI2] "Beilsteins Handbuch der Organischen Chemie", Springer-Verlag, Berlin, 1983 (citing US Patent 2,650,250, Distillers Co.).

[84MI1] V. L. King, "Synthesis and Evaluations of Crosslinked Polystyrenes Containing Thiol Functional Groups", Master thesis, Univ. of Florida, Gainesville, Florida, 1984.

[84MI2] G. R. Rao and G. Zerbi, *Applied Spectroscopy.*, 38, 795, 1984.

[84MI3] J. C. Leighton, "Synthesis and Kinetic Investigations of Macromolecular Polymeric Catalysts", Ph.D. dissertation, Univ. of Florida, Gainesville, Florida, 1984.

[85MI1] "Encyclopedia of Polymer Science and Engineering", J. I. Kroschwitz, Ed.-in-Chief, vol. 3, 1985, p.293.

[86MI1] "Polymer-supported Reactions in Organic Synthesis", eds. P. Hodge and D. C. Sherrington, Wiley-Interscience, Chichester, England, 1980.

[86MI2] W. T. Ford in: "Polymeric Reagents and Catalysts", ed. W. T. Ford, ACS series 308, Washington, D.C., 1986, Chapter 11.

[86MI3] W. T. Ford in: "Polymeric Reagents and Catalysts", ed. W. T. Ford, ACS series 308, Washington, D.C., 1986, pp.250-1.

[86MI4] M. A. Sharaf, D. L. Illman, B. R. Kowalski, Chemometrics, volume 82 of Chemical Analysis, Wiley-Interscience, New York, 1986, pp.11, 316.

[87MI1] J. L. Koenig, Analytical Chemistry, 59, 1141A, 1987.

[87MI2] "Computer-Enhanced Analytical Spectroscopy", eds. H. L. C. Meuzelaar and T. L. Isenhour, Plenum Press, New York, 1987, pp.67-102.

[89MI1] M. Periyasamy and W. T. Ford, Journal of Polymer Science, 27, 2357, 1989.

BIOGRAPHICAL SKETCH

Kenneth Jones was born on February 21, 1958, in Delhi, Louisiana; the hospital was later condemned. His academic career improved after receiving an F for conduct in the first grade.

After attending three universities, he obtained his B.S. degree in chemistry in 1981 from Louisiana State University. He worked with a little company while taking more coursework, and obtained a B.S. degree in chemical engineering from Louisiana State University in 1983.

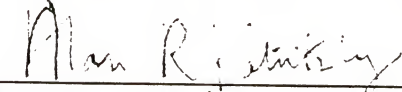
After working and taking yet more coursework at LSU, he decided to leave Louisiana, came to the University of Florida in September 1986 and later chose to work with Dr. James A. Deyrup. Following graduation he will take a research associate position with the Naval Research Laboratory in Washington, D.C.

I certify that I have read this study and that in my opinion it conforms to acceptable standards of scholarly presentation and is fully adequate, in scope and quality, as a dissertation for the degree of Doctor of Philosophy.



James A. Deyrup, Chairman
Professor of Chemistry

I certify that I have read this study and that in my opinion it conforms to acceptable standards of scholarly presentation and is fully adequate, in scope and quality, as a dissertation for the degree of Doctor of Philosophy.



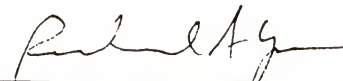
Alan R. Katritzky
Kenan Professor of Chemistry

I certify that I have read this study and that in my opinion it conforms to acceptable standards of scholarly presentation and is fully adequate, in scope and quality, as a dissertation for the degree of Doctor of Philosophy.



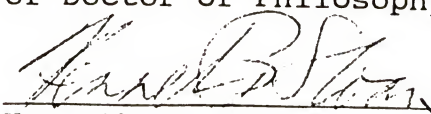
John A. Zoltewicz
Professor of Chemistry

I certify that I have read this study and that in my opinion it conforms to acceptable standards of scholarly presentation and is fully adequate, in scope and quality, as a dissertation for the degree of Doctor of Philosophy.



Richard A. Yost
Professor of Chemistry

I certify that I have read this study and that in my opinion it conforms to acceptable standards of scholarly presentation and is fully adequate, in scope and quality, as a dissertation for the degree of Doctor of Philosophy.



Kenneth B. Sloan
Associate Professor of Medicinal Chemistry

This dissertation was submitted to the Graduate Faculty of the College of Liberal Arts and Sciences and to the Graduate School and was accepted as partial fulfillment of the requirements for the degree of Doctor of Philosophy.

December, 1991

Dean, Graduate School